Human Pluripotent Stem Cell Models of Huntington's Disease

Jacquet, Laureen Esther-Mae

Awarding institution:
King's College London

Human Pluripotent Stem Cell Models of Huntington's Disease

By

Laureen Esther-Mae Jacquet

A thesis presented for the fulfilment of the degree of Doctor of Philosophy at King's College London, University of London

September 2013

Stem Cell Research Laboratory
Kings College London School of Medicine
Division of Women's Health
Assisted Conception Unit
11th Floor Tower Wing
Guy's Hospital
London SE1 9RT

ABSTRACT

Huntington's disease (HD) is a late-onset, autosomal, dominant and progressive neurodegenerative disorder for which there is no disease-modifying therapy. An abnormal trinucleotide CAG repeats expansion (>36 CAG repeats) in exon 1 of the gene coding for the Huntingtin (HTT) protein is the causative mutation for the disease. Animal models of HD, such as the R6/2 mouse model, already exist. Yet, in order to understand the disease at a molecular level, cellular models of HD are also needed. At the beginning of this project, existing models had been developed from tumour cell lines using genome-integrating lentiviral delivery system carrying a mutated HTT exon 1. This model was not optimal, as the cells will always have non-innate extra copies of HTT, which expression is driven by exogenous promoter. In order to circumvent this, we were aiming to develop two human stem cell models of HD and use them as tools in drug discovery and further understanding of molecular mechanisms of the disease.

The first model is human embryonic stem cells (hESCs) isolated from clinically unsuitable embryos, donated by consenting couples. The embryos carrying a mutation in HTT gene, as determined by Preimplantation Genetic Diagnosis (PGD), were used to derive HD-specific mutation-carrying hESC lines (HD-hESC). Seven HD- hESCs lines were derived at the Assisted Conception Unit (ACU) at Guy's Hospital, King's College London (KCL).

The second model is induced pluripotent stem cells (iPSCs) that I would derive from keratinocytes obtained from plucked hairs of consenting HD patients. Their greater availability means that we would be able to derive lines representing a larger spectrum of HD phenotype due to variations in CAG repeats expansion. Reprogramming will be done using a combination of modified mRNAs and/or a lentiviral vector encoding the transcription factors needed for reprogramming.

The overall goal of the project was to optimize culture conditions for the HD-hESC and HD-iPS cell lines, fully characterise them, and differentiate them *in vitro.* Epidemiology studies suggest that cardiac failure is the second cause of death in HD patients. For this reasons, HD-ESCs were differentiated into cardiac cells (cardiomyocytes) in order to define and characterize the cardiac HD phenotype.

Here, I am describing thorough characterization of normal and HD-hESC lines and their differentiation into cardiomyocytes. I am also presenting my data on reprogramming of human fibroblasts into iPSC using synthetic modified mRNA. Due to time limit and several technical issues outlined in the text, I was unable to successfully reprogram cells from keratinocytes obtained from plucked hairs of consenting HD patients.

DECLARATION

I, Laureen Esther-Mae Jacquet, confirm that the work presented in this thesis is the work of the author. As such, copyright of this thesis rests with the author and no quotations from it or information derived from it may be published without the prior consent of the author.

TABLE OF CONTENT

LIST OF FIGURES

LIST OF TABLES

ABBREVIATIONS

β-ME	B-Mercaptoethanol
3-NP	3-Nitropropionic Acid
A	Absorbance
aCGH	Array Comparative Genomic Hybridisation
ACU	Assisted Conception Unit
AFP	Alpha-Fetoprotein
AP	Alkaline Phosphatase
bFGF	Basic Fibroblast Growth Factor
BMP	Bone Morphogenic Protein
cDNA	Complementary DNA
CNS	Central Nervous System
CO_2	Carbon Dioxide
CS	Cellstart
Ct	Threshold Cycle
cTNT	Cardiac Troponin T
DAB	Diaminobenzidin
DAPI	4',6-Diamidino-2-Phenylindole
dNTP	Deoxyribonucleotide triphosphate
DMEM	Dubelco Modified Eagle Medium
DMSO	Dimethylsulphoxide
DNA	Deoxyribonucleic Acid
DOC	Sodium Deoxycholate
DPX	Di-N-Butyl Phthalate (DPX).
EB	Embryoid Body

ECM	Extracellular Matrix
EMEM	Eagle's Minimal Essential Medium
F-12	Nutrient Mix F-12
FBS	Fetal Bovine Serum
GFP	Green Fluorescent Protein
GFR	Growth Factor Reduced
GOI	Gene Of Interest
H&E	Haematoxylin & Eosin
HCl	Hydrochloric Acid
HD	Huntington's Disease
HDAC	Histone Deacetylase
hESC	Human Embryonic Stem Cell
hESC-CM	Human Embryonic Stem Cell-derived Cardiomyocyte
HF	Hair Follicule
HFEA	Human Fertilisation And Embryology Authority
HFF	Human Foreskin Fibroblast
HIER	Heat-Induced Epitope Retrieval
HK	Housekeeping
HKGS	Human Keratinocyte Growth Supplement
HLA	Human Leukocyte Antigen
HRP	Horseradish Peroxidase
HTT	Huntingtin Protein
ICM	Inner Cell Mass
IMS	Industrial Methylated Spirit
iPSCs	Induced Pluripotent Stem Cells

IVF	In Vitro Fertilisation
JHD	Juvenile Huntington's Disease
KCL	Kings College London
KO	Knock-Out
LN_2	Liquid Nitrogen
KO-DMEM	Knockout Dubelcco's Modified Eagle Medium
KOSR-XF	Knock Out Serum Replacement Xeno-Free
MEF	Mouse Embryonic Fibroblast
MEF-CM	Mouse Embryonic Fibroblast Conditionned Medium
MET	Mesenchymal-Epithelial Transition
mHTT	Mutant Huntingtin Protein
NaBu	Sodium Butyrate
NNEA	Non-Essential Amino Acids
NOD-SCID	Non Obese Diabetic Severe Combined Immunodeficiency
NSC	Neural Stem Cell
NuFF	Newborn Human Foreskin Fibroblast
O_2	Oxygen
ORS	Outer Root Sheath
P	Passage
PBS	Phosphate-Buffered Saline
PCR	Polymerase Chain Reaction
PFA	Paraformaldehyde
PFT-α	Pifithrin-A
PGD	Preimplantation Genetic Diagnosis
PSC	Pluripotent Stem Cell

qPCR	Quantitative Polymerase Chain Reaction
RNA	Ribonucleic Acid
ROCK	Rho-Associated Kinase
rpm	Revolutions Per Minute
RPMI	Roswell Park Memorial Institute
RT	Room Temperature
SEM	Standard Error Of The Mean
SMA	Smooth Muscle Actin
TBS	Tris Buffered Saline
TEM	Transmission Electron Microscopy
TGF-β	Transforming Growth Factor B
Tris	Tris(Hydroxymethyl)Aminomethane
VPA	Valproic Acid
WT	Wild Type

ACKNOWLEDGEMENT

I would first like to thank my supervisors, Dr. D. Ilic and Prof. G. Bates. It has been an honor to work under your guidance and to have two experts in their fields as supervisors. Thank you for your help in guiding my research and for always encouraging me and reassuring me when needed be. I have learnt a lot as a scientist and as a person over the past four years.

I am also especially grateful to the patients who donated their embryos and hair samples.

I would like to thank past and present members of the Ilic and Bates labs. You were all always so kind to give a hand and help me troubleshooting. I have learnt a lot from all of you. Special thanks go to Dimitra, Excel is now part of my life thanks to you. Heema, thanks for sharing your wisdom with me. Andreas, thank you for opening the doors of Molecular Biology. Dale, it has been a pleasure to work with you.

“Merci” to all of my friends for their support and for being so patient. Thank you for always being the ones coming to visit when I could not be away from the lab at the weekends. Claire, thank you for your unconditional support. Darren, many thanks for repeating the “it will be fine” mantra to me.

To my wonderful family, from Mamie to little Jules, this thesis is for you. Mum, you are the best personal cheerleader anybody could ask for. I am very privileged to have in my life somebody that believes in me as much as you do. Paps, I cherish all our conversations and the time we spend together. I learn a lot from you. Alice, my wonderful sister and best friend, you made this year in London the best. Warm thanks as well to the Monk family for offering me a home from home.

Lawrence, I cannot thank you enough for the support you have given me over the past four years. You have been my rock, always believing in me and helping me everyday to reach my goal. I could not have done it without you.

"A smooth sea never made a skilled sailor."

English proverb

CHAPTER 1

GENERAL INTRODUCTION

Chapter 1 GENERAL INTRODUCTION

1.1 Huntington's Disease

1.1.1 Clinical features of HD

Huntington's disease (HD) was named after George Huntington, who very accurately described the disease in his brief report "On Chorea" in 1872 (Huntington, 1872, Figure 1-1). His precise observations are still relevant today and admirably describe the major traits associated with HD. They can serve as an introduction to the disease.

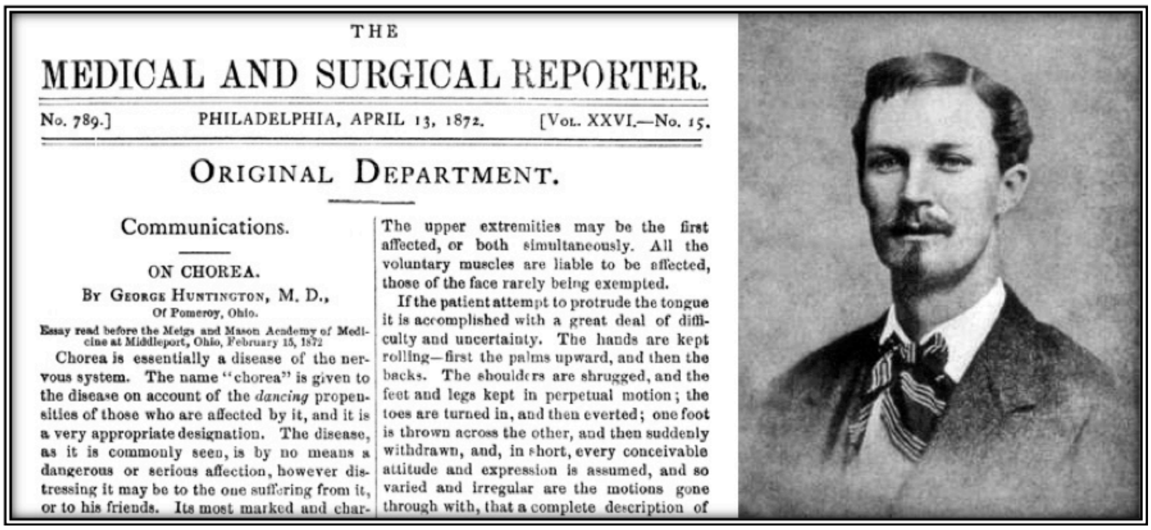
THE

MEDICAL AND SURGICAL REPORTER.

No. 789.] PHILADELPHIA, APRIL 13, 1872. [Vol. XXVI.—No. 15.

ORIGINAL DEPARTMENT.

Communications.

ON CHOREA.

By George Huntington, M. D.,
Of Pomeroy, Ohio.

Essay read before the Meigs and Mason Academy of Medicine at Middleport, Ohio, February 15, 1872

Chorea is essentially a disease of the nervous system. The name "chorea" is given to the disease on account of the *dancing* propensities of those who are affected by it, and it is a very appropriate designation. The disease, as it is commonly seen, is by no means a dangerous or serious affection, however distressing it may be to the one suffering from it, or to his friends. Its most marked and char-

The upper extremities may be the first affected, or both simultaneously. All the voluntary muscles are liable to be affected, those of the face rarely being exempted.

If the patient attempt to protrude the tongue it is accomplished with a great deal of difficulty and uncertainty. The hands are kept rolling—first the palms upward, and then the backs. The shoulders are shrugged, and the feet and legs kept in perpetual motion; the toes are turned in, and then everted; one foot is thrown across the other, and then suddenly withdrawn, and, in short, every conceivable attitude and expression is assumed, and so varied and irregular are the motions gone through with, that a complete description of

Figure 1-1: Picture of G. Huntington aged 22, and of the title page of his article "On Chorea" in the *Medical and Surgical Reporter*, 1872.

i) Chorea is one of the hallmarks of HD.

> *"Chorea is essentially a disease of the nervous system. The name "chorea" is given to the disease on account of the dancing propensities of those who are affected by it, and it is a very appropriate designation. […] The disease commonly begins by slight twitchings in the muscles of the face, which gradually increase in violence and variety. The eyelids are kept winking, the brows are corrugated, and then elevated, the nose is screwed first to the one side and then to the other, and the mouth is drawn in various directions, giving the patient the most ludicrous appearance imaginable. The upper extremities may be the first affected, or both simultaneously. All the voluntary muscles are liable to be affected, those of the face rarely being exempted."*

Chorea, derived from the Greek word *χορεία*, to dance, describes the involuntary movements suffered by HD patients. They are associated with the neurodegeneration of the central nervous

system (CNS) and will only worsen throughout the duration of the illness. The beginning of chorea usually marks the onset of the disease (Margolis and Ross, 2003).

ii) HD is an autosomal, dominantly inherited disease.

> *"Of its hereditary nature. When either or both the parents have shown manifestations of the disease, and more especially when these manifestations have been of a serious nature, one or more of the offspring almost invariably suffer from the disease, if they live to adult age. But if by any chance these children go through life without it, the thread is broken and the grandchildren and great-grandchildren of the original shakers may rest assured that they are free from the disease."*

G. Huntington was able to describe the autosomal, dominant inheritance pattern of HD thanks to long epidemiological studies carried out by himself, his father and his grandfather. Together, these three generations of physicians cumulated 78 years of clinical observations. This was prior to our current knowledge on genetics and the acceptation of Mendel's theory of the principle of hereditary transmission (Mendel, 1865)

iii) HD patients also suffer from cognitive decline and a tendency to suicide.

> *"A tendency to insanity and suicide. […] The tendency to insanity, and sometimes that form of insanity which leads to suicide, is marked. I know of several instances of suicide of people suffering from this form of chorea, or who belonged to families in which the disease existed. As the disease progresses the mind becomes more or less impaired, in many amounting to insanity, while in others mind and body both gradually fail until death relieves them of their sufferings. At present I know of two married men, whose wives are living, and who are constantly making love to some young lady, not seeming to be aware that there is any impropriety in it. They are suffering from chorea to such an extent that they can hardly walk, and would be thought, by a stranger, to be intoxicated. They are men of about 50 years of age, but never let an opportunity to flirt with a girl go past unimproved. The effect is ridiculous in the extreme."*

Cognitive decline, irritability and depression are common features of HD that can affect up to 80% of HD patients. They can manifest before the onset of motor-deficits and are usually most prominent in the year preceding clinical diagnosis and during the early stages of the development of motor symptoms (Epping and Paulsen, 2011; Margolis and Ross, 2003). Depression is not a symptom measured relative to disease progression (Epping and Paulsen, 2011), nevertheless suicide is a significant cause of mortality amongst HD patients (Chiu and

Alexander, 1982; Lanska *et al.*, 1988; Sorensen and Fenger, 1992) and patients have to be monitored for it to minimise risks.

iv) HD is a late onset, progressive neurodegenerative disorder.

> *"I do not know of a single case that has shown any marked signs of chorea before the age of thirty or forty years, while those who pass the fortieth year without symptoms of the disease, are seldom attacked. It begins as an ordinary chorea might begin, by the irregular and spasmodic action of certain muscles, as of the face, arms, etc. These movements gradually increase, when muscles hitherto unaffected take on the spasmodic action, until every muscle in the body becomes affected (excepting the involuntary ones), and the poor patient presents a spectacle which is anything but pleasing to witness. I have never known a recovery or even an amelioration of symptoms in this form of chorea; when once it begins it clings to the bitter end. No treatment seems to be of any avail, and indeed nowadays its end is so well-known to the sufferer and his friends, that medical advice is seldom sought. It seems at least to be one of the incurables."*

G. Huntington accurately describes the late-onset and progressive nature of HD. However, a juvenile form of the disease (JHD) also exists, with a different clinical manifestation. Age of onset of HD is predominantly determined by the size of the mutation of the HD gene, which will be discussed in section 1.1.2. JHD patients also suffer from dementia and other cognitive deficits. However, their major motor feature manifestation tends to be rigidity rather than chorea (Siesling *et al.*, 1997).

Unfortunately, G. Huntington's description of the fatal nature of HD with the absence of treatment is still factual, despite the discovery of the cause of the disease 20 years ago. Intriguingly, epidemiology studies indicate that cardiac failure is the second cause of death amongst HD patients (Sorensen and Fenger, 1992; Lanska *et al.*, 1988; Chiu and Alexander, 1982). The cause for this is yet to be investigated.

1.1.2 Huntingtin

The HD gene, Huntingtin (*HTT*), was discovered by The Huntington Disease Collaborative Research Group in 1993 (The Huntington Disease Collaborative Research Group, 1993). It is located on chromosome 4 and is characterised by an increased polymorphic polyglutamine trinucleotide motif (CAG) in its first exon. This causes the translation of an abnormally long polyglutamine track within the Huntingtin (HTT) protein. In healthy individuals, the CAG repeat number ranges from 11 to 34 while HD-specific repeats are above 36. There is a strong negative correlation between the number of CAG repeats and the age of onset / severity of the symptoms (The Huntington Disease Collaborative Research Group, 1993; Trottier *et al.*, 1994; Squitieri *et al.*, 2001; Figure 1-2).

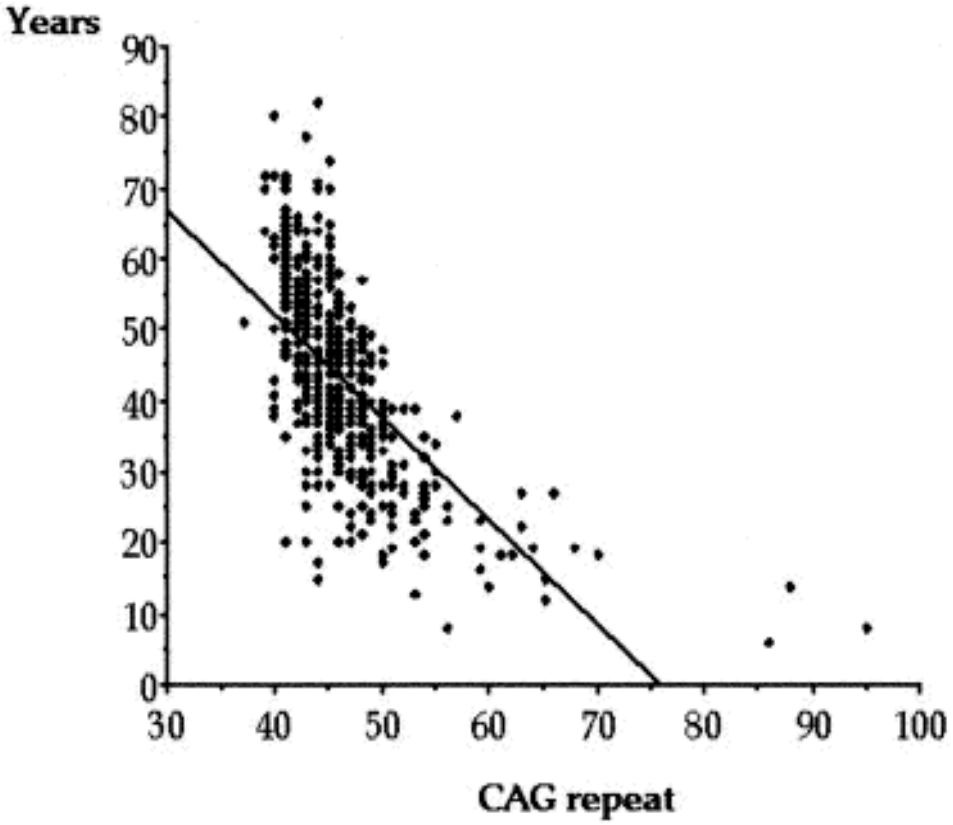

Figure 1-2: Negative correlation between HD age of onset and CAG repeat size.
"Linear correlation obtained by simple regression analysis plotting the age at onset (y-axis) with the CAG repeat expansion (x-axis; n = 464, r^2 = 0.54, p = 0.0001)" taken from Squitieri *et al.*, (2001)

Individuals who have CAG repeat numbers in the higher abnormal range i.e. above 55 repeats tend to develop Juvenile Huntington's Disease (JHD), a more severe form of the disease, with slightly different clinical manifestations that develop in their youth instead of in their third to fifth decade. The mutation is unstable, showing both decreases and increases in size (Duyao *et al.*, 1993; The Huntington Disease Collaborative Research Group, 1993). The largest increases are found during spermatogenesis, leading to JHD mainly being the result of anticipation with a bias towards paternal inheritance (Telenius *et al.*, 1993; Duyao *et al.*, 1993). HD patients baring homozygous mutations do not automatically have a lower age of onset, nevertheless they will have a more severe phenotype and faster disease progression (Squitieri *et al.*, 2001). Instability of the CAG repeat sizes have also been reported in somatic tissues, with the largest expansion being observed in the brain (Telenius *et al.*, 1994; Kennedy *et al.*, 2003).

The discovery of *HTT* allowed for the development of predictive testing for individuals at risk, including embryos, and the development of *in vivo* and *in vitro* models of the disease.

1.1.3 Function of Huntingtin

HTT is a large protein (348 kD) that is ubiquitously expressed, with the highest levels found in the brain and testis (The Huntington Disease Collaborative Research Group, 1993; Li, S.H. *et al.*, 1993; Strong *et al.*, 1993; Sharp *et al.*, 1995). Its endogenous function is still not completely understood as it has very little homology to other known proteins (The Huntington Disease Collaborative Research Group, 1993). Nevertheless it has been discovered that HTT is essential for development, its double knockout (KO) causes embryonic lethality in mice. Apoptotic cell death is observed from embryonic day 6 (E6.0), primarily in the distal region of the epiblast. By E11.5, no embryonic tissue could be observed; only extraembryonic tissues (mostly yolk sac membrane) could be recovered (Zeitlin *et al.*, 1995). HTT is also important for neurodevelopment and fertility. Its KO (by Cre/loxP-mediated inactivation in the forebrain and cerebellum using the *Camk2a* promoter in E.15 or postnatal mice day 5) or knockdown (in *Htt*-shRNA-transfected E12.5) in mice resulted in the progressive neurodegeneration and sterility of these latter (Dragatsis *et al.*, 2000; Tong *et al.*, 2011). HTT is also involved in cellular trafficking as a scaffold protein, interacts with different organelles such as the Golgi apparatus, mitochondria and the endoplasmic reticulum, is also involved in the endosome–lysosome pathway and plays a role in transcriptional regulation (Landles and Bates, 2004; Harjes and Wanker, 2003). When HTT misfolds, it aggregates and forms inclusions pre-dominantly in the neural cells of the central nervous system (CNS) and to a lesser extent in peripheral tissue cells. WT-HTT is predominantly found in the cytoplasm while aggregates tend to be found in the nucleus. The nuclear localisation of mutant HTT can lead to its abnormal binding to different transcription factors, subsequently leading to the formation of aggregates and the disruption of transcriptional expression (Harjes and Wanker, 2003). This could be described as a WT-HTT *loss of function*, coupled with a mutant HTT *gain of function*, which could explain the defects, mainly neurological, observed in HD (Davies *et al.*, 1997; Scherzinger *et al.*, 1997; Sathasivam *et al.*, 1999).

1.2 Models of Huntington's Disease

In order to study human diseases, researchers have strived to create disease models. These range from animals to primary or genetically modified cell types. It is expected for a valid HD model to exhibit key features of HD in a progressive and measurable way. For instance, it is preferable for murine models to have a mid-to late-life disease onset characterised by motor impairment.

1.2.1 *In vivo* models of HD

HD does not naturally develop in animals. Therefore, *in vivo* models were created by the use of toxins that mimic the mutation or by the transgenic expression of the mutation.

1.2.1.1 Toxin-induced models of Huntington's Disease

Prior to the discovery of *HTT*, HD models were developed by the delivery of toxins to rodent and non-human primates to reproduce an HD-like phenotype. Toxins such as quinolinic acid and 3-Nitropropionic Acid (3-NP), a mitochondrial inhibitor, can cause neuronal cell death. This in turn induces symptoms such as cognitive deficit and motor impairment which are also found in HD. Drawbacks associated with these models are the lack of progressive cell death and the absence of HTT aggregates, two hallmarks of the disease (Ramaswamy *et al.*, 2007).

1.2.1.2 Murine models of HD

Murine models of HD can be divided into three categories: i) transgenic mice expressing fragments of both the promoter and exon 1 of the human *HTT* gene, ii) transgenic mice expressing the full-length human *HTT* gene and iii) knock-in mice expressing murine HTT with a pathogenic CAG repeat expansion.

i) One of the first murine models of HD was developed in 1996 (Mangiarini *et al.*, 1996). They carry a transgene allele of the promoter sequence and the *HTT* exon 1 N-terminal sequences with a CAG expansion of approximately 130 repeats. Of these, the R6/2 strain is the best characterised and displays an aggressive phenotype as from 4 weeks of age resulting in death between 10 and 13 weeks. Disease progression can be observed by reduced brain weight and body weight, chorea-like tremors, motor and cognitive deficits (Mangiarini *et al.*, 1996), as well as cardiac dysfunction (Mihm *et al.*, 2007). The ability of mutant HTT to form intranuclear inclusions or aggregates, particularly in neurons was also discovered thanks to the R6/2 model (Davies *et al.*, 1997). It can also be noted that the transgene is expressed in every tissue, as expected from the ubiquitous expression of HTT (Mangiarini *et al.*, 1996; Sathasivam *et al.*, 1999; Moffitt *et al.*, 2009; Sassone *et al.*, 2009)

ii) Inserting full-length HTT using yeast artificial chromosomes or bacterial artificial chromosomes respectively generated the YAC and BAC murine HD models respectively (Hodgson *et al.*, 1999; Gray *et al.*, 2008). Unlike the R6/2 models, the YAC murine strains were at first generated to study CAG repeat sizes comparable to those present in either adult or juvenile HD patients (YAC46 and YAC72 have 46 or 72 CAG repeats respectively) (Hodgson *et al.*, 1999). Disease progression in these models is much less aggressive than in the R6/2. Particularly in the YAC46, HD behavioral phenotypic characteristics cannot be observed for up to 20 months. In order to have a model with a faster disease onset, YAC murine strains with 128 CAG repeats, the YAC128, were later engineered (Slow *et al.*, 2003). This confirms that there is a strong negative correlation between CAG repeats number, age of disease onset and severity of HD symptoms (Hodgson *et al.*, 1999).

iii) HD knock-in murine models have been generated by engineering the murine *HTT* homologue (*Hdh)* to carry a pathogenic CAG repeat number (Levine *et al.*, 1999; Shelbourne *et*

al., 1999; Wheeler *et al.*, 2000). This approach presents the advantage of having *HTT* expressed in an endogenous genomic and proteomic context. Similarly to other full-length HTT murine models, the disease phenotype is milder and progression occurs in a longer lifespan than the transgenic fragment models (Menalled *et al.*, 2003). This further emphasizes that the HTT fragments generated by the expression of exon 1 only are very toxic, and sufficient to cause the disease phenotype (Mangiarini *et al.*, 1996; Davies *et al.*, 1997)

There is no doubt that murine models of HD have immensely contributed to the current knowledge on HD, especially from a molecular and genetic aspect, as well as pre-clinical standpoint. For instance, they led to the discovery of the aggregate phenotype in HD. However there are issues associated with these *in vivo* models. Firstly, they are short lived. In can be argued that despite their short lifespan, murine models of HD still recapitulate HD phenotypes that can take decades to manifest in humans. Yet, this restricts the study of the disease to very short time period, particularly in models such as the R6/2 mice that have a very aggressive phenotype manifestation. The size of the HD murine models and consequently the size of their brain could also be a limitation associated with these models. Indeed, treatment delivery means or doses that are applicable and effective to some extent in murine models cannot necessarily be scaled up in humans. It can also be noted that most of the existing HD *in vivo* models manifest a wide-range of symptoms with different timings. For these reasons the need for the standardisation of experimental protocols and their statistical analysis has been enounced (Hockly *et al.*, 2003). Furthermore, it has been suggested that, prior to being considered for clinical trial, a compound of interest should show efficacy in at least two different murine models in two different laboratories (Bates and Hockly, 2003).

1.2.1.3 Large animal models of HD

Large animal models of HD include non-human primates, which were given HD by the transgenic expression of *HTT* exon 1. When expressing exon 1 with 84 CAG repeats the monkeys showed motor deficits, chorea and presented HTT neuronal aggregates (Yang, S.H. *et al.*, 2008). Compared to murine or non-vertebrate models, non-human primates could offer the possibility of a wider range of cognitive tests similar to the ones performed in humans. However, the transgenic primates suffered from early deaths (within one day to one month post-natal), possibly due to the high expression levels of mutant HTT. HD-specific phenotypes such as chorea and apoptotic neurons were also found in HD transgenic pigs expressing a N-terminal (208 amino acids) portion of HTT with 105 CAG repeats (Yang *et al.*, 2010). However, like the HD monkeys, the pigs suffered from early deaths. This is unlike transgenic HD murine models, which can survive longer with even larger CAG repeat sizes. This highlights that the endogenous context in which mutant HTT is expressed can influence the resulting phenotype. HD transgenic sheep have also been developed (Jacobsen *et al.*, 2010) and survival of up to three years has been reported in this model. Unlike the HD monkey, they express the full-length human HTT (with 73 CAG repeats), and not only a fragment of exon 1, which seems to be

better tolerated. Like monkeys and pigs, sheep have the advantage of having larger brains that further resemble those of humans, and advanced cognitive functions (Morton and Avanzo, 2011).

1.2.1.4 Invertebrate and eukaryotic models of HD

S.cerevisiae (Mason and Giorgini, 2011), *C. elegans* (Parker *et al.*, 2001) and *D. melanogaster* (Jackson *et al.*, 1998) are invertebrate species used to model HD, mainly by forced expression of HTT exon 1. Their small size and the absence of a blood-brain barrier make them useful for high-throughput screening of therapeutic compounds. They also have the advantage of being relatively inexpensive, which allows the generation of numerous biological replicates. These models have contributed to better understand HTT aggregation and provided further insight into the role of HTT, for example by linking HTT interaction with the mitochondria misfunction and screen for therapeutics that can later be further validated in other HD models.

1.2.2 *In vitro* models of Huntington's Disease

To complement HD *in vivo* models, HD *in vitro* models have also been developed from mouse, rat and human cells. Cellular models of HD, such as the transgenic ones presented in Table 1-1, recapitulate some of the hallmarks features of HD, notably increased cell death and the formation of aggregates. They can then be used as a screening platform for therapeutic agents that will prevent or delay aggregate formation and / or cell death.

Cell line	Species origin	Cell type	Phenotype	CAG (Q) repeat size	Reference
NG108-15	Mouse / Rat cell hybrid	Neuroblastoma / Glioma	Presence of aggregates and increased apoptotic cell death	FL (15Q, 73Q, 116Q), N502 (15Q, 73Q, 116Q), N80 (15Q, 73Q, 116Q)	Lunkes and Mandel (1998)
X57	Mouse cell hybrid	E18 Strial primordial / Neuroblastoma	Presence of aggregate	FL (18Q, 46Q, 100Q), N3221 (18Q, 100Q)	Kim, M. *et al.* (1999)
Neuro2A (N2A)	Mouse	Neuroblastoma	Presence of aggregates and increased apoptotic cell death	Exon 1 (16Q, 60Q, 150Q)	Wang, G.H. *et al.*(1999), Yamamoto *et al.* (2006)
				Exon 1 (25Q, 65Q and 103Q) 103Q)	Yamamoto *et al.* (2006)
ST14A	Rat	Striatal primordial (E14)	Increased apoptotic cell death	FL (23Q, 82Q), N548(15Q, 120Q), N63 (18Q, 82Q),	Rigamonti *et al.*, (2000), Legleiter *et al.* (2010)
				Exon 1 (20Q, 35Q, 46Q, 53Q)	Legleiter *et al.*, (2010)
StHdhQ111	Mouse	Striatal primordial (E14)	Disrupted cellular pathway	Conditional immortalisation from knock-in mice (111Q)	Trettel *et al.*, (2000)
293	Human	Embryonic kidney	Presence of aggregate and increased cell toxicity	Exon 1 (20Q, 51Q, 83Q)	Waelter *et al.*, (2001)
HD43	Rat	ST14A derivative	Transcription abnormality	N548 (26Q, 67Q, 105Q, 118Q)	Sipione *et al.*, (2002), Bari *et al.* (2013)

Table 1-1 continued

Cell line	Species origin	Cell type	Phenotype	CAG (Q) repeat size	Reference
PC12	Rat	Adrenal gland tumour	Aggregate formation	N17, Exon 1 or N584 with CAG/CAA 25-300Q.	Apostol *et al.*, (2003), Arrasate *et al.* (2004), Sahl *et al.* (2012)
M213	Rat	Striatal primordial (E14)	Reduced BDNF expression, formation of aggregates	Exon 1 (47Q, 72Q and 103Q	Canals *et al.* (2004)
Htt14A2.6	Rat	Adrenal gland tumour	Presence of aggregates	N17 (103Q)	Fox *et al.* (2004)
HeLa	Human	Cervical cancer	Presence of aggregates and increased apoptotic cell death	Exon 1 (25Q, 65Q and 103Q	Yamamoto *et al.* (2006)
A1	Human	Cerebral-neuroblastoma hybrid	Presence of aggregates	N3221 (18Q, and 100Q	Lim *et al.* (2008)
HN10	Mouse	Hippocampal (E18-21) and N18TG2 neuroblastoma l somatic cell hybrid	Presence of aggregates, transcription abnormality and increased apoptotic cell death	Exon 1 and N857 (25Q and 72Q	Weiss *et al.* (2009)
*Hdh*CAG	Mouse	Embryonic stem cells	Large CAG repeat sizes increase neurogenesis	Derived from Hdh knock-in mice (7Q, 77Q and 150Q)	Lorincz and Zawistowski (2009)
TrES1	Monkey	Pluripotent stem cells	Presence of aggregates	Exon 1 (84Q)	Laowtammathron *et al.* (2010)

Table 1-1: Summary of transgenic cellular models of HD.
FL: Full-length; N: N-terminal, Q: glutamine. Adapted and completed from Sipione and Cattaneo (2001)

As can be seen from Table 1-1, many transgenic HD cell lines have been developed. The vast majority of them features HD-specific phenotypes, notably with the formation of aggregates and increased apoptotic cell death. The same phenotypes have been found in primary cell models such as non-immortalised striatal neurons (Saudou *et al.*, 1998; Jovicic *et al.*, 2013; Sontag *et al.*, 2012), myoblasts (Ciammola *et al.*, 2006) or organotypic brain slice cultures (Smith and Bates, 2004). They have been used as a screening platform for therapeutic agents that can prevent or delay aggregate formation and or cell death. These cellular models present the important advantage of having isogenic controls. However, apart from the *Hdh*CAG and the TrES1 models, which were derived from embryonic stem cells (ESCs), all the other models are committed to one cell lineage, mainly neuronal. This restricts the *in vitro* study of HD. Furthermore; these models will always have non-innate extra copies of HTT, whose expression is driven by the exogenous promoter. On possibility to circumvent this is to develop human embryonic stem cell (hESC) models of HD. HD-hESCs have the great advantage of baring the endogenous mutation, can be differentiated into multiple cell lineages and can be kept in culture *ad infinitum*, circumventing the limitations associated with primary cell culture.

1.3 Pluripotent stem cells as disease models

1.3.1 Human Embryonic Stem Cells

1.3.1.1 Human Embryonic Stem Cell derivation

hESCs were first derived by Thomson (Thomson *et al.*, 1998) from the inner cell mass (ICM) of preimplantation blastocysts (day 5-7 post *in vitro* fertilization, IVF). hESCs are pluripotent. They can self-renew *ad infinitum*, provided that they are maintained in the right culture conditions. They also have the ability to differentiate into the three embryonic germ layers i.e. endoderm, mesoderm and ectoderm.

1.3.1.2 PGD and disease-baring hESCs

Preimplantation Genetic Diagnosis (PGD) is a prenatal genetic diagnostic procedure performed on a single blastomere biopsied from *in vitro fertilisation* (IVF) embryos at risk of inheritable single-gene disorders, provided that the mutated gene has been identified, prior to the embryo's implantation in the at risk patient. PGD has been rendered possible by the polymerase chain reaction (PCR), a technique that allows the amplification of specific DNA sequences (Mullis *et al.*, 1986), and has been successfully used as a diagnostic tool on human IVF embryos since the early 1990s (Handyside *et al.*, 1990). As a result of the discovery of the *HTT* gene by the Huntington Disease Collaborative Research Group in 1993 (The Huntington Disease Collaborative Research Group, 1993), it is possible to offer PGD services to patients at risk of transmitting HD (Schulman *et al.*, 1996). Non-mutation carrying embryos can then be implanted

while mutated ones will be discarded or, if the couple consents, can be given to research such as the derivation of HD-hESCs. Due to its autosomal dominant nature, HD-hESC lines are amongst the most numerous (20 out of 187; 10.7%) disease-bearing hESC lines to have been derived between 2005 and 2012. A summary of the 187 diseased-bearing hESC lines is presented in Table 1-2.

DISEASE	Number of lines
Adrenoleukodystrophy	1
Albinism Ocular, Type1	2
Alpha-Thalassaemia	2
Alport Syndrome	2
Beta thalassemia	6
Beta thalassemia carrier	3
Breast cancer	2
Breast cancer and endocrine neoplasia	1
Charcot-Marie Tooth Disease, Type 1A	3
Charcot-Marie Tooth Disease, Type 1B	1
Cystic fibrosis	22
Cystic fibrosis carrier	1
Epidermolysis Bullosa	1
Fabry Syndrome	1
Fanconi Anemia – A carrier	1
Fragile Site Mental Retardation 1, carrier	1
Fragile X Syndrome	6
Fragile X Syndrome, carrier	5
Gaucher Disease	1
Hemoglobin Alpha Locus	1
Hemoglobin Beta Locus mutation	3
Hemophilia A	1

Table 1-2. continued

DISEASE	Number of lines
Huntington's Disease	20
Huntington's Disease & Marfan Syndrome	1
Hypochondroplasia	1
Incontinentia Pigmenti	1
Infantile Neuroaxonal Dystrophy	1
Juvenile Retinoschisis	1
Marfan Syndrome	3
Merosin-Deficient Congenital Muscular Dystrophy, Type 1A	1
Multiple Endocrine Neoplasia, Type 1	1
Multiple Endocrine Neoplasia, Type 2	3
Muscular Dystrophy, Becker	1
Muscular Dystrophy, Becker, carrier	1
Muscular Dystrophy, Duchenne	5
Muscular Dystrophy, Duchenne, carrier	1
Muscular Dystrophy, Emery-Dreifuss	1
Muscular Dystrophy, Emery-Dreifuss, carrier	3
Muscular Dystrophy, Facioscapulohumeral	9
Muscular Dystrophy, Facioscapulohumeral and Turner syndrome	1
Muscular Dystrophy, Facioscapulohumeral, putative	2
Myotonic Dystrophy	6
Myotonic Dystrophy, type 1	4
Myotonic Dystrophy, type 2	1

Table 1-2. continued

DISEASE	Number of lines
Nemaline Myopathy 2	2
NEMO Deficiency	2
Neurofibromatosis, Type I	9
Osteogenesis Imperfecta, Type 1	1
Patau Syndrome	1
Pelizaeus-Merzbacher Disease	1
Popliteal Pterygium Syndrome	1
Saethre-Chotzen Syndrome	1
Sandhoff Disease	1
Sickle Cell Anemia	2
Spinal Muscular Atrophy, Type I	3
Spinocerebellar Ataxia, Type 2	1
Spinocerebellar Ataxia, Type 7	1
Torsion Dystonia	1
Torsion Dystonia 1	4
Translocation, 7:12	1
Translocation, 7:17	1
Translocation, 11:22	1
Treacher Collins-Francescetti Syndrome	2
Tuberous Sclerosis, Type 1	3
Turner Syndrome, mosaic cell line	1
Vitelliform Macular Dystrophy	2

Table 1-2. continued

DISEASE	Number of lines
Von Hippel-Lindau Disease	5
Wilms' Tumour	1
Wiskott-Aldrich Syndrome, Cystic Fibrosis carrier	1
X-linked Myotubular Myopathy	2
Zellweger Syndrome	1

Table 1-2: Specific mutation-carrying hESC lines reported by May 17, 2012. (Loser *et al.*, 2010;Strulovici *et al.*, 2007); University of Massachusetts Medical School, International Stem Cell Registry http://www.umassmed.edu/iscr/GeneticDisorders.aspx; http://www.stemride.com/ accessed on May 17, 2012, including those derived at Assisted Conception Unit at Guy's Hospital as of May 17, 2012, sorted by disease type**.** To be published in Stephenson *et al.* (2014).

1.3.1.3 hESCs culture conditions

The first hESCs were derived and maintained for long-term culture on a feeder layer of mouse embryonic fibroblasts (MEF), combined with a culture medium containing foetal bovine serum (FBS) (Thomson *et al.*, 1998). Many laboratories continued to use these culture conditions for the derivation of new lines and their long-term maintenance. However, despite the efficiency of feeder-based culture, it is not optimal as it is not a fully defined condition and it requires manual hESC passaging, which is very labour intensive, time consuming and limits the scalability of the hESCs cultures. This can prevent downstream applications such as hESC differentiation. Indeed, some differentiation protocols can require large amounts of hESCs as a starting point (Laflamme *et al.*, 2007). Furthermore, experiments are limited as there is a risk that obtained data could be a hindered or altered due to presence of feeders. For these reasons, feeder-free culture systems that support the long-term, undifferentiated and pluripotent growth of hESCs have been developed.

One of the most commonly used feeder-free matrix is Matrigel (Xu *et al.*, 2001). Matrigel is a gelatinous substance secreted by Engelbreth-Holm-Swarm (EHS) mouse sarcoma cells, composed of a complex mixture of laminin, collagen IV and heparan sulfate proteoglycan (Xu *et al.*, 2001;Kleinman *et al.*, 1982). It supports the long-term (≈ 130 population doublings) feeder-free culture of undifferentiated, karyotypically normal hESCs. Moreover, it allows the hESCs to maintain their capacity to differentiate into the three germ layers (Xu *et al.*, 2001). Along with the development of feeder-free matrices, fully defined media have been developed. One of the most reliable media to be used in conjunction with Matrigel is mTeSR1 (Ludwig and J, 2007; Akopian *et al.*, 2010). mTeSR1 is a fully defined and serum-free culture medium. It mainly maintains

hESCs pluripotency by having high concentrations of basic Fibroblast Growth Factor (bFGF) and transforming growth factor-β (TGF-β).

Feeder-free hESC culture present many advantages such as the absence of feeder-cells contamination and the facility of hESC culture upscaling. Furthermore, it gives the possibility to have a fully defined, xeno-free culture system, which is an advantage to generate hESCs for therapeutic uses (Stephenson *et al,* 2012). However, it cannot be dismissed that feeder-free culture maintenance may promote karyotype abnormalities and can prevent downstream cell differentiation.
In the work presented in this thesis, it could be observed that, in our hands, the pluripotency maintenance medium of the hESCs had a direct influence on cardiac differentiation outcome and efficiency. This will be further discussed in Chapter 5.

1.3.1.4 Limitations of hESCs

Disease modelling with hESCs is limited by embryo availability and whether or not the disease is due to a unique genetic mutation that can be screened by PGD. Furthermore, the destruction of the embryo associated with hESC line derivation poses some ethical concerns and has limited hESC research in countries such as the USA or France. This gap was breached in 2006 by the generation of a new type of pluripotent stem cells (PSCs) (Takahashi and Yamanaka, 2006).

1.3.2 Human Induced Pluripotent Stem Cells

Human induced Pluripotent Stem Cells (iPSCs) are pluripotent stem cells derived from the reprogramming of adult somatic cells. This can be achieved by the forced expression of pluripotency genes now known as the "Yamanaka factors", *OCT3/4, SOX2*, *KLF4* and *c-MYC* (Takahashi *et al.*, 2007; Takahashi and Yamanaka, 2006). Less ethical issues are associated with iPSC work than with hESCs generation, as it does not require the destruction of an embryo. Once reprogrammed, iPSCs have the same morphology, pluripotency and differentiation potential as hESCs. However, iPSCs generation is not an easy task and efficiencies were as low as 0.01% when the technique was first developed (Takahashi *et al.*, 2007; Takahashi and Yamanaka, 2006). As for hESCs, disease-specific iPSC can be generated. However, iPSCs are not limited to single gene disorders and can be derived from complex diseases such as Alzheimer's disease (Yagi *et al.*, 2011; Israel *et al.*, 2012). Like hESCs, they can then be differentiated into specific tissues affected by the disease in order to gain further insight into the molecular mechanisms of the disease. Disease-baring PSCs can allow the identification of *in vitro* phenotypic assay that can help identify therapeutic targets.

Since iPSCs were first derived, different reprogramming approaches have been developed in order to improve efficiency. Variability between protocols includes i) the source of somatic cells to be reprogrammed, ii) the vector used for forced ectopic expression of "pluripotency-genes"

and iii) the combination of genes used for reprogramming. A summary of the different methods used for reprogramming somatic cells into iPSCs is presented in Table 1-3.

Vector	Vector type	Cell type	Reprogramming factors	Efficiency (%)	Advantage	Disadvantage	Reference
Retroviral	Integrating	Fibroblasts, neural stem cells, stomach cells, liver cells, keratinocytes, amniotic cells, blood cells and	OSKM, OSK, OSK + VPA or OS + VPA	≈0.001-1	Reasonably efficient	Genomic integration, incomplete proviral silencing and slow kinetics	Takahashi *et al.* (2007), Takahashi and Yamanaka (2006), Lowry *et al.* (2008), Huangfu *et al.* (2008)
Lentiviral	Integrating	Fibroblasts and keratinocytes	OSKM or mir302/367 cluster + VPA	≈0.1-1.1	Reasonably efficient and transduces dividing and non-dividing cells	Genomic integration and incomplete proviral silencing	Yu, J. *et al.* (2007) Stadtfeld *et al.*, (2008b), Sommer *et al.* (2009), Anokye-Danso *et al.* (2011)
Inducible lentiviral	Integrating	Fibroblasts, β cells, keratinocytes, blood cells and melanocytes	OSKM or OSKMN	≈0.1-2	Reasonably efficient and allows controlled expression of factors	Genomic integration and requirement for transactivator expression	Stadtfeld *et al.* (2008a), Maherali *et al.* (2008)
Transposon	Excisable	Fibroblasts	OSKM	≈0.1	Reasonably efficient and no genomic integration	Labour-intensive screening of excised lines	Woltjen *et al.* (2009)

Table 1-3 continued

Vector	Vector type	Cell type	Reprogramming factors	Efficiency (%)	Advantage	Disadvantage	Reference
loxP-flanked lentiviral8	Excisable	Fibroblasts	OSK	≈0.1-1	Reasonably efficient and no genomic integration	Labour-intensive screening of excised lines, and loxP sites retained in the genome	Somers *et al.* (2010)
Adenoviral	Non-integrating	Fibroblasts and liver cells	OSKM	≈0.001	No genomic integration	Low efficiency	Zhou, W. and Freed, (2009), Stadtfeld *et al.* (2008c)
Plasmid	Non-integrating	Fibroblasts	OSKL	≈0.001	Only occasional genomic integration	Low efficiency and occasional vector genomic integration	Okita *et al.* (2008), Si-Tayeb *et al.* (2010)
Sendai virus	DNA-free	Fibroblasts	OSKM	≈1	No genomic integration	Sequence-sensitive RNA replicase, and difficulty in purging cells of replicating virus	Fusaki *et al.* (2009)

Table 1-3 continued

Vector	Vector type	Cell type	Reprogramming factors	Efficiency (%)	Advantage	Disadvantage	Reference
Protein	DNA-free	Fibroblasts	OS	≈0.001	No genomic integration, direct delivery of transcription factors and no DNA-related complications	Low efficiency, short half-life, and requirement for large quantities of pure proteins and multiple applications of protein	Kim, D. *et al.*, (2009), Zhou, H. *et al.* (2009)
Modified mRNA	DNA-free	Fibroblasts	OSKM or OSKML+ VPA	≈1-4.4	No genomic integration, bypasses innate antiviral response, faster reprogramming kinetics, controllable and high efficiency	Requirement for multiple rounds of transfection	Warren *et al.* (2010)
MicroRNA	DNA-free	Adipose stromal cells and dermal fibroblasts	miR-200c, miR-302s or miR-369s	≈0.1	Efficient, faster reprogramming kinetics than commonly used lentiviral or retroviral vectors, no exogenous transcription factors and no risk of	Lower efficiency than other commonly used methods	Miyoshi *et al.* (2011)

Table 1-3: Summary of the methods for reprogramming somatic cells to iPSCs.
Table taken from Robinton and Daley, (2012). OSKM and similar factor names represent combinations of reprogramming factors: O, OCT4; S, SOX2; K, KLF4; M, c-MYC and VPA, valproic acid.

It can be seen from Table 1-3 that since the development of iPSCs in 2006 (Takahashi and Yamanaka, 2006), a wide range of somatic cell types can be reprogrammed, using different delivery vectors and reprogramming gene combinations. The somatic cell type to be reprogrammed can be chosen based on its availability. For instance fibroblasts are a commonly used somatic cell type as they can efficiently be derived from a skin biopsy and are easy and robust to culture. Keratinocytes, on the other hand, can be chosen for their greater reprogramming efficiency. Compared to fibroblasts, reprogramming keratinocytes can be up to 100-folds more efficient and twofold faster (Aasen *et al.*, 2008). It is worth noting however that it has been established that despite reprogramming, iPSCs retain an "epigenetic memory" from their somatic source (Kim, K. *et al.*, 2011), which influences their downstream differentiation potential. In this way, cord-blood-derived iPSCs will more readily differentiate into hematopoietic colonies than iPSCs derived from keratinocytes (Kim, K. *et al.*, 2011).

1.4 Pluripotent stem cells disease-modelling.

PSC disease modelling requires three major steps: i) PSC generation, ii) PSC differentiation into a relevant cell type, iii) disease-specific phenotype identification (summarised in Figure 1-3).

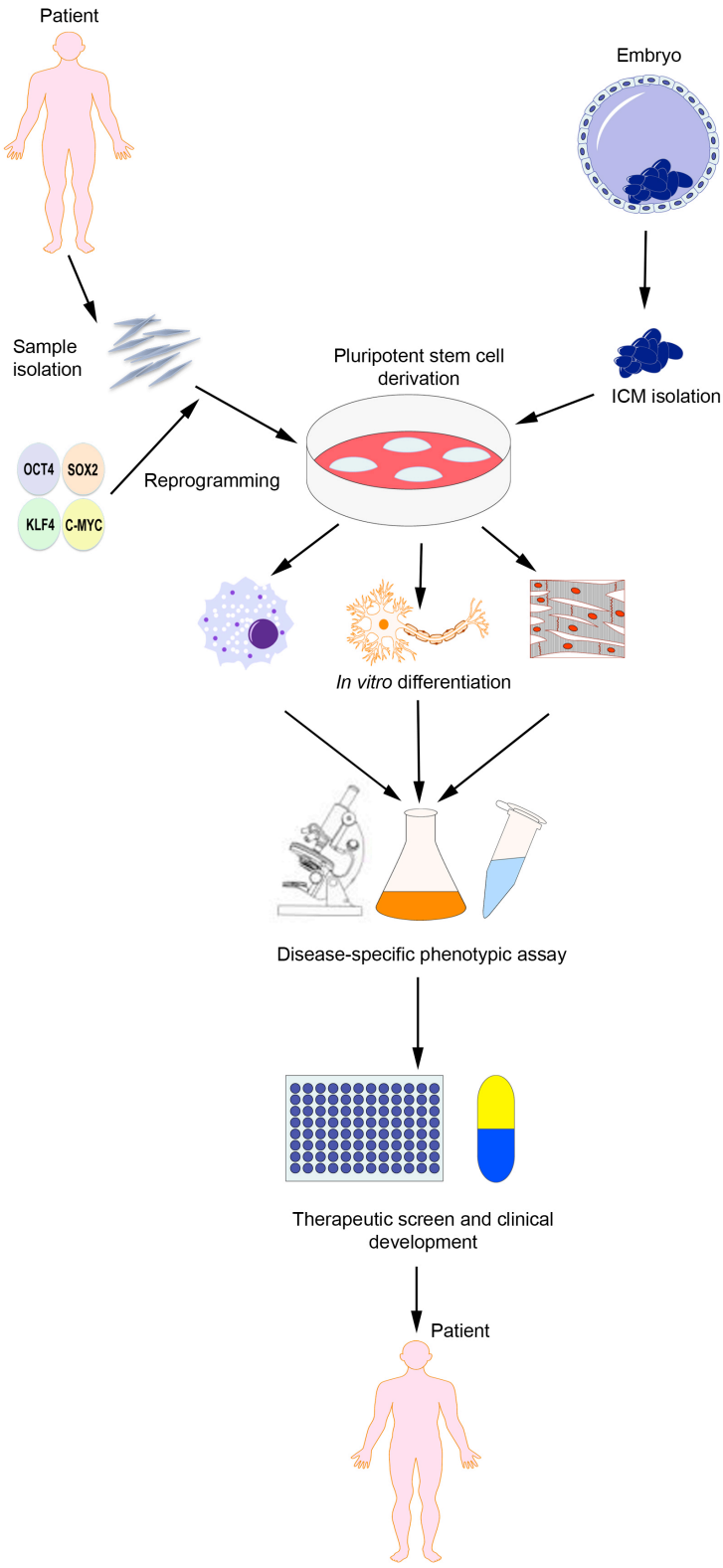

Figure 1-3: Disease modelling, therapeutic screen and clinical development using pluripotent stem cells (PSCs).
PSC can be derived from i) patient-derived somatic cells reprogrammed using the "Yamanaka factors" or ii) the inner cell mass (ICM) isolated from an embryo. Upon derivation, PSCs are characterised and expanded. They can then be differentiated into mature cells to study disease-specific phenotypes and develop assays. These assays can be used for high-throughput therapeutic screening and clinical development to reverse the disease phenotype and benefit the patient. Figure realised using the biomedical PPT toolkit by motifolio.

i) Disease PSC generation

Together, hESCs and iPSCs are great complimentary tools for *in vitro* disease modelling. hESCs present the advantage of higher line derivation success. With a well-established protocol, hESC line derivation can reach efficiencies as high as 50%-60% (Stephenson *et al.*, 2012). However, hESC-disease modelling is limited to single single-gene disorders (Verlinsky *et al.*, 2005). Despite their lower rate of derivation (0.01% with retroviruses and the four Yamanaka factors, (Takahashi *et al.*, 2007; Takahashi and Yamanaka, 2006), iPSCs confer the advantage of enabling the derivation of PSCs baring multifactorial diseases, without the limited life-span usually associated with primary cell cultures. iPSC generation will be further discussed in chapter 4.

ii) Disease PSC differentiation

PSCs have the ability to differentiated into the endoderm, mesoderm and ectoderm germ layers. Part of their pluripotency characterisation consists of spontaneously differentiating them *in vivo* to generate teratomas, which comprise derivatives of the three germ layers (Thomson *et al.*, 1998). For this project, we were interested in differentiating the HD-PSCs into cardiomyocytes. PSC differentiation into cardiomyocytes needs to replicate 4 major developmental steps: i) the commitment of the PSCs to the mesoendoderm germ layer, ii) cardiomesoderm commitment, iii) cardiac progenitor formation and iv) cardiomyocyte maturation. Several strategies exist in order to achieve this. One popular approach to generate PSC-derived cardiomyocytes relies on the characteristic that PSCs can be spontaneously differentiated *in vitro* by forming aggregates in suspension called embryoid bodies (EBs) (Itskovitz-Eldor *et al.*, 2000) in the absence of bFGF. The EBs become cystic and form derivatives of the three germ layers. Although EB-based differentiation is not specific, it has been demonstrated that when plated on gelatin after 7-10 days in suspension, EBs can reproducibly (8.1%) give rise to cardiomyocytes (Kehat *et al.*, 2001). Another strategy to differentiate PSCs into a specific lineage consists of PSC co-culture with another cell type. For instance, PSCs can be differentiated into cardiomyocytes by co-culture with the END-2 visceral endoderm-like cells (Mummery *et al.*, 2003). Similarly, PSCs can be differentiated into the hematopoietic lineage by co-culture with the S17 mouse bone marrow stromal cell line or the C166 mouse yolk-sac endothelial cell line (Kaufman *et al.*, 2001). A third method, to generate PSC-derived cardiomyocytes consists of directed differentiation by temporal cytokine treatment. In this method, which was chosen for this study, Activin A treatment is used to trigger mesoendoerm formation and exposure to Bone Morphogenic Protein 4 (BMP4) then further commit the cells to cardiac differentiation (Laflamme *et al.*, 2007). Table 1-4 summarises key PSC cardiac differentiation protocol. Cardiac differentiation of HD-hESCs will also be further discussed in Chapter 5.

Cardiac differentiation method	Protocol outline	Reference
Embryoid Body (EB) based differentiation		
Spontaneous EB differentiation with FBS containing medium	Formation of embryoid bodies (EBs), suspension aggregates, in the absence of bFGF. The EBs become cystic and form derivatives of the three germ layers. After 7-10 days of culture in suspension, EBs are plated on gelatin and give rise to cardiomyocytes (8.1%).	Kehat *et al.*, 2001
Forced aggregation EB based differentiation in chemically defined medium.	Use of force aggregation for EB formation and exposure to PVA, Insulin, 1-thioglycerol, BMP4, bFGF, and Y-27632. Very high and rapid efficiency (≈95% cardiomyocytes in 9 days) reproducible across multiple cell lines.	Burridge *et al.*, 2011
Directed EB based differentiation	Successive exposure to combinations of BMP4, bFGF, Activin A, VEGF and DKK1. Up to 40% differentiation efficiency. When used on a cell monolayer, this protocol gives rise to up to 50% cardiomyocyte differentiation	Yang *et al.*, 2008
Controlled size EBs	Generation of EBs containing 1,000 cells by forced aggregation in micro-wells. The cells were then exposed to the Yang *et al.* differentiation protocol. Yields up to 75% cardiomyocytes	Bauwens *et al.*, 2011

Table 1-4 continued

Cardiac differentiation method	Protocol outline	Reference
END-2 co-culture differentiation		
END-2 co-culture	PSC differentiation into cardiomyocytes by co-culture with the END-2 visceral endoderm-like cell line. Up to 35% of the culture wells contained beating cardiomyocytes.	Mummery *et al.*, 2003
END-2 conditioned medium	PSC differentiation by exposure to END-2 cell conditioned medium and SB203580, a p38 MAPK inhibitor. Up to 20% efficiency.	Graichen *et al.*, 2008
Monolayer based differentiation		
Cell monolayer	High density PSC monolayer culture with high concentrations of Activin A and BMP4. Up to 30% cardiomyocytes	Laflamme *et al.*, 2007
The matrix sandwich differentiation		
Cell monolayer overlayed by Matrigel	High density PSC monolayer culture overlayed by a fine layer of Matrigel and exposure to high concentrations of Activin A followed by BMP4 and bFGF. Gives rise to high purity of cardiomyocytes (98%)	Zhang *et al*., 2012

Table 1-4: Key pluripotent stem cell cardiac differentiation methods

iii) Disease-specific phenotype identification

Disease-baring PSCs are complementary tools to animal models. As discussed previously, HD *in vivo* models have successfully recapitulated HD-specific phenotypes. However, this is also tampered by the fact that the mutated protein is not expressed in an endogenous context, and not in a range usually seen in patients. The advantage of HD-PSCs and other disease-baring PSC lies in their expression of the endogenous mutation in the right context, and in their pluripotency and ability to differentiation into an array of somatic cell types. Despite HD being a late onset disorder HD-PSCs have been differentiated into neural cells (Camnasio *et al.*, 2012; Niclis *et al.*, 2009; An *et al.*, 2012; Zhang, N. *et al.*, 2010;The HD iPSC Consortium, 2012), which in some cases replicated HD-specific phenotypes *in vitro* (Table 1-5). Yet, HD *in vitro* study is not limited to PSC-derived neural cells and we have chosen to differentiated HD-hESCs into cardiomyocytes in order to study the HD cardiac phenotype. This holds great promise for the development of disease-specific phenotypic assays and the screening of HD therapeutic compounds. In this way, Timothy syndrome (TS)-iPSCs were differentiated in to both cardiomyocytes (Yazawa *et al.*, 2011) and neural cells (Pasca *et al.*, 2011). TS-iPSCs recplicated *in vitro* TS-specific phenotypes (Table 1-5) in both somatic cell types, giving a better insight into the disease mechanism. More importantly, they are helping to validate potential therapeutic targets. In this example, Roscovitine (Ros), a cycline-dependent kinase inhibitor, or Ros related drugs could help rescue the phenotype in both TS-cardiomyocytes and TS-neuronal cells (Yazawa *et al.*, 2011; Pasca *et al.*, 2011). Therapeutic compound identification was also facilitated using Gaucher's disease (GD)-iPSCs (Tiscornia *et al.*, 2013). GD-iPSCs were differentiated into dopaminergic neurons and macrophages. Both cell type presented with acid-β-glucosidase expression deficiency, a common phenotype of the disease. Using the cells as a screening platform, they identified two nojirimycin analogues that could rescue the GD-specific phenotype.

One limitation, but potentially an advantage, that could be associated with PSC disease modelling is the modelling of non-cell autonomous conditions. HD is primarily a neurological disorder. However, cardiac failure is a common cause of death amongst HD patients (Sorensen and Fenger, 1992; Lanska *et al.*, 1988; Chiu and Alexander, 1982). As described previously, PSC-derived cardiomyocytes are able to replicate cardiac disease-specific phenotypes *in vitro.* Since HTT is ubiquitously expressed, by studying PSC-derived HD-cardiomyocytes *in vitro*, this will give us further insight on whether cardiac defects in HD are caused by a cell autonomous or a non-cell autonomous process.

Disease	Mutation	*In vitro* phenotype	Cell type	Reference
Huntington's Disease	Extended CAG repeats in exon 1 of *HTT*	Increased lysosomal activity	Undifferentiated iPSCs	Camnasio *et al.* (2012)
		Increased caspase activity	iPSC-derived neural cells	Zhang, N. *et al.* (2010)
		Differential gene expression	Undifferentiated iPSCs	An *et al.* (2012)
		Increased TUNEL and caspase activity	iPSC-derived neural stem cells	
		Differential gene expression	iPSC-derived neural stem cells	The HD iPSC Consortium (2012)
		Change in the actin cytoskeleton, decreased cell adhesion, compromised energy metabolism, aberrant electrophysiology and increased cell death.	iPSC-derived neural cells	
Rett's syndrome	Mutation in *MECP2*	Defect in neuronal maturation	iPSC-derived neural cells	Kim, K.Y. *et al.* (2011)
Alzheimer's disease	*APP* duplication	Increased levels of amyloid-β (1–40), phospho-tau (Thr 231) and active glycogen synthase kinase-3β (aGSK-3β).	iPSC-derived neural cells	Israel *et al.* (2012)

Table 1-5. continued.

Disease	Mutation	*In vitro* phenotype	Cell type	Reference
Dyskeratosis Congenita	Mutations in TERT (P704S and R979W), TCAB1 (H376Y/G435R) and DKC1 (DKC1_L54V and ΔL37)	Reduction of TCAB1 accumulation in Cajal bodies and reduction of telomerase activity	Undifferentiated iPSCs	Batista *et al.*, (2011)
Timothy syndrome	Mutation in *CACNA1C*	Electrical defects (irregular cardiomyocyte contractions, longer action potential)	iPSC-derived cardiomyocytes	Yazawa *et al.*, (2011)
		Increased norepinephrine and dopamine production, and defective calcium signaling.	iPSC-derived neural cells	Pasca *et al.*, (2011)

Table 1-5: Examples of iPSC-modelled disease with an in vitro phenotype.

1.5 Aims of the project

The aim of the work presented in this thesis was to develop, characterise and differentiate PSC models of HD. To achieve this, this work is divided in three parts:

i) Characterisation of five HD-hESC lines derived at the Assisted Conception Unit (ACU), King's College London, and their adaptation to feeder-free culture conditions required for downstream differentiations.

ii) The generation of iPSC lines. The final aim was to generate HD-iPSCs from HD-HF-keratinocytes. To achieve this, HF-keratinocyte derivation protocols and iPSC generation using synthetic modified mRNA were optimised.

iii) hESC differentiation into cardiomyocytes in order to study the effect of the HD mutation in this somatic cell type and determine whether or not the cardiac failure suffered by HD patients is a cell autonomous or non-cell autonomous process.

Chapter 2

Experimental Procedures

Chapter 2 EXPERIMENTAL PROCEDURES

2.1 Human Embryonic Stem Cells

The hESC used in this study are summarised in Table 2-1.

WT-hESC	HD-hESC
KCL020	KCL012_HD 3
KCL031	KCL013_HD 4
KCL034	KCL027_HD 5
KCL040	KCL028_HD 6
	KCL036_HD 7

Table 2-1: Summary of the Wild Type (WT) and HD-hESCs used in this study

Unless specified differently, all cells were cultured at 37°C, 5% O_2 and 6% CO_2 in a HERAcell 240 incubator (Heraeus) or a benchtop MINC incubators (Cook). All tissue culture procedures were conducted aseptically in a class II biological safety cabinet.

2.1.1 Preparation of Human Foreskin Fibroblast (HFF)-feeders

The hESC lines were derived and cultured on Human Foreskin Fibroblast (HFF)-feeders (Forticell). Frozen stocks had previously been inactivated by γ-irradiation at 5,000 rad (50 Gy) with a caesium-source irradiator (Nordion International, GammaCell 1000 Elite). Feeder-cells were plated in CELLstart (CS) (Gibco, Invitrogen)-coated 4-well plates (Nunc) in M199 (72% Dulbecco's Modified Eagle Medium (DMEM, Invitrogen) supplemented with 18% medium 199 (Invitrogen) and 10% FBS, (Hyclone). CS coating was performed 2 h before HFF plating by diluting CS 1:75 in Dulbecco's Phosphate Buffered Saline with calcium and magnesium ($DPBS^{Ca2+/Mg2+}$, Lonza). A volume of 250 µL of diluted CS was added to each well of a 4-well dish and the dish placed at 37°C for 2 h. After the incubation, CS was removed and 2.25 x 10^4 cells/cm^2 inactivated HFF in 500µL of M199 were plated in each well. The HFF-feeders were

then returned to the incubator, the medium was changed every two to three days and the cells used within two weeks or discarded.

2.1.2 Human ESCs derivation

Human ESC lines used in this study were derived at the Assisted Conception Unit, Guy's Hospital (London, UK). hESCs were derived under the Human Fertilisation and Embryology Authority (HFEA; research license number R0133) and local ethical approval (UK National Health Service Research Ethics Committee Reference 06/Q0702/90) from healthy cryopreserved In Vitro Fertilisation (IVF) embryos and fresh embryos diagnosed with HD following Preimplantation Genetic Diagnosis (PGD). Informed consent was obtained from all patients and the experiments were compliant with the WMA Declaration of Helsinki and the NIH Belmont Report principles. No financial inducements were offered for donation. A sample of each line that is derived is deposited in the UK Stem Cell Bank for distribution to academic and research centres internationally.

2.1.3 hESCs maintenance on HFF-feeders

All hESC lines were initially grown and maintained as colonies on an HFF-feeder layer prepared as described in 2.1.1. The KOSR-XF complete medium used in this study consisted of KnockOut Dulbecco's Modified Eagle Medium (KO-DMEM) supplemented with 15% KnockOut Serum Replacement Xeno-Free (KOSR-XF), 2 mM GlutaMax-1, 2% KOSR Growth Factor Cocktail and 0.1 mM β-Mercaptoethanol (β-ME) (all from Gibco, Invitrogen). The medium was filtered through a 0.22 μm Polyethersulfone (PES) membrane filter system (Corning), stored at 4°C and used within 10 days. Cells were fed every two to three days with medium supplemented with 24 ng/mL of bFGF (R&D Systems) and pre-equilibrated at 37°C for a minimum of 30 min prior to use.

hESCs were manually passaged once or twice per week. M199 medium was removed from the HFF-feeders, the wells rinsed three times with Phosphate Buffer Saline (PBS, Gibco) and replaced with 500 μL of KOSR-XF complete medium supplemented with 24 ng/mL of bFGF. The HFF-feeders were then returned to the incubator for 30 min prior to use. Colonies were first dissected under a Nikon SMZ1000 Stereomicroscope, and pieces were detached using a hooked disposable Pasteur Pipette (Volac Cole-Parmer). The seeding of 6-10 pieces onto a pre-conditioned fresh cell culture dish marked a single passage. Undifferentiated hESCs form tightly packed colonies with well-defined edges and are clear from differentiated cells. Prior to passaging, colony regions that presented sign of differentiation were discarded (illustrated in Figure 2-1).

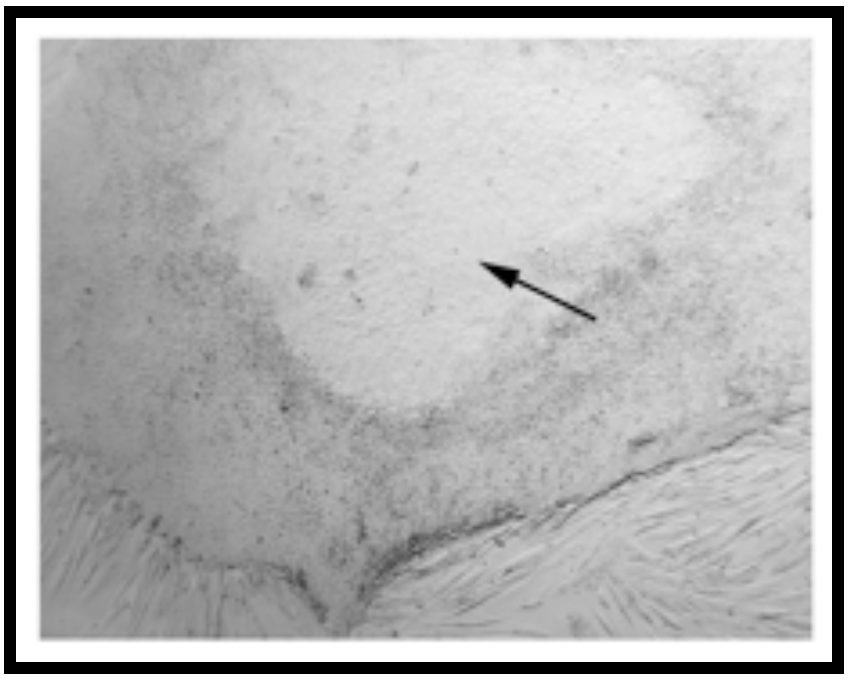

Figure 2-1: hESC colony presenting signs of differentiation.

KCL012_HD3 p8. Black arrow indicates differentiated area that needs removal prior to passaging. Image was taken at 40x magnification.

2.1.4 hESCs maintained on HFF-feeders cryopreservation and thawing

2.1.4.1 Vitrification

hESCs cultured on HFF-feeders were cryopreserved by vitrification. All cryopreservation solutions (Table 2-2) were prepared fresh, stored at 4°C and used within one week.

ES-HEPES solution	Volume (mL)	Manufacturer
DMEM/F-12	15.6	Invitrogen
KOSR-XF	4.0	Invitrogen
1M HEPES	0.4	Invitrogen
1M Sucrose	**Volume (mL)**	**Manufacturer**
Sucrose	3.42g	Sigma
ES-HEPES solution	8.0	Made as above
KOSR-XF	2.0	Invitrogen
10% Vitrification	**Volume (mL)**	**Manufacturer**
ES-HEPES solution	2.0	Made as above
Ethylene Glycol	0.25	Sigma
DMSO	0.25	VWR
20% Vitrification	**Volume (mL)**	**Manufacturer**
ES-HEPES solution	0.75	Made as above
1M Sucrose	0.75	Made as above
Ethylene Glycol	0.5	Sigma
DMSO	0.5	VWR

Table 2-2: hESCs vitrification media formulations.
DMEM/F-12: DMEM/Nutrient Mix F-12; KOSR-XF: Knock Out Serum Replacement Xeno-Free

Prior to starting vitrification, all the cryopreservation solutions were pre-warmed in the incubator for a minimum of 30 min. The hESC culture medium of the cells to vitrify was replaced by pre-warmed KO-DMEM. Colonies were scored and cut into pieces approximately twice the size as those generated for subculture. They were then placed in a well of ES-HEPES solution. Microdrops of 10% and 20% vitrification solutions were disposed in an inverted culture dish lid as illustrated in Figure 2-2.

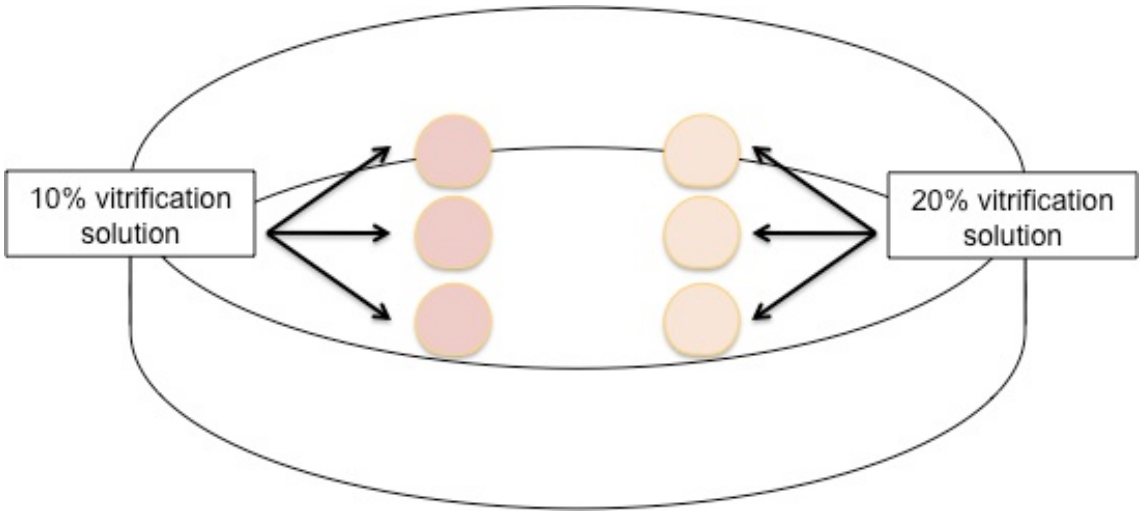

Figure 2-2: Schematic of an inverted lid with microdrops of 10% and 20% vitrification solution for the freezing of human embryonic stem cells cultured on feeders.

Six to ten colony pieces at a time were pipetted from the ES-HEPES solution and incubated for 1 min in the 10% vitrification solution microdrop before being transferred to a 20% vitrification solution microdrop for 25 s. Using capillary action, the colony pieces were aspirated into a labelled open pulled vitrification straw (MTR), quickly held horizontally with sterile forceps and plunged into liquid nitrogen (LN_2). Still in LN_2, the straw was then placed into a 5 mL labelled cryovial (Nunc). This process was repeated for the remaining colony pieces. Each cryovial held a maximum of 12 frozen straws.

2.1.4.2 Thawing

Prior to thawing the cells, the M199 medium in one HFF-feeder plate per cell line was removed, cells were washed three times with PBS, and 500 µL of KOSR-XF complete medium supplemented with 24 ng/mL bFGF was added per well. Additionally, one thaw plate per cell line was prepared by adding complete KOSR-XF medium (without bFGF) to two empty wells of a 4-well plate. The HFF-feeder and the thaw plates were left to pre-equilibrate for at least 30 min at 37°C prior to use.

A straw of the desired hESC line was removed from LN_2 and its tip immediately placed into the first well of the thaw dish. In case the medium and colony pieces would not expel immediately, the process was aided by inserting the tip of a 100-µL Gilson tip on the opposite side of the straw to lightly expel the content. The colony pieces were rapidly moved to the second well of the thaw dish to ensure complete removal of any cryopreservation reagents and thoroughly wash the cells, left to incubate for 5 min, and transferred to the pre-equilibrated feeder dish.

2.1.5 hESCs adaptation to feeder-free culture

In order to adapt the cells to feeder-free culture, two substrates, Growth Factor Reduced (GFR)-Matrigel (BD) and extracellular matrix (ECM) from decellularised feeder layer were tested, as well as two media, complete KOSR-XF and mTeSR1 (STEMCELL Technologies).

2.1.5.1 GFR-Matrigel preparation

GFR-Matrigel was thawed overnight on ice at 4°C, and checked for the presence of any gel formation. If there were no visible clumps, GFR-Matrigel stock was diluted to a final concentration of 0.34 mg/mL in DMEM/Nutrient Mix F-12 (DMEM/F-12, Invitrogen). Four-well plates or 6-well plate were coated with 250 µL/well or 1 mL/well of the solution respectively and placed in the incubator at 37°C for 2 h. GFR-Matrigel was then removed and replaced with the appropriate medium before use.

2.1.5.2 Decellularised feeder preparation

In order to prepare the decellularised feeder matrix, HFF-feeders were cultured and plated in 4-well plates as described in 2.1.1. Two protocols using different detergents, either sodium deoxycholate (DOC) or Triton X-100 (both from Sigma), were tested for the quality of cell monolayer extraction and ECM structure preservation. Both protocols were tried on one to three weeks old HFF-feeders monolayer.

2.1.5.2.1 DOC protocol

Cell monolayer extraction was performed as described by Klimanskaya *et al.* (2005). Briefly, cells were rinsed twice with PBS before being incubated at 4°C for 30 min with the cell extraction buffer (0.5% DOC in 10 mmol/L tris(hydroxymethyl)aminomethane-Hydrochloric acid (Tris-HCl), pH 8.0). The decellularised feeder matrices were then gently rinsed five times with PBS. The appropriate pre-equilibrated medium could then be added for immediate use or they could be stored at 4°C in PBS for up to one week.

2.1.5.2.2 Triton x-100 protocol

Cell lysis using Triton X-100 was adapted from the published protocols by Beacham *et al.* (2007) and Vlodavsky (2001). Briefly, cells were rinsed twice with PBS before being incubated at 37°C for 3-5 min with the cell extraction buffer (0.5% v/v Triton X-100 and 20 mM NH_4OH in PBS). The decellularised feeder matrices were then gently rinsed five times with PBS. The appropriate medium could then be added for immediate use or they could be stored at 4°C in PBS for up to one week.

2.1.5.2.3 Decellularised feeder matrix immunostaining

To confirm the ECM integrity, samples were immunostained for fibronectin. To do so, PBS was removed from the decellularised feeder matrices and they were fixed with 3.7% paraformaldehyde (PFA; Sigma) for 20 min at room temperature (RT) and then washed three times with $DPBS^{Ca2+/Mg2+}$. $DPBS^{Ca2+/Mg2+}$ was chosen over PBS as it helps to keep the cells fixed to the dish. Fixed cells were kept at 4°C in $DPBS^{Ca2+/Mg2+}$ for up five days if they were not processed immediately. The anti-human fibronectin antibody (Sigma, F3648), developed in rabbit, was diluted in $DPBS^{Ca2+/Mg2+}$ to a final concentration of 5 µg/mL. A final volume of 250µL/well was added to the cells overnight at 4°C. The solution was then removed and cells washed three times for 5 min with $DPBS^{Ca2+/Mg2+}$ before adding 15 µg/mL of Donkey anti-rabbit IgG, Rhodamine Red™- X-conjugated (Jackson ImmunoResearch, 711-295-152) diluted in $DPBS^{Ca2+/Mg2+}$ for 40 min at RT, shielded from light. Cells were then washed three times for 5 min in $DPBS^{Ca2+/Mg2+}$, mounted in Vectashield mounting medium containing 4',6-diamidino-2-phenylindole (DAPI, Vector Laboratories), and covered with a coverslip. Samples were assessed using Eclipse 50i upright epifluorescence microscope (Nikon). Images were captured with cooled CCD camera Infinity 3

2.1.6 hESCs adaptation to enzymatic passaging

hESCs were first adapted to feeder-free culture conditions in 4-well plates and were manually passaged as described in 2.1.3. hESCs cultures were then manually expanded to tissue culture treated 6-well plates (Corning). Once adapted to 6-well plate feeder-free culture, the cells were enzymatically passaged with 1 mg/mL dispase (STEMCELL Technologies). Briefly, differentiated cells were manually removed and discarded. The well was then rinsed with pre-warmed DMEM. Dispase (1 mL/well of a 6-well plate) was then applied and left to incubate at 37°C for 7 min or until the edges of the colonies began to curl up. Once the colonies edges were slightly curled, the dispase was removed and two DMEM washes were performed. 1 mL of mTeSR1 was then added to each well before the cells could be scraped off into little clumps. The clumps were then seeded at a 1:6 to 1:12 ratio in freshly GFR-Matrigel-coated dishes containing 2 mL of mTeSR1. Enzymatic passaging took place once or twice a week.

2.1.7 hESCs maintained in feeder-free conditions cryopreservation and thawing

Unlike hESCs cultured on feeders, hESCs cultured feeder-free were not cryopreserved by vitrification (refer to 2.1.4) but by slow freezing. Only high quality hESCs colonies (less than 20% of the cells being differentiated based on the assessment of morphology criteria described in 2.1.3) were cryopreserved when the confluency in the well reached approximately 70%. Any differentiated cells were manually removed prior to the procedure. The colonies were passaged as described in 2.1.6, generating cell clumps bigger than for usual subculture. Following, the second DMEM wash, the cell suspension was resuspended in 5 mL of DMEM, transferred to a 15-mL centrifugation tube and centrifuged for 5 min at 1,000 x g. The supernatant was

discarded and the cell pellet resuspended in RT-pre-warmed mFreSR (1 mL per well of a 6-well plate, STEMCELL Technologies) using a 5-mL pipette, taking care not to generate small clumps. The hESCs suspension was aliquoted 1 mL per labelled cryovial and stored overnight at -80°C into a Mr. Frosty isopropanol cryovessel (Nalgene). Mr. Frosty allows the cells to have a cooling rate of –1°C per minute. The following day, the cryovials were transferred into a dewar and stored in the LN_2 vapor phase.

To recover hESCs from LN_2, cryovials were quickly thawed in a 37°C heating block until only a small frozen chunk remained. The contents were transferred into a 15-mL centrifuge tube (Falcon) using a 5 mL pipette in order to prevent the generation of very small clumps. Pre-warmed mTeSR1 (5 mL) was added to the tube dropwise to avoid a sudden change in osmolality. The cells were centrifuged 5 min at 1,000 x g. The supernatant was discarded and the pellet resuspended in 2 mL of mTeSR1 containing 10 µM of Rho-associated kinase (ROCK) I inhibitor Y-27632 (Source Bioscience), still taking care not to disaggregate the clumps further. ROCK I inhibitor prevents apoptosis and enhance survival of dissociated hESCs (Watanabe *et al.*, 2007). The cells were then seeded in GFR-Matrigel pre-coated 6-well plates (refer to 2.1.5.1 for GFR-Matrigel preparation). Generally, hESCs cryopreserved from 1 well of a 6-well plate were thawed back into 1 well of a 6-well plate. The cells were placed back in the incubator.

2.1.8 hESCs pluripotency characterisation

2.1.8.1 *In vitro* spontaneous differentiation

hESCs were cultured for a minimum of three weeks in KOSR-XF medium supplemented with 5% FBS and without bFGF. Medium was changed every two to three days.

2.1.8.2 Immunofluorescence

The presence of pluripotency or germ layer markers was assessed by immunofluorescence. To do so, medium was removed from the cells prior to washing them once with $DPBS^{Ca2+/Mg2+}$. They were then fixed with 3.7% PFA for 20 min at RT and then washed three times with $DPBS^{Ca2+/Mg2+}$. Fixed cells were kept at 4°C in $DPBS^{Ca2+/Mg2+}$ for up five days if they were not processed immediately. Permeabilisation was effectuated with 0.5% Triton X-100/$DPBS^{Ca2+/Mg2+}$ for 5 min at RT when staining for pluripotency markers; or with cold 90% acetone (Alfa Aesar) for 10 min at 4°C when staining for germ layers markers. In both cases, cells were then washed three times with $DPBS^{Ca2+/Mg2+}$. The appropriate primary antibody (Table 2-3) was diluted in $DPBS^{Ca2+/Mg2+}$ and added to the cells overnight at 4°C. The solution was then removed and cells washed three times for 5 min with $DPBS^{Ca2+/Mg2+}$ before adding the appropriate secondary antibody (Table 2-4) diluted in $DPBS^{Ca2+/Mg2+}$ for 40 min at RT, shielded from light. Cells were then washed three times for 5 min in $DPBS^{Ca2+/Mg2+}$ mounted in Vectashield mounting medium containing DAPI, and covered with a coverslip. Samples were assessed using Eclipse 50i

upright epifluorescence microscope. Images were captured with cooled CCD camera Infinity 3 utilising Infinity Capture software and processed in Adobe Photoshop CS5.

Primary antibody	Final Dilution	Manufacturer
Antibodies for pluripotency staining		
Anti-TRA-1-60 mouse IgM	10 µg/mL	Chemicon Millipore (MAB4360)
Anti-TRA-1-81 mouse IgM	10 µg/mL	Chemicon Millipore (MAB4381)
Anti-human Nanog goat IgG	1 µg/mL	R&D Systems (AF1997)
Anti-human Oct3/4 rabbit IgG	2 µg/mL	Sata Cruz Biotechnology (sc-9081)
Antibodies for differentiation staining		
Anti-α-fetoprotein mouse IgG Clone C3	50 µg/mL	Sigma-Aldrich (A 8452)
Anti- α-smooth muscle actin mouse IgG Clone 1A4	20 µg/mL	Sigma-Aldrich (A 5228)
Anti-β-tubulin isotype III mouse IgG Clone SDL.3D10	20 µg/mL	Sigma-Aldrich (T 5076)

Table 2-3 Primary antibodies used for pluripotency and germ layer immunodetection of human embryonic stem cells

Secondary antibody	Final Dilution	Manufacturer
Donkey anti-mouse IgM, DyLight 488-conjugated	15 µg/mL	Jackson ImmunoResearch (715-485-140)
Donkey anti-goat IgG, FITC-conjugated	15 µg/mL	Jackson ImmunoResearch (705-095-147)
Donkey anti-goat IgG, Rhodamine Red-X-conjugated	15 µg/mL	Jackson ImmunoResearch (705-295-147)
Donkey anti-rabbit IgG, FITC-conjugated	15 µg/mL	Jackson ImmunoResearch (711-095-152)
Donkey anti-rabbit IgG, Rhodamine Red- X-conjugated	15 µg/mL	Jackson ImmunoResearch (711-295-152)

Table 2-4 Secondary antibodies used for pluripotency and germ layer immunodetection of human embryonic stem cells

2.1.8.3 Alkaline phosphatase activity detection

Endogenous Alkaline Phosphatase (AP) activity was detected in hESCs using ELF Phosphatase Detection Kit (ATCC) according to manufacturer's protocol. Briefly, cells were rinsed twice with PBS before being fixed with a 10% Formalin solution (4% formaldehyde w/v; Sigma). Cell membranes were permeabilized with 0.2% Tween 20 (Sigma) in $DPBS^{Ca2+/Mg2}$ for 10 min at RT. After several rinses in $DPBS^{Ca2+/Mg2}$ the provided ELF phosphate substrate was diluted 1:20 in the kit detection buffer before being added to each well for 5 min at RT. Next, the cells were washed once for 15 min in wash buffer ($DPBS^{Ca2+/Mg2}$ with 25 mM EDTA and 5 mM Levamisole, pH 8.0, both Sigma-Aldrich) and twice for 15 min with rhodamine phalloidin (Gibco Invitrogen) diluted 1:250 in the wash buffer at RT protected from light. Finally, cells were rinsed twice with wash buffer, mounted in a drop of the provided mounting medium, and covered with a coverslip. Samples were assessed using Eclipse 50i upright epifluorescence microscope. Images were captured with cooled CCD camera Infinity 3 utilising Infinity Capture software and processed in Adobe Photoshop CS5.

2.1.8.4 Teratoma assay

2.1.8.4.1 Cell preparation and mice injection

hESCs cultures were expanded feeder-free in 6-well plates as described in section 2.1.6. Approximately 6 x 10^6 cells from (one confluent 6-well plate) were used per one injection into female, beige, non-obese diabetic severe immunodeficiency (NOD-SCID) mice (Charles River). The day prior to hESCs harvesting, an aliquot of GFR-Matrigel was thawed overnight at 4°C. To harvest the cells, each well of a 6-well plate was washed with 1 mL of PBS before adding 1 mL of accutase (STEMCELL Technologies) per well. The plate was incubated at 37°C, 5% O_2, for approximately 3 min. Human ESCs were observed under the phase contrast microscope (Nikon) to confirm the formation of a single cell suspension. If needed, the cells were returned to the incubator for an extra 2 min. If not, the single cell suspension was added to a 15-mL centrifuge tube containing 7 mL of DMEM/F-12. Using 1 mL of DMEM/F-12 per well, each well was further rinsed to collect any remaining cells. The cells were then centrifuged at 1,000 x g for 5 min, after which the supernatant was discarded. The cell pellet was resuspended in a final volume of 240 µL 1:3 GFR-Matrigel:DMEM/F-12. The cell suspension was kept on ice until the time of injection in order to prevent the GFR-Matrigel from polymerizing. Just prior to injection, it was loaded in a 1-mL syringe (Terumo) fitted with a 30-gauge needle (BD Microlance). Air was expelled from the syringe and cells were injected subcutaneously in the right or left flank of the NOD-SCID mouse. A total of two to three NOD-SCID mice per hESCs line were injected. They were observed on a weekly basis and palpated for tumour formation detection. Typically the tumours would be observed 6-12 weeks post injection. When sufficient tumour growth was achieved (at least 1cm^3) and before their discomfort had become too acute, the mice were sacrificed using a Schedule 2 method. Mice were cared for and sacrificed in accordance with the Home Office license guidelines.

2.1.8.4.2 Teratoma harvesting and preparation for immunohistochemistry analysis

The mice were sacrificed and the tumours removed. After rinsing with PBS, the tumours were placed in 4% PFA to fix the tissue. To ensure rapid, even fixation, the specimens were placed on a Rotator at RT, fixed for 2 h, bisected longitudinally and then fixed for a further 48 h. If the tumours could not be immediately processed, they were stored at 4°C in PBS containing 0.1% azide (Sigma) to prevent microbial and fungal contamination.

The teratomas preparation, histological staining, immunohistochemistry staining and sample analysis were done at the Wolfson CARD Histology laboratory at King's College London.

Briefly, the teratomas were placed into individual, coded, processing cassettes and processed to Paraffin wax (VWR), using a Leica 2010 Processing machine. Upon completion of processing, the teratomas were embedded into heated moulds containing molten wax. The moulds were then cooled at 4°C until the wax had solidified. The wax-embedded teratomas were sectioned in 6 µm serial slices using a rotary microtome, and allowed to float on the surface of 45°C heated water to softens the wax and allow the tissues to flatten out. Sections

were then mounted onto Superfrost Plus Microscope slide (Fisher Scientific). These slides have a special pre-treatment that allows the tissue sections to electrostatically adhere to the glass. Section–mounted slides were then placed into a 60°C oven for 1 h to ensure maximum adhesion. Slides were then stored at RT until required.

2.1.8.4.3 Histological staining and analysis

It is essential to de-wax the samples prior to histology as wax is hydrophobic and would repel the aqueous solution used for histological staining. To do so, two 10 min xylene (SLS) washes under agitation at RT were performed to de-solubilize the wax. This was followed by rehydration in four short absolute alcohol baths and a final wash in water. Sections were then sequentially stained using Mayer's Haematoxylin (for nuclei) (VWR) and Eosin (for cytoplasmic and all extracellular structures) (Sigma).

2.1.8.4.4 Immunohistochemical staining and analysis

As recognisable tissue structures from each germ layer could not always be readily identified by Haematoxylin & Eosin (H&E) examination, additional immunohistochemical staining and analysis of the teratomas was performed. Immunohistochemistry using germ layer-specific markers allowed confirmation of hESC differentiation into endoderm, mesoderm and ectoderm tissues.

As for histological staining (section 2.1.8.4.3), the teratoma sections required de-waxing prior to immunohistochemical staining after which sections were taken to water and blocked for endogenous peroxidases using 3% hydrogen peroxide aqueous solution for 10 min at RT (Sigma). This step deactivates the samples' endogenous peroxidase activity, which is essential as the detection system is based on a peroxidase activity (Horseradish peroxidase).

Next, Heat Induced Epitope Retrieval (HIER) was performed on the sections: this is necessary as Formalin-fixation and then paraffin wax processing (alcohol dehydration and the 62°C heat of the wax) can either destroy or mask antigenic sites (epitopes) of proteins. The precise mechanism whereby HIER unmasks hidden epitopes is not known but it appears to be either by calcium removal or Heat-inducing conformational changes to the protein, or both, allowing the epitopes to be revealed.

Once completed, slides were rinsed well in tap water before applying blocking solution (1 % bovine serum albumin in 1x Tris Buffered Saline (TBS) and 0.1 % azide, pH 7.6) for at least 5 min to quench (by ionic attraction) non-specific attachment of antibodies.

After blocking, primary antibodies specific for differentiated germ layers were diluted in blocking solution and left for 2 h at RT. The dilutions at which the antibodies were used are indicated in Table 2-5. After the primary antibody incubation, the slides were gently rinsed in 1X TBS and then washed in 500 mL 1X TBS, with stirring, for 10 min. Excess buffer solution was then flicked

off the slides before incubating them for 60 min at RT with the biotinylated secondary antibody (Table 2-6), also diluted in blocking solution.

	Primary antibody	Manufacturer	Final concentration
Human specific	Anti-MTCO2 Mouse IgG	Abcam (110258)	4 µg/mL
Endoderm	Anti-α-fetoprotein Mouse IgG	Sigma (A8452)	12.5 µg/mL
	Anti-GATA4 Goat IgG	R&D (AF2606)	1.3 µg/mL
Mesoderm	Anti-Desmin Mouse IgG	Sigma (D-1033)	1:1500*
	Anti-Tenascin C Rabbit IgG	Abcam (ab108930)	1:250**
Ectoderm	Anti-β-tubulin isotype III Mouse IgG	Abcam (ab7751)	2 µg/mL
	Anti-GFAP Rabbit IgG	Abcam (ab7260)	1:2500**

Table 2-5: Primary antibodies used for germ layer immunodetection on teratomas.
*Anti-Desmin is an ascites fluid and the final antibody concentration has not been determined.
**Anti-Tenascin C and anti-GFAP are whole anti-sera and the final antibody concentration has not been determined.

Secondary biotinylated antibody	Manufacturer	Final concentration
Goat anti-rabbit IgG	Vectorlab BA-1000	3 µg/mL
Goat anti-mouse IgG	Vectorlab BA-9200	3 µg/mL

Table 2-6: Secondary Biotinylated antibodies used for germ layer immunodetection on teratomas

After incubation with the biotinylated secondary antibodies, the slides were rinsed once briefly in 1X TBS followed by a 10 min wash with stirring in 1X TBS. This was immediately followed by a 30 min incubation at RT with the StreptABC-HRP complex (VectorLabs), which was made in 1X Tris Buffer. The slides were then washed in 1X TBS as above.

The samples were then developed for 10 min in diaminobenzidin solution (DAB) (VectorLabs) prepared following the manufacturer's instruction, under gentle agitation. Following this, the

sections were washed under running tap water for 5 min, counterstained in Mayer's Haematoxylin for 2 min in order to be able to visualise the cells' nuclei, and washed again under tap water it latter was running clear. Before being mounted on the coverslip, the sections had to be dehydrated. For this, they were washed in four successive 2 min alcohol baths of 100% Industrial Methylated Spirit (IMS) followed by two 5 min Xylene washes to render the section hydrophobic. The slides were then ready to be mounted with Di-n-butyl phthalate (DPX, VWR). Controls procedures with the omission of either the primary or secondary antibody were performed to check the specificity of the antigen:antibody interactions.

Images were taken with an Axiocam MR colour camera (medium resolution, Zeiss) mounted on an axioscope upright microscope (Zeiss) and processed with Photoshop CS5.

2.1.9 CAG repeat number determination

2.1.9.1 Total DNA extraction

Total DNA was extracted from trypsinised and pelleted cells using the DNeasy kit (Qiagen) according to manufacturer's protocol. Briefly, cell lysis was performed by the resuspension of the pellet in 200 µL of PBS supplemented with 12 mAU/mL proteinase K, followed by the addition of 200 µL of buffer AL (with ethanol added), vortexing and a 10 min incubation at 56°C. The sample was homogenised by the addition of 200 µL of 100% ethanol and vortexing before being pipetted into a QIAgen DNeasy mini spin column and centrifuged at 6,000 x g for 1 min. The flow through was discarded and the column was washed with the addition of 500 µL of buffers AW1 and AW2 followed by a 6,000 x g for 1 min and a 20,000 x g for 3 min centrifugations respectively. To elute the DNA, 200 µL of buffer AE or water was pipetted to the column, left to incubate for 1 min at RT and centrifuged for 1 min at 6,000 x g into a DNAse-free 1.5-mL microcentrifuge tube. DNA concentration was determined using a Nanodrop ND1000 UV-Vis Spectrophotometer (Labtech Int). The DNA concentration was adjusted to 50 ng/µL before proceeding to the repeat sizing polymerase chain reaction (PCR).

2.1.9.2 Repeat sizing PCR

Determination of the CAG repeat sizing of the different hESC lines was carried out by PCR. The 10 µL PCR reaction set up is described in Table 2-7 and thermocycling conditions used on the Bio-rad MyCycler Thermal Cycler are described in Table 2-8.

Component	Volume
DNA (50 ng/µL)	2 µL
dNTPs (2mM)	1 µL
DMSO	1 µL
AM Buffer (2mM) with β-mercaptoethanol	1 µL
Forward Primer (10 pmol/µL) GAGTCCCTCAAGTCCTTCCAGCA	0.8 µL
Reverse primer (10 pmol/µL) GCC CAAACTCACGGTCGGT	0.8 µL
AmpiTaq (5 U/µL)	0.1 µL
RNAse/DNAse free dH_20	3.3 µL

Table 2-7: PCR reaction set up for CAG repeat sizing.
dNTPs are from Invitrogen and Ampitaq polymerase is from Applied Biosystem. All the other components are from Sigma.

Step	Temperature	Time	
Enzyme activation	94ºC	90 s	
Denaturation	94ºC	30 s	
Annealing	65ºC	30 s	X 35 cycles
Elongation	72ºC	90 s	
Final elongation	72ºC	10 min	

Table 2-8: Repeat sizing PCR thermocycling conditions

After the PCR, for each sample, 1 µL of PCR product was mixed with 9 µL of HiDi Formamide (Applied Biosystems) and 0.03 µL l MegaBACE ET900-R Size standards (GE Healthcare) and denatured at 95ºC for 5 min. The PCR reaction was stopped by immediately putting the samples on ice.

2.1.9.3 CAG repeat size determination

The samples were then run on an ABI 3730xl PCR machine at GSTS Pathology, Guy's Hospital, London.

Using the GeneMapper software (Applied Biosystem), the standards' size were checked first. If they were correct, the amplicon's size could then be established. To determine the actual CAG repeat size, the following formula was used:

CAG Repeat size = (amplicon size in base pairs – 185)/3

where 185 corresponds to the products amplified in the 5' and 3' sequence of the uninterrupted CAG repeat tract.

2.1.10 Array Comparative Genomic Hybridisation karyotyping

Array Comparative Genomic Hybridisation (aCGH) was performed on each hESC line in order to monitor the karyotype and the genomic copy number variation of each cell line by the Cytogenetics laboratory (GSTS Pathology, Guy's Hospital, London). DNA extractions were performed on cell pellets of each line using a Chemagen DNA extraction robot according to the manufacturer's instructions. The DNA concentrations were measured using a NanoDrop and DNA integrity was confirmed by agarose gel electrophoresis. Following the manufacturer's instructions, 1 µg of DNA was labelled using a CGH labelling kit (Enzo Life Sciences) before being purified using the QIAquick PCR purification kit (Qiagen) and run on an Agilent 4 x 44 K platform using either Wessex NGRL design 017457 or design 028469. Hybridization, washing and scanning of the arrays were all performed according to the manufacturer's protocols. Analysis of the results and interpretation of the data was performed by the Cytogenetics team using feature extraction and DNA analytics software packages (Agilent). Only lines with a normal karyotype were used in this study.

2.1.11 DNA Fingerprinting

DNA fingerprinting was performed on each newly derived hESC line by the Cytogenetics laboratory (GSTS Pathology, Guy's Hospital, London). DNA was extracted and quantified as described in section 2.1.10. DNA was amplified using two PCR multiplexes (Heath *et al.*, 2000). The first one targeted 17 polymorphic microsatellite markers on chromosomes 13, 18 and 21. The second targeted 14 markers on the X and Y chromosomes. The various PCR products

were separated using an ABI PRISM 3100 Genetic Analyzer, and results were analysed using the ABI Genotyper software and interpreted by recording the allele sizes for each marker in order to give a unique fingerprint of each cell line by the Cytogenetics laboratory team.

1.1.1 Human Leukocyte Antigen (HLA) typing

HLA typing was performed and analysed by the Cytogenetics Department and the Clinical Transplantation Laboratory, Guy's Hospital, London as per the method described in Jacquet *et al*. (2013).

2.2 Reprograming of somatic cells into iPSCs using synthetic modified mRNA

The generation of iPSCs using modified synthetic mRNA as a reprogramming vector was first successful in 2010 (Warren *et al.*, 2010). This technique was then modified and commercialised by Stemgent. We further improved the protocol and the final protocol that gave rise to iPSCs will be described in this section. Key modifications and differences between the original protocol, Stemgent's and mine will be discussed in Chapter 4.

2.2.1 BJ cell culture

The commercially available neonatal foreskin BJ fibroblasts (CRL-2522, ATCC) were used as a positive control. The purchased cryovial containing 6.7 x 10^5 cells was recovered for culture by being quickly transferred from LN_2 to a 37°C heating block until most of the cell suspension was thawed. The cells were then transferred to a 15-mL centrifuge tube containing 4 mL of pre-warmed complete BJ medium consisting of Eagle's Minimum Essential Medium (ATCC) supplemented with 10% FBS (Sigma). The cells were centrifuged for 5 min at 1,000 x g and were resuspended in 10 mL of complete BJ medium after removal of the supernatant. BJs were plated in a T75 flask (Corning) and were fed every 2-3 days.

Cells were passaged when they reached 80 to 90% confluency. To do so, the cells were washed once with PBS and incubated 5 min with 3 mL of TrypLE Select (Invitrogen). The cell suspension was then collected in 7 mL of complete BJ medium and centrifuged at 1,000 x g for 5 min. Once the supernatant was discarded, the cells were resuspended in complete BJ medium and subcultured at a 1:6 to 1:10 ratio. In order to store the bank of cells generated, a cell pellet was generated as previously described. This latter was resuspended in complete BJ medium containing 5% DMSO (VWR), placed in cryovials and put at -80°C in a Mr. Frosty isopropanol cryovessel before being transferred to LN_2 24 h later.

2.2.2 Newborn foreskin fibroblast (NuFF) donor 11

Gamma-irradiated NuFF donor 11 were purchased from Global Stem (GSC-3001G) and recovered as described in 2.2.1 in NuFF culture medium (DMEM, 10% FBS, 1% Glutamax and 1% Penicillin/Streptomycin). Each vial contains 4-5 x 10^6 cells.

2.2.2.1 Feeders preparation

Four wells of a 6-well plate were coated with 0.2% gelatin (Millipore) for a minimum of 30 min before evenly plating 2.5 x 10^5 NuFF per well in 2.5 ml of NuFF medium.

2.2.2.2 Medium conditioning

The 3-4 x 10^6 inactivated NuFFs cells unused for feeders preparation were plated in one T75, in 10 mL of NuFF culture medium, and left to attach overnight in a 37°C, 20% O_2 and 5% CO_2 incubator (Nuaire). The following day, the NuFF culture medium was removed from the T75, the cells washed once with PBS and medium replaced with 25 mL of Pluriton (Stemgent) supplemented with 4 ng/mL of bFGF and left to incubate overnight. For a total of six days after each 24 h incubation the NuFF-conditioned Pluriton was collected, frozen at -20°C and replaced by 25 mL of fresh Pluriton supplemented with 4 ng/mL bFGF.

On the sixth day of conditioned-medium collection, all the previously collected aliquots of NuFF-conditioned Pluriton Medium were thawed at 4°C. They were all pooled with the final collection and filtered using a 0.22 µm pore size, low protein-binding filter (Corning). The filtered NuFF-conditioned Pluriton medium was re-aliquoted (40 mL aliquots) and re-frozen at -20°C until used in the reprogramming protocol or for up to three months.

2.2.3 Hair-follicle derived keratinocyte culture

The hair-follicle (HF)-keratinocyte derivation protocol used in this study was modified from previously published work Aasen and Belmonte (2010).

2.2.3.1 Patients samples collection

Sample collection for optimisation of the keratinocyte derivation technique was done under study *REC Ref: 10/H0716/90 Induced Pluripotent Stem Cells from Keratinocytes: A neuronal model of Huntington's disease, a neurodegenerative disorder (K-iPS cells HD).* Patient consenting and sample collection to be used for iPSCs generation was done by Dr. S. Haider. A repertory of the samples collected is presented in Chapter 4, Table 4-3.

2.2.3.2 Hair plucking

After explaining the procedure to the patient and taking consent, a small scalp area of the temporal or the occipital part of the head was washed with a 70% ethanol wipe. A few hairs were then plucked using single forceps. Hairs in the anagene phase with a visible outer root

sheath (ORS, Figure 2-3) were placed into RT DMEM supplemented with 1X of antibiotic/antimycotic (Sigma). Hairs with no visible ORS were discarded.

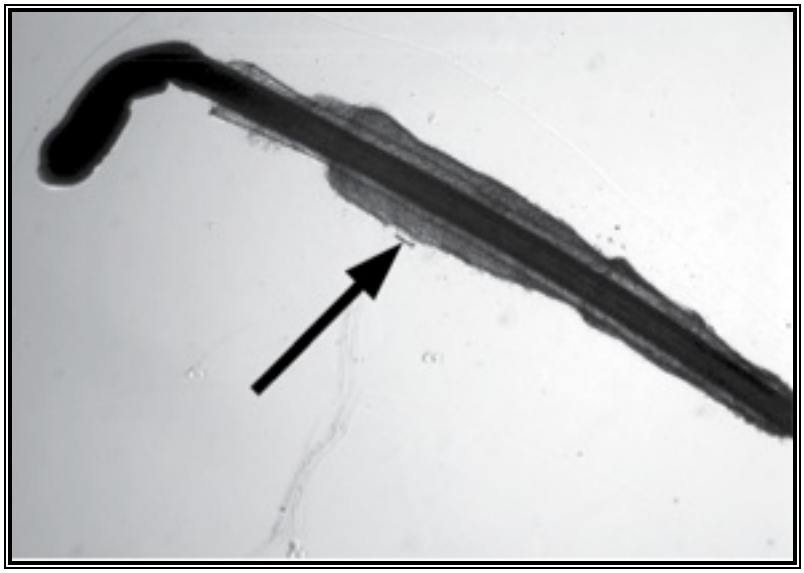

Figure 2-3: Hair follicle in the anagene phase. Arrow indicates the Outer Root Sheath (ORS)

2.2.3.3 Hair plating

Hair plating was adapted from Aasen and Belmonte (2010). Briefly, plucked hairs were single-plated into wells of a 6-well plates pre-coated with GFR-Matrigel (prepared as in 2.1.5.1). A 22-mm coverslip (SLS) was then placed onto the hair before 1 mL of mTeSR1 medium supplemented with 1X antibiotic/antimycotic mixture was added to each well. Unless otherwise indicated, hairs and derived keratinocytes were cultured at 37°C, 20% O_2 and 5% CO_2 (Nuaire incubator). Hair cultures were not disturbed for 72 h to ensure good attachment. Coverslips were removed after 72 h. In the event that the hair had attached to the coverslip and not to the GFR-Matrigel, the coverslip was just flipped over.

2.2.3.4 Keratinocyte derivation and maintenance

The mTeSR1 medium was replaced every two days until an outgrowth was observed. At this stage, keratinocytes were fed every two to three days with Epilife medium supplemented with Human Keratinocyte Growth Supplement (HKGS) (both from Invitrogen) until cells were confluent enough to be passaged.

Prior to passaging, wells of a 6-well plate were coated with recombinant human collagen I in order to improve keratinocyte attachment and growth. To do so, the Coating Matrix Kit (Invitrogen) was used where recombinant human collagen I was diluted with the provided Dilution Medium to a final concentration of 15 µg/mL and added to the wells. The 6-well plate was rocked back and forth briskly to ensure even distribution of the Coating Matrix in the well and left to incubate at RT for 30 min. Excess coating matrix was removed prior to cell plating.

To passage the cells, 1 mL of Tryple Select (Invitrogen) was put in each well before the cells were returned to the incubator for 7-10 min. To stop the reaction, 1 mg/mL of trypsin inhibitor (Sigma) was used. Cells were collected and centrifuged at 1,200 x g for 5 min. The pellet was then resuspended in Epilife and cells split at a 1:3 ratio. Hairs that did not present any outgrowth after 10 days were discarded.

2.2.3.5 Keratinocyte cryopreservation and thaw

As for hESCs, HF-keratinocyte cryopreservation was done when the cells reached 70-80% confluency to ensure the cells were actively dividing. Cells were passaged as described in 2.2.3.4. After the 5 min centrifugation at 1,000 x g, the supernatant was discarded and the cell pellet resuspended pre-chilled FBS supplemented with 10% DMSO. Approximately 1 x 10^6 cells were aliquoted in 1 mL per labelled cryovial and stored overnight at -80°C into a Mr. Frosty isopropanol cryovessel. They were transferred into a LN_2 vapor tank the following day. To recover the keratinocytes from liquid nitrogen, cryovials were quickly thawed in a 37°C heating block until only a small frozen chunk remained. The contents were transferred into a 15-mL centrifuge tube using a 5-mL pipette in order to prevent the generation of very small clumps. Pre-warmed Epilife (5 mL) was added to the tube drop wise and the cells were centrifuged 5 min at 1,000 x g. The supernatant was discarded and the pellet resuspended in 2 mL of Epilife before plating the cells in a well of a 6-well plate pre-coated with Coating Matrix (refer to 2.2.3.4).

2.2.4 Target cell plating

Primary somatic cells, BJs and HF-keratinocytes, to be reprogrammed into iPSCs are also referred to as target cells. The day prior to the beginning of the reprogramming protocol, BJs or HF-keratinocytes were passaged as described in 2.2.1 and 2.2.3.4 respectively, counted and plated in their culture medium at a density of 7 x 10^3 or 6 x 10^4 cells respectively on the NuFF feeders prepared as in 2.2.2.1.

2.2.5 Modified mRNA synthesis

The intronless coding sequences (CDS) of *OCT4*, *SOX2*, *KLF4*, *c-MYC* and *LIN28* were retrieved from NCBI (see appendix II). As published by Warren et *al*. (2010), a KOZAK translational initiation signal was added in 5' UTR and the 3' UTR terminated with an alpha-globin driven oligo(dT) sequence for templated addition of a polyA tail.

The CDS were then codon optimised with the GeneOptimizer expert software by Geneart/Life Technologies. Codon optimisation allows more efficient transcription, by avoiding RNA secondary structures, adjusting GC content and removing splice-sites for an overall increased

protein yield (Fath *et al.*, 2011). The codon optimised CDSs were synthesized and subcloned into a pTNT plasmid (Promega) to allow mRNA synthesis (see appendix II).

Amsbio synthesized the modified mRNA. To do so, PCR templates were generated from the linearized plasmids using the same upstream primers for all 6 constructs with six different gene-specific downstream T120-heeled reverse primers for the addition of the poly(A) tail. The templates were transcribed with T7 polymerase and further modified according to Warren et *al*. (2010). Modifications include the complete substitution of 5-methylcytidine (5mC) for cytidine and the substitution of pseudouridine (psi) for uridine to increase mRNA viability and ectopic protein expression. Furthermore, to promote efficient translation and increase mRNA half-life a synthetic 5' guanine cap was added and 5'-triphosphates were eliminated by phosphatase treatment. A "mRNA cocktail" containing *OCT4*, *SOX2*, *KLF4*, *C-MYC*, *LIN28* and d2eGFP in molar ratios of (3:1:1:1:1:1) at a final concentration of 100ng/mL was prepared, aliquoted in single-use 50 µl aliquots and stored at -80˚C.

2.2.6 mRNA transfection

On day 0 of the protocol, fresh Pluriton medium was equilibrated at 37°C and low O_2 tension for a minimum of 2 h prior to use. 1X Pluriton supplement and 300ng/mL B18R (ebioscience) was added to Pluriton medium.

The mRNA transfection complex (for 4 wells of a 6-well plate) was prepared using RNAse-free material and working on RNAZAP (Life Technologies) treated surfaces. To do so, a single-use 50 µL aliquot of the mRNA cocktail (prepared prior to the beginning of the reprogramming) was thawed on ice. It was then mixed with 200 µL of Opti-MEM (Invitrogen) and mixed by gentle pipetting. In a separate tube, 25 µL of RNAiMAX (Sigma), a lipofectamine transfection reagent, was diluted in 225 µL of Opti-MEM and mixed by gentle pipetting. The diluted lipofectamine was then carefully added to the diluted mRNA cocktail with gentle pipetting to generate the mRNA transfection complex. The complex was incubated at RT for 15 min before 120 µL was in a dropwise fashion to each of the 4 wells to be transfected. To ensure uniform distribution of the mRNA transfection complex, the 6-well plate was gently rocked from side to side and front to back before being incubated for 4 h at 37°C and 5% O_2.

During this time, more Pluriton medium was equilibrated. Just prior to exchanging the transfection medium, the equilibrated Pluriton was supplemented with 1X Pluriton supplement as well as 300 ng/mL B18R. The cells were returned to incubate overnight at 37°C and 5% O_2.

2.2.7 Somatic cell reprogramming with synthetic modified mRNA

A summary of the mRNA reprogramming protocol adapted from Warren et *al*. (2010) is presented in Table 2-9. The impact of the different modification on the success of the protocol will be discussed in Chapter 4.

Step	Day	Adapted mRNA reprogramming protocol
Feeder cell plating	-2	Plating of NuFF cells donor 11 cells, 2.5 x 10^5 cells/well of a 6-well plate and the remainder into a T75 flask
Target cell plating	-1	Plating of target cells at a density of 7 x 10^3 cells/well (BJ) or 6 x 10^4 cells/well (HF-keratinocytes)
mRNA transfection	0	B18R Pre-treatment (300 ng/mL), cell transfection with mRNA cocktail in Pluriton medium supplemented with 300 ng/mL B18R and 1X Pluriton supplement
Optional	2 to 17	Optional 1 μM Pithilthrin-α treatment
mRNA transfection	1 to 17	Cell transfection with mRNA cocktail in Pluriton medium supplemented with 300 ng/mL B18R and 1X Pluriton supplement
Use of conditioned medium	6 to 17	Day -1 to Day 6 NuFF-conditioned Pluriton medium is pooled together, filtered, supplemented with 0.5 mM sodium butyrate and used from Day 6 onwards.
Colony identification	18 to 20	Potential colonies are left to expand and fed daily with Pluriton medium
Colony picking	21	Manual picking of primary iPSC colonies and passaging on to HFF in KOSR-XF medium
iPSC line expansion, freezing, maintenance and adaptation to feeder-free culture conditions	22+	Daily refeeding. Maintenance and expansion of the culture on HFF-feeder in KOSR-XF complete medium and adaptation to Matrigel/Nutristem feeder-free conditions

Table 2-9:Summary of mRNA reprogramming protocol adapted from Warren et al (2010)

2.2.8 iPSCs freezing

iPSCs cultured on feeders were vitrified and thawed similarly to hESCs (described in section 2.1.4) while iPSCs cultured feeder-free were cryopreserved and thawed similarly to hESCs (described in section 2.1.7.)

2.2.9 iPSCs characterisation

2.2.9.1 iPSCs pluripotency characterisation

iPSCs pluripotency characterisation was identical to hESC characterisation (described in section 2.1.8).

2.2.9.2 Array CGH karyotyping

The protocol for iPSCS karyotyping is identical to the protocol for hESC karyotyping (described in section 2.1.10).

2.2.9.3 DNA Fingerprinting

The protocol for iPSC DNA fingerprinting is identical to the protocol for hESC DNA fingerprinting (described in section 2.1.11).

2.3 Human Pluripotent Stem Cells (hPSCs) differentiation

2.3.1 Human pluripotent stem cell culture

In order to ensure good cardiac differentiation, cells were cultured for at least three passages on GFR-Matrigel (refer to 2.1.5.1) with Nutristem medium (Stemgent). Enzymatic passaging was performed using dispase (refer to 2.1.6).

2.3.2 Directed cardiac differentiation

Directed cardiac differentiation was based on the work published by (Laflamme *et al.*, 2007). Briefly, undifferentiated hESCs (KCL020, KCL027_HD5, KCL028_HD6, KCL031, KCL034, KCL036_HD7 and KCL040) were dissociated into a single-cell suspension by a 3-5 min incubation with accutase. Cells were then centrifuged, resuspended, counted and seeded in Nutristem onto GFR-Matrigel coated 24-well plates at a density of 2 x 10^5 cells/cm^2, with the addition of 10 μM Y-27632 to ensure good cell attachment. This marked day -5 of the differentiation protocol. Until day 0, cells were fed daily with 2 mL/well of Nutristem. At day 0, cardiac differentiation was induced by feeding the cells with 0.5 mL/well Roswell Park Memorial Institute medium (RPMI)-B27 medium (Invitrogen) supplemented with 100 ng/mL of human recombinant Activin A (Miltenyi). The following day, the medium was replaced by 1.5 mL/well RPMI-B27 supplemented with 10 ng/ml human recombinant BMP4, (Miltenyi) and left unchanged for four days. The medium was then exchanged for unsupplemented RPMI-B27

every two days for up to 30 days. Figure 2-4 summarises the directed cardiac differentiation protocol.

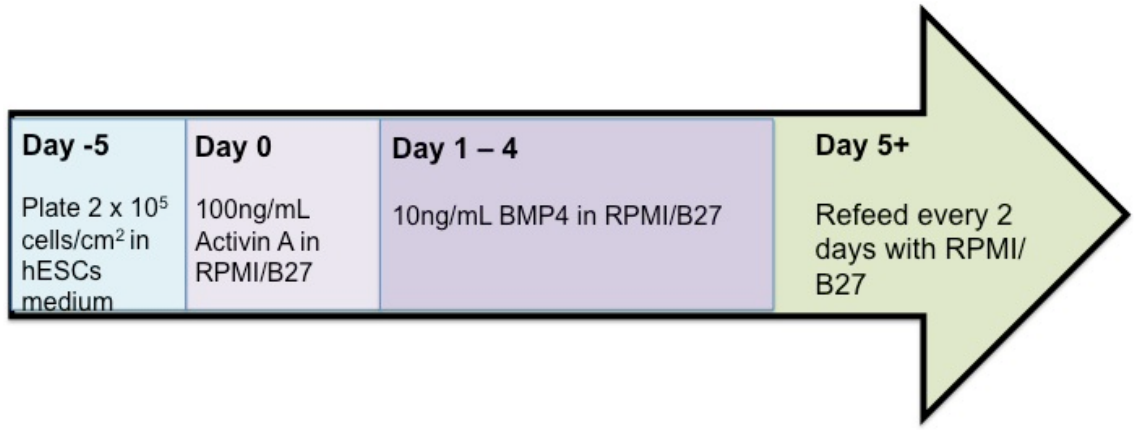

Figure 2-4: Timeline of the directed cardiac differentiation protocol

2.3.3 Cardiomyocytes immunofluorescence

For immunofluoresence analysis cardiomyocytes were plated on GFR-Matrigel (refer to 2.1.5.1 for GFR-Matrigel preparation) pre-coated glass-bottomed dishes (MatTek Corporation). The medium was removed from the cardiomyocytes monolayers, the cells were rinsed once with $DPBS^{Ca2+/Mg2+}$ and then inbubated with 1 mL accutase for 10-15 min at 37˚C. The cells were then washed with DMEM, centrifuged at 1,000 x g for 5 min and resuspended in 200 µL/dish of RPMI-B27 supplemented with 10 µM Y-27632. They were then fixed with 3.7% PFA for 20 min at RT and washed three times with $DPBS^{Ca2+/Mg2+}$. Fixed cells were kept at 4°C in $DPBS^{Ca2+/Mg2+}$ for up five days if not processed immediately. Permeabilisation was effectuated with 0.1% Triton X-100/$DPBS^{Ca2+/Mg2+}$ for 10 min at RT, followed by three $DPBS^{Ca2+/Mg2+}$ washes. The samples were then blocked in PBS with 4% FBS for 2 h at RT. Without rinsing, the anti-Cardiac Troponin T antibody (Abcam, ab45932), developed in rabbit, was diluted in $DPBS^{Ca2+/Mg2+}$ to a final concentration of 5 µg/mL and added to the cells for 1 h at RT. The solution was then removed and cells washed 3 times for 5 min with $DPBS^{Ca2+/Mg2+}$ before adding Donkey anti-rabbit IgG, FITC-conjugated secondary (Jackson ImmunoResearch, 711-095-152) at 15 µg/mL in $DPBS^{Ca2+/Mg2+}$ for 40 min at RT, shilded from light. Cells were then washed three times for 5 min in $DPBS^{Ca2+/Mg2+}$, mounted in Vectashield mounting medium containing DAPI, and covered with a coverslip. Samples were assessed using Eclipse 50i upright epifluorescence microscope. Images were captured with cooled CCD camera Infinity 3 utilising Infinity Capture software and processed in Adobe Photoshop CS5.

2.3.4 Quantitative PCR (qPCR)

2.3.4.1 Total RNA preparation

Total RNA was extracted using the RNeasy kit (Qiagen). The cell monolayer was rinsed once with PBS before the addition of 350 µL or 600 µL of buffer RLT (for < 5 x 10^6 or 5 x 10^6 – 1 x 10^7

cells respectively), supplemented with 10 µL/mL of β-ME to protect the sample from endogenous RNases (Frenkel *et al.*, 1987). Samples were homogenised by vortexing for 1 min or by going through a QIAshredder spin column for 2 min at 8,000 x g. Equal volumes of 70% ethanol were added to the homogenised lysates before loading the samples in an RNeasy spin column placed in a collection tube. The columns were centrifuged at 8,000 x g for 15 s and the flow-through discarded. 350 µL of buffer RW1 was added and centrifuged at 8,000 x g for 15 s to wash the column. After discarding the flow-through, the samples were incubated for 15 min at RT with DNase I (27 Kunitz units final) in order to eliminate genomic DNA. Another 350 µL RW1 wash and centrifugation for 15 s at 8,000 x g stopped the digestion, followed by two 500 µL RPE washes with 15 s and 2 min centrifugations at 16,000 x g. In order to prevent ethanol carryover, another centrifugation was performed for 1 min at 16,000 x g using an empty collection tube. To elute the purified total RNA, 30 µL of RNase-free water was added to the column and left to incubate for 1 min before a final 1 min centrifugation at 8,000 x g. RNA concentration and purity were determined using a Nanodrop ND1000 UV-Vis Spectrophotometer. RNA has a maximal absorbance (A) of 260 nm while proteins have a maximal A of 280 nm. Only samples with an A260/A280 ration between 1.8 and 2.1 were used for complementary DNA (cDNA) formation. Samples that were not used immediately were stored at -80°C.

2.3.4.2 Complementary DNA (cDNA) preparation

cDNA was prepared from 50 ng of total RNA using the Precision nanoScript Reverse Transcription kit (Primer design). Briefly, 0.5 µg of total RNA was mixed with 1 µL oligo-dT and brought to a final volume of 10 µL with RNase free water. The samples were heated at 65°C for 5 min to denature any RNA secondary structures and then directly transferred on to ice to allow primer annealing. A 10 µL mastermix consisting of nanoscript 10x buffer, 0.5 mM deoxyribonucleotide triphosphate (dNTPs), 10 mM Dithiothreitol, water and 0.7 U/µL final reverse transcriptase was added to the samples before incubating them at 55°C for 20 min followed by a 15 min inactivation step at 75°C using a MyCycler Thermal Cycler (Bio-rad). cDNA samples were stored at -20°C until use.

2.3.4.3 Primer design

The primer sequences of the target genes used to characterise hESC-derived cardiomyocytes are presented in Table 2-10. Information concerning the housekeeping genes used to characterise hESC-derived cardiomyocytes are presented in Table 2-11.

Gene	Accession number	Sense Primer	Anti-sense primer
OTC3/4	NM_002701	GCCGTGAAGCTGGAGAAG	GTGTATATCCCAGGGTGATCC
NANOG	NM_024865	ATGTCTTCTGCTGAGATGCC	GTTGTTTGCCTTTGGGACTG
TNNT2	NM_000364	CAAAGCCCAGGTCGTTCAT	GCAACTCATTCAGGTCCCTTCT
NKX2.5	NM_004387	GCACCCACCCGTATTTATGT	GGGTCAACGCACTCTCTTTAA
HTT	NM_002111	TCTGGGCATCGCTATGGAAC	ATTTCTGAGGCCGAACCAGG

Table 2-10: Sense and Antisense primers of target genes used for hESC-derived cardiomyocytes characterisation.
Primers in blue were designed by PrimerDesign Ltd.

Gene	Accession number	Anchor nucleotide:	Amplicon length
EIF4A2	NM_001967	900	113
SDHA	NM_004168	1032	120

Table 2-11 Housekeeping genes designed and synthesized by PrimerDesign Ltd used for hESC-derived cardiomyocyte characterisation amplicon context.
The primer sequences are commercially sensitive information but the details provided in this table are MIQE compliant (Bustin *et al.*, 2011)

2.3.4.4 qPCR

qPCR was performed using the Precision 2X qPCR SYBR green-based Mastermix (PrimerDesign). As the cDNA is being amplified, SYBR green proportionally intercalates its fluorescent dyes in to the double stranded DNA, emitting fluorescence at the 522 nm wavelength. This can be measured by the apparatus and used to quantify gene expression. According to the manufacturer's instruction, cDNA prepared as described in section 2.3.4.2 was diluted 1:10 in DNAse/RNAse free water prior to use. The components described in Table 2-12 were added for each 20 µL qPCR reaction.

Components	Per reaction
Precision 2X qPCR Mastermix	10 µL
Forward and Reverse Primers mix (6 mM stock)	1 µL
Template cDNA (1:10 diluted)	5 µL
DNAse/RNAse free water	4 µL

Table 2-12: Components of each 20 µL qPCR reaction using the Precision 2x Mastermix from PrimerDesign Ltd.

All samples were run in technical triplicates in 96-well hard shell white PCR plates (Bio-rad). No positive template controls were included. DNAse/RNAse free water was used instead of template cDNA as a negative control (refer to Table 2-12). The plate was sealed with a microseal adhesive sealer film (Bio-rad). The Bio-Rad CFX96 thermal cycler and accompanying software were used to run the qPCRs. Thermocycling conditions are described in Table 2-13.

Step	Temperature	Time	
Enzyme activation - HotStart	95ºC	10 min	
Denaturation	95ºC	15 s	X 40 cycles
Data collection	60ºC	30 s	
Melt Curve	59ºC to 95ºC with 0.5ºC increment	10 s	

Table 2-13 Cycling conditions used for qPCR reactions using the Bio-Rad CFX96 thermal

Considering that SYBR green can bind to non-specific product amplicons or primer-dimers, a dissociation melt curves step was added to the thermocycling programme to ensure the accuracy of the PCR products analysed. Each PCR product has a particular temperature at which it becomes single-stranded and loses the SYBR green fluorescence, corresponding to a single peak in the melt-curve analysis.

Once specific PCR amplification was insured, mRNA quantification could be done using the $2^{\Delta\Delta Ct}$ relative quantification method. In this method the difference in Ct (threshold cycle) value of genes of interest (GOI) and of housekeeping (HK) genes is first calculated to generate the ΔCt value. Next, the control-condition ΔCt (undifferentiated hESCs) is subtracted from the experimental-condition ΔCt (differentiated hESCs) to yield the ΔΔCt value. The negative value of this subtraction, the −ΔΔCt, is then used as the exponent of 2 to calculate the "corrected" expression level of the samples. The newly calculated expression value of the control-condition

was set to 1, and the experimental-conditions' expression levels were normalised by dividing the mean $2^{\Delta\Delta Ct}$ value by the control-condition mean $2^{-\Delta\Delta Ct}$ value.

2.3.4.5 Cardiomyocyte-specific biomarker gene expression

The Human Cardiomyocyte Differentiation qBiomarker PCR Array (IPHS-102, Qiagen) was used to determine the gene expression of cardiomyocyte-specific biomarkers. For this, cDNA was synthesized using the RT^2 First Strand Kit (Qiagen). The kit includes a genomic DNA elimination step (GE). This was performed by mixing 0.5 µg of total RNA with 2 µL of buffer GE and water to a final volume of 10 µL. The GE mix was incubated at 42ºC for 5 min after which it was immediately put on ice for at least 1 min. The reverse transcription mix was prepared as described in Table 2-14 and added to the GE mix.

Component	Volume
BC3 (5X buffer 3)	4 µL
P2 (primer and external control mix)	1 µL
RE3 (RT enzyme mix 3)	2 µL
H2O	3 µL
Final volume	10 µL

Table 2-14: Qiagen RT^2 First Strand Kit reverse transcription mix (one reaction).

The reverse transcription synthesis was performed by incubating the mix at 42ºC for 15 min, immediately followed by an incubation at 95ºC for 5 min. The cDNA was diluted 1:5, mixed with RT^2 Real Time SYBR® Green/ROX™ qPCR Master Mix (Qiagen) and added to the Human Cardiomyocyte Differentiation qBiomarker PCR Array. The array was then loaded in a 7900HT Fast Real-Time PCR System (Applied Biosystem). Results were analysed using the web-based Qiagen qBiomarker iPSC Data Analysis Software.

Chapter 3

hESC Pluripotency Characterisation

Chapter 3 hESC Pluripotency Characterisation

Pluripotent hESCs have distinct characteristics. When undifferentiated, they grow as uniform, tightly packed colonies with defined edges. They present a large nucleus and a high nucleus to cytoplasm ratio. hESCs have the ability to self-renew into the same cell type, provided that they are maintained in the correct culture conditions. They also express an array of specific "pluripotency markers" and importantly, have the ability to differentiate into any of the three germ layers: endoderm, mesoderm and ectoderm (Thomson *et al.*, 1998). The cell lines used in this study were characterised using a set of seven criteria as we previously published (Stephenson *et al.*, 2012; methods described in section 2.1.8). An "identification card" could then be generated for each hESC line. Once the hESC lines were characterised, they could be adapted to feeder-free culture conditions for downstream applications.

3.1 hESC Pluripotency Characterisation

Most of the hESC lines used in this study were characterised following seven criteria. A representative characterisation set of five out of seven criteria is presented in Figure 3-1.

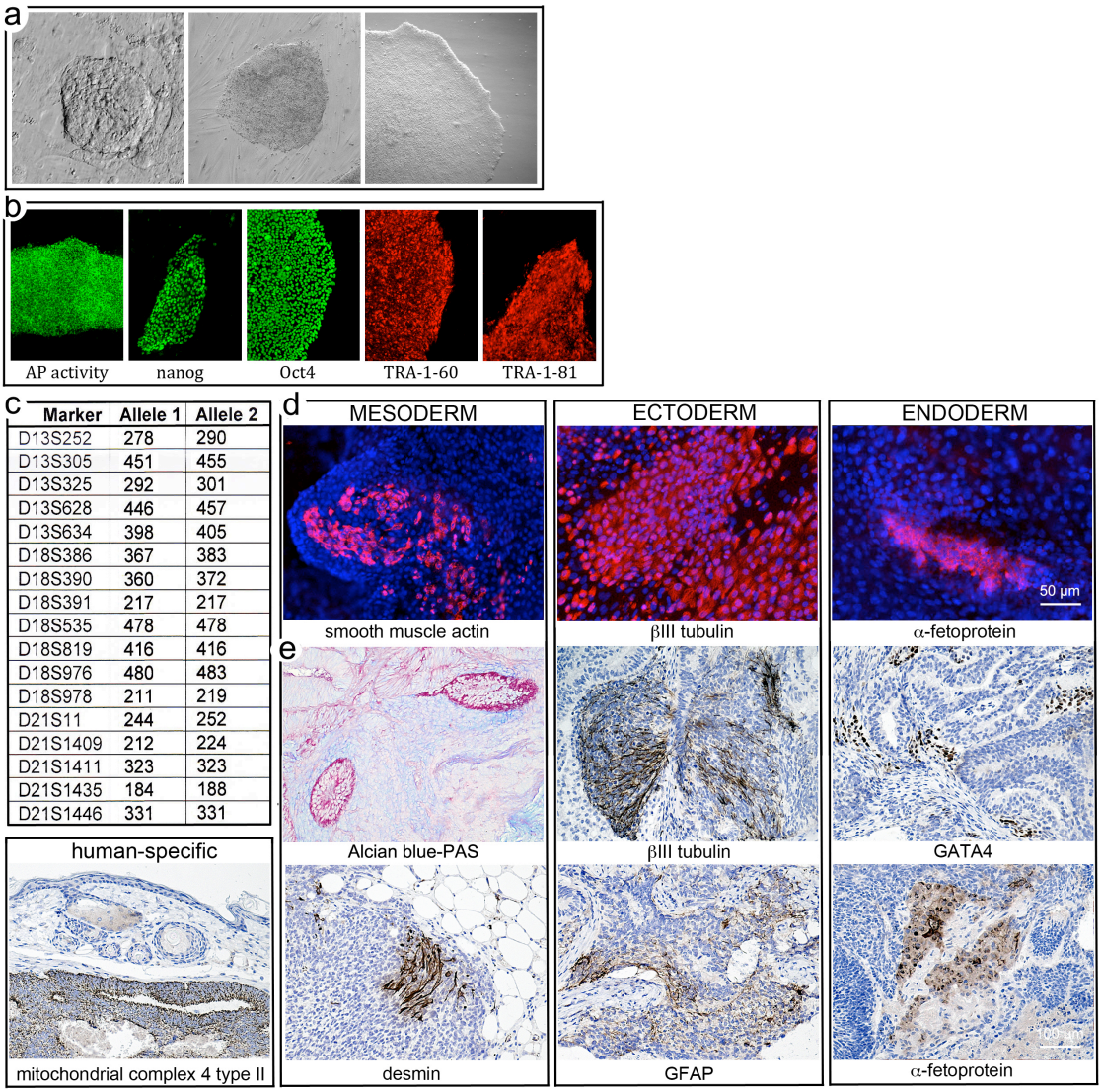

Marker	Allele 1	Allele 2
D13S252	278	290
D13S305	451	455
D13S325	292	301
D13S628	446	457
D13S634	398	405
D18S386	367	383
D18S390	360	372
D18S391	217	217
D18S535	478	478
D18S819	416	416
D18S976	480	483
D18S978	211	219
D21S11	244	252
D21S1409	212	224
D21S1411	323	323
D21S1435	184	188
D21S1446	331	331

Figure 3-1: Representative hESC characterisation.
The characterisation set of HD-hESC KCL012_HD3 is presented in this figure. **a)** Morphological criteria. Initial outgrowth (left), KCL012_HD3 cell colony on HFF (middle) and feeder-free condition (right). **b)** Pluripotency markers: alkaline phosphatase (AP) activity, OCT4, NANOG, TRA-1–60 and TRA-1–81. **c)** Genotyping: microsatellite markers specific for chromosomes 13, 18, 21, X and Y were amplified. The allele sizes in base pair for markers on chromosomes 13, 18, and 21 are listed in the table. Array comparative genomic hybridization (CGH) did not detect any copy number changes using Promega female G1521 as a standard. **d)** *In vitro* differentiation markers for the three germ layers: smooth muscle actin (mesoderm), β-III tubulin (ectoderm) and α-fetoprotein (endoderm). **e)** *In vivo* differentiation. Teratoma sections were counterstained with hematoxylin and eosin and specific stains are either light blue (Alcian blue) or brown (all immunohistochemistry). Mesoderm germ layer markers: Alcian blue– and periodic acid–Schiff (PAS)-stained cartilage and desmin. Ectoderm germ layer markers: β-III tubulin and glial fibrillary acidic protein (GFAP). Endoderm germ layer marker: GATA4 and α-fetoprotein. Positive immunostaining for complex IV type II marker confirms the human origin of the tumour (adjacent section of the one stained for desmin). Images were taken at 40x magnification.

1) Morphological criteria: Undifferentiated hESCs form tightly packed colonies with well-defined edges and are clear from differentiated cells, as represented in Panel a. hESCs were considered to be adapted to a new culture condition when they could be propagated undifferentiated under said culture condition for a minimum of three passages.

2) Detection of pluripotency marker: Pluripotency was evaluated by immunofluorescence detection of two pluripotency transcription factors, NANOG and OCT3/4, and two pluripotency surface markers, TRA-1-60 and TRA-1-81; as well as by AP enzymatic activity as showed in Panel b.

3) Differentiation into three germ layers *in vitro*: hESCs colonies were differentiated *in vitro* for a period of three weeks before performing immunofluorescence to detect markers representative of the three germ layers such as α-fetoprotein and/or GATA4 for endoderm, smooth muscle actin and/or Brachyury T for mesoderm and β-III tubulin and/or PAX6 for ectoderm as showed in Panel d.

4) Differentiation into three germ layers *in vivo*: hESCs were injected subcutaneously into NOD/SCID mice and tumours were harvested 6–12 weeks post injection. Tumour sections were stained with hematoxylin and eosin (H&E) as well as stained by immunohistochemistry to confirm the presence of the three germ layers and its human specificity as showed in Panel e.

5) Genotyping: Each cell line was identified at the molecular level after derivation. For this, DNA Fingerprinting by the amplification 17 polymorphic microsatellite markers on chromosomes 13, 18 and 21 was used. A result example is presented in Panel c.

6) Determination of genomic stability: Genomic stability was confirmed by the absence of chromosomal abnormalities such as deletion or duplications as well as abnormal karyotyping. This was assessed at the time of derivation and after 10-20 passages by array-comparative genomic hybridization. KCL040 presented a microdeletion at q13.2 of chromosome 5 at passage 4 and KCL027_HD5 showed a microdeletion in the long arm of chromosome 2 at passage 18. However these were considered as not significant as they are normal population polymorphisms. However, KCL013_HD4 showed the addition of a whole chromosome 12 at passage 12 and was dismissed from the rest of this study.

7) Human leukocyte antigen (HLA) typing: HLA typing was performed for HLA-A, -B, -C, and DRB1. Results were entered into the MatchView1 database (Be the Match Registry, http://marrow.org/Patient/Transplant_Process/Search_Process/View_Potential_Matches/View_Potential_Matches.aspx, Accessed 17 May 2012) to determine the match level frequency in the population.

In addition to these seven characterisation criteria, the HD-hESCs had their CAG repeat number determined. The representative repeat sizing of KCL012_HD3 is presented in Figure 3-2.

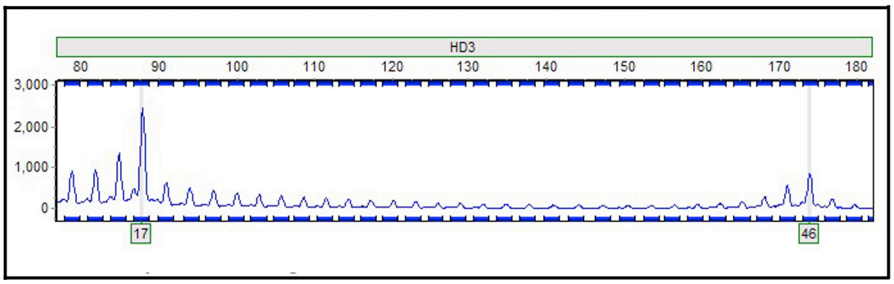

Figure 3-2: CAG repeat sizing of KCL012_HD3.
Repeat sizes were of 17 and 46 CAGs.

A summary of the remaining hESC lines' characterisation is presented in Table 3-1 and additional figures are in appendix I.

	Morphology	Pluripotency	*In vitro* differentiation	*In vivo* differentiation	Genotyping	Genomic stability	HLA Typing
KCL012_HD3	+	+	+	+	+	+	+
KCL013_HD4	+	+	+	ND	+	-	+
KCL020	+	+	+	ND	+	+	+
KCL027_HD5	+	+	+	+	+	+	+
KCL028_HD6	+	+	+	+	+	+	+
KCL031	+	+	+	+	+	+	+
KCL034	+	+	+	+	+	+	+
KCL036_HD7	+	+	+	+	+	+	+
KCL040	+	+	+	ND	+	+	+

Table 3-1: Summary of the hESC characterisation.
+: Positive result, **-**; negative result, **ND**: non-determined.

3.2 Adaptation of hESCs to feeder-free culture

Feeder cells such as mitotically-inactivated HFF are commonly used to support the derivation and long-term maintenance of pluripotent stem cells. The hESCs lines used in this study are no exception. HFF-feeders maintain the pluripotent state of hESCs by notably secreting bFGF (Park *et al.*, 2011) as well as other unknown growth factors and cytokines. Feeders also assemble ECM, a required physical support for hESCs to attach and grow. One goal when using hESCs as disease-in-a-dish models is to differentiate them into a specific somatic cell type, such as cardiomyocytes, that is affected by the disease. There are a variety of protocols describing hESCs differentiation. However, in order to obtain a sufficient yield of differentiated cells, large-scale hESCs culture is needed to start with. This is not achievable when cultured on feeders, as manual passaging is required. Furthermore, as much as feeder-free culture is required in order to obtain enough hESCs for differentiation purposes, it is absolutely essential when it comes to the study of a disease-specific phenotype. Indeed, the presence of feeder cells could cloud the apparent effects of drugs, small molecules and genetic modifications specific to a disease. For these reasons, all the hESCs lines used in this study were adapted to feeder-free culture conditions. Two different matrices were tested for this purpose: i) A commercially available matrix, GFR-Matrigel (refer to section 2.1.5.1 for preparation) and ii) custom made ECM from decellularised feeders from two different protocols (refer to section 2.1.5.2 for preparation).

Matrigel is a gelatinous substance secreted by Engelbreth-Holm-Swarm (EHS) mouse sarcoma cells. It is composed of a complex mixture of laminin, collagen IV and heparan sulfate proteoglycan (Xu *et al.*, 2001; Kleinman *et al.*, 1982). When diluted and allowed to polymerize, it can form a matrix that allows the long-term (≈ 130 population doublings) feeder-free culture of undifferentiated, karyotypically normal, hESCs. Moreover, it allows the hESCs to maintain their capacity to differentiate into the three germ layers (Xu *et al.*, 2001). Matrigel also has the advantage of being commercially available and very rapid to prepare (≈1 h). However, matrices generated with Matrigel contain animal products and could lack the endogenous 3 dimensional (3D) structure provided by HFF-feeders. For this reason, we also trialed custom made ECM from decellularised human fibroblasts. Several decellularisation protocols exist (Beacham *et al.*, 2007; Vlodavsky, 2001; Klimanskaya *et al.*, 2005) and such decellularised feeder matrices have already been successfully used for hESC derivation and culture (Klimanskaya *et al.*, 2005).

3.2.1 Comparison of two protocols for generating decellularised feeders

In order to obtain an ECM assembled by HFF with optimally preserved 3D structures, two protocols were compared in an initial set of experiments. One protocol contained an anionic detergent, DOC, and the other one Triton X-100, which is a non-ionic detergent.

Figure 3-3 demonstrates the presence of fibronectin as an ECM component secreted by fibroblasts. To confirm that the cell removal process preserved intact ECM, the decellularised feeder matrices were immunostained for fibronectin (Figure 3-4). The staining revealed that

both protocols are equivalent in terms of decellularisation as no cell nuclei can be observed (negative DAPI staining). However, the DOC protocol left intact mostly high molecular weight fibronectin aggregates (arrowheads), whereas the Triton X-100 protocol was gentler and both high molecular weight fibronectin aggregates as well as numerous fine fibronectin fibrils (arrows) could be seen. According to these results, it was decided that future decellularised feeders matrix would only be prepared according to the Triton X-100 protocol as it keeps a better integrity of the ECM and from now on, the term decellularised feeder matrix will only refer to ECM prepared as such.

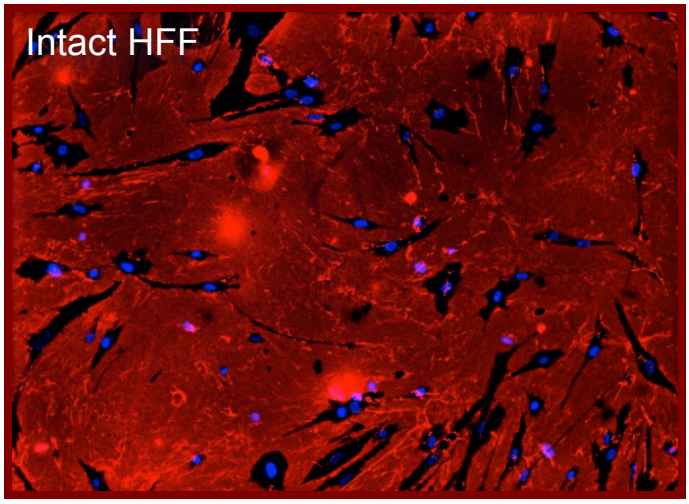

Figure 3-3: HFF-generated ECM immunostaining prior to decellularisation.
Fibronectin (red) and DAPI staining (blue). Images were taken at 40x magnification (Previously published in (Ilic *et al.*, 2012)

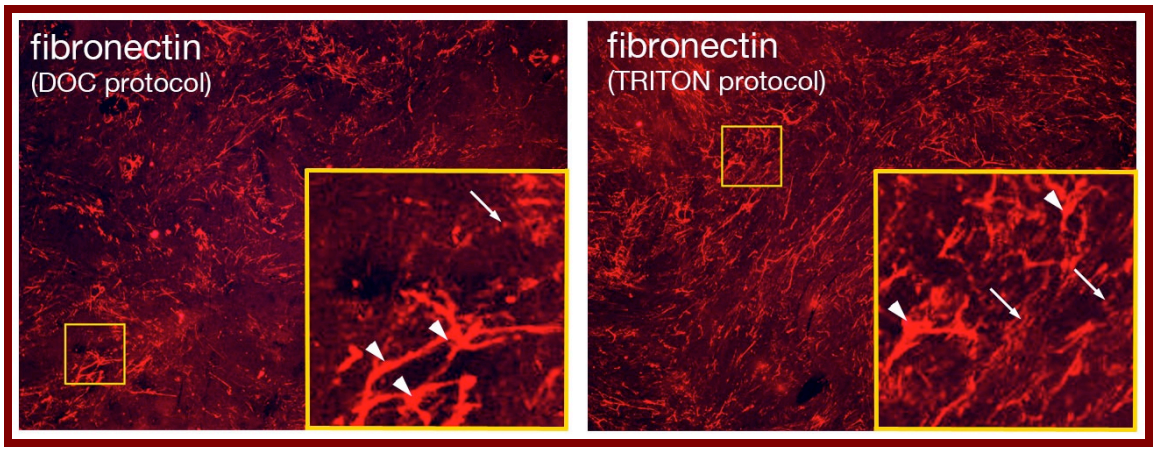

Figure 3-4: Decellularised feeder fibronectin immunostaining.
Decellularised feeder matrices made using DOC (left) and Triton X-100 (right) were immunostained for fibronectin (red). Images were taken at 100x magnification. In the insets, arrowheads indicate high molecular weight fibronectin aggregates and arrows indicate fine fibronectin fibrils. DAPI negative result indicates complete decellularisation.

3.2.2 Comparison of two defined media for hESCs feeder-free culture

We trialled two defined hESC culture media, complete KOSR-XF medium and mTeSR1, in combination with GFR-Matrigel or decellularised feeder matrices for hESC feeder-free culture, making a total of four feeder-free culture condition to test. They are summarised in Table 3-2.

Medium	Complete KOSR-XF	mTeSR1
Matrix	Decellularised feeder matrix	Decellularised feeder matrix
	GFR-Matrigel	GFR-Matrigel

Table 3-2: Summary of the feeder-free culture conditions tested on the hESCs

As mentioned in section 3.1, we considered that a hESC line is adapted to a new culture condition when propagated undifferentiated for over three passages under said condition. Maintenance hESC pluripotency was assessed by the following morphological criteria: i) well-defined colony edges; ii) tightly packed colonies and iii) absence of differentiated cells. The results are presented in Table 3-3.

Pluripotency criteria	Complete KOSR-XF		mTeSR1	
	Decellularised feeder matrix	**GFR-Matrigel**	Decellularised feeder matrix	**GFR-Matrigel**
Propagation for >3 passages in a culture condition	**-**	**-**	**+**	**+**
Well defined colony edges	**+/-**	**+/-**	**+**	**+**
Tightly packed colony	**+/-**	**+/-**	**+**	**+**
Absence of differentiated cells	**+/-**	**+/-**	**+**	**+**

Table 3-3: Comparison of hESCs culture on different feeder-free conditions.
+ = positive ; - = negative ; +/- = intermediate.

Complete KOSR-XF medium did not support the propagation of hESCs for over three passages on decellularised feeder matrix or on GFR-Matrigel. On the contrary, mTeSR1 allowed hESCs feeder-free propagation on both matrices for over three passages. hESC colonies remained positive for morphological criteria characteristic of undifferentiated hESCs (Figure 3-5). They were also positive for pluripotency markers as illustrated by immunostaining in Figure 3-6 and Figure 3-7.

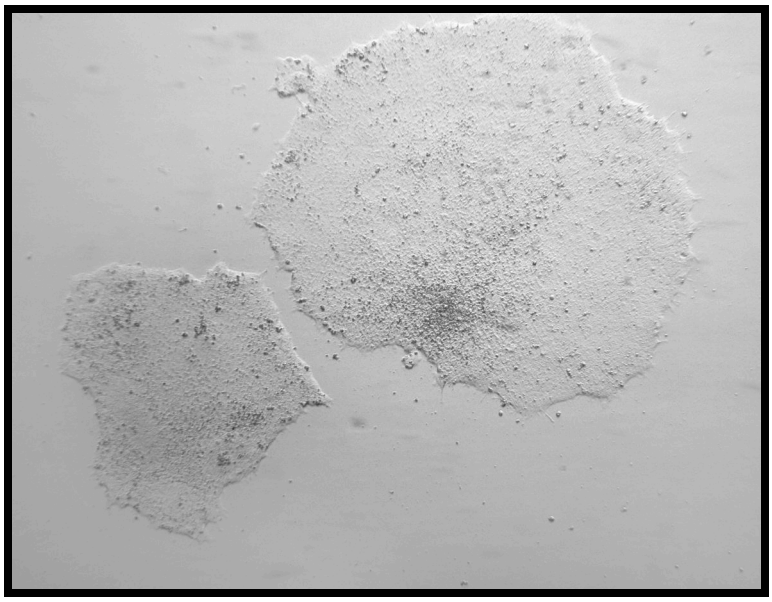

Figure 3-5: Undifferentiated KCL012_HD3 P14 cultured for five passages on GFR-Matrigel with mTeSR1 medium.
The image was taken at 40x magnification.

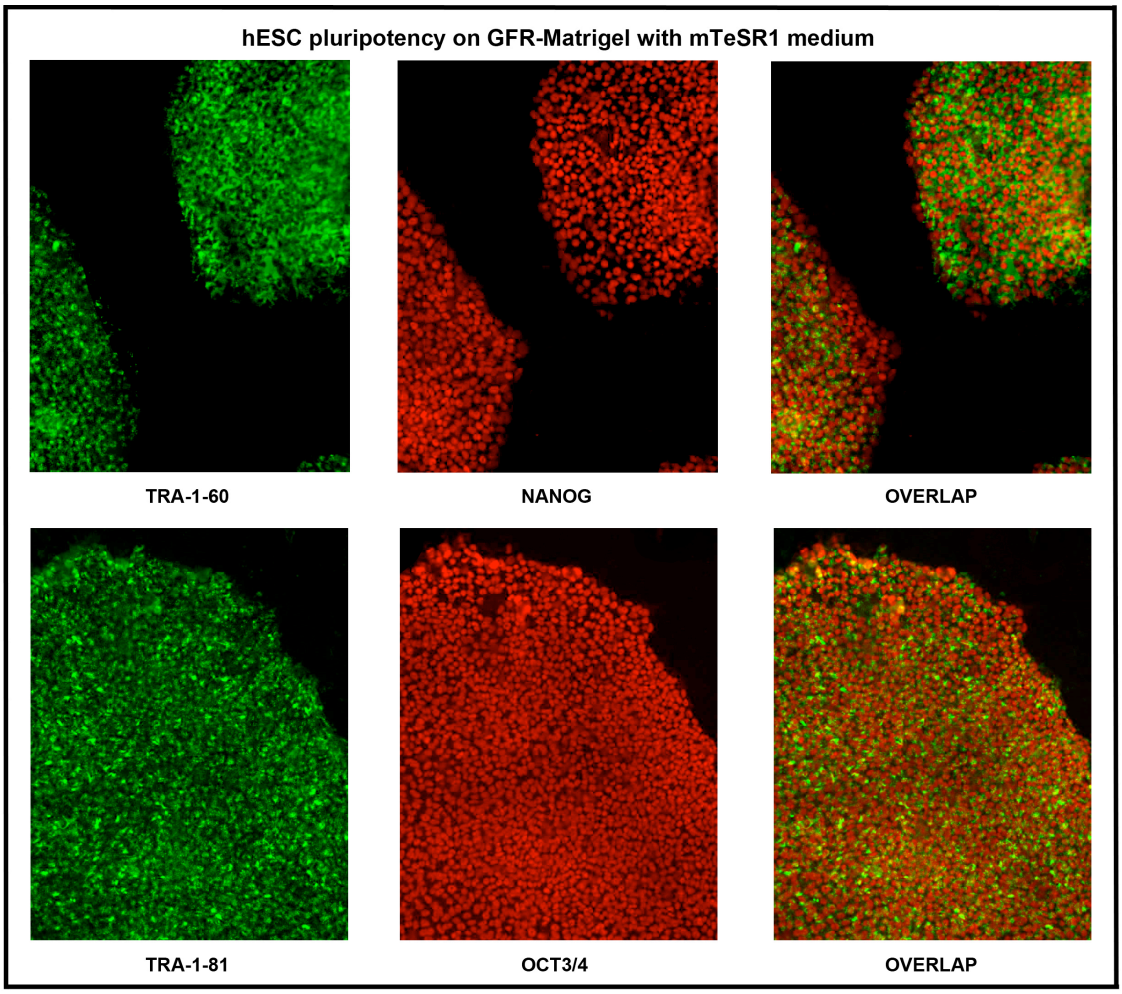

Figure 3-6 KCL012_HD3 P13 pluripotency on GFR-Matrigel in mTeSR1 medium.
All images were taken at 100x magnification.

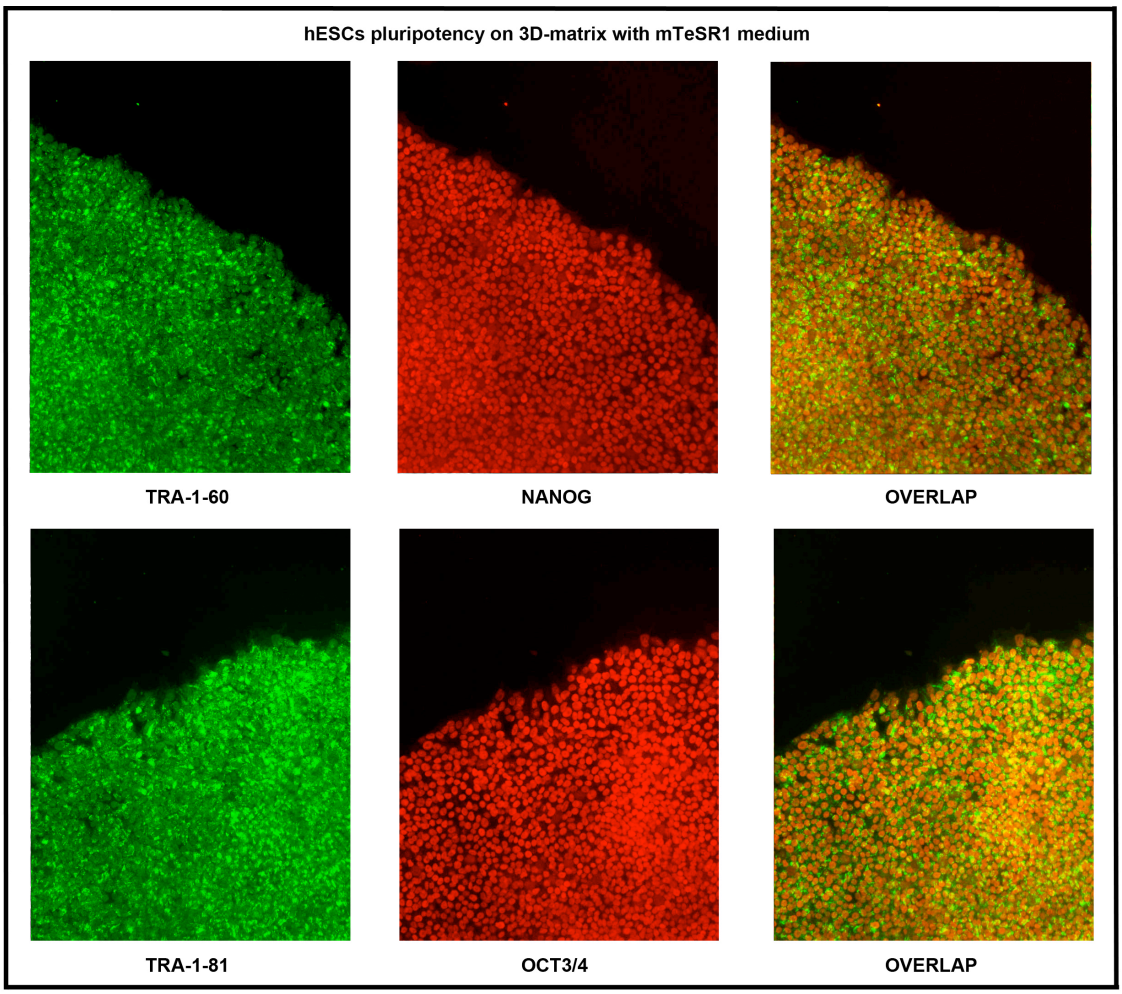

Figure 3-7: KCL012_HD3 P14 pluripotency on decellularised feeder matrix in mTeSR1 medium.
All images were taken at 100x magnification.

Once cultured feeder-free, enzymatic passaging of the hESCs with dispase was attempted. Only the mTeSR1/GFR-Matrigel feeder-free culture condition allowed enzymatic passaging. Subsequently, hESCs were only cultured in mTeSR1/Matrigel and passaged with dispase.

3.3 Discussion

In this set of experiments, we investigated whether KCL012_HD3, KCL020, KCL031, KCL034, KCL027_HD5, KCL028_HD6, KCL036_HD7 and KCL040, the eight hESCs lines derived at the ACU, King's College London used in this study would fulfil the two main hESC characteristics: i) indefinite self-renewal and ii) differentiation in all three germ layers. In order to demonstrate this, the hESCs lines, were first tested for the presence of pluripotency markers in undifferentiated hESCs and then subjected to differentiation *in vitro* and *in vivo*. All eight hESC lines used in this study fulfilled these criteria.

We also followed genomic stability of each cell lines over an extended period of culture. They all presented a normal karyotype upon derivation. However, KCL013_HD4 acquired an extra chromosome 12 over time and was thus removed from the study to prevent any biased future observation. Genomic instability in pluripotent stem cell culture, especially feeder-free, has been extensively discussed (Maitra *et al.*, 2005; Amps *et al.*, 2011; Lefort *et al.*, 2008). Chromosome 12 aneuploidy in particular has been suggested to provide a selective growth advantage (Catalina *et al.*, 2008; Mayshar *et al.*, 2010; Lefort *et al.*, 2008; Draper *et al.*, 2004).

Prior to any differentiation work, the eight hESCs lines used in this study had to be adapted to feeder-free culture conditions as well as enzymatic passaging. Indeed, a differentiation protocol such as Laflamme's cardiogenesis one, requires high undifferentiated hESCs cell numbers to begin with (2-4 x 10^5 cells / cm^2) (Laflamme *et al.*, 2007). A feeder-free culture condition with enzymatic passaging allows reaching such numbers in a considerably shorter-time. For this, two matrices, HFF-feeder-derived ECM from decellularised feeders and GFR-Matrigel, as well as two media, complete KOSR-XF medium and mTeSR1, were tested. It was first determined by morphological assessment that in our hands, mTeSR1 was the best medium for feeder-free culture with either matrix.

In addition to the ones tested in this study, there are many other feeder-free matrices available for hESC feeder-free culture. Human serum matrix has been shown to support undifferentiated hESC culture for over three months when used in combination with medium conditioned by hESC-derived fibroblast-like cells (Stojkovic *et al.*, 2005). ECM from human placenta, rich in collagen IV, laminin and fibronectin, has also been used for feeder-free hESC culture (Wang, Q. *et al.*, 2012).). Many ECM components of GFR-Matrigel and decellularised feeders e.g. laminin, fibronectin and vitronectin, can be used as individual ECM proteins to support feeder-free hESC culture. These are attractive as they are fully defined and can offer less batch-to-batch variability. Laminin can be used as a matrix when used in combination with high concentrations of bFGF (Li, Y. *et al.*, 2005). Amit *et al*. (2004) cultured hESCs on 2D layers of fibronectin for over 50 passages when used with a medium containing KOSR, bFGF, TGF-β and leukemia inhibitory factor LIF. Cells interact with their matrices via integrins. Vitronectin (Braam *et al.*, 2008; Kim, H.T. *et al.*, 2013), E-cadherin (Nagaoka *et al.*, 2010) and collagen I (Furue *et al.*, 2008) are also matrices supporting long-term feeder-free culture. Some groups have now moved on from biological components to fully chemically defined synthetic matrices (Irwin *et al.*, 2011; Melkoumian *et al.*, 2010), which could in the long term be cheaper and better for up-scaling hESC cultures. Another alternative is to completely bypass a 2D or 3D adherent cell culture system and culture the hESCs in suspension. Using mTeSR1 medium supplemented with Y-27632, Rho-associated kinase (ROCK) I inhibitor, hESC suspension culture has been shown to be efficient for long-term (over 20 passages) hESC feeder-free maintenance (Olmer *et al.*, 2010). The cells retained pluripotency and their ability to differentiate into the three germ layers. Interestingly, the hESCs cultured in suspension had a higher proliferation rate than cells cultured on feeder or on 2D-feeder-free matrices. This is attractive for the upscaling required by some differentiation protocols.

The eight hESC lines used in this study all had satisfactory undifferentiated morphologies when cultured in mTeSR1 with either GFR-Matrigel or decellularised feeder matrix. The pluripotency of the hESCs was nevertheless further confirmed by immunostaining for NANOG, OCT3/4, TRA-1-60 and TRA-1-81 (Figure 3-6 and Figure 3-7). The results were positive and support a previous comparative study that demonstrated that hESCs cultured feeder-free have a similar global gene expression pattern as hESCs cultured on feeders (Yoon *et al.*, 2010). In our hand, enzymatic passaging with dispase was only possible with the mTeSR1/GFR-Matrigel culture condition. This latter feeder-free culture condition was therefore used for the rest of this study. This is consistent with the International Stem Cell Initiative Consortium's results of a multicentre study that concluded that mTeSR1 used with Matrigel as a matrix and dispase for enzymatic passaging is one of the best combinations to support maintenance of most undifferentiated hESC lines (Akopian *et al.*, 2010).

This set of experiments confirms that the hESCs used in this study, whether wild-type of HD-specific, are i) pluripotent and ii) can be maintained in feeder-free culture conditions with enzymatic passaging, which is essential for up-scaling to obtain the large numbers of cells required for lineage specific differentiation.

Chapter 4

Induced Pluripotent Stem Cell Generation

Chapter 4 Induced Pluripotent Stem Cell Generation

The use of synthetic modified mRNA for fibroblast cell reprogramming resulted in a twice as fast, 36-fold higher reprogramming efficiency than retroviral reprogramming (Warren *et al.*, 2010). This method also presents the advantage of being non-integrative, meaning that the cells' genome will not be altered.

In this chapter are presented the repetition of the original Warren protocol (Warren *et al.*, 2010) on fibroblasts and HF-keratinocytes. When using retroviral vectors, HF-keratinocytes have been showed to reprogram 100 fold more efficiently and twofold faster than fibroblasts (Aasen *et al.*, 2008). It was hypothesized that combining HF-keratinocytes as a somatic cell source and synthetic modified mRNA as a delivery vector would result in a very efficient and rapid iPSC generation protocol. Furthermore, HF-keratinocytes are an easily accessible source of somatic cells. Hair plucking is a non-invasive and non-painful procedure, two important aspects when collecting patient samples. The original mRNA reprogramming protocol could not generate iPSCs in either cell type. It was later modified and allowed the successful reprogramming of the BJ fibroblast cells.

4.1 Fibroblast reprogramming with synthetic modified mRNA

4.1.1 Original mRNA reprogramming protocol (Warren *et al.*, 2010)

We first tested fibroblast reprogramming with synthetic modified mRNA on HFFs, which will be referred to as target cells. To do so, we plated 0.5 x 10^5 target cells on a layer of 1 x 10^5 HFF-feeders and transfected daily with mRNA reprogramming cocktail using RNAimax, a lipofectamine transfection reagent. The mRNA cocktail contains low-stability GFP (d2eGFP) mRNA, rendered nuclear with a 3' nuclear localisation sequence, for monitoring transfection efficiency. As indicated in the original mRNA reprogramming protocol (Warren *et al.*, 2010). Nutristem, a reprogramming medium, and 200 ng/mL of B18R, an interferon inhibitor, were included in the protocol. These conditions, however, did not support HFF reprogramming in our hands. Despite good transfection efficiency shown by uniform d2eGFP expression (data not shown), no mesenchymal-epithelial transition (MET) was observed. The experiment was terminated at day 15, as the cells survival was too low. It is worth noticing that even the cells that endured a 15 days mock transfection regimen (all the reagents but the mRNA) also had high cell death by day 15 (Figure 4-1). Lipofectamine had previously been reported to be of high efficiency and low toxicity. However, this was when used for two consecutive transfections, not 17 as required by this protocol (Zhao, M. *et al.*, 2008).

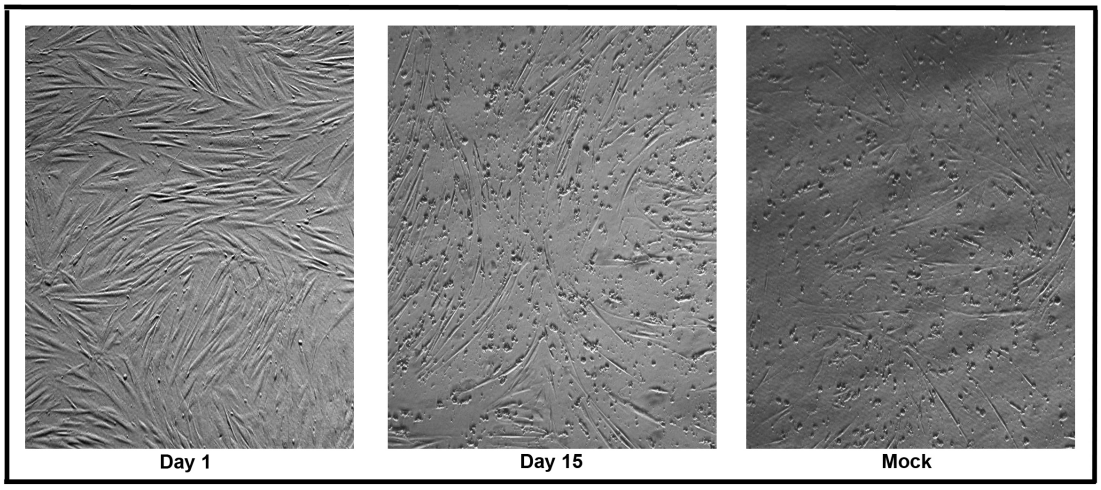

Figure 4-1: Human Foreskin Fibroblast at day 1 and 15 of the Warren (2010) mRNA reprogramming protocol.
On the far right are presented fibroblasts after 15 mock transfections (no mRNA). Images were taken at 40x magnification.

In this first experiment, we used three-times less HFF-feeders than in the original publication, which could be a factor contributing to the high cell death observed. In the second round of experiments, the number of feeders was increased to 3 x 10^5 cells/well of a 6-well dish, as outlined in the original protocol. Furthermore, different target cell densities ranging from 0.5-1.5 x 10^5 cells/well were evaluated. Reprogramming was still unsuccessful due to great cell death.

Valproic Acid (VPA), a Histone Deacetylase (HDAC) inhibitor, was reported to greatly increase fibroblast reprogramming (Huangfu *et al.*, 2008). Therefore, on our subsequent mRNA reprogramming experiment, we supplemented the reprogramming medium with 1 mM of VPA as from day five of the reprogramming protocol. In our hands, VPA did not improve reprogramming efficiency. No MET could be observed and the protocol had to be discontinued due to high cell death within 15 days of reprogramming. Even though VPA has been demonstrated to improve fibroblast reprogramming (Huangfu *et al.*, 2008), possibly by increasing protein production (Wulhfard *et al.*, 2010), VPA can also inhibit clonal cell proliferation and increase apoptosis even when used at doses lower than the one used in this protocol (Takai *et al.*, 2004; Fujiki *et al.*, 2013; Fortson *et al.*, 2011).

These results are in agreement with Warren's who trialled adding VPA to the mRNA reprogramming regimen and did not observe an increased reprogramming efficiency either.

4.1.2 Modified mRNA reprogramming protocol

During the course of this study, Stemgent started commercialising an mRNA reprogramming kit with a protocol that contained substantial modifications to the original published one. Modifications included: i) a lower target cells plating density, ii) a new reprogramming medium, iii) the use of conditioned-medium as from day 6 of the reprogramming protocol, iv) a different source and density of feeder cells and v) the elimination of the passaging step during the reprogramming protocol.

We took these changes into account in the next round of mRNA reprogramming protocol optimisation. Therefore, the target cell density was decreased from 0.5 x 10^5 cells / well of a 6-well plate to 7 x 10^3 per well of a 6-well plate. NuFF feeders from donor 11 were used instead of our regular HFF-feeders. Pluriton cell culture medium was used instead of Nutristem and NuFF-conditioned Pluriton was used from day 6 of the reprogramming protocol. Due to the high cell loss experienced previously, B18R concentration was increased from 200 ng/mL to 300 ng/mL. This was to further suppress the innate immune response triggered by the exogenous mRNA cocktail, which in turn would be beneficial for the cells to resist the consecutive transfections required by our protocol (Angel and Yanik, 2010). Furthermore, the cells were incubated with the B18R 4 h prior to the first transfection in order to condition the cells. Our last variation to the protocol was to add 0.5 mM final of Sodium Butyrate (NaBu) as from day 6 of the mRNA reprogramming protocol, with or without 1 µM of pifithrin-α (PTA-α) from day 2 of the mRNA reprogramming protocol. NaBu is an HDAC inhibitor which when used at 0.5 mM, can not only improve cell reprogramming, but do so at a greater efficiency than VPA (Zhang, Z. *et al.*, 2011). p53 negatively regulates somatic cell reprogramming, notably by its pro-apoptotic role. Transiently inhibiting it with an inhibitor such as PTA-α can increase iPSC generation by up to four folds (Hong *et al.*, 2009; Kawamura *et al.*, 2009; Zhao, Y. *et al.*, 2008; Marion *et al.*, 2009). A summary of the modifications is presented in Table 4-1.

Procedure	**Warren *et al*.(2010)**	**Modified protocol**
Feeder cell density	3 x 10^5 cells/well of 6-well dish	2.5 x 10^5 cells/well
Target cell density	5-30 x 10^4 cells/well	7 x 10^3 cells/well
Reprogramming medium	Nutristem with 100 ng/mL bFGF	Pluriton with 1X Pluriton supplement
Use of conditioned medium	No	Yes, as from day 6
B18R concentration	200 ng/mL	300 ng/mL
Sodium butyrate (NaBu) concentration	0	0.5 mM
Pifithrin-α (PTA-α) concentration	0	1 µM from day 2 (optional)

Table 4-1: Summary of the differences between the original Warren *et al*. (2010) mRNA reprogramming protocol and our modified one.

The modified protocol allowed the reprogramming of BJ fibroblasts into iPSCs using mRNA reprogramming cocktail. The cells were monitored daily for morphological changes and d2eGFP expression. The reprogramming experiments are presented in Figure 4-2 and Figure 4-3.

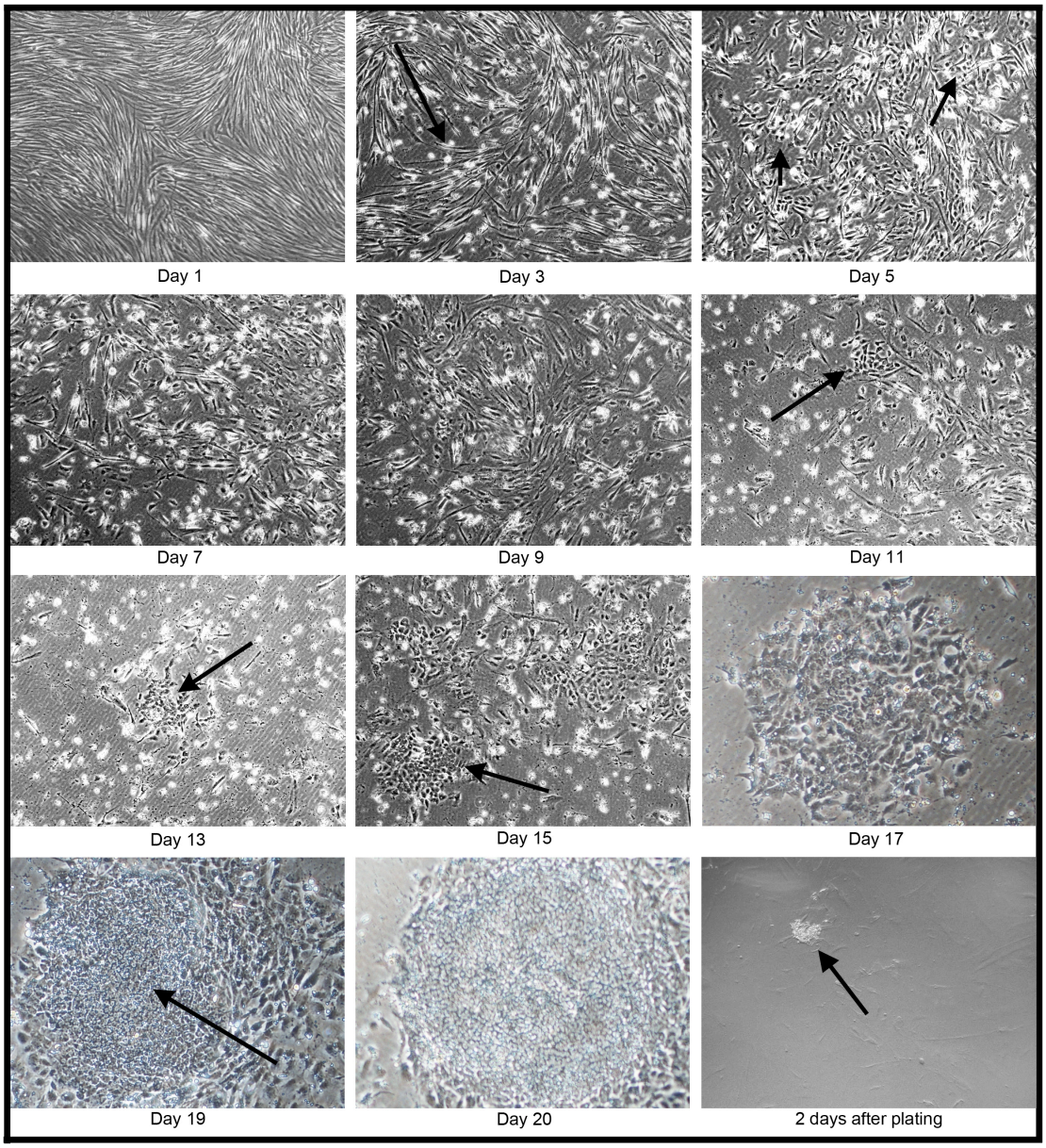

Figure 4-2: Representative morphology of BJ fibroblasts plated on NuFF-feeders undergoing mRNA reprogramming with daily transfections and NaBu treatment.
Images were taken at 40x magnification. **Day 1:** Healthy cells after the first transfection. **Day 3:** Cell loss and cell rounding, a pre-apoptotic sign (arrows) can be observed. **Day 5:** Cells start undergoing MET and adopt an epithelial morphology (arrows) **Day 7 and 9:** Increase in cell death. Surviving cells are transitioning. **Day 11:** First sign of compaction and colony formation (arrow). **Day 13:** Increased compaction. Cells become smaller and more hESC-like (arrow). **Day 15**. Increase in colony size (arrow). **Day 17:** Last transfection. Note that only reprogrammed cells survived all 17 transfections and keep increasing in colony size. **Day 19:** Cells are fed with NuFF-conditioned Pluriton. Colony center (arrow) keeps compacting as cells continue to reprogram and adopt a stem cell morphology. **Day 20:** The colony center is ready for picking and being plated on HFF-feeders in complete KOSR medium. **2 days after plating:** All the colonies plated have attached and can be left to expand.

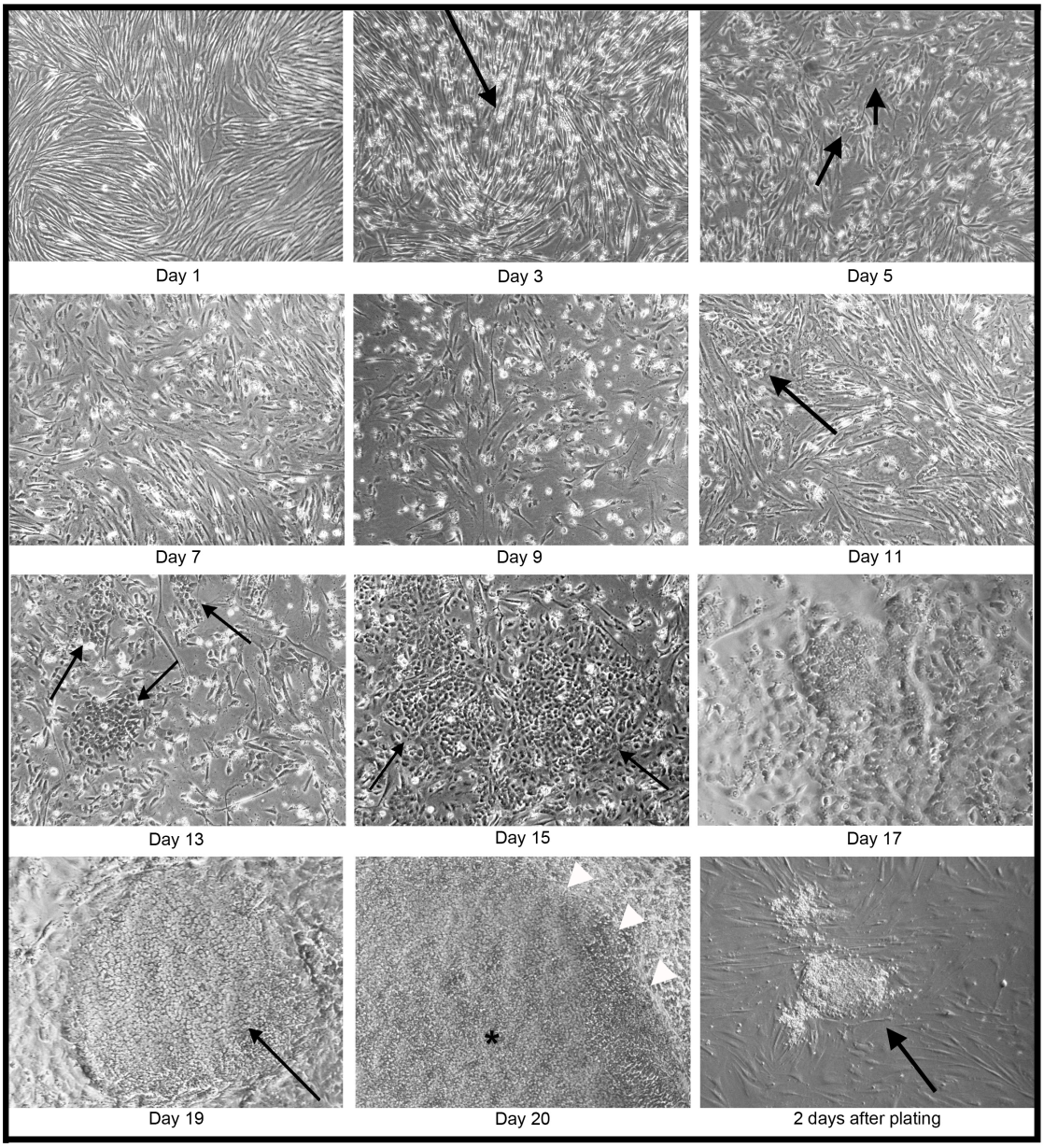

Figure 4-3: Representative morphology of BJ fibroblasts plated on NuFF-feeders undergoing mRNA reprogramming with daily transfections and NaBu and PTA-α treatment.
Images were taken at 40x magnification. **Day 1:** Healthy cells after the first transfection. **Day 3:** Cell loss and cell rounding, a pre-apoptotic sign (arrow) can be observed. **Day 5:** Cells start undergoing MET and adopt an epithelial morphology (arrows) **Day 7 and 9:** Increase in cell death. Surviving cells are transitioning. **Day 11:** First sign of compaction and colony formation (arrow). **Day 13:** Increased compaction. Cells become smaller and more hESC-like (arrows). **Day 15**. Increase in colony size (arrows). **Day 17:** Last transfection. Colonies are compact and increase in size. **Day 19:** Cells are fed with NuFF-conditioned Pluriton. Colony center (arrow) keeps compacting as cells continue to reprogram and adopt a hESC-like morphology. **Day 20:** Colonies are very big with defined edges (white arrow heads). Colony center (asterix) is ready for picking and being plated on HFF-feeders in complete KOSR medium. **2 days after plating:** All the colonies plated have attached and can be left to expand (arrow).

The modified mRNA reprogramming protocol successfully gave rise to iPSC colonies. Good d2eGFP, representing good transfection efficiency, could be observed throughout the reprogramming experiments (data not shown). Less cell death was observed in the presence of PTA-α (Figure 4-2), and the emerging colonies were more compact and easier to pick. Reprogramming efficiency was greater in the presence of 1 μM PTA-α (0.86% vs. 0.66%, illustrated in Figure 4-4). Nevertheless, this was still lower than the 4% efficiency reported by Warren *et al*. (2010).

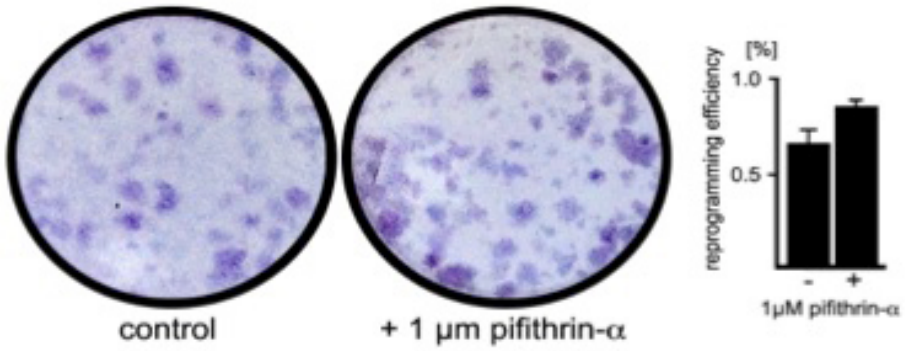

Figure 4-4 Trypan blue staining of colonies formed in the presence or absence of 1 μM PTA-α in one well of 6-well plate and an average reprogramming efficiency from two independent experiments.

Good d2eGFP could be observed throughout the reprogramming experiments (data not shown). Less cell death was observed in the presence of PTA-α, and the emerging colonies were more compact and easier to pick. Reprogramming efficiency seemed greater in the presence of PTA-α. However, by day 20 of the reprogramming protocols, the iPSC colonies were big and merged together. A final number of iPSC colonies could not be determined. Regardless, iPSC colonies from both treatment groups could successfully be plated in our regular hESCs culture conditions (i.e. on HFF-feeders in complete KOSR medium). The cells attached and expanded well. Upon passaging on HFF-feeders, they maintained typical undifferentiated hESC morphology and presented with typical hESC morphology (**Figure 4-5**).

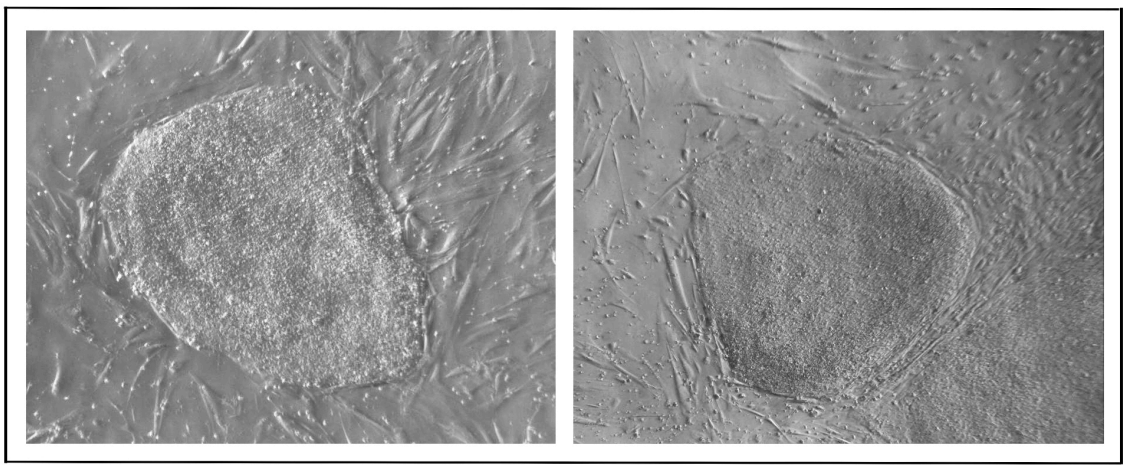

Figure 4-5: iKCL004 and iKCL011 colonies cultured in complete KOSR medium on HFF-feeders.

iKCL004 P2 (left) and iKCL011 P2 (right). The cells have typical hESC morphology. Images were taken at 40x magnification.

4.2 Adaptation of iPSCs to feeder-free culture conditions.

Two iPSC lines with similar population doublings were selected for characterisation, iKCL004 and iKCL011. The former was reprogrammed with NaBu treatment only and the latter was reprogrammed with both NaBu and PTA-α treatments. Both iPSC lines were successfully adapted to feeder-free culture conditions (GFR-Matrigel / mTeSR1) as illustrated in Figure 4-6. No differences in morphology or proliferation rate could be observed between the cell lines.

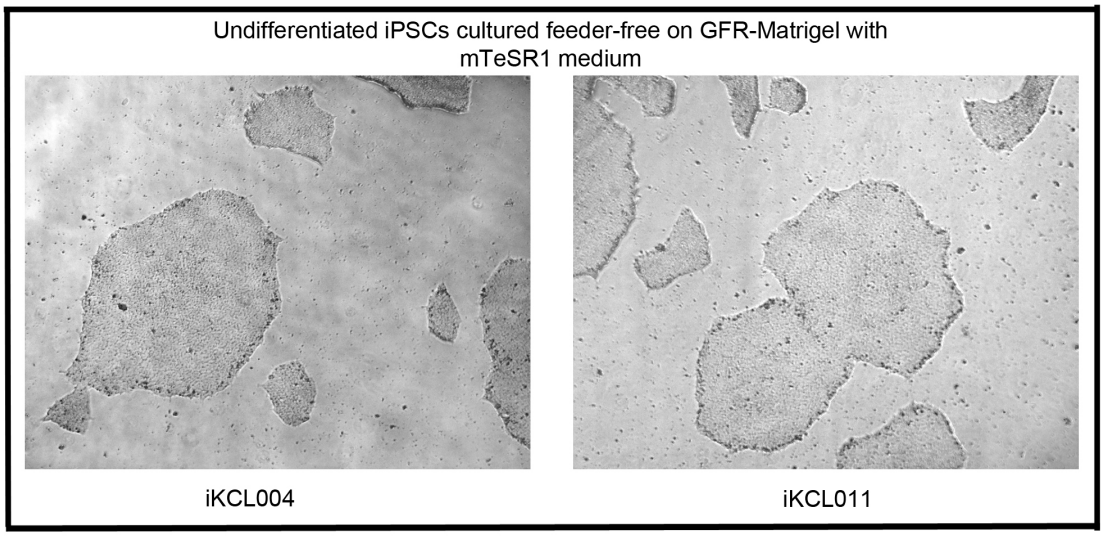

Figure 4-6: iKCL004 P11 and iKCL011 P11 iPSCs lines cultured feeder-free on GFR-Matrigel with mTeSR1 medium.
Both lines have morphologies characteristic of undifferentiated iPSCs. Images were taken at 40x magnification.

4.3 iPSCs characterisation

4.3.1 Pluripotency characterisation

The two chosen iPSC lines, iKCL004 and iKCL011, were characterised by following the methods described in section 2.1.9 according to five criteria: i) morphological criteria, ii) detection of pluripotency markers: alkaline phosphatase activity, OCT4, NANOG, TRA-1-60 and TRA-1-8, iii) differentiation into three germ layers *in vivo*, iv) genotyping, v) determination of genomic stability. HLA typing was omitted since the cell lines will be used for research only and not clinically. The morphological criteria were met for both lines as the cells presented with an hESC-like undifferentiated morphology (Figure 4-5 and Figure 4-6). The pluripotency characterisation and teratoma formation results for iKCL004 are presented in Figure 4-7 and Figure 4-8 respectively and the pluripotency characterisation and teratoma formation results for

iKCL011 are presented in Figure 4-9 and Figure 4-10 respectively. The positive results confirm that the iPSCs derived from the BJ cell line using the modified mRNA reprogramming protocol. iPSCs generated with or without p53 inhibition are equally pluripotent and express the same *in vitro* pluripotency markers as the hESCs used in this study. Similarly to our hESC lines, both iPSC lines also have the ability to differentiate *in vivo* into the three germ layers.

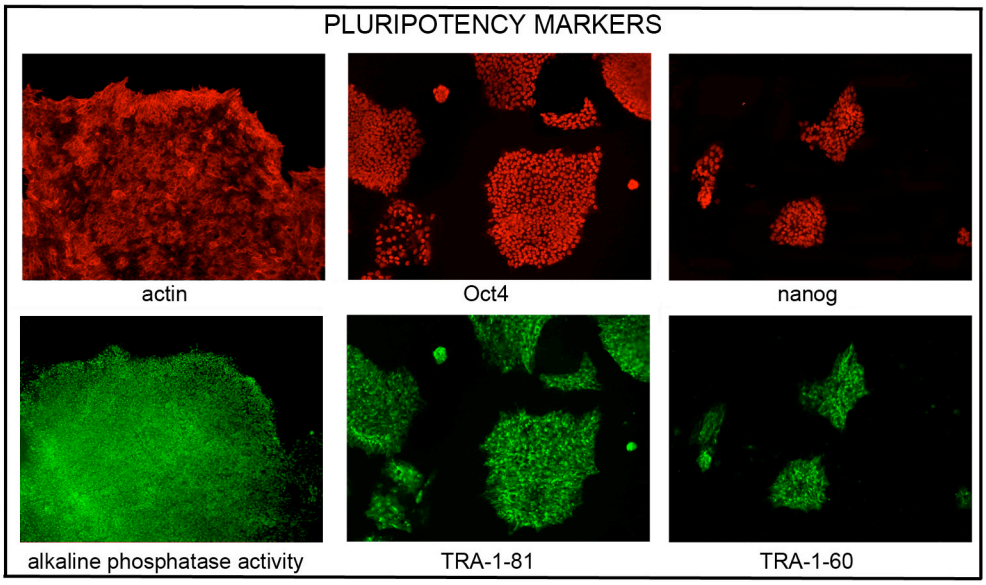

Figure 4-7: iKCL004 cultured on GFR-Matrigel with mTeSR1 pluripotency characterisation.
All images were taken at 40x magnification.

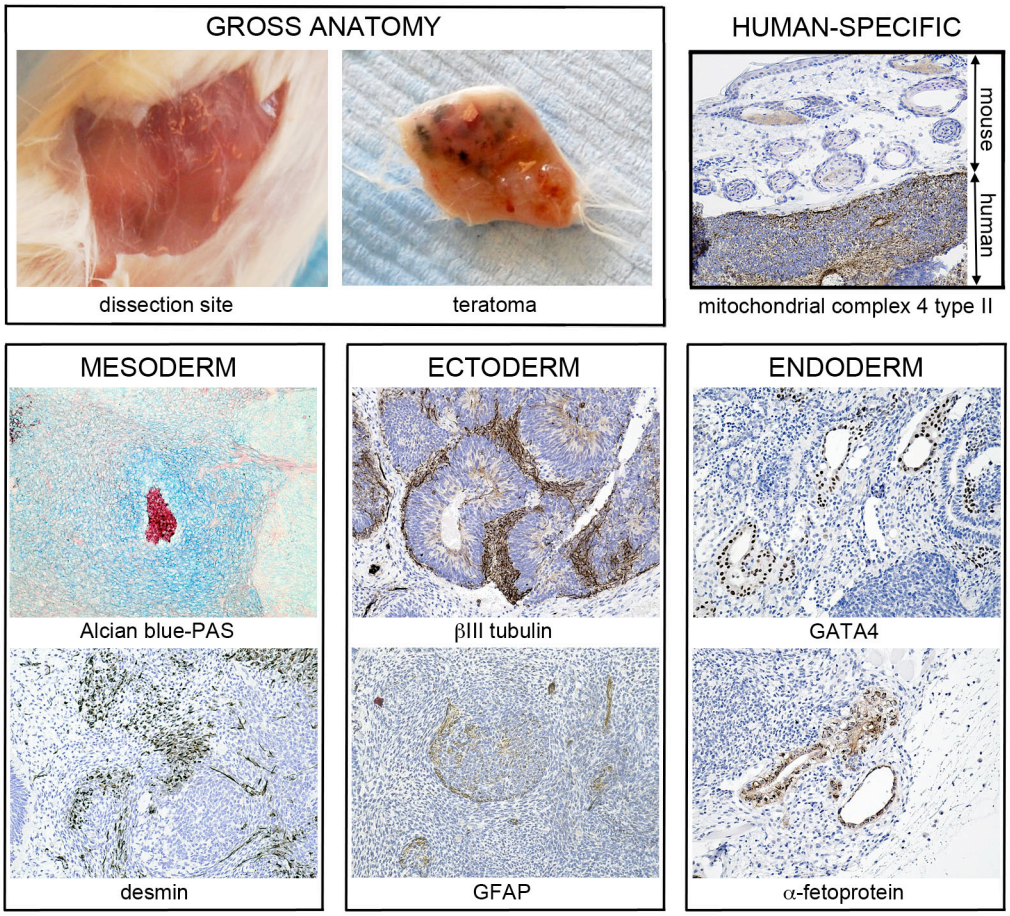

Figure 4-8: iKCL004 Teratoma characterisation
Histological images were taken at 40x magnification.

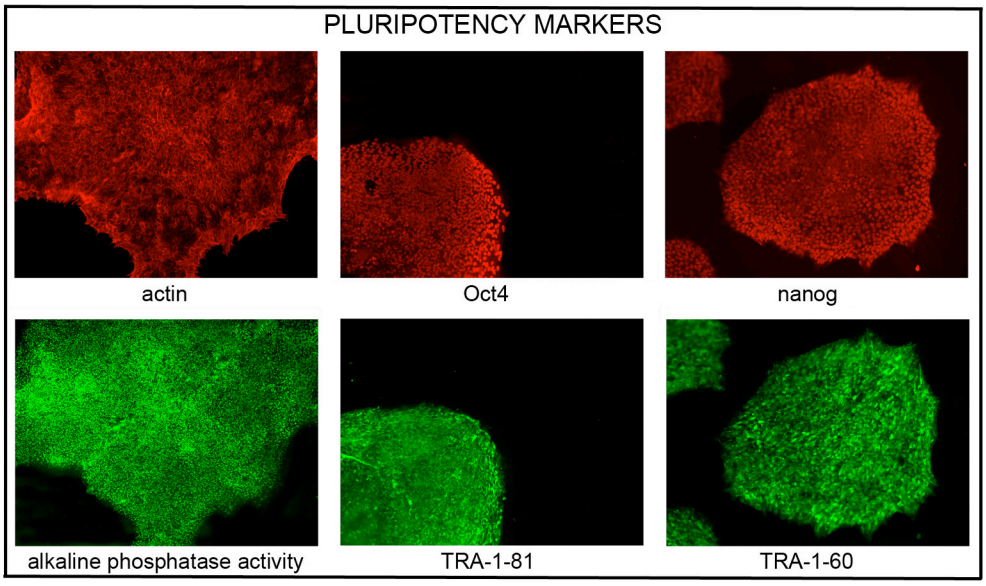

Figure 4-9: iKCL011 cultured on GFR-Matrigel with mTeSR1 pluripotency characterisation.
All images were taken at 40x magnification.

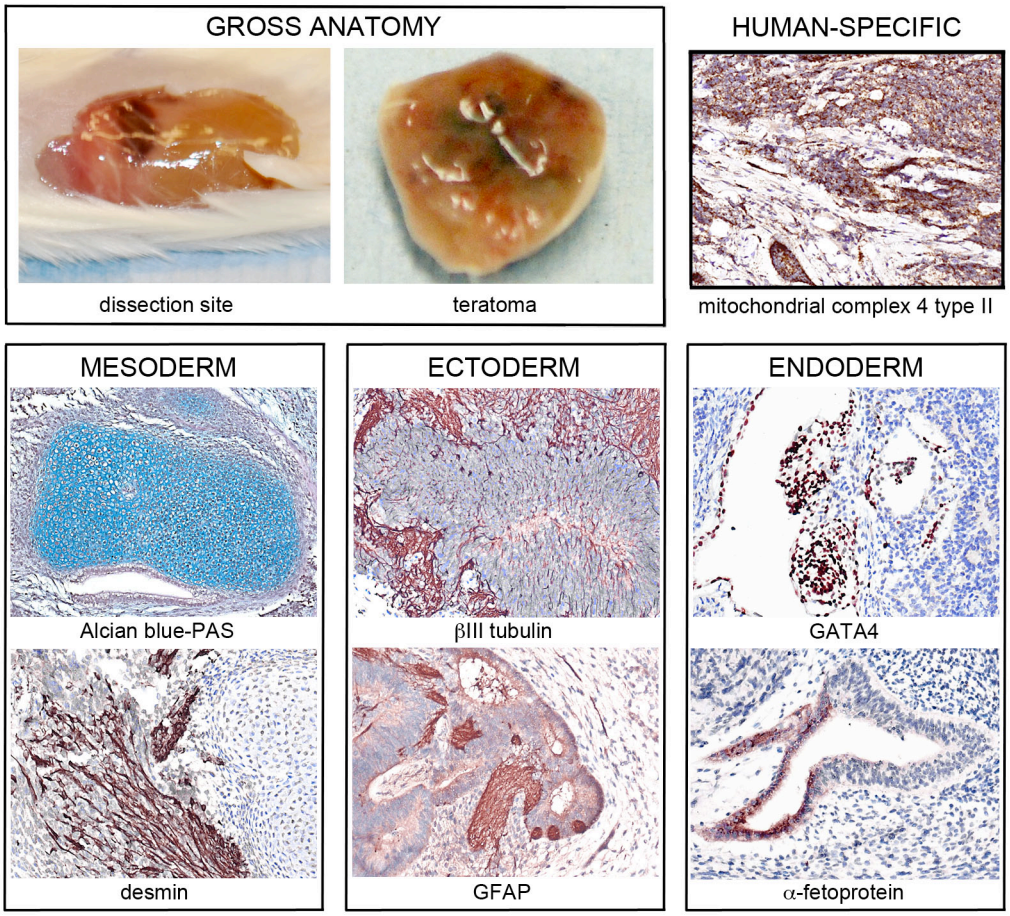

Figure 4-10: iKCL011 teratoma characterisation.
Histological images were taken at 40x magnification.

4.3.2 DNA Fingerprinting

We confirmed that the two preferred iPSC lines, iKCL004 and iKCL011 were derived from the BJ somatic donor cells with DNA fingerprinting. Results are presented in Table 4-2.

	BJ		iKCL004		iKCL011	
Marker	**Allele 1**	**Allele 2**	**Allele 1**	**Allele 2**	**Allele 1**	**Allele 2**
D13S252	299	299	298	298	299	299
D13S325	289	293	289	293	289	293
D13S628	454	457	454	457	454	457
D13S634	403	415	403	415	403	415
D18S386	381	386	381	386	380	386
D18S390	368	376	368	376	368	376
D18S391	217	217	217	217	218	218
D18S535	486	490	486	490	486	491
D18S819	408	416	407	416	407	415
D18S976	472	481	472	480	472	481
D18S978	207	211	207	211	207	211
D21S11	245	245	245	245	245	245
D21S1409	216	224	216	224	216	224
D21S1411	308	328	308	328	308	328
D21S1435	180	184	180	184	181	185
D21S1446	311	325	311	325	312	326

Table 4-2: DNA fingerprinting results for the BJ somatic fibroblast cell line and the iKCL004 and iKCL011 iPSC lines derived from it.
The occasional 1bp size difference is due to the size differentiation by capillary electrophoresis.

4.4 Keratinocyte-derived iPSCs generation using synthetic modified mRNA

4.4.1 Keratinocytes derivation and culture

As mentioned previously, the target HD somatic cells for iPSC reprogramming were HF-keratinocytes. Firstly, HF-keratinocytes derivation and culture were optimised from the Aasen protocol (Aasen *et al.*, 2008) on samples from healthy donors. After taking patient consent, hairs were plucked and only hair follicles with a visible ORS, and indication of being in the proliferative anagene phase (Alonso and Fuchs, 2006), were kept. The adapted protocol (described in 2.2.3) allowed good HF-keratinocyte derivation and culture. Positive immunostaining for Keratin 14 (K14), a basal epithelial keratinocyte marker. confirmed that the cells migrating out of the ORS are keratinocytes (Figure 4-11).

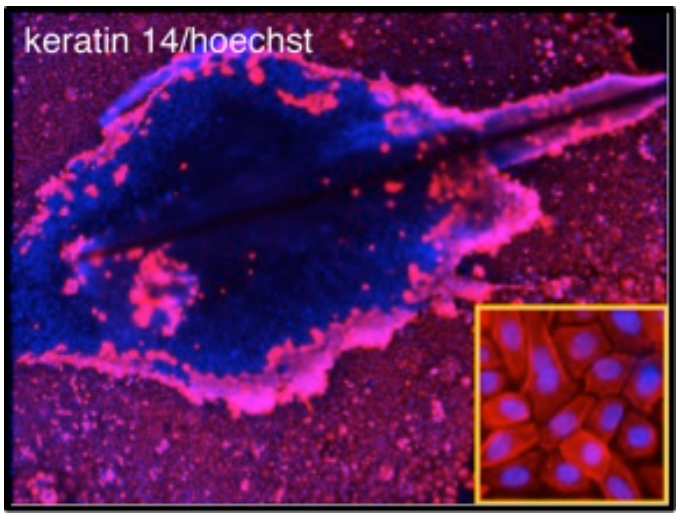

Figure 4-11: Keratinocyte keratin 14 immunostaining.
Keratin 14 (red) and Hoechst (blue) staining of hair follicle-derived keratinocytes. Image was taken at 40x magnification. Inset image is 400x magnification.

4.4.2 HD Patients keratinocyte sample collection

Patient hair sample collection was performed in the same way as for healthy individuals. However, there was a great variability in the quality of the samples collected and the subsequent good isolation and culture of the HF-keratinocytes. No HD-patient HF-keratinocytes culture could be expanded in sufficient number to allow mRNA reprogramming (Table 4-3).

Patient	Project	Anonymous ID number	KCL nb	date	plucking by	Symptomatic	CAG rpt nb	number of hairs plated	hairs attached	outgrowth	outcome
patient 1	K_iPSC_HD	486583344	HD1_K	20/10/2012	SH/LJ	yes	19/49	6	2	1	Poor growth, not possible to expand. discarded 16/12/10. No frozen stock
patient 2	K_iPSC_HD	36112102X	HD2_K	05/07/2012	SH	yes	19/43	4	4	0	Discarded on 23/7/12
patient 3	K_iPSC_HD	623563615	HD3-K	05/07/2012	SH	yes	-/42	6	6	0	Discarded on 23/7/12
NA	K_iPSC_HD	667-793-735	NA	02/08/2012	SH		13/45	0	0		
patient 4	K_iPSC_HD	917-669-620	HD4-K	02/08/2012	SH	no	17/43	15	14	7	discarded 2/9/12. passaged cells never divided
patient 5	K_iPSC_HD	336-899-812	HD5-K	02/08/2012	SH	no	18/42	6	6	3	discarded 2/9/12. passaged cells never divided
patient 6	K_iPSC_HD	994-352-93x	HD6-K	02/08/2012	SH	yes	24/42	7	6	0	dicarded 16/8/12, no outgrowth
patient 7	K_iPSC_HD	737-785-88X	HD7-K	16/08/2012	SH	yes	21/46	4	3	1	discarded 5/10/12, cells senescing
patient 7	K_iPSC_HD	737-785-88X	HD7-K	10/09/2012	SH	yes	21/46	2	0	1	discarded 16/9/12
patient 8	K_iPSC_HD	755-859-71X	HD8-K	06/09/2012	SH	no	n/a	6	1	1	discarded 1/10/12
patient 9	K_iPSC_HD	131-076-837	HD9-K	06/09/2012	SH	no	-/42	6	2	2	discarded 5/11/12 p1. senescing
patient 10	K_iPSC_HD	594-436-170	HD11-K	12/09/2012	SH	yes	18/45	9	9	9	discarded 5/11/12 p1. senescing
patient 11	K_iPSC_HD	852-862-483	HD10-K	17/09/2012	SH	yes	21/45	9	4	0	discarded 1/10/12

Table 4-1 Repertory of the patient samples collected for this study.
CAG corresponds to the CAG repeat number of *HTT.*

4.4.3 Keratinocytes reprogramming with synthetic modified mRNA

4.4.3.1 Original Warren *et al.* (2010) mRNA reprogramming protocol

Even though it was not possible to attempt reprogramming HD keratinocytes due to insufficient cell number derivation (Table 4-3) we tried the original Warren protocol on HF-keratinocytes isolated from healthy individuals. To do so, 0.6–1 x 10^5 HF-keratinocytes were plated on 3 x 10^5 HFF-feeders/well of a 6-well dish and the cells were transfected daily with the mRNA reprogramming cocktail. As for the fibroblasts, excessive cell loss rapidly occurred no colony formation was observed. The experiments were terminated at day 15, without generating iPSCs (Figure 4-12).

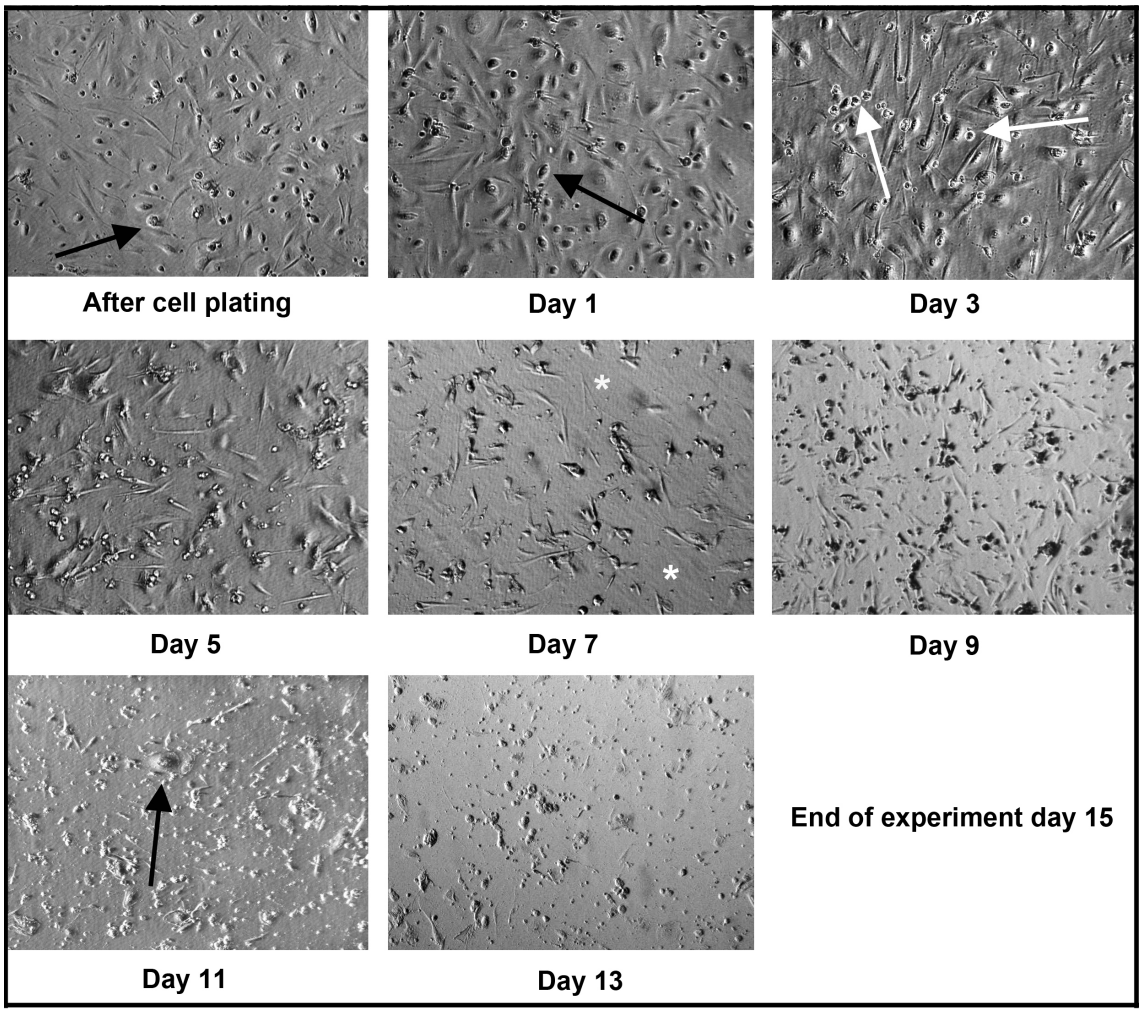

Figure 4-12: Representative morphology of healthy HF-keratinocytes plated on HFF-feeders undergoing mRNA reprogramming with daily transfections.
Images were taken at 40x magnification. **After cell plating:** Healthy HF-keratinocytes (black arrow) on an HFF-feeder layer. **Day 1:** Healthy HF-keratinocytes after the first transfection (black arrow). **Day 3:** Cell rounding, a pre-apoptotic sign (white arrows) can be observed. **Day 5:** Overall cell loss is observed. **Day 7:** Excessive cell loss observed. Areas indicated by the white asterisks are completely depleted from cells. **Day 9:** No improvement and no signs of cells starting to reprogram. **Day 11:** Only a few HF-keratinocytes (black arrow) can be observed in culture. Their morphology indicates that they are not reprogramming. **Day 13:** No more healthy cells left in culture. The experiment was terminated at **day 15**.

4.4.3.2 Modified mRNA reprogramming protocol

The modified mRNA reprogramming protocol using Pluriton medium was experimented on the HF-keratinocytes. Unlike with the fibroblasts, it did not improve mRNA reprogramming and did not give rise to iPSCs. After two days in Pluriton medium, the HF-keratinocytes differentiated and adopted a stratified morphology (Figure 4-13). Keratinocytes are sensitive to calcium-induced differentiation, which can be triggered by extracellular calcium concentrations greater than 0.06 mM (Aasen and Belmonte, 2010). Pluriton's calcium concentration is a proprietary information and we cannot confirm whether it is the cause for the keratinocyte differentiation we observed. The differentiated keratinocytes could not be transfected by our mRNA cocktails, as observed by the negative d2eGFP expression (data not shown).

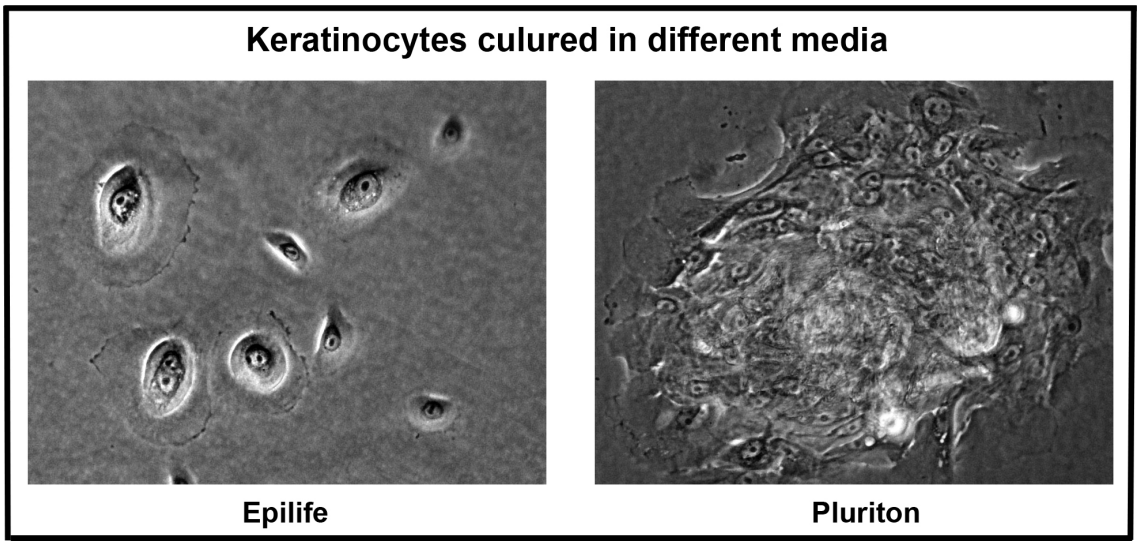

Figure 4-13: Keratinocytes cultured in Epilife (keratinocyte medium) and Pluriton (mRNA reprogramming medium) for 48h.
Keratinocytes differentiated and exhibited a stratified morphology after exposure to Pluriton. Images were taken at 100x magnification.

4.5 Discussion

We trialled the mRNA reprogramming protocol originally published by Warren *et al*. (2010) on fibroblasts but could not be reproduce it due to high cell death. We optimised the mRNA reprogramming protocol, notably by increasing the concentration of B18R and using NaBu with or without PTA-α. Both treatment groups successfully gave rise to iPSCs. One iPSC line from each treatment group (iKCL004 and iKCL011 respectively) was adapted to feeder-free culture before being characterised. Both iPSC lines equally maintained hESC-like morphology and tested positive for the presence of pluripotency markers. The lines were also differentiated *in vivo* and tested positive for the presence of the three germ layers. Finally, DNA fingerprinting

confirmed that the iKCL004 and iKCL011 iPSCs lines were derived from the same BJ fibroblast somatic donor line.

Other groups have demonstrated transient inactivation of p53 during reprogramming is beneficial and leads to an increased reprogramming efficiency (Hong *et al.*, 2009; Kawamura *et al.*, 2009; Zhao, Y. *et al.*, 2008; Marion *et al.*, 2009). We observed an overall decreased cell death and more compact iPSC colonies in cells treated with PTA-α. We observed a 30% increase in iPSC colony numbers upon PTA-α treatment. Basic characterisation of iKCL004 and iKCL011 does not suggest any obvious differences between the lines. p53 mainly ensures fidelity of DNA replication and maintenance of cellular epigenetic stability, by inducing apoptosis in cells undergoing undesirable changes in order to prevent their proliferation (Jackson-Grusby *et al.*, 2001; Leonova *et al.*, 2013; Marion *et al.*, 2009). Even though p53 activation during iPSC generation is partly responsible for poor reprogramming efficiency, it could also to some extent be seen as beneficial as it prevents the reprogramming of cells with DNA damages. In the absence of p53, interferon I-mediated cell death can take over to prevent the proliferation of cells with a disturbed epigenetic state (Leonova *et al.*, 2013). Yet, our mRNA reprogramming protocol includes B18R, an interferon I inhibitor required to suppress the native immune response triggered by the multiple exogenous mRNA transfections required by our reprogramming protocol (Angel and Yanik, 2010; Warren *et al.*, 2010). B18R treatment could prevent interferon-mediated cell death to take place in the absence of p53. Transient p53 inactivation coupled with interferon I inhibition could lead to the generation of iPSC lines with higher DNA damage rates. Therefore, further complementary characterisation of iKCL004 and iKCL011 is necessary. It would include pairwise comparison of the iPSC lines for whole-genome DNA methylation and whole-exome sequencing. We are anticipating DNA demethylation of pluripotency-associated genes in both iPSCs lines compared to the BJ somatic donor line (Reik, 2007; Guenther *et al.*, 2010). When comparing to one of our hESC lines, we are likely to observe some differences as iPSCs have a distinct gene signature from hESCs, partly because of the persistence of some of the donor somatic cell's gene expression even after reprogramming (Ghosh *et al.*, 2010; Streckfuss-Bomeke *et al.*, 2012; Ruiz *et al.*, 2012; Chin *et al.*, 2009). Yet, regardless of the donor cell type, iPSCs can have up to nearly 3% of differentially methylated CpG site, mainly due to *de novo* hypermethylations acquired during reprogramming. These epigenetic differences can then in turn be associated with changes in gene expression (Ruiz *et al.*, 2012). It would be interesting to see if such differences are more prominent in iKCL011, our PTA-α-treated iPSC line. For complementary information, whole-exome sequencing could be performed on our iPSCs. It would allow us to determine if PTA-α treatment induced any somatic mutations or rare genetic variants (Ng, S.B. *et al.*, 2009).

HF-keratinocytes was the ultimate somatic cell type to be reprogrammed using mRNA. For this, we derived HF-keratinocytes from anagen-phase hair follicles. This was achieved by successfully adapting the Aasen *et al*. (2008) protocol on hair follicles plucked from healthy donors. Keratin 14 positive keratinocytes cultures could be isolated and expanded. As for the fibroblasts, the original Warren *et al.* (2010) mRNA reprogramming protocol was tried on the HF-keratinocytes. No iPSCs could be derived due to high cell death. The protocol modifications

that led to a successful fibroblast mRNA reprogramming protocol could not be applied to the HF-keratinocytes. Indeed, the new reprogramming medium, Pluriton, led to HF-keratinocytes differentiation and cell cycle arrest. HF-keratinocytes are an attractive source of somatic cells for iPSC generation due to their higher efficiency and rapidity to reprogram compared to fibroblasts (Aasen *et al.*, 2008). Several groups reprogrammed keratinocytes from various origins with retroviral or lentiviral vectors (Linta *et al.*, 2012; Kim, K. *et al.*, 2011; Zhu *et al.*, 2010; Novak *et al.*, 2010; Petit *et al.*, 2012). However, it seems that in our hands HF-keratinocytes are not as robust as fibroblasts to survive the 18 consecutive mRNA transfections required by the Warren protocol. Furthermore, the Pluriton medium used in the optimised protocol induced differentiation of the HF-keratinocytes, which in turn prevented them from being transfected. The other constraint associated with HF-keratinocytes encountered in this project was the high variability in HF-keratinocytes derivation success. No HD HF-keratinocytes could be derived in sufficient number for reprogramming. Patients were in their mid 40s to 50s and age could explain less efficient HF-keratinocyte derivation. It was observed that HF-keratinocytes could not be derived from white hairs for instance. Other environmental factors could also be responsible for poor HF-keratinocytes derivation. Patient 6 was notably taking Methotrexate, a chemotherapy drug that can affect hair growth (Table 4-3).

At the time of writing, no other group published iPSC lines generated using the original Warren *et al*. (2010) protocol. It has been acknowledged in recent publications by the authors that Pluriton medium is more robust and better to use with this protocol than Nutristem (Warren *et al.*, 2012; Mandal and Rossi, 2013). One option to improve HF-keratinocytes mRNA reprogramming would be to progressively switch them from the HF-keratinocyte culture medium to the iPSC reprogramming medium in order to prevent calcium-induced HF-keratinocytes differentiation. Furthermore, the addition of 10 µM of Y-27632 during HF-keratinocytes reprogramming could be beneficial as ROCK inhibitor blocks keratinocyte terminal differentiation, increases cell proliferation and prevents apoptosis (Mcmullan *et al.*, 2003; Chapman *et al.*, 2010).

It should also be highlighted that the NuFF-feeder cells play a crucial role on the favourable outcome of the reprogramming protocol. Indeed, even when using Pluriton medium, the protocol cannot be reproduced when using HFF-feeders other than NuFF cells from donor 11. It is not known how exactly these specific cells support better mRNA reprogramming but their central role in the protocol could explain why Warren had to further modify the synthetic mRNA in order to develop a feeder-free mRNA protocol (Warren *et al.*, 2012).

On top of the labour-intensity of the protocol, another significant limitation associated with mRNA reprogramming is its very high cost, which restricted the number of experimental conditions that could be tested.

All in all, modified synthetic mRNA was, in our hands, not the right reprogramming vector for HF-keratinocytes. Multiple reprogramming method exist and choosing one depends i) on the

starting cell population e.g. keratinocytes, fibroblasts or adipocytes and ii) the purpose of reprogramming e.g. disease modeling or cell therapy. Fibroblasts are still the “go to” cells to be reprogrammed, as they are very easy to culture and robust to various reprogramming method. In our case, they survived the daily transfections required by synthetic modified mRNA reprogramming. Moreover, for the purpose of disease modeling, cell repositories such as Coriell bank disease fibroblasts, making it an easily available source of samples for scientists. Another source of patient sample that can be readily accessible to researcher are peripheral blood mononuclear cells (PBMCs). PBMCs can be reprogrammed to iPSCs with efficiencies comparable to fibroblasts (Loh *et al,* 2010). Keratinocytes are also a great source of patient samples, and their isolation via hair follicle collection is a non-invasive, non-painful procedure. Keratinocytes have been shown to reprogram up to 100-folds more efficiently and twofold faster than fibroblasts, probably due to their endogenous levels of KLF4 and c-MYC (Aasen *et al.*, 2008). Although not readily available, neural stem cells are also a competent source of cells for reprogramming due to their endogenous levels of reprogramming factors, leading them to being reprogrammed in the absence of *SOX2* or *c-MYC* or with *OCT4* alone *(*Kim, J. B. *et al.,*2008; Kim, J. B. *et al.,*2009*).* Though not applicable to any cell type, non-integrative reprogramming strategies such as synthetic modified mRNA reprogramming are attractive not only by their kinetics, but also by the great advantage of leaving no permanent genetic mutation, due to random viral transgene insertion, in the derived-iPSCS. This would reduce genetic heterogeneity amongst the generated iPSC lines.

There are still many options to generate iPSCs derivation strategies. They still mainly depend on the available source of sample, purpose of reprogramming, reprogramming vector availability as well as time and budget limitations.

Chapter 5

hESC differentiation into cardiomyocytes

Chapter 5 hESC DIFFERENTIATION INTO CARDIOMYOCYTES

5.1 Cardiac failure and Huntington's Disease

HTT is ubiquitously expressed and despite neurodegeneration being the main phenotype of HD, non-CNS HD-associated pathologies have been reported (Van Der Burg *et al.*, 2009; Sassone *et al.*, 2009; Sathasivam *et al.*, 1999). Epidemiology studies suggest that cardiac failure is the second cause of death amongst HD patients (Sorensen and Fenger, 1992; Lanska *et al.*, 1988; Chiu and Alexander, 1982). Cardiac defects, including atrophy, have previously been described In HD murine models (Sathasivam *et al.*, 1999; Mihm *et al.*, 2007; Wood, 2012; Kiriazis *et al.*, 2012). HD-iPSCs have proven to be good *in vitro* models by replicating some HD-neuronal phenotypes (Zhang, N. *et al.*, 2010; An *et al.*, 2012; Camnasio *et al.*, 2012;The HD iPSC Consortium, 2012). However, the HD cardiac phenotype is yet to be studied *in vitro* in order to determine whether the cardiac defects observed in HD murine models are due to a cell autonomous or a non-cell autonomous process. Therefore, here we differentiate the hESCs previously characterised in Chapter 3 into cardiomyocytes in order to address this and investigate possible HD-specific cardiac phenotypes. To our knowledge, this work is the first human cardiac HD *in vitro* model.

5.2 hESCs cardiac differentiation

This hESC cardiac differentiation work was first undertaken in collaboration with Prof. Harding's groups (Imperial College London). The Harding group has successfully differentiated the H7 hESCs line into hESC-derived cardiomyocytes (hESC-CM) (Thomson *et al.*, 1998; Foldes *et al.*, 2011). This collaboration enabled us to use the H7 line as a positive control for the differentiation conditions. The observation of beating cell clusters no later than 30 days post-initiation of differentiation was used as a cut-off point to determine the success of a differentiation protocol and the generation of functional cardiomyocytes.

5.2.1 hESCs cultured in mTeSR1

As described in Chapter 3, the eight hESC lines used in this study were successfully adapted to feeder-free culture conditions by culturing them in mTeSR1 medium in combination with GFR-Matrigel coating matrix. The H7 hESC line was thus adapted to the latter and was maintained in it for at least three passages prior to cardiac differentiation induction.

5.2.1.1 Spontaneous cardiac differentiation of hESCs cultured in mTeSR1

As described in Chapter 3, hESCs have the ability to spontaneously differentiate into all three germ layers in the presence of FBS and absence of bFGF. We explored to which extent they spontaneously differentiate into the mesoderm vs. other two germ layers (endoderm and ectoderm) when cultured under these conditions. This property was exploited to differentiate hESCs into cardiomyocytes.

One commonly used method for cardiac differentiation relies on the formation of spherical aggregates known as EBs, which enable the hESCs to differentiate into derivatives of the three germ layers, including cardiomyocytes (Germanguz *et al.*, 2011; Dolnikov *et al.*, 2006; Ma *et al.*, 2012; Gherghiceanu *et al.*, 2011; Xu *et al.*, 2001; Kehat *et al.*, 2001). To form EBs, H7 hESCs colonies were manually broken following dispase treatment as described in 2.1.6. Cell clusters were placed into low adherence dishes and fed daily with KOSR medium supplemented with 20% FBS and without bFGF. After four days of culture in suspension, the EBs were plated onto 0.5% gelatin-coated dishes, fed every two or three days and monitored for the formation of spontaneously beating areas. Although inefficient due to the cells also differentiating into endoderm and ectoderm derivatives (Xu *et al.*, 2001), it is expected that approximately 8.1% of the plated EBs will give rise to contractile foci within 30 days of differentiation (Kehat *et al.*, 2001). The observation of spontaneously beating areas within 30 days of differentiation was considered as our endpoint to determine whether or not the hESCs had successfully differentiated into functional cardiomyocytes. No beating was observed within 30 days of plating for the H7 hESCs.

The endocrine and chemical composition of FBS varies from batch-to-batch (Honn *et al.*, 1975). One possibility to explain our negative outcome is that the batch of FBS used in this study was not supportive of cardiac differentiation. Another drawback associated with this EB-based differentiation protocol is that the size of manually generated EBs cannot be controlled. Yet, It has been demonstrated that EB-based differentiation outcomes can be greatly influenced by the initial EB size. EBs of 1,000 cells are optimal for cardiac differentiation (Bauwens *et al.*, 2011). In order to generate size-controlled EBs of 1,000 cells/aggregate, Aggrewell plates (STEMCELL Technologies) were used. Aggrewell plates contain microwells that allow the even distribution of a single cell suspension in order to generate EBs of a chosen size. hESCs were seeded in Aggrewell plates in KOSR medium with 20% FBS and without bFGF to generate EBs of 1,000 cells. After 24 h in the Aggrewell plates, EBs were placed into low-adhesion plates for four days before being plated on 0.5% gelatin (Figure 5-1). No beating was observed in wells with the H7 hESC line within 30 days of differentiation. The protocol was repeated with EBs of 3,000 and 10,000 cells. Indeed, the 1,000 cells EBs were smaller than the manually generated EBs that had a positive differentiation outcome in MEF-conditioned Medium (MEF-CM) cultured H7 hESCs (Foldes *et al.*, 2011) (personal communication from Dr. M. Mioulane). However, no beating was observed within 30 days of differentiation.

Additionally, we trialled the EB-based spontaneous hESC cardiac differentiation using STEMDiff APEL medium (STEMCELL Technologies) as a basal medium, supplemented with 20 % FBS.

Its xeno-free, serum-free formulation was originally developed for EB-based hESC differentiation (Ng, E.S. *et al.*, 2008). STEMCELL Technologies recommended it, as its formulation could be more suitable for cells cultured in mTeSR1. As summarised in Table 5-1, this differentiation condition was trialled with EBs of 1,000, 3,000 and 10,000 cells. No beating could be observed within 30 days of differentiation.

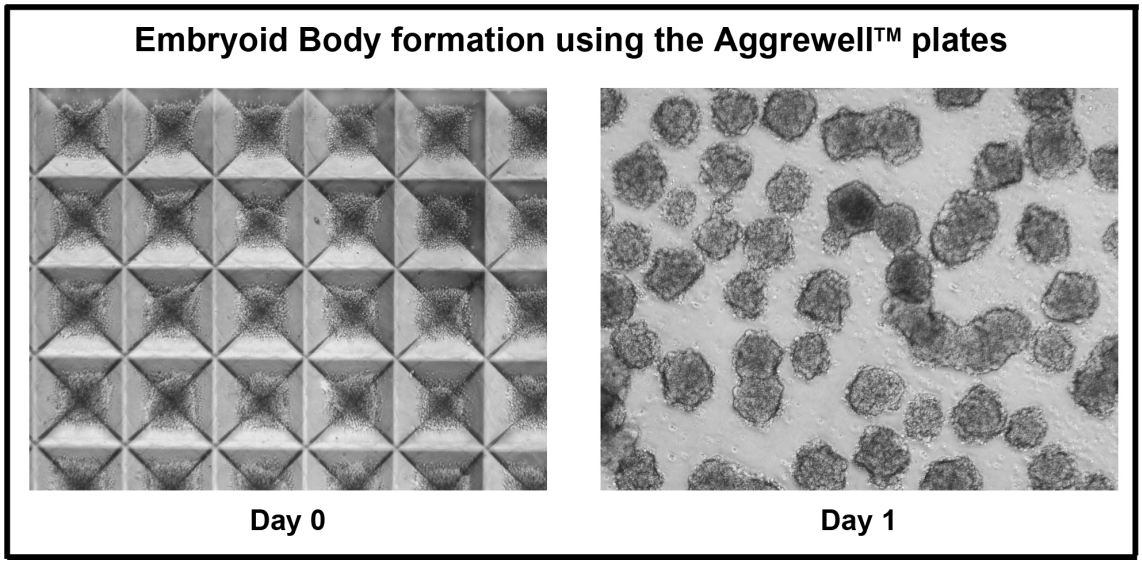

Figure 5-1: Embryoid Body (EB) formation using the Aggrewell plates.
Day 0: 1,000 cells per microwell were seeded in KOSR medium supplemented with 20% FBS and without bFGF. Day 1: 24 h later, EBs uniform in size could be cultured in suspension. Images were taken at 40x magnification.

5.2.1.2 Directed cardiac differentiation of hESCs cultured in mTeSR1

Due to the lack of success of the EB-based spontaneous cardiac differentiation protocol, a directed cardiac differentiation approach was trialled. Directed cardiac differentiation relies on exposing the hESCs to successive cytokine treatments to direct them into the cardiac lineage. Directed cardiac differentiation protocols also have the advantage of being fully defined and of bypassing the use of FBS.

5.2.1.2.1 Yang protocol

First, using H7 hESC line cultured in mTeSR1, we tested an EB-based protocol for directed cardiac differentiation (Yang, L. *et al.*, 2008). However, the EBs rapidly disaggregated. One reason for this could be that the differentiation medium did not support survival of mTeSR1 cultured cells. We repeated the protocol generating EBs of 1,000 cells as described in 5.2.1.1, using STEMDiff APEL medium as a basal medium. This time, the cells were left in the Aggrewell plate throughout the differentiation. However, within 15 days of differentiation, the EBs disaggregated and no beating could be observed (Figure 5-2).

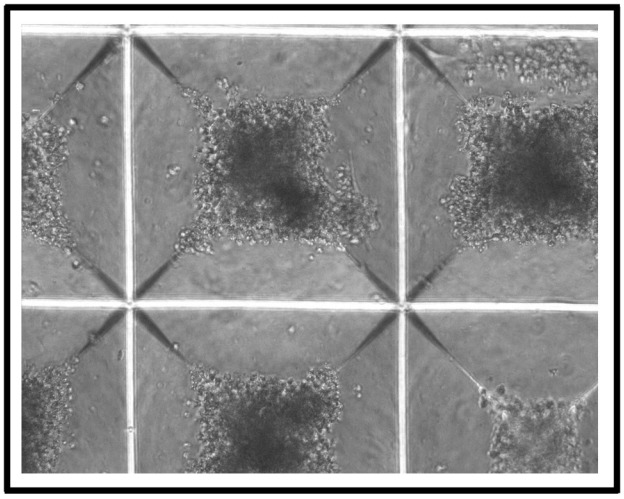

Figure 5-2. Disaggregating EBs 15 days post differentiation in STEMDiff APEL.
Image was taken at 100x magnification.

5.2.1.2.2 Laflamme protocol

Considering the negative outcomes of the EB-based differentiation protocols, we decided to try a monolayer directed differentiation protocol, which can be up to 50-fold more efficient than EB-based cardiac differentiation protocols (Laflamme *et al.*, 2007). As for the Yang protocol, the Laflamme protocol consists of a succession of cytokine treatments and is detailed in section 2.3.2. This protocol was chosen because it is not FBS-based and is fully defined. More importantly, it was originally developed on the H7 hESC line and was since successfully reproduced by Prof. Harding's group (Foldes *et al.*, 2011). Using the H7 hESC line as a positive control, all the eight hESC lines used in this study were subjected to this protocol. Within 15 days of differentiation, the cells formed clusters but none of them started beating within 30 days. Two examples of the clusters formed after 15 days of cardiac differentiation with the Laflamme protocol are presented in Figure 5-3.

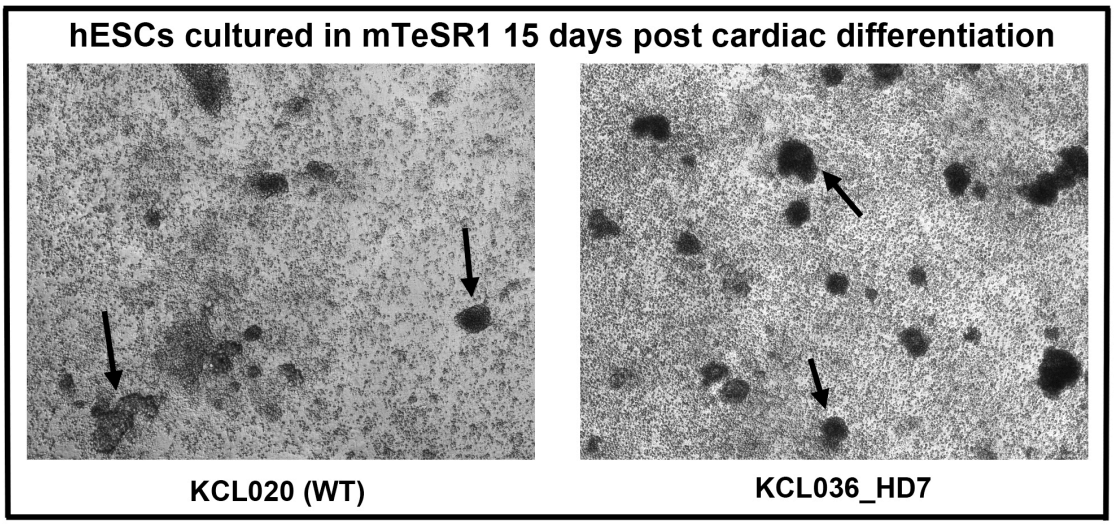

Figure 5-3: Day 15 day of cardiac differentiation in mTeSR1 medium (Laflamme protocol).

KCL020 (WT-hESC) and KCL036_HD7 (HD-hESC) formed clusters (arrows) 15 days post cardiac differentiation. No beating was observed within 30 days. Images were taken at 40x magnification.

5.2.1.2.3 Lian protocol

All of the above protocols were originally developed on cells cultured on MEF or on GFR-Matrigel with MEF-CM, which could explain why they gave poor outcomes on cells cultured in mTeSR1. During our cardiac differentiation protocol development, Lian *et al*. (2012a) published a cardiac differentiation protocol that started with cells cultured feeder-free in mTeSR1 and GFR-Matrigel. It is based on the Laflamme protocol (Laflamme *et al*., 2007), with the addition of a three-day cell pre-treatment with a glycogen synthase kinase 3 (Gsk3) inhibitor (CHIR99021) and the use of a B27 supplement without insulin. Indeed, Lian *et al*. also published that low insulin levels were beneficial to cardiomyocytes differentiation (Lian *et al*., 2012b, 2013) One WT-hESC line (KCL031) and one HD-hESC line (KCL027_HD5) were subjected to this protocol. We also tested a range of CHIR99021 concentrations in combination with B27 with no insulin as indicated.

Within eight days of the Lian cardiomyocytes differentiation protocol, cell survival decreased. No beating cardiomyocytes could be observed within 30 days of differentiation in the two cell lines tested (Figure 5-4).

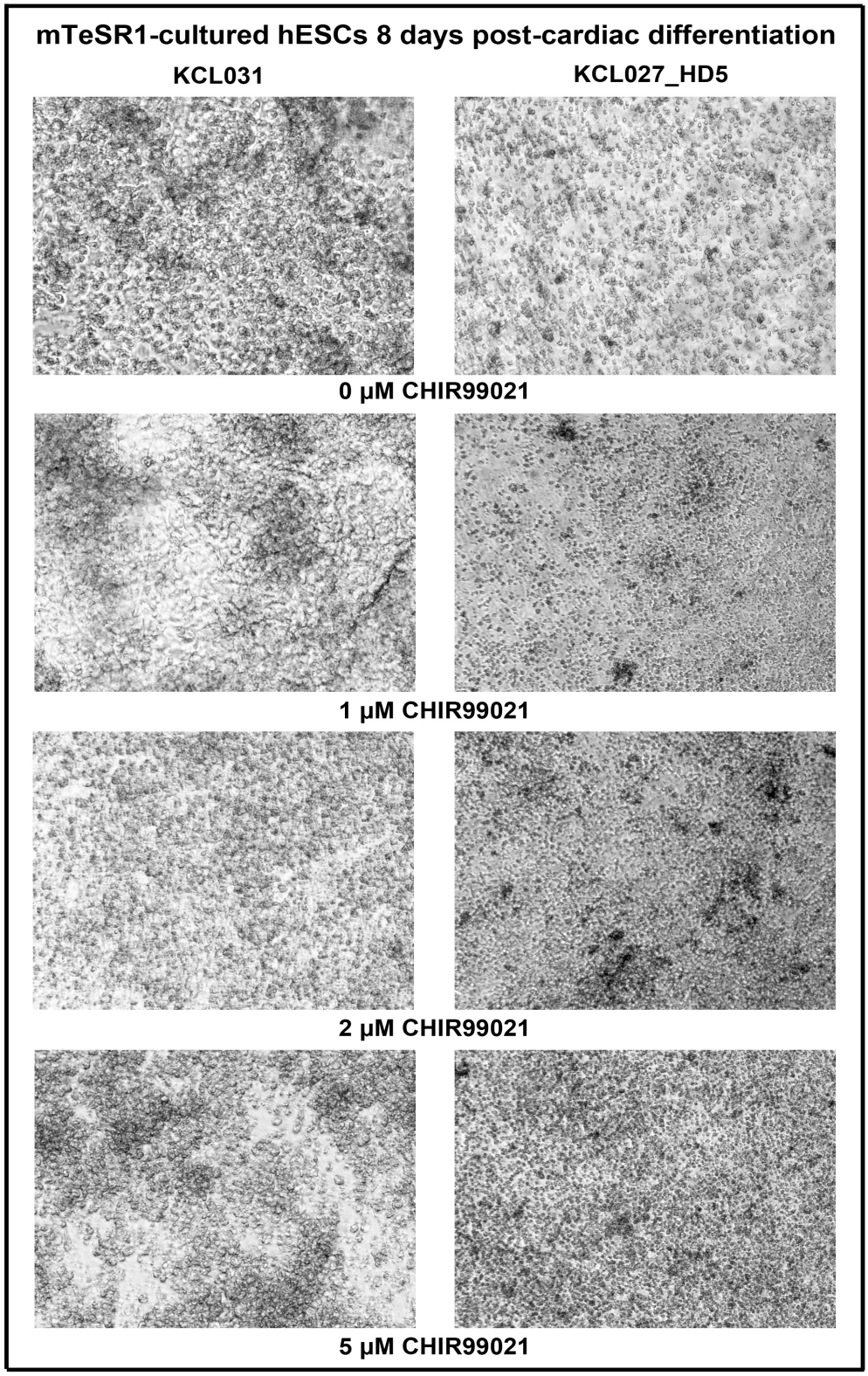

Figure 5-4: Day 8 of cardiac differentiation in mTeSR1 medium (Lian protocol).
Different concentrations of CHIR99021 were tested. KCL031 and KCL027_HD5 cell survival started decreasing from 8 days post cardiac differentiation. Images were taken at 40x magnification.

5.2.1.3 Summary of the cardiac differentiation protocols trialled on mTeSR1-cultured hESCs.

hESC culture medium	Protocol	Additional Info	Beating
mTeSR1	EB (20%FBS)	Manually formed EBs	Negative
mTeSR1	EB (20%FBS)	1,000 cells/EB	Negative
mTeSR1	EB (20%FBS)	3,000 cells/EB	Negative
mTeSR1	EB (20%FBS)	10,000 cells/EB	Negative
mTeSR1	STEMDiff APEL + 20%FBS	1,000 cells/EB	Negative
mTeSR1	STEMDiff APEL + 20%FBS	3,000 cells/EB	Negative
mTeSR1	STEMDiff APEL + 20%FBS	10,000 cells/EB	Negative
mTeSR1	Yang *et al*. (2008)	Manually formed EBs	Negative
mTeSR1	Yang *et al*. (2008)	1,000 cells/EB	Negative
mTeSR1	Laflamme *et al*. (2007)	Monolayer of 2 x 10^5 cells/cm^2	Negative
mTeSR1	Laflamme *et al*. (2007) with STEMDiff APEL as a basal medium	Monolayer of 2 x 10^5 cells/cm^2	Negative
mTeSR1	Lian *et al*. (2012a) *	Monolayer of 2 x 10^5 cells/cm^2	Negative
MEF-CM	EB (20%FBS)	Manually formed EBs	**Positive**
MEF-CM	Laflamme	Monolayer of 2 x 10^5 cells/cm^2	**Positive**

Table 5-1: Summary of the cardiac differentiation conditions trialled on the H7 hESC lines cultured feeder-free in mTeSR1 medium or mouse embryonic fibroblast-conditioned medium (MEF-CM).

* This condition was only trialled on WT-hESC KCL031 and HD-hESC KCL027_HD5 lines.

The differentiation conditions where the cells were cultured feeder-free in mTeSR1 medium all had a negative outcome (no beating within 30 days of differentiation) while the differentiation protocols were successful when the cells were cultured in MEF-CM prior to differentiation. This led to suggest that rather than the differentiation protocol; the undifferentiated hESC culture conditions could be impeding downstream cardiac differentiation. We thus decided to adapt the hESCs to a new culture medium.

5.2.2 hESCs cultured In Nutristem

All eight hESC lines but HD-hESC KCL012_HD3 could be adapted from culture in mTeSR1 medium to culture in Nutristem medium (Stemgent) on GFR-Matrigel as a matrix. KCL012_HD3 could not be cultured in these conditions for a minimum of three passages without excessive spontaneous differentiation and could thus not be used for cardiac differentiation. It cannot be excluded that KCL012_HD3 acquired a chromosomal abnormality during the study, which could explain the excessive differentiation. Nutristem was chosen over MEF-CM as it has a fully defined formulation, which would bypass any variability associated with different batches of MEFs. The hESCs were maintained in this culture condition for at least three passages prior to cardiac differentiation.

5.2.2.1 Spontaneous cardiac differentiation of hESCs cultured in Nutristem

Among seven feeder-free hESC lines adapted to Nutristem medium, and subjected to the spontaneous cardiac differentiation protocol described In 5.2.1.1, only one WT- (KCL031) and one HD- (KCL028_HD6) hESC line gave rise to beating clusters within 30 days of differentiation (**Figure 5-5**).

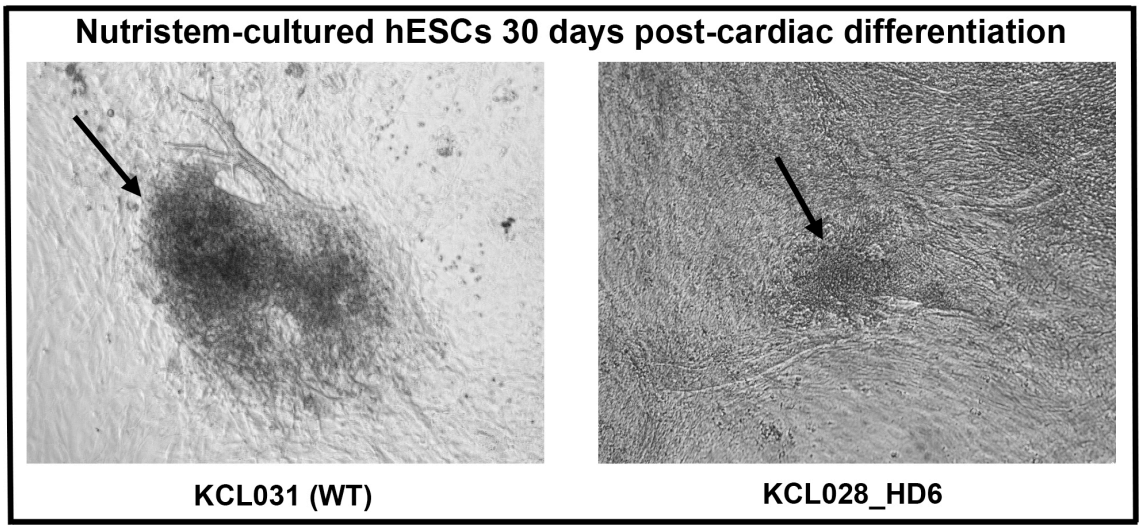

Figure 5-5: hESCs cultured in Nutristem after 30 days of cardiac differentiation (Spontaneous EB-based protocol).

KCL031 and KCL028_HD6 formed beating clusters (arrows) 30 days post cardiac differentiation. Images were taken at 40x magnification.

Considering this protocol only had a positive outcome on 2/7 hESC lines and the variability across different batches of FBS, we decided to differentiate the hESCs adapted to Nutristem feeder-free culture with the Laflamme directed differentiation protocol. This protocol offers a tighter control over the different variables of differentiation, which could lead to a better reproducibility across the seven different hESCs lines.

5.2.2.2 Directed cardiac differentiation of hESCs cultured in Nutristem (Laflamme protocol)

As in 5.2.1.2.2, we subjected seven hESCs lines adapted to Nutristem feeder-free culture to the Laflamme directed differentiation protocol.

All the hESC lines but KCL040 presented beating areas within 30 days of differentiation. In our hands, the Laflamme protocol on cells cultured feeder-free in Nutristem medium was the most dependable despite a wide range of differentiation efficiency (summarised in Table 5-2).

Cell line	% wells with beating cardiomyocytes (day 30)
KCL020	4.2% (2/48)
KCL027_HD5	16.7% (8/48)
KCL028_HD6	4.2% (2/48)
KCL031	20.8% (10/48)
KCL034	6.3% (3/48)
KCL036_HD7	6.3% (3/48)
KCL040	0% (0/48)

Table 5-2: Summary of percentage of wells presenting beating areas by day 30 of cardiac differentiation by the Laflamme protocol.

Next, the hESC line that presented beating by day 30 of the Laflamme differentiation protocol were analysed by qPCR for two pluripotency markers (*NANOG* and *OCT3/4*), two cardiac markers (*NKX2.5* and *TNNT2*) and *HTT*. The relative gene expression and the gene expression normalised to the undifferentiated hESCs are presented in Table 5.3.A and B respectively.

A

	Nanog	OCT3/4	NKX2.5	TNNT2	HTT
Kcl020	119.627552	746.469166	8.4529023	3.86576582	2.55848858
kcl020-CM	18.1231515	18.9085305	35.878625	19.4088115	1.89713298
kcl031	46.2655091	487.128073	8.4863608	1.87538385	1
kcl031-CM	15.5062779	22.7154712	72.242232	19.4877193	2.28501644
kcl034	67.0392425	659.089709	14.648569	2.36069449	1.65261732
kcl034-CM	10.2184697	21.3031205	46.590654	4.85861817	2.14238053
kcl027_HD5	60.8269203	651.133194	1	2.06584688	1.91931805
kcl027_HD5-CM	10.654272	14.9138828	9.8117884	23.6726584	1.38011531
kcl028_HD6	69.7536574	471.898454	2.0919443	3.9062605	1.08626136
kcl028_HD6-CM	20.1939222	6.98791407	42.797738	38.0784834	2.12247416
kcl036_HD7	76.9756752	636.206146	2.8751853	3.13046425	1.46766577
kcl036_HD7-CM	14.6508143	26.9955446	9.244438	10.2874502	2.36135853

B

	Nanog	OCT3/4	NKX2.5	TNNT2	HTT
Kcl020	1	1	1	1	1
kcl020-CM	0.1514965	0.0253306	4.2445333	5.0206899	0.741505352
kcl031	1	1	1	1	1
kcl031-CM	0.3351585	0.0466314	8.5127457	10.391323	2.285016438
kcl034	1	1	1	1	1
kcl034-CM	0.1524252	0.032322	3.1805601	2.0581309	1.296356097
kcl027_HD5	1	1	1	1	1
kcl027_HD5-CM	0.1751572	0.0229045	9.8117884	11.459058	0.719065459
kcl028_HD6	1	1	1	1	1
kcl028_HD6-CM	0.2895034	0.0148081	20.458355	9.7480655	1.953925857
kcl036_HD7	1	1	1	1	1
kcl036_HD7-CM	0.1903304	0.0424321	3.2152495	3.2862379	1.608921178

Table 5-3: Gene expression of hESC and hESC-CM at day 30 of the Laflamme protocol.
A. Relative gene expression of the hESC and hESC-CM (day 30). **B.** Gene expression levels in hESC-CMs normalised to the respective hESC line.

The results presented in Table 5-3 confirm that the six hESC lines presenting beating areas by day 30 of the Laflamme differentiation protocol had a down-regulation of their pluripotency associated genes *NANOG* and *OCT3/4*, and an up-regulation of the cardiac-associated genes *NKX2.5* and *TNNT2*. KCL031 and KCL027_HD5, which are the two cell lines that presented the most beating areas (Table 5-2), have the highest expression of *NKX2.5* and *TNNT2*, whether looking at the relative or the normalised gene expression (Table 5-3). *HTT* expression remained similar between hESCs and hESC-CMs.

The results presented in Table 5-3 support a study published by Allegrucci and Young (Allegrucci and Young, 2007) that demonstrated that hESC lines have variable in gene expressions. We have also observed this cell line variability, as shown in part A of Table 5-3,

where the undifferentiated hESCs have a wide array of expression of their pluripotency genes. This could explain the differences in differentiation efficiency observed.

Next we assessed the gene expression of the normalised means of WT- and HD-hESCs and WT- and HD-hESC-CMs (Figure 5-6). This confirmed that both WT- and HD-hESCs had significant down-regulation of their pluripotency genes at 30 days of the Laflamme cardiomyocytes differentiation protocol. Both WT- and HD-hESCs had an up-regulation of cardiac-associated genes after 30 days of cardiac differentiation. However, the increase was only significant for *NKX2.5* in WT-hESCs. *HTT* expression remained the same between both group in hESCs and hESC-CMs.

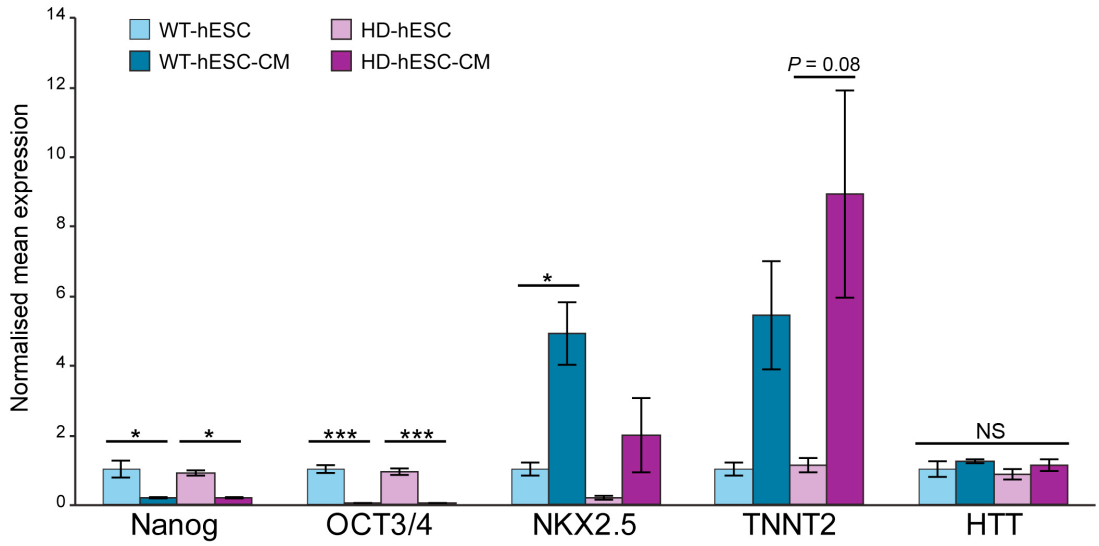

Figure 5-6: Gene expression of the normalised means of WT-hESCs, WT-hESC-CM, HD-hESCs and HD-hESC-CMs.
WT-hESC are compared with WT-hESC-CM and HD-hESC are compared with HD-hESC-CM. Data are given by normalised mean ± standard error of the mean (n = 3); statistical significance was calculated by two-way ANOVA with Bonferroni post-hoc test. * $P < 0.05$, *** $P < 0.01$, NS: non significant.

We further confirmed the positive outcome of the Laflamme protocol and the presence of beating cardiomyocytes by immunostaining the cells against cardiac troponin T (cTnT), a cardiac marker specific to beating cardiomyocytes (Figure 5-7).

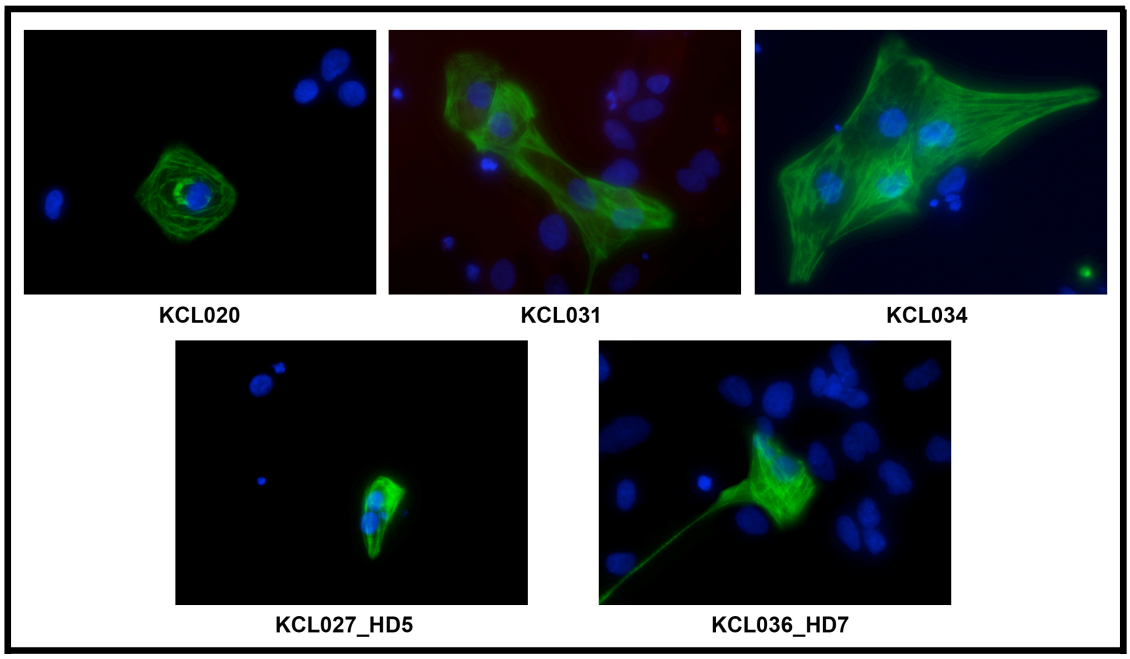

Figure 5-7: Representative cardiac troponin T (cTnT) immunostaining on day 30 of cardiac differentiation.
cTnT: green and Hoechst: blue. Images were taken at 400x magnification.

After 30 days of cardiac differentiation, positive cTnT staining could be observed for three WT-hESC-CM lines (KCL020, KCL031 and KCL034) and two HD-hESC-CM lines (KCL027_HD5 and KCL036-HD7). cTnT immunostaining on HD-hESC-CM KCL028, which also presented beating areas within 30 days of differentiation, was not performed. We found no obvious difference between WT-hESC-CMs and HD-hESC-CMs, suggesting that HTT mutation does not prevent HD-hESCs from differentiating into cardiomyocytes.

5.2.2.3 Comparison of WT- and HD-hESC-CMs.

5.2.2.3.1 Cardiomyocyte-specific biomarker expression in WT- and HD-hESC-CMs

We choose one WT- (KCL031) and one HD- (KCL027_HD5) hESC line with the best differentiation efficiency (20.8% and 16.7% respectively, see Table 5-2) and the highest gene expression of cardiac-associated genes to be screened for any disparities in differentiation potential and any potential molecular HD-specific phenotype. Samples from undifferentiated hESCs and hESC-CMs at day 30 of differentiation were analysed by qPCR using the Qiagen Human Cardiomyocyte Differentiation qBiomarker PCR Array. The array contains 19 cardiomyocyte-specific biomarkers and two housekeeping genes for normalisation (summarised in Table 5-4).

Biomarker	Gene
Cardiomyocyte Structural Constituent:	*ACTN2* (Actinin alpha2)*, DES* (Desmin), *MYH7* (MyHC-beta)*, MYL2* (MLC-2, MLC-2v)*, MYL3, MYL7, TNNI3* (cTnI), *TNNT2* (cTnT)
Cardiomyocyte Transcription Factors	*GATA4, HAND2* (dHAND)*, NKX2-5*
Cardiomyocyte Receptors	*ADRB1, NPPA, RYR2,*
Cardiomyocyte Ion Channels	*KCNQ1, PLN, SLC8A1*
Cardiomyocyte Enzyme	*CKM*
Cardiomyocyte Transporter	*MB* (myoglobin)
Housekeeping Gene	*NAT1, GAPDH*

Table 5-4: List of cardiac biomarker genes present on the Qiagen Human Cardiomyocyte Differentiation qBiomarker PCR Array.
Adapted from Qiagen (http://www.sabiosciences.com/qbiomarker_product/HTML/IPHS-102A.html, accessed on 20/07/2013)

Samples from the undifferentiated and the differentiated conditions for the two chosen hESC lines were run in technical triplicates on the qBiomarker array and were analysed using the Web-based Qiagen qBiomarker iPSC Data Analysis Software. Upon data analysis, *glyceraldehyde-3-phosphate dehydrogenase* (*GAPDH*) was determined to be the most stable housekeeping genes and the sample were normalised against its expression. A clustergram of the samples' normalised gene expression was generated and is presented in Figure 5-8.

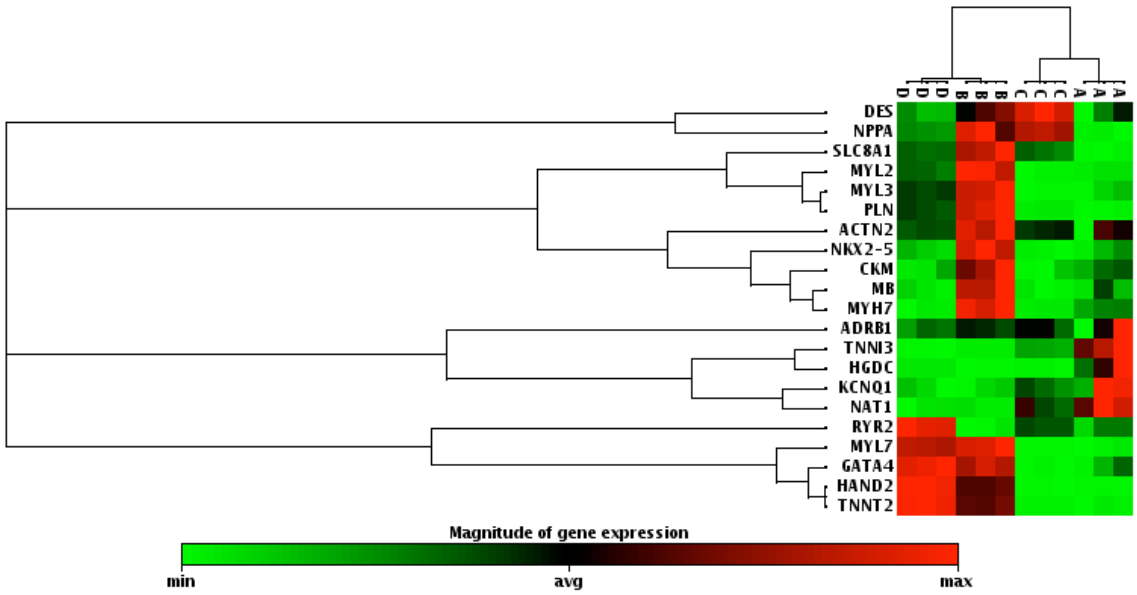

Figure 5-8: Clustergram of expression values of cardiac genes in undifferentiated hESCs and hESC-CM at day 30 of cardiac differentiation (Laflamme protocol).
A) Undifferentiated KCL031, **B)** KCL031-CM, **C) undifferentiated** KCL027, **D)** KCL027-CM. Green colour represents minimal gene expression and red colour represents maximal gene expression.

The results of the clustergram presented in Figure 5-8 show that the undifferentiated hESCs populations (A and C) are well separated from the differentiated hESCs populations (B and D). The data confirmed that the majority of cardiac-specific genes such as *NKX2*.5 and *TNNT2* are minimally or not at all expressed in the undifferentiated hESCs populations (A and C) (the magnitude of gene expression is in green). This is in line with the data presented in Table 5-3 and Figure 5-6. On the contrary, these genes were expressed in the differentiated hESCs populations (B and D), suggesting that the cardiac differentiation is taking place (the magnitude of gene expression is in red). Interestingly, a high proportion of cardiomyocyte biomarkers such as *MYH7* and *NKX2*.5 appear to be less expressed in the HD-hESC-CMs (sample D) than in the WT-hESC-CMs (sample B) though whether this is of any significance should be confirmed.

We next compared the cardiomyocyte biomarkers expression in KCL027_HD5-CM versus KCL031-CM and performed a scatter plot analysis where the Log10 of 2-^Delta-Ct expression of HD-hESC-CM KCL027 was plotted against the Log10 of 2-^Delta-Ct expression of WT-hESC-CM KCL031. A fold change of two or more was considered significant. The scatter plot is presented in Figure 5-9 and a summary table of the genes with a fold change of two or more is presented in Table 5-5.

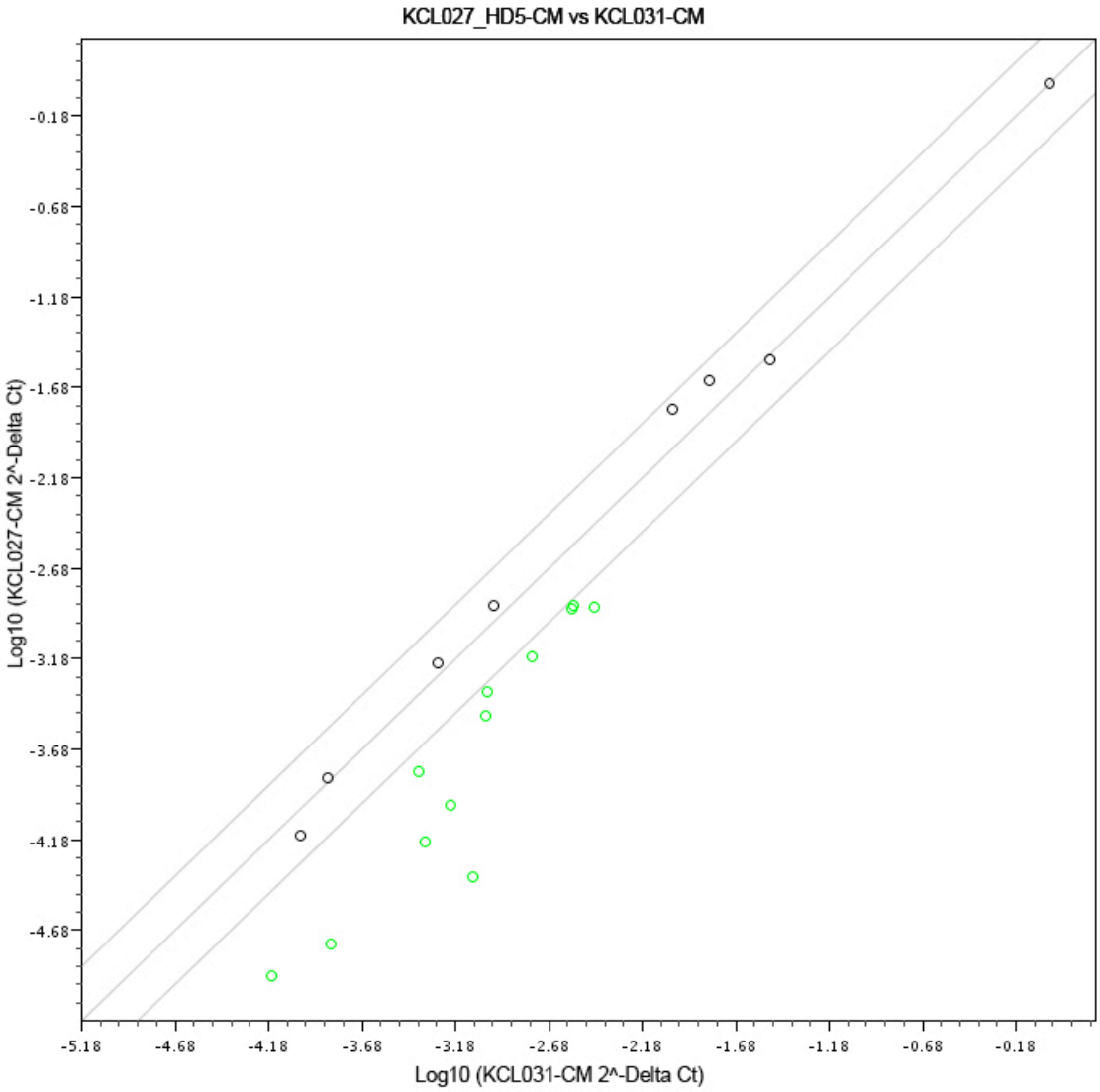

Figure 5-9: Relative comparison expression of cardiomyocyte biomarkers gene in KCL027_HD5-CM compared to KCL031-CM at day 30 of the Laflamme protocol.
Scatter plot showing the Log10 of 2-^Delta-Ct expression of HD-hESC-CM KCL027 plotted against the Log10 of 2-^Delta-Ct expression of WT-hESC-CM KCL031. Green dots represent HD-hESC-CM genes with a fold expression lower than WT-hESC-CM and grey lines indicate ± 2 folds expression.

Gene	Fold Regulation
ACTN2	-2.2631
CKM	-5.9351
DES	-2.8504
MB	-8.103
MYH7	-20.0035
MYL2	-2.7055
MYL3	-2.1997
NKX2-5	-6.9687
NPPA	-2.9925
PLN	-2.1939
SLC8A1	-2.4645
TNNI3	-6.0878

Table 5-5: Summary table of the relative expression of cardiomyocyte biomarker genes with a fold change of two or more in HD-hESC-CM KCL027 compared to WT-hESC-CM KCL031.

It can be seen from Figure 5-9 and Table 5-5 that day 30 KCL027_HD5-CMs have 12 genes with a lower expression by two folds or more compared to day 30 KCL031-CMs. This further confirms the trend indicated by the clustergram presented in Figure 5-8. The gene expression of *ACTN2, NKX2.5*, *DES*, *MYL2* and MYH7 has been shown to increase as the hESC-CM mature (Segev *et al.*, 2005; Puppala *et al.*, 2013; Dubois *et al.*, 2011). Their lower expression in day 30 KCL027_HD5-CMs compared to day 30 KCL031-CMs suggest that the HD-hESC-CMs might be less mature than the WT-hESC-CMs. However, it cannot be excluded that this difference could be due to hESC variability and not HD.

5.2.2.4 CAG repeat stability in HD-hESC-derived cardiomyocytes

The trinucleotide HD mutation is subject to mosaicism in HD sufferers, especially in the CNS and gonads (Telenius *et al.*, 1994). However, there are also contradictory reports on whether CAG repeats increase during PSC differentiation (The HD iPSC Consortium, 2012; Niclis *et al.*,

2009; Seriola *et al.*, 2011; Camnasio *et al.*, 2012). We therefore looked at CAG repeat stability in the HD-hESC-CMs after 30 and 60 days of cardiac differentiation with the Laflamme protocol. The results are presented in Figure 5-10.

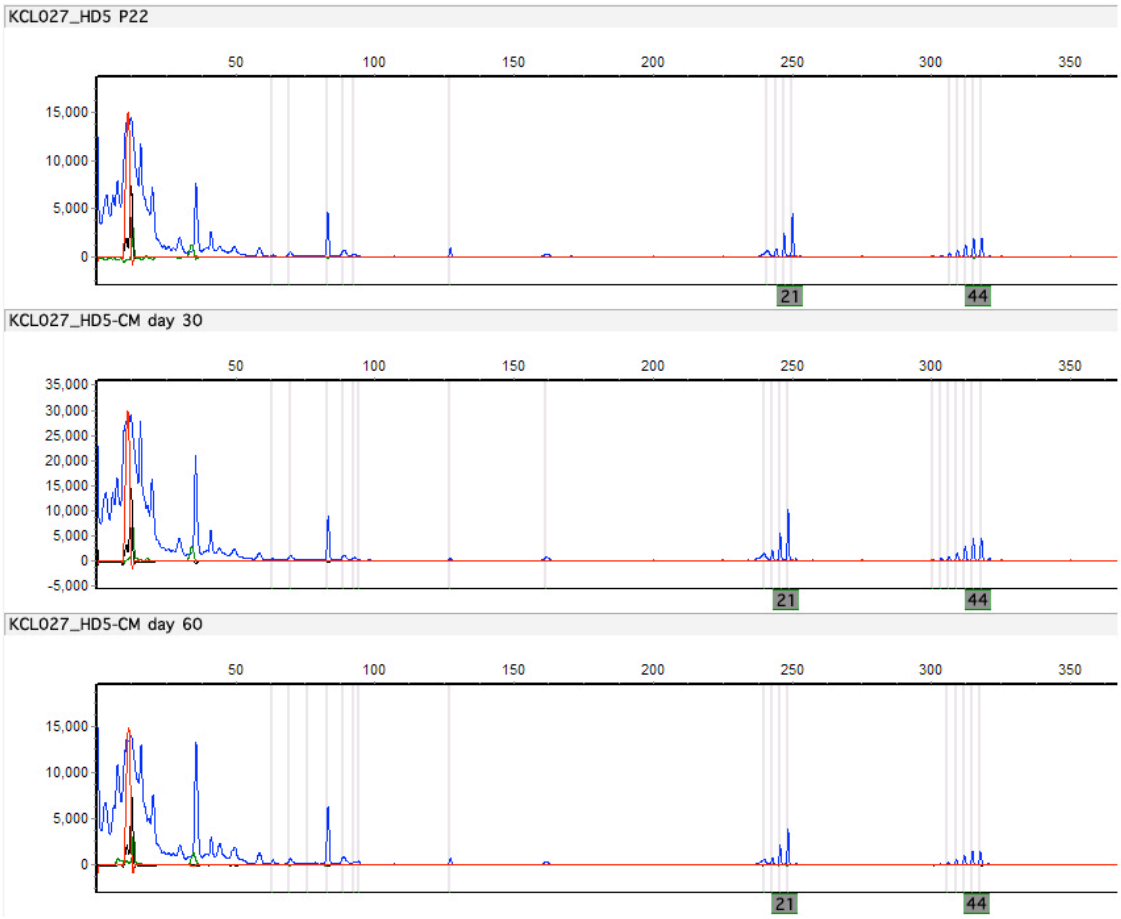

Figure 5-10: CAG repeat number in undifferentiated hESC KCL027_HD5 P22 and post 30 and 60 days of cardiac differentiation (Laflamme protocol).
The CAG repeat number remained stable at 44 CAG repeats. CAG repeats of over 36 are HD positive.

The CAG repeat number of KCL027_HD5 remained stable at 44 CAG repeats throughout differentiation. These results are consistent with some previously published studies that showed that the CAG repeats were stable in undifferentiated HD-hESCs even after multiple passages, as well as in differentiated hESCs (osteogenic progenitor-like, neural progenitors and neurons) (Seriola *et al.*, 2011; Camnasio *et al.*, 2012). However, this may not be a rule. In some other publications, CAG repeats have been found to be instable with documented trinucleotide expansion of five and eight repeats in neurons (Niclis *et al.*, 2009; The HD iPSC Consortium, 2012).

5.2.3 Discussion

Here I described the development of the first HD-specific human cardiac *in vitro* model. To generate this model, we characterised eight hESCs lines, four WT (KCL020, KCL031, KCL034 and KCL040) and four carrying HD-specific mutation (KCL012, KCL027, KCL028, and KCL036) (Chapter 3).

Using the H7 hESC line as a positive control, we subjected all the hESC lines cultured feeder-free in mTeSR1 medium on GFR-Matrigel substrate to one spontaneous (5.2.1.1) and three directed differentiation protocols (5.2.1.2). All four differentiation protocols were unsuccessful at giving rise to beating cardiomyocytes, our endpoint to determine whether a cardiac differentiation protocol successfully generated functional cardiomyocytes or not. During our cardiac differentiation protocol development, Ojala *et al*. published a study demonstrating that hESC culture conditions prior to cardiac differentiation can have an impact on the differentiation outcome. Notably, their study on the H7 line demonstrated that the mTeSR1 with GFR-Matrigel substrate culture condition was the least favourable one to give rise to beating cardiomyocytes (Ojala *et al.*, 2012). However, they used a co-culture method with END2 endothelial cells to differentiate H7 into cardiomyocytes, a condition not tested in our study. Taking this report into account, we decided to adapt the eight hESC lines to Nutristem medium. All but KCL012_HD3 could be adapted to feeder-free culture in Nutristem / GFR-Matrigel. In these conditions, KCL012_HD3 presented excessive spontaneous differentiation. It cannot be excluded that at the time of Nutristem adaptation the cell line had acquired karyotypic abnormalities resulting in poor maintenance of pluripotency in these culture conditions The seven remaining hESCs were subjected to the spontaneous differentiation protocol 5.2.2.1, which resulted in a positive outcome (beating), though in two cell lines only (KCL031 and KCL028_HD6). This highlights the poor outcome of this protocol in our hands. In order to increase the cardiac differentiation outcome, we subjected the seven remaining hESC lines to the Laflamme directed differentiation protocol (5.2.2.2). Beating could be observed with various efficiencies (refer to Table 5-2) within 30 days Beating could be observed within 30 days in all lines except one, WT-hESC KCL040. Since the cells were cultured on an identical substrate (GFR-Matrigel) and the only difference in culture condition was the culture medium, this positive outcome across multiple hESC cell lines suggested that in our hands, mTeSR1 might have an inhibitory effect on cardiac differentiation in the hESC lines used in this study. Feeder-free hESC culture presents many advantages such as culture upscaling and prevention of feeder–cell contamination. However, as observed in this study, it can also inhibit downstream differentiation. One way to prevent this would be to use feeder-free culture as a transient step for feeder-cell depletion prior to differentiation, rather than for long term culture (>20 passages) as in this study.

Although with a wide range of efficiency, the positive cardiac differentiation results across the six different hESC lines confirmed that like WT-hESCS, HD-hESCs could be differentiated into cardiomyocytes. This is not unexpected as HD is characterised by a late onset and slow progression, with individuals that develop normally. Furthermore, this is in line with findings on other human and murine *in vitro* HD ESC models that HD-hESCs can be differentiated into other cell types, notably neurons (Castiglioni *et al.*, 2012; Niclis *et al.*, 2009; Camnasio *et al.*,

2012; Seriola *et al.*, 2011; Lorincz and Zawistowski, 2009). Gene expression analysis and positive cTnT immunostaining of the five tested hESC-derived CMs lines at day 30 of the Laflamme protocol, further confirmed that both WT and HD-hESCs could be differentiated into cardiomyocytes with no significant difference. One WT-hESC line (KCL031) and one HD-hESC line (KCL027_HD5) were then chosen for the molecular characterisation of cardiomyocyte biomarkers as they had the highest differentiation efficiency. Analysis of the cardiomyocyte biomarkers expression 30 days post-differentiation revealed that both the WT-hESC and the HD-hESC cell lines had differentiated into cardiomyocytes, as the cardiomyocyte biomarkers were more expressed in differentiated cells than in undifferentiated cells. However, expression levels of cardiomyocyte-specific genes such as *MYH7* and *NKX2.5* were somewhat lower in the HD-hESC-CMs than in the WT-hESC-CMs, raising the interesting possibility that HD-hESC-CMs might be less mature than the WT-hESC-CMs.

Unfortunately, I ran out of time and I could not repeat the Laflamme differentiation protocol at least three times on all the lines in order to have differentiation triplicates on top of biological replicates. If results were consistent, to avoid the possibility of an hESC line-specific bias, I would repeat the Qiagen Human Cardiomyocyte Differentiation qBiomarker PCR Array on the six hESC lines that generated beating cardiomyocytes within 30 days of the Laflamme cardiac differentiation protocol (KCL020, KCL031, KCL034, KCL027_HD5, KCL028_HD6 and KCL036_HD7). This would enable me to generate a stronger baseline of WT cardiomyocyte biomarker gene expression. Comparing the HD-hESC-CMs to this baseline would then give a better insight on whether or not the lower cardiomyocyte biomarker gene expression is an HD-specific phenotype or if it is a hESC line specificity. Results presented in Table 5-3 and Figure 5-6 confirm that all the cell lines down-regulate their pluripotency-associated genes. This indicates that poor cardiac differentiation efficiency is likely due to the cells not committing to the cardiac lineage. This could be investigated by looking at the gene expression of genes from the ectoderm and endoderm cell lineages. Their expression should be minimal. Lower levels of cardiomyocyte-specific biomarker expression in HD-hESCs could be due to inefficient differentiation rather than an HD-specific phenotype. Until then, no definitive conclusion can be drawn from these results. Furthermore, quantitative analysis of the hESC-derived cardiomyocytes could be performed by flow cytometry for markers such as cTNT, MCL2a or SMA. This would enable us to further investigate whether or not there is a difference in cardiomyocyte differentiation propensity between WT-hESCs and HD-hESCs. Moreover, electrophysiological analysis of the WT-hESC-CM and HD-hESC-CM is necessary to further investigate a potential difference between the cell lines due to the HD mutation.

Using the KCL027_HD5 hESC lines, we also investigated CAG repeat stability in the HD-hESC-CMs after 30 and 60 days of cardiac differentiation with the Laflamme protocol. In our hands, the CAG repeats (44) of KCL027_HD5 remained unchanged throughout cardiac differentiation with this protocol. Other groups have published contradictory reports on whether CAG repeats increase during PSC differentiation (The HD iPSC Consortium, 2012; Niclis *et al.*, 2009; Seriola *et al.*, 2011; Camnasio *et al.*, 2012). However, it has been established that like in patients, there is an *in vitro* CAG repeat expansion associated phenotype, notably in iPSC-derived neurons

(The HD iPSC Consortium, 2012). To confirm the presence of an *in vitro* HD-specific phenotype in HD-hESC-CMs, they should be generated from HD-PSCs with greater CAG repeat numbers. In this instance we tried to generate HD-iPSCs and aimed to target JHD patients.

One drawback of the Laflamme directed differentiation protocol used in this study is that it does not generate a pure cardiomyocytes population (≈ 30%) (Laflamme *et al.*, 2007), which was also observed from the wide range of differentiation efficiency presented in Table 5-2 and from the immunostaining presented in Figure 5-7. Treating the cells with 1-2% DMSO has recently been found to be beneficial for cardiac differentiation (Chetty *et al.*, 2013). Removing insulin from certain stages of the differentiation protocol could also improve efficiency as the latter has been found to inhibit cardiac differentiation (Lian *et al.*, 2012b; Burridge *et al.*, 2011; Lian *et al.*, 2013). Challenging the ratios of cytokines used in the differentiation protocol is another approach that could be beneficial for the cell lines used in this study. Thanks to an elegant *NKX2.5* reporter hESC line, Elliot *et al*. could track cardiac differentiation. They tested 96 Activin A and BMP4 concentration combinations and determined that in their differentiation conditions, a ratio of BMP4:Activin A of 1:1 or 1:2 was optimal (Elliott *et al.*, 2011). Finally, the use of small molecules in addition to cytokines has the capacity to give differentiation of great efficiency. Even though our attempt with CHIR99021 compound was not successful (5.2.1.2.3), it helped give rise to a $cTnT^+$ population of approximately 85% in the original study (Lian *et al.*, 2012a). Another small molecule with great potential is KY02111, which can increase cardiac differentiation by 80 folds (Minami *et al.*, 2012). Interestingly, both CHIR99021 and KY02111 modulate the Wnt signaling pathway, but in opposite ways. Indeed, the Wnt signaling pathway needs to be activated in order to promote mesoderm differentiation, and then inhibited at later stages in order to ensure cardiac differentiation and not differentiation into cells from the hematopoietic or vascular lineage (Mignone *et al.*, 2010; Naito *et al.*, 2006). Consequently, Lian *et al.* (2012a) used the CHIR99021 Wnt activator as a pre-treatment before starting cardiac differentation via cytokine induction, while Minami *et al.* (2012) used KY02111, a Wnt signaling inhibitor 3 days post-cardiac differentiation induction. Another alternative is to modify the differentiation ECM. Zhang *et al*. could get up to 98% $cTnT^+$ cells by using a GFR-Matrigel “sandwich” method. It is worth noting that Zhang *et al*. obtained these results with hESCs cultured in mTeSR1 prior to differentiation. However mTeSR1 was not used for long-term maintenance of undifferentiated hESCs but rather for feeder-cell depletion three to six days prior to starting cardiac differentiation (Zhang, J. *et al.*, 2012).

If cardiac differentiation cannot be enhanced, another approach is to perform “cardiac enrichment” in order to have a purer cell population prior to molecular analysis. Cardiomyocyte enrichment techniques include dissection of the beating areas prior to dissociation, or the use of a discontinuous Percoll gradient centrifugation step for density separation of the cardiomyocytes, which can lead to a four-fold enrichment (Xu *et al.*, 2002). Another strategy could be to use the SIRPA or ALCAM cardiomyocytes surface markers for enrichment by fluorescence-activated cell sorting (FACS) or magnet-assisted cell separation (Dubois *et al.*, 2011; Rust *et al.*, 2009). Finally, establishing hESC lines with a cardiomyocyte-specific promoter fluorescent reporter vector would also enable us to enrich the differentiated cell populations by

FACS. This approach has already been successful using *α-myosin heavy chain*, *myosin light chain 2V* and *Troponin-I* promoters (Kita-Matsuo *et al.*, 2009;Ritner *et al.*, 2011;Huber *et al.*, 2007;Gallo *et al.*, 2008). However, there is a risk for random insertion of the transgene in the genome or for the transgene to rearrange. Thorough characterisation of the transgene's expression and stability would thus be needed.

Given more time and resources, I would also have characterised the cardiomyocytes by electrophysiological analysis to look at action potential properties. iPSC-derived cardiomyocytes from patients have already proven to replicate disease phenotypes of Timothy syndrome, long QT-disease, dilated cardiomyopathy, arrhythmogenic right ventricular cardiomyopathy and familial hypertrophic cardiomyopathy *in vitro* (Yazawa *et al.*, 2011; Lahti *et al.*, 2011; Ma *et al.*, 2012; Tse *et al.*, 2013; Lan *et al.*, 2013). The HD cardiac phenotypes found in the R6/2 murine model comprise a decreased heart weight and left ventricular defects, including a 50% reduction in cardiac output (Mihm *et al.*, 2007; Wood, 2012). Interestingly, *MYH7*, which is mostly expressed in cardiac ventricles, was expressed ≈ 20 folds lower in our HD-hESC-CMs (Table 5-5) than in our WT-hESC-CMs. However, *in vivo*, these phenotypes are found in 12 weeks old mice that have a very aggressive and rapid form of HD. Such phenotype might not develop in HD hESC-derived cardiomyocytes within the timeframe allowed by their *in vitro* culture, even if it can reach several months. Furthermore, R6/2 mice present severe neurodegeneration at this age and lose a lot of weight, including heart weight. It cannot be excluded that the cardiac phenotype observed in these studies is only an indirect consequence of the latter. This hypothesis is reinforced by a recent publication from Kiriazis *et al*., which suggests in their study of the R6/1 murine HD model that the observed cardiac defects are consequences of neurocardiac dysregulations and neurogenic arrhythmias (Kiriazis *et al.*, 2012). R6/1 and WT mice displayed different heart rate responses to isoprotenerol and atropine. The action potential of our HD-hESC-CM could be studied and such drug treatments could be replicated, with the unique advantage of not having any neuronal influence. This would give further highlight on whether HD cardiac defects are a direct or indirect consequence of HD. Finally, given more time and resources, I would have liked to study the HD-hESC-CMs calcium handling properties. Our model displays a 20-fold lower expression of *MYH7*. A βMYH (chick analogue of MYH7) knockdown in cardiac ventricle shows calcium transients deregulations, notably by the induction of a decrease in the rise time during the calcium transient. Correct calcium transients are essential for the cardiomyocytes to contract and beat properly (Rutland *et al.*, 2011; Lan *et al.*, 2013).

HD cardiac mitochondria have a disrupted morphology and density in 12 weeks old R6/2 mice (Mihm *et al.*, 2007). High magnification microscopic techniques, like e.g. Transmission Electron Microscopy (TEM) could be used to verify this phenotype in our model. TEM has enabled the modelling of pathological cardiac phenotypes in iPSC-derived cardiomyocytes, such as increased cell width, disorganised Z-band and differences in lipid droplets (Ma *et al.*, 2012). TEM could be used in our *in vitro* model to compare the ultra-structure of HD-hESC-CM and WT-hESC-CM, notably for the mitochondria, and to look for the presence of aggregates. Aggregates have been found in sparse quantities in hearts of the *Hdh*Q150 and the R6/2

murine models of HD (Moffitt *et al.*, 2009; Sathasivam *et al.*, 1999) and a study on polyglutamine amyloids revealed that transgenic mice expressing 83 CAG repeats residues in the cardiac tissues only suffered from reduced cardiac function and dilation by five months and died by eight months (Pattison *et al.*, 2008). However, for practical reasons, TEM needs to be prepared from EB-based cardiomyocytes (Dr. G. Vizcay-Barrena, personal communication) so the TEM sample preparation does not interfere with cardiomyocyte morphology. This correlates with recent methods described in the literature where TEM was performed on contractile EBs or cardiac bodies (Ma *et al.*, 2012; Gherghiceanu *et al.*, 2011; Yu, T. *et al.*, 2013; Tse *et al.*, 2013; Kensah *et al.*, 2013). Cardiomyocytes derived by the Laflamme differentiation protocol would not be suitable for TEM analysis.

A good positive control would be to try replicating in our HD-hESC lines some HD-phenotypes found in another *in vitro* HD modeling study, such as higher lysosomal activation (Camnasio *et al.*, 2012). Even though it has been stressed previously that this study requires more biological replicates in order to generate a baseline of WT gene expression, the best control would be to have isogenic hESC lines where only the HD mutation would differ. Such HD-hESCs were successfully generated by insertion of *HTT* exon 1 transgene baring different CAG repeats length into the H9 WT-hESC line (Lu and Palacino, 2013) or by homologous recombination where the 72 CAG repeats allele was corrected to 21 CAG repeats. This latter correction did not affect the pluripotency of hESCs nor their neuronal differentiation potential, and allowed the correction of HD-specific phenotype such as elevated caspase-3/7 activity (An *et al.*, 2012). Isogenic iPSCs have also been generated for Rett syndrome by X-Chromosome inactivation selection (Ananiev *et al.*, 2011), and by zinc finger nuclease (ZFN)-mediated genome editing for Parkinson's disease iPSCs (Soldner *et al.*, 2011). Genetic engineering of hESCs is also possible with Transcription Activation-Like Effector Nucleases (TALENs), which offer more flexibility in the sequence reading than ZFN and have the advantage of recognising single nucleotides (Hockemeyer *et al.*, 2011; Miller *et al.*, 2011).

Chapter 6

Summary

Chapter 6 Summary

6.1 Development of pluripotent models of HD

The work presented in this thesis focuses on the characterisation, development and differentiation of pluripotent stem cell models of HD. HD is an autosomal dominant, late onset disease caused by a single mutation, which offers a large window for therapy. *In vivo* and *in vitro* disease models were therefore developed for a better understanding of the disease, phenotype identification and therapeutic compound screening and development. Yet, at the beginning of this project, existing cellular models of HD had been developed from tumour cell lines using genome-integrating lentiviral delivery system carrying a mutated HTT exon 1. These models were not optimal, as the cells would always have non-innate extra copies of HTT, with CAG repeat sizes rarely seen in patients, and whose expression was driven by an exogenous promoter. Furthermore, none of the existing human HD cellular models were pluripotent, therefore restricting the somatic cell type in which the mutation could be studied.

In order to circumvent this, we aimed to develop two human pluripotent stem cell models of HD. The first model was HD-hESCs, isolated after PGD and donated to research by consenting couples. Seven HD-hESC lines were derived at the ACU, Guy's Hospital, King's College London. The second model to be developed was iPSCs generated from HF-keratinocytes using synthetic modified mRNA as a reprogramming vector. Although the technique was successfully optimised to reprogramme WT-fibroblasts, in the timeframe of this project I was not successful in optimising the protocol for the mRNA reprogramming of HF-keratinocytes. One possibility for the future would be to reprogramme HD fibroblasts with the optimised mRNA reprogramming protocol instead of HD-HF-keratinocytes.

6.2 Characterisation of HD-PSCs

Five HD-hESC lines were fully characterised in this study, along with four WT-hESC counterparts. I also characterised two iPSC lines generated with the optimised mRNA reprogramming protocol. The PSCs were characterised according to seven criteria: their morphology, the presence of pluripotency markers, their ability to differentiated *in* vitro and *in vivo*, DNA fingerprinting, genomic stability and HLA typing. Only one hESC line (KCL013_HD4) presented with genomic instability and was eliminated from this study. The other eight hESC lines were suitable for downstream differentiation.

The iPSCs generated in this study were exposed to different treatments, one of which comprised the transient inhibition of the p53 pathway. One iPSC line from each treatment group was selected for further investigation. Upon preliminary characterisation, no differences could

be observed between the two lines. Additionally, they behaved similarly to the hESCs used in this study. Nevertheless, future characterisation of these iPSCs would include full-exome sequencing and whole-genome DNA methylation analysis to confirm whether or not the transient p53 treatment could have induced any somatic mutations.

6.3 HD-PSC differentiation

Prior to their differentiation, the PSC were adapted to feeder-free culture conditions. The feeder-dependant culture system is not fully defined, requires manual passaging, which is labour-intensive and time consuming, this limits the scalability of PSC culture. Therefore, I trialled two different feeder-free matrices: GFR-Matrigel and decelullarised feeders matrix and two fully defined pluripotent stem cell media: complete KOSR and mTeSR1, for the feeder-free adaptation of the PSCs used in this study. It was determined that GFR-Matrigel and mTeSR1 was the best combination for feeder-free culture and PSC culture expansion. These results are in accordance with those published by a multicentre investigation that also determined that these were the best, defined, feeder-free PSC culture conditions (Akopian *et al.*, 2010). Once adapted to feeder-free culture conditions, the PSCs could be differentiated. For time constraints, it was decided to focus on the differentiation of the eight hESCs only.

HD is primarily a neurodegenerative disorder. Nevertheless, HTT is an ubiquitously expressed protein and disease-specific phenotypes are also present in peripheral tissues (Van Der Burg *et al.*, 2009; Sassone *et al.*, 2009; Sathasivam *et al.*, 1999). Epidemiology studies show that cardiac defects are a prevalent cause of death amongst HD patients (Sorensen and Fenger, 1992; Lanska *et al.*, 1988; Chiu and Alexander, 1982). Furthermore, cardiac defects, including atrophy, have previously been described in HD murine models (Sathasivam *et al.*, 1999; Mihm *et al.*, 2007; Wood, 2012; Kiriazis *et al.*, 2012). For these reasons, it was decided to differentiate the hESCs into cardiomyocytes in order to explore the HD phenotype in this cell type, and determine if the reported cardiac defects are a cell autonomous or non-cell autonomous consequence of HD. To our knowledge, other *in vitro* human HD cardiomyocytes model currently does not exist.

Several cardiac differentiation protocols were tried, either based on spontaneous or directed cardiac differentiation. In our hands, mTeSR1 had an inhibitory effect on cardiac differentiation. This observation was further supported by a study by Ojala *et al.* (2012) that also reported GFR-Matrigel and mTeSR1 to be the least favourable for cardiac differentiation. Consequently, the hESCs were adapted to another fully defined medium, Nutristem. All the hESCs lines but KCL012_HD3 could be adapted to it. KCL012_HD3 presented with a lot of spontaneous differentiation in these new culture conditions and was excluded from the rest of the study. It cannot be excluded that KCL012_HD3 could have acquired a chromosomal abnormality which could explain this increased rate of spontaneous differentiation.

Using Nutristem and GFR-Matrigel, the Laflamme directed cardiac differentiation protocol (Laflamme *et al.*, 2007) was the most dependable in our hands. All the differentiated hESC lines but KCL040 presented beating areas within 30 days of differentiation. Despite a range of efficiency, the observation of beating areas, the positive immunofluorescence and gene expression study of cardiac-specific markers confirmed that the HD-hESCs could be differentiated into cardiomyocytes similarly to WT-hESCs. I next chose one WT- and one HD-hESC line (KCL031 and KCL027_HD5 respectively) with the best cardiac differentiation efficiency at 30 days for further investigation. In these samples, I looked at the gene expression of 16 cardiac-specific biomarkers. This further confirmed that the HD-hESCs differentiated into cardiomyocytes. However, the data also suggested that the HD-hESCs could be less mature than the WT-hESCs at 30 days of cardiac differentiation with the Laflamme protocol.

Next, I looked at the stability of the CAG mutation in the HD-hESC line KCL027_HD5 in undifferentiated samples and after 30 and 60 days of cardiac differentiation with the Laflamme protocol. The mutation (44 CAG) remained stable throughout differentiation.

6.4 Future prospects of HD-PSC modelling

HD being a late-onset disease, one could wonder if *in vitro* HD-PSCs could display HD-specific phenotypes. Several HD studies have identified HD specific *in vitro* phenotypes, such as increased lysosomal activity in undifferentiated hESCs (Camnasio *et al.*, 2012) and elevated caspase in HD-iPSCs derived neurons (Zhang, N. *et al.*, 2010). In the work presented in this study our undifferentiated HD-hESCs cannot be distinguished from WT-hESCs. They can also be differentiated into cardiomyocytes to study the HD mutation in this somatic cell type.

However, it is known that there is variability in gene expression in hESCs (Allegrucci and Young, 2007), an observation that could also be made in our undifferentiated hESCs (Table 5.3). Therefore, it is recommended to repeat the cardiac differentiation of the hESCs used in this study to further distinguish what could be a potential HD-specific phenotype from cell line variability. To completely exclude this possibility, it would be best to work with isogenic lines. An *et al.* (2012) were able to correct the HD mutation by homologous recombination and rescue the HD phenotype in their lines this way.

In this study, gene expression was analysed at 30 days post differentiation. HD being a progressive disease, it would be interesting to study later time points. . Further investigation of HD-specific cardiac phenotypes could also be complemented by electrophysiology work at the single cell level by patch-clamping for instance. Indeed, this technique allows distinguishing between different types of cardiomyocytes action potential i.e. ventricular-, atrial- or nodal-like. In the case of Long-QT Syndrome iPSC-derived cardiomyocytes, patch clamping revealed differences in spontaneous beating of ventricular and atrial Long-QT Syndrome cardiomyocytes compared to wild-type cardiomyocytes, while no significant differences could be reported for

nodal Long-QT Syndrome cardiomyocytes compared to wild-type cardiomyocytes (Moretti *et al*., 2010). On top of studying spontaneous cardiomyocyte beating, the WT-hESC-CMs and the HD-hESC-CMs could also be electrically stimulated in order to study their adaptive response to changing rates of electrical stimulation. Other functional studies that could be performed on the cardiomyocytes generated in this study could include comparing the β-adrenergic regulation of the WT-hESC-CMs and the HD-hESC-CMs. To do so, the cardiomyocytes could be treated with a nonselective β-adrenergic receptor agonist such as isoproterenol. If the cardiomyocytes are functional, an increase in heart and decrease in action potential should be observed. Finally, analyzing the calcium transients during spontaneous or stimuli-induced beating of the WT-hESC-CMs and the HD-hESC-CMs could be used for the characterization of the calcium channels.

Recent studies on HD-iPSC-derived neurons observed increased cell death and increase caspase activity after growth factor removal (An *et al.*, 2012; Zhang, N. *et al.*, 2010; The HD iPSC Consortium, 2012). Stressing the cells by the use of toxic agents or growth factor removal might be required in order to observe a phenotype in HD-hESC-CMs. Lastly, as discussed in chapter 5, even though beating was observed after 30 days of differentiation in six hESC lines, to further explore the HD in vitro cardiac phenotype, the yield of cardiomyocytes needs to be improved. This could be achieved by further optimising the cardiac differentiation protocol or by enriching the cardiomyocyte population post-differentiation.

The HD iPSC consortium recently published that the positive correlation between CAG repeat size and severity of symptoms observed in HD patients could also be observed in vitro in HD-iPSC derived neurons (The HD iPSC Consortium, 2012). Even though the CAG-repeat expansion associated phenotypes were already reported in transgenic models of HD, this is of critical importance as it is from the endogenous mutation. These data further highlight the need to generate HD-iPSCs with a wider range of repeats, possibly from JHD patients in the future.

References

REFERENCES

Aasen, T. & Belmonte, J. C. 2010. Isolation and cultivation of human keratinocytes from skin or plucked hair for the generation of induced pluripotent stem cells. *Nat. Protoc.,* 5**,** 371-82.

Aasen, T., Raya, A., Barrero, M. J., Garreta, E., Consiglio, A., Gonzalez, F., Vassena, R., Bilic, J., Pekarik, V., Tiscornia, G., Edel, M., Boue, S. & Izpisua Belmonte, J. C. 2008. Efficient and rapid generation of induced pluripotent stem cells from human keratinocytes. *Nat. Biotechnol.,* 26**,** 1276-84.

Akopian, V., Andrews, P. W., Beil, S., Benvenisty, N., Brehm, J., Christie, M., Ford, A., Fox, V., Gokhale, P. J., Healy, L., Holm, F., Hovatta, O., Knowles, B. B., Ludwig, T. E., Mckay, R. D., Miyazaki, T., Nakatsuji, N., Oh, S. K., Pera, M. F., Rossant, J., Stacey, G. N. & Suemori, H. 2010. Comparison of defined culture systems for feeder cell free propagation of human embryonic stem cells. *In vitro cellular & developmental biology. Animal,* 46**,** 247-58.

Allegrucci, C. & Young, L. E. 2007. Differences between human embryonic stem cell lines. *Hum. Reprod. Update,* 13**,** 103-20.

Alonso, L. & Fuchs, E. 2006. The hair cycle. *J. Cell Sci.,* 119**,** 391-3.

Amit, M., Shariki, C., Margulets, V. & Itskovitz-Eldor, J. 2004. Feeder layer- and serum-free culture of human embryonic stem cells. *Biol. Reprod.,* 70**,** 837-45.

Amps, K., Andrews, P. W., Anyfantis, G., Armstrong, L., Avery, S., Baharvand, H., Baker, J., Baker, D., Munoz, M. B., Beil, S., Benvenisty, N., Ben-Yosef, D., Biancotti, J. C., Bosman, A., Brena, R. M., Brison, D., Caisander, G., Camarasa, M. V., Chen, J., Chiao, E., Choi, Y. M., Choo, A. B., Collins, D., Colman, A., Crook, J. M., Daley, G. Q., Dalton, A., De Sousa, P. A., Denning, C., Downie, J., Dvorak, P., Montgomery, K. D., Feki, A., Ford, A., Fox, V., Fraga, A. M., Frumkin, T., Ge, L., Gokhale, P. J., Golan-Lev, T., Gourabi, H., Gropp, M., Lu, G., Hampl, A., Harron, K., Healy, L., Herath, W., Holm, F., Hovatta, O., Hyllner, J., Inamdar, M. S., Irwanto, A. K., Ishii, T., Jaconi, M., Jin, Y., Kimber, S., Kiselev, S., Knowles, B. B., Kopper, O., Kukharenko, V., Kuliev, A., Lagarkova, M. A., Laird, P. W., Lako, M., Laslett, A. L., Lavon, N., Lee, D. R., Lee, J. E., Li, C., Lim, L. S., Ludwig, T. E., Ma, Y., Maltby, E., Mateizel, I., Mayshar, Y., Mileikovsky, M., Minger, S. L., Miyazaki, T., Moon, S. Y., Moore, H., Mummery, C., Nagy, A., Nakatsuji, N., Narwani, K., Oh, S. K., Olson, C., Otonkoski, T., Pan, F., Park, I. H., Pells, S., Pera, M. F., Pereira, L. V., Qi, O., Raj, G. S., Reubinoff, B., Robins, A., Robson, P., Rossant, J., Salekdeh, G. H., Schulz, T. C*., et al.* 2011. Screening ethnically diverse human embryonic stem cells identifies a chromosome 20 minimal amplicon conferring growth advantage. *Nat. Biotechnol.,* 29**,** 1132-44.

An, M. C., Zhang, N., Scott, G., Montoro, D., Wittkop, T., Mooney, S., Melov, S. & Ellerby, L. M. 2012. Genetic correction of Huntington's disease phenotypes in induced pluripotent stem cells. *Cell Stem Cell,* 11**,** 253-63.

Ananiev, G., Williams, E. C., Li, H. & Chang, Q. 2011. Isogenic pairs of wild type and mutant induced pluripotent stem cell (iPSC) lines from Rett syndrome patients as in vitro disease model. *PLoS One,* 6**,** e25255.

Angel, M. & Yanik, M. F. 2010. Innate immune suppression enables frequent transfection with RNA encoding reprogramming proteins. *PLoS One,* 5**,** e11756.

Anokye-Danso, F., Trivedi, C. M., Juhr, D., Gupta, M., Cui, Z., Tian, Y., Zhang, Y., Yang, W., Gruber, P. J., Epstein, J. A. & Morrisey, E. E. 2011. Highly efficient miRNA-mediated reprogramming of mouse and human somatic cells to pluripotency. *Cell Stem Cell,* 8**,** 376-88.

Apostol, B. L., Kazantsev, A., Raffioni, S., Illes, K., Pallos, J., Bodai, L., Slepko, N., Bear, J. E., Gertler, F. B., Hersch, S., Housman, D. E., Marsh, J. L. & Thompson, L. M. 2003. A cell-based assay for aggregation inhibitors as therapeutics of polyglutamine-repeat disease and validation in Drosophila. *Proc. Natl. Acad. Sci. U. S. A.,* 100**,** 5950-5.

Arrasate, M., Mitra, S., Schweitzer, E. S., Segal, M. R. & Finkbeiner, S. 2004. Inclusion body formation reduces levels of mutant huntingtin and the risk of neuronal death. *Nature,* 431**,** 805-10.

Bari, M., Battista, N., Valenza, M., Mastrangelo, N., Malaponti, M., Catanzaro, G., Centonze, D., Finazzi-Agro, A., Cattaneo, E. & Maccarrone, M. 2013. In vitro and in vivo models of Huntington's disease show alterations in the endocannabinoid system. *The FEBS journal,* 280**,** 3376-88.

Bates, G. P. & Hockly, E. 2003. Experimental therapeutics in Huntington's disease: are models useful for therapeutic trials? *Curr. Opin. Neurol.,* 16**,** 465-70.

Batista, L. F., Pech, M. F., Zhong, F. L., Nguyen, H. N., Xie, K. T., Zaug, A. J., Crary, S. M., Choi, J., Sebastiano, V., Cherry, A., Giri, N., Wernig, M., Alter, B. P., Cech, T. R., Savage, S. A., Reijo Pera, R. A. & Artandi, S. E. 2011. Telomere shortening and loss of self-renewal in dyskeratosis congenita induced pluripotent stem cells. *Nature,* 474**,** 399-402.

Bauwens, C. L., Song, H., Thavandiran, N., Ungrin, M., Masse, S., Nanthakumar, K., Seguin, C. & Zandstra, P. W. 2011. Geometric control of cardiomyogenic induction in human pluripotent stem cells. *Tissue Eng Part A,* 17**,** 1901-9.

Beacham, D. A., Amatangelo, M. D. & Cukierman, E. 2007. Preparation of extracellular matrices produced by cultured and primary fibroblasts. *Curr. Protoc. Cell Biol.,* Chapter 10**,** Unit 10 9.

Braam, S. R., Zeinstra, L., Litjens, S., Ward-Van Oostwaard, D., Van Den Brink, S., Van Laake, L., Lebrin, F., Kats, P., Hochstenbach, R., Passier, R., Sonnenberg, A. & Mummery, C. L. 2008. Recombinant vitronectin is a functionally defined substrate that supports human embryonic stem cell self-renewal via alphavbeta5 integrin. *Stem Cells,* 26**,** 2257-65.

Burridge, P. W., Thompson, S., Millrod, M. A., Weinberg, S., Yuan, X., Peters, A., Mahairaki, V., Koliatsos, V. E., Tung, L. & Zambidis, E. T. 2011. A universal system for highly efficient cardiac differentiation of human induced pluripotent stem cells that eliminates interline variability. *PLoS One,* 6**,** e18293.

Bustin, S. A., Benes, V., Garson, J. A., Hellemans, J., Huggett, J., Kubista, M., Mueller, R., Nolan, T., Pfaffl, M. W., Shipley, G. L., Vandesompele, J. & Wittwer, C. T. 2011. Primer sequence disclosure: a clarification of the MIQE guidelines. *Clin. Chem.,* 57**,** 919-21.

Camnasio, S., Carri, A. D., Lombardo, A., Grad, I., Mariotti, C., Castucci, A., Rozell, B., Riso, P. L., Castiglioni, V., Zuccato, C., Rochon, C., Takashima, Y., Diaferia, G., Biunno, I., Gellera, C., Jaconi, M., Smith, A., Hovatta, O., Naldini, L., Di Donato, S., Feki, A. & Cattaneo, E. 2012. The first reported generation of several induced pluripotent stem cell lines from homozygous and heterozygous Huntington's disease patients demonstrates mutation related enhanced lysosomal activity. *Neurobiol. Dis.,* 46**,** 41-51.

Canals, J. M., Pineda, J. R., Torres-Peraza, J. F., Bosch, M., Martin-Ibanez, R., Munoz, M. T., Mengod, G., Ernfors, P. & Alberch, J. 2004. Brain-derived neurotrophic factor regulates the onset and severity of motor dysfunction associated with enkephalinergic neuronal degeneration in Huntington's disease. *The Journal of neuroscience : the official journal of the Society for Neuroscience,* 24**,** 7727-39.

Castiglioni, V., Onorati, M., Rochon, C. & Cattaneo, E. 2012. Induced pluripotent stem cell lines from Huntington's disease mice undergo neuronal differentiation while showing alterations in the lysosomal pathway. *Neurobiol. Dis.,* 46**,** 30-40.

Catalina, P., Montes, R., Ligero, G., Sanchez, L., De La Cueva, T., Bueno, C., Leone, P. E. & Menendez, P. 2008. Human ESCs predisposition to karyotypic instability: Is a matter of culture adaptation or differential vulnerability among hESC lines due to inherent properties? *Mol. Cancer,* 7**,** 76.

Chapman, S., Liu, X., Meyers, C., Schlegel, R. & Mcbride, A. A. 2010. Human keratinocytes are efficiently immortalized by a Rho kinase inhibitor. *The Journal of clinical investigation,* 120**,** 2619-26.

Chetty, S., Pagliuca, F. W., Honore, C., Kweudjeu, A., Rezania, A. & Melton, D. A. 2013. A simple tool to improve pluripotent stem cell differentiation. *Nature methods,* 10**,** 553-6.

Chin, M. H., Mason, M. J., Xie, W., Volinia, S., Singer, M., Peterson, C., Ambartsumyan, G., Aimiuwu, O., Richter, L., Zhang, J., Khvorostov, I., Ott, V., Grunstein, M., Lavon, N., Benvenisty, N., Croce, C. M., Clark, A. T., Baxter, T., Pyle, A. D., Teitell, M. A., Pelegrini, M., Plath, K. & Lowry, W. E. 2009. Induced pluripotent stem cells and embryonic stem cells are distinguished by gene expression signatures. *Cell Stem Cell,* 5**,** 111-23.

Chiu, E. & Alexander, L. 1982. Causes of death in Huntington's disease. *The Medical journal of Australia,* 1**,** 153.

Ciammola, A., Sassone, J., Alberti, L., Meola, G., Mancinelli, E., Russo, M. A., Squitieri, F. & Silani, V. 2006. Increased apoptosis, Huntingtin inclusions and altered differentiation in muscle cell cultures from Huntington's disease subjects. *Cell Death Differ.,* 13**,** 2068-78.

Davies, S. W., Turmaine, M., Cozens, B. A., Difiglia, M., Sharp, A. H., Ross, C. A., Scherzinger, E., Wanker, E. E., Mangiarini, L. & Bates, G. P. 1997. Formation of neuronal intranuclear inclusions underlies the neurological dysfunction in mice transgenic for the HD mutation. *Cell,* 90**,** 537-48.

Dolnikov, K., Shilkrut, M., Zeevi-Levin, N., Gerecht-Nir, S., Amit, M., Danon, A., Itskovitz-Eldor, J. & Binah, O. 2006. Functional properties of human embryonic stem cell-derived

cardiomyocytes: intracellular Ca2+ handling and the role of sarcoplasmic reticulum in the contraction. *Stem Cells,* 24**,** 236-45.

Dragatsis, I., Levine, M. S. & Zeitlin, S. 2000. Inactivation of Hdh in the brain and testis results in progressive neurodegeneration and sterility in mice. *Nat. Genet.,* 26**,** 300-6.

Draper, J. S., Smith, K., Gokhale, P., Moore, H. D., Maltby, E., Johnson, J., Meisner, L., Zwaka, T. P., Thomson, J. A. & Andrews, P. W. 2004. Recurrent gain of chromosomes 17q and 12 in cultured human embryonic stem cells. *Nat. Biotechnol.,* 22**,** 53-4.

Dubois, N. C., Craft, A. M., Sharma, P., Elliott, D. A., Stanley, E. G., Elefanty, A. G., Gramolini, A. & Keller, G. 2011. SIRPA is a specific cell-surface marker for isolating cardiomyocytes derived from human pluripotent stem cells. *Nat. Biotechnol.*

Duyao, M., Ambrose, C., Myers, R., Novelletto, A., Persichetti, F., Frontali, M., Folstein, S., Ross, C., Franz, M., Abbott, M. & Et Al. 1993. Trinucleotide repeat length instability and age of onset in Huntington's disease. *Nat. Genet.,* 4**,** 387-92.

Elliott, D. A., Braam, S. R., Koutsis, K., Ng, E. S., Jenny, R., Lagerqvist, E. L., Biben, C., Hatzistavrou, T., Hirst, C. E., Yu, Q. C., Skelton, R. J., Ward-Van Oostwaard, D., Lim, S. M., Khammy, O., Li, X., Hawes, S. M., Davis, R. P., Goulburn, A. L., Passier, R., Prall, O. W., Haynes, J. M., Pouton, C. W., Kaye, D. M., Mummery, C. L., Elefanty, A. G. & Stanley, E. G. 2011. NKX2-5(eGFP/w) hESCs for isolation of human cardiac progenitors and cardiomyocytes. *Nat Methods*.

Epping, E. A. & Paulsen, J. S. 2011. Depression in the early stages of Huntington disease. *Neurodegener. Dis. Manag.,* 1**,** 407-414.

Fath, S., Bauer, A. P., Liss, M., Spriestersbach, A., Maertens, B., Hahn, P., Ludwig, C., Schafer, F., Graf, M. & Wagner, R. 2011. Multiparameter RNA and codon optimization: a standardized tool to assess and enhance autologous mammalian gene expression. *PLoS One,* 6**,** e17596.

Foldes, G., Mioulane, M., Wright, J. S., Liu, A. Q., Novak, P., Merkely, B., Gorelik, J., Schneider, M. D., Ali, N. N. & Harding, S. E. 2011. Modulation of human embryonic stem cell-derived cardiomyocyte growth: a testbed for studying human cardiac hypertrophy? *J. Mol. Cell. Cardiol.,* 50**,** 367-76.

Fortson, W. S., Kayarthodi, S., Fujimura, Y., Xu, H., Matthews, R., Grizzle, W. E., Rao, V. N., Bhat, G. K. & Reddy, E. S. 2011. Histone deacetylase inhibitors, valproic acid and trichostatin-A induce apoptosis and affect acetylation status of p53 in ERG-positive prostate cancer cells. *Int. J. Oncol.,* 39**,** 111-9.

Fox, J. H., Barber, D. S., Singh, B., Zucker, B., Swindell, M. K., Norflus, F., Buzescu, R., Chopra, R., Ferrante, R. J., Kazantsev, A. & Hersch, S. M. 2004. Cystamine increases L-cysteine levels in Huntington's disease transgenic mouse brain and in a PC12 model of polyglutamine aggregation. *J. Neurochem.,* 91**,** 413-22.

Frenkel, G. D., Walcott, A. & Middleton, C. 1987. Inhibition of RNA and DNA polymerases by the product of the reaction of selenite with sulfhydryl compounds. *Mol. Pharmacol.,* 31**,** 112-6.

Fujiki, R., Sato, A., Fujitani, M. & Yamashita, T. 2013. A proapoptotic effect of valproic acid on progenitors of embryonic stem cell-derived glutamatergic neurons. *Cell Death Dis.,* 4**,** e677.

Furue, M. K., Na, J., Jackson, J. P., Okamoto, T., Jones, M., Baker, D., Hata, R., Moore, H. D., Sato, J. D. & Andrews, P. W. 2008. Heparin promotes the growth of human embryonic stem cells in a defined serum-free medium. *Proc. Natl. Acad. Sci. U. S. A.,* 105**,** 13409-14.

Fusaki, N., Ban, H., Nishiyama, A., Saeki, K. & Hasegawa, M. 2009. Efficient induction of transgene-free human pluripotent stem cells using a vector based on Sendai virus, an RNA virus that does not integrate into the host genome. *Proc. Jpn. Acad. Ser. B Phys. Biol. Sci.,* 85**,** 348-62.

Gallo, P., Grimaldi, S., Latronico, M. V., Bonci, D., Pagliuca, A., Ausoni, S., Peschle, C. & Condorelli, G. 2008. A lentiviral vector with a short troponin-I promoter for tracking cardiomyocyte differentiation of human embryonic stem cells. *Gene Ther.,* 15**,** 161-70.

Germanguz, I., Sedan, O., Zeevi-Levin, N., Shtrichman, R., Barak, E., Ziskind, A., Eliyahu, S., Meiry, G., Amit, M., Itskovitz-Eldor, J. & Binah, O. 2011. Molecular characterization and functional properties of cardiomyocytes derived from human inducible pluripotent stem cells. *J. Cell. Mol. Med.,* 15**,** 38-51.

Gherghiceanu, M., Barad, L., Novak, A., Reiter, I., Itskovitz-Eldor, J., Binah, O. & Popescu, L. M. 2011. Cardiomyocytes derived from human embryonic and induced pluripotent stem cells: comparative ultrastructure. *J. Cell. Mol. Med.,* 15**,** 2539-51.

Ghosh, Z., Wilson, K. D., Wu, Y., Hu, S., Quertermous, T. & Wu, J. C. 2010. Persistent donor cell gene expression among human induced pluripotent stem cells contributes to differences with human embryonic stem cells. *PLoS One,* 5**,** e8975.

Graichen, R., Xu, X., Braam, S. R., Balakrishnan, T., Norfiza, S., Sieh, S., Soo, S. Y., Tham, S. C., Mummery, C., Colman, A., Zweigerdt, R. & Davidson, B. P. 2008. Enhanced Cardiomyogenesis Of Human Embryonic Stem Cells By A Small Molecular Inhibitor Of P38 MAPK. *Differentiation,* 76**,** 357-70.

Gray, M., Shirasaki, D. I., Cepeda, C., Andre, V. M., Wilburn, B., Lu, X. H., Tao, J., Yamazaki, I., Li, S. H., Sun, Y. E., Li, X. J., Levine, M. S. & Yang, X. W. 2008. Full-length human mutant huntingtin with a stable polyglutamine repeat can elicit progressive and selective neuropathogenesis in BACHD mice. *The Journal of neuroscience : the official journal of the Society for Neuroscience,* 28**,** 6182-95.

Guenther, M. G., Frampton, G. M., Soldner, F., Hockemeyer, D., Mitalipova, M., Jaenisch, R. & Young, R. A. 2010. Chromatin structure and gene expression programs of human embryonic and induced pluripotent stem cells. *Cell Stem Cell,* 7**,** 249-57.

Handyside, A. H., Kontogianni, E. H., Hardy, K. & Winston, R. M. 1990. Pregnancies from biopsied human preimplantation embryos sexed by Y-specific DNA amplification. *Nature,* 344**,** 768-70.

Harjes, P. & Wanker, E. E. 2003. The hunt for huntingtin function: interaction partners tell many different stories. *Trends Biochem. Sci.,* 28**,** 425-33.

Heath, K. E., Day, I. N. & Humphries, S. E. 2000. Universal primer quantitative fluorescent multiplex (UPQFM) PCR: a method to detect major and minor rearrangements of the low density lipoprotein receptor gene. *J. Med. Genet.,* 37**,** 272-80.

Hockemeyer, D., Wang, H., Kiani, S., Lai, C. S., Gao, Q., Cassady, J. P., Cost, G. J., Zhang, L., Santiago, Y., Miller, J. C., Zeitler, B., Cherone, J. M., Meng, X., Hinkley, S. J., Rebar, E. J., Gregory, P. D., Urnov, F. D. & Jaenisch, R. 2011. Genetic engineering of human pluripotent cells using TALE nucleases. *Nat. Biotechnol.,* 29**,** 731-4.

Hockly, E., Woodman, B., Mahal, A., Lewis, C. M. & Bates, G. 2003. Standardization and statistical approaches to therapeutic trials in the R6/2 mouse. *Brain Res. Bull.,* 61**,** 469-79.

Hodgson, J. G., Agopyan, N., Gutekunst, C. A., Leavitt, B. R., Lepiane, F., Singaraja, R., Smith, D. J., Bissada, N., Mccutcheon, K., Nasir, J., Jamot, L., Li, X. J., Stevens, M. E., Rosemond, E., Roder, J. C., Phillips, A. G., Rubin, E. M., Hersch, S. M. & Hayden, M. R. 1999. A YAC mouse model for Huntington's disease with full-length mutant huntingtin, cytoplasmic toxicity, and selective striatal neurodegeneration. *Neuron,* 23**,** 181-92.

Hong, H., Takahashi, K., Ichisaka, T., Aoi, T., Kanagawa, O., Nakagawa, M., Okita, K. & Yamanaka, S. 2009. Suppression of induced pluripotent stem cell generation by the p53-p21 pathway. *Nature,* 460**,** 1132-5.

Honn, K. V., Singley, J. A. & Chavin, W. 1975. Fetal bovine serum: a multivariate standard. *Proceedings of the Society for Experimental Biology and Medicine. Society for Experimental Biology and Medicine,* 149**,** 344-7.

Huangfu, D., Osafune, K., Maehr, R., Guo, W., Eijkelenboom, A., Chen, S., Muhlestein, W. & Melton, D. A. 2008. Induction of pluripotent stem cells from primary human fibroblasts with only Oct4 and Sox2. *Nat. Biotechnol.,* 26**,** 1269-75.

Huber, I., Itzhaki, I., Caspi, O., Arbel, G., Tzukerman, M., Gepstein, A., Habib, M., Yankelson, L., Kehat, I. & Gepstein, L. 2007. Identification and selection of cardiomyocytes during human embryonic stem cell differentiation. *FASEB journal : official publication of the Federation of American Societies for Experimental Biology,* 21**,** 2551-63.

Huntington, G. 1872. On Chorea. *Medical and Surgical Reporter,* 26**,** 317-321.

Ilic, D., Stephenson, E., Wood, V., Jacquet, L., Stevenson, D., Petrova, A., Kadeva, N., Codognotto, S., Patel, H., Semple, M., Cornwell, G., Ogilvie, C. & Braude, P. 2012. Derivation and feeder-free propagation of human embryonic stem cells under xeno-free conditions. *Cytotherapy,* 14**,** 122-8.

Irwin, E. F., Gupta, R., Dashti, D. C. & Healy, K. E. 2011. Engineered polymer-media interfaces for the long-term self-renewal of human embryonic stem cells. *Biomaterials,* 32**,** 6912-9.

Israel, M. A., Yuan, S. H., Bardy, C., Reyna, S. M., Mu, Y., Herrera, C., Hefferan, M. P., Van Gorp, S., Nazor, K. L., Boscolo, F. S., Carson, C. T., Laurent, L. C., Marsala, M., Gage, F. H., Remes, A. M., Koo, E. H. & Goldstein, L. S. 2012. Probing sporadic and familial Alzheimer's disease using induced pluripotent stem cells. *Nature,* 482**,** 216-20.

Itskovitz-Eldor, J., Schuldiner, M., Karsenti, D., Eden, A., Yanuka, O., Amit, M., Soreq, H. & Benvenisty, N. 2000. Differentiation of human embryonic stem cells into embryoid bodies compromising the three embryonic germ layers. *Mol. Med.,* 6**,** 88-95.

Jackson, G. R., Salecker, I., Dong, X., Yao, X., Arnheim, N., Faber, P. W., Macdonald, M. E. & Zipursky, S. L. 1998. Polyglutamine-expanded human huntingtin transgenes induce degeneration of Drosophila photoreceptor neurons. *Neuron,* 21**,** 633-42.

Jackson-Grusby, L., Beard, C., Possemato, R., Tudor, M., Fambrough, D., Csankovszki, G., Dausman, J., Lee, P., Wilson, C., Lander, E. & Jaenisch, R. 2001. Loss of genomic methylation causes p53-dependent apoptosis and epigenetic deregulation. *Nat. Genet.,* 27**,** 31-9.

Jacquet, L., Stephenson, E., Collins, R., Patel, H., Trussler, J., Al-Bedaery, R., Renwick, P., Ogilvie, C., Vaughan, R. & Ilic, D. 2013. Strategy for the creation of clinical grade hESC line banks that HLA-match a target population. *EMBO Mol Med*, 5, 10-7.

Jacobsen, J. C., Bawden, C. S., Rudiger, S. R., Mclaughlan, C. J., Reid, S. J., Waldvogel, H. J., Macdonald, M. E., Gusella, J. F., Walker, S. K., Kelly, J. M., Webb, G. C., Faull, R. L., Rees, M. I. & Snell, R. G. 2010. An ovine transgenic Huntington's disease model. *Hum. Mol. Genet.,* 19**,** 1873-82.

Jovicic, A., Zaldivar Jolissaint, J. F., Moser, R., Silva Santos Mde, F. & Luthi-Carter, R. 2013. MicroRNA-22 (miR-22) overexpression is neuroprotective via general anti-apoptotic effects and may also target specific Huntington's disease-related mechanisms. *PLoS One,* 8**,** e54222.

Kaufman, D. S., Hanson, E. T., Lewis, R. L., Auerbach, R. & Thomson, J. A. 2001. Hematopoietic colony-forming cells derived from human embryonic stem cells. *Proc. Natl. Acad. Sci. U. S. A.,* 98**,** 10716-21.

Kawamura, T., Suzuki, J., Wang, Y. V., Menendez, S., Morera, L. B., Raya, A., Wahl, G. M. & Izpisua Belmonte, J. C. 2009. Linking the p53 tumour suppressor pathway to somatic cell reprogramming. *Nature,* 460**,** 1140-4.

Kehat, I., Kenyagin-Karsenti, D., Snir, M., Segev, H., Amit, M., Gepstein, A., Livne, E., Binah, O., Itskovitz-Eldor, J. & Gepstein, L. 2001. Human embryonic stem cells can differentiate into myocytes with structural and functional properties of cardiomyocytes. *The Journal of clinical investigation,* 108**,** 407-14.

Kennedy, L., Evans, E., Chen, C. M., Craven, L., Detloff, P. J., Ennis, M. & Shelbourne, P. F. 2003. Dramatic tissue-specific mutation length increases are an early molecular event in Huntington disease pathogenesis. *Hum. Mol. Genet.,* 12**,** 3359-67.

Kensah, G., Roa Lara, A., Dahlmann, J., Zweigerdt, R., Schwanke, K., Hegermann, J., Skvorc, D., Gawol, A., Azizian, A., Wagner, S., Maier, L. S., Krause, A., Drager, G., Ochs, M., Haverich, A., Gruh, I. & Martin, U. 2013. Murine and human pluripotent stem cell-derived cardiac bodies form contractile myocardial tissue in vitro. *Eur. Heart J.,* 34**,** 1134-46.

Kim, D., Kim, C. H., Moon, J. I., Chung, Y. G., Chang, M. Y., Han, B. S., Ko, S., Yang, E., Cha, K. Y., Lanza, R. & Kim, K. S. 2009. Generation of human induced pluripotent stem cells by direct delivery of reprogramming proteins. *Cell Stem Cell,* 4**,** 472-6.

Kim, H. T., Lee, K. I., Kim, D. W. & Hwang, D. Y. 2013. An ECM-based culture system for the generation and maintenance of xeno-free human iPS cells. *Biomaterials,* 34**,** 1041-50.

Kim, K., Zhao, R., Doi, A., Ng, K., Unternaehrer, J., Cahan, P., Hongguang, H., Loh, Y. H., Aryee, M. J., Lensch, M. W., Li, H., Collins, J. J., Feinberg, A. P. & Daley, G. Q. 2011. Donor cell type can influence the epigenome and differentiation potential of human induced pluripotent stem cells. *Nat. Biotechnol.*

Kim, K. Y., Hysolli, E. & Park, I. H. 2011. Neuronal maturation defect in induced pluripotent stem cells from patients with Rett syndrome. *Proc. Natl. Acad. Sci. U. S. A.*

Kim, M., Lee, H. S., Laforet, G., Mcintyre, C., Martin, E. J., Chang, P., Kim, T. W., Williams, M., Reddy, P. H., Tagle, D., Boyce, F. M., Won, L., Heller, A., Aronin, N. & Difiglia, M. 1999. Mutant huntingtin expression in clonal striatal cells: dissociation of inclusion formation and neuronal survival by caspase inhibition. *The Journal of neuroscience : the official journal of the Society for Neuroscience,* 19**,** 964-73.

Kiriazis, H., Jennings, N. L., Davern, P., Lambert, G., Su, Y., Pang, T., Du, X., La Greca, L., Head, G. A., Hannan, A. J. & Du, X. J. 2012. Neurocardiac dysregulation and neurogenic arrhythmias in a transgenic mouse model of Huntington's disease. *The Journal of physiology,* 590**,** 5845-60.

Kita-Matsuo, H., Barcova, M., Prigozhina, N., Salomonis, N., Wei, K., Jacot, J. G., Nelson, B., Spiering, S., Haverslag, R., Kim, C., Talantova, M., Bajpai, R., Calzolari, D., Terskikh, A., Mcculloch, A. D., Price, J. H., Conklin, B. R., Chen, H. S. & Mercola, M. 2009. Lentiviral vectors and protocols for creation of stable hESC lines for fluorescent tracking and drug resistance selection of cardiomyocytes. *PLoS One,* 4**,** e5046.

Kleinman, H. K., Mcgarvey, M. L., Liotta, L. A., Robey, P. G., Tryggvason, K. & Martin, G. R. 1982. Isolation and characterization of type IV procollagen, laminin, and heparan sulfate proteoglycan from the EHS sarcoma. *Biochemistry,* 21**,** 6188-93.

Klimanskaya, I., Chung, Y., Meisner, L., Johnson, J., West, M. D. & Lanza, R. 2005. Human embryonic stem cells derived without feeder cells. *Lancet,* 365**,** 1636-41.

Laflamme, M. A., Chen, K. Y., Naumova, A. V., Muskheli, V., Fugate, J. A., Dupras, S. K., Reinecke, H., Xu, C., Hassanipour, M., Police, S., O'sullivan, C., Collins, L., Chen, Y., Minami, E., Gill, E. A., Ueno, S., Yuan, C., Gold, J. & Murry, C. E. 2007. Cardiomyocytes derived from human embryonic stem cells in pro-survival factors enhance function of infarcted rat hearts. *Nat. Biotechnol.,* 25**,** 1015-24.

Lahti, A. L., Kujala, V. J., Chapman, H., Koivisto, A. P., Pekkanen-Mattila, M., Kerkela, E., Hyttinen, J., Kontula, K., Swan, H., Conklin, B. R., Yamanaka, S., Silvennoinen, O. & Aalto-Setala, K. 2011. Model for long QT syndrome type 2 using human iPS cells demonstrates arrhythmogenic characteristics in cell culture. *Dis. Model. Mech.*

Lan, F., Lee, A. S., Liang, P., Sanchez-Freire, V., Nguyen, P. K., Wang, L., Han, L., Yen, M., Wang, Y., Sun, N., Abilez, O. J., Hu, S., Ebert, A. D., Navarrete, E. G., Simmons, C. S., Wheeler, M., Pruitt, B., Lewis, R., Yamaguchi, Y., Ashley, E. A., Bers, D. M., Robbins, R. C., Longaker, M. T. & Wu, J. C. 2013. Abnormal calcium handling properties underlie familial hypertrophic cardiomyopathy pathology in patient-specific induced pluripotent stem cells. *Cell Stem Cell,* 12**,** 101-13.

Landles, C. & Bates, G. P. 2004. Huntingtin and the molecular pathogenesis of Huntington's disease. Fourth in molecular medicine review series. *EMBO reports,* 5**,** 958-63.

Lanska, D. J., Lavine, L., Lanska, M. J. & Schoenberg, B. S. 1988. Huntington's disease mortality in the United States. *Neurology,* 38**,** 769-72.

Laowtammathron, C., Cheng, E. C., Cheng, P.-H., Snyder, B. R., Yang, S.-H., Johnson, Z., Lorthongpanich, C., Kuo, H.-C., Parnpai, R. & Chan, A. W. S. 2010. Monkey hybrid stem cells develop cellular features of Huntington's disease. *BMC Cell Biol.,* 11**,** 12.

Lefort, N., Feyeux, M., Bas, C., Feraud, O., Bennaceur-Griscelli, A., Tachdjian, G., Peschanski, M. & Perrier, A. L. 2008. Human embryonic stem cells reveal recurrent genomic instability at 20q11.21. *Nat. Biotechnol.,* 26**,** 1364-6.

Legleiter, J., Mitchell, E., Lotz, G. P., Sapp, E., Ng, C., Difiglia, M., Thompson, L. M. & Muchowski, P. J. 2010. Mutant huntingtin fragments form oligomers in a polyglutamine length-dependent manner in vitro and in vivo. *The Journal of biological chemistry,* 285**,** 14777-90.

Leonova, K. I., Brodsky, L., Lipchick, B., Pal, M., Novototskaya, L., Chenchik, A. A., Sen, G. C., Komarova, E. A. & Gudkov, A. V. 2013. p53 cooperates with DNA methylation and a suicidal interferon response to maintain epigenetic silencing of repeats and noncoding RNAs. *Proc. Natl. Acad. Sci. U. S. A.,* 110**,** E89-98.

Levine, M. S., Klapstein, G. J., Koppel, A., Gruen, E., Cepeda, C., Vargas, M. E., Jokel, E. S., Carpenter, E. M., Zanjani, H., Hurst, R. S., Efstratiadis, A., Zeitlin, S. & Chesselet, M. F. 1999. Enhanced sensitivity to N-methyl-D-aspartate receptor activation in transgenic and knockin mouse models of Huntington's disease. *J. Neurosci. Res.,* 58**,** 515-32.

Li, S. H., Schilling, G., Young, W. S., 3rd, Li, X. J., Margolis, R. L., Stine, O. C., Wagster, M. V., Abbott, M. H., Franz, M. L., Ranen, N. G. & Et Al. 1993. Huntington's disease gene (IT15) is widely expressed in human and rat tissues. *Neuron,* 11**,** 985-93.

Li, Y., Powell, S., Brunette, E., Lebkowski, J. & Mandalam, R. 2005. Expansion of human embryonic stem cells in defined serum-free medium devoid of animal-derived products. *Biotechnol. Bioeng.,* 91**,** 688-98.

Lian, X., Hsiao, C., Wilson, G., Zhu, K., Hazeltine, L. B., Azarin, S. M., Raval, K. K., Zhang, J., Kamp, T. J. & Palecek, S. P. 2012a. Robust cardiomyocyte differentiation from human pluripotent stem cells via temporal modulation of canonical Wnt signaling. *Proc. Natl. Acad. Sci. U. S. A*.

Lian, X., Zhang, J., Zhu, K., Kamp, T. J. & Palecek, S. P. 2012b. Insulin Inhibits Cardiac Mesoderm, not Mesendoderm, formation during Cardiac Differentiation of Human Pluripotent Stem Cells and Modulation of Canonical Wnt Signaling Can Rescue this Inhibition. *Stem Cells*.

Lian, X., Zhang, J., Zhu, K., Kamp, T. J. & Palecek, S. P. 2013. Insulin inhibits cardiac mesoderm, not mesendoderm, formation during cardiac differentiation of human pluripotent stem cells and modulation of canonical Wnt signaling can rescue this inhibition. *Stem Cells,* 31**,** 447-57.

Lim, H. C., Lee, S. T., Chu, K., Joo, K. M., Kang, L., Im, W. S., Park, J. E., Kim, S. U., Kim, M. & Cha, C. I. 2008. Neuroprotective effect of neural stem cell-conditioned media in in vitro model of Huntington's disease. *Neurosci. Lett.,* 435**,** 175-80.

Linta, L., Stockmann, M., Kleinhans, K. N., Bockers, A., Storch, A., Zaehres, H., Lin, Q., Barbi, G., Bockers, T. M., Kleger, A. & Liebau, S. 2012. Rat embryonic fibroblasts improve reprogramming of human keratinocytes into induced pluripotent stem cells. *Stem cells and development,* 21**,** 965-76.

Lorincz, M. T. & Zawistowski, V. A. 2009. Expanded CAG repeats in the murine Huntington's disease gene increases neuronal differentiation of embryonic and neural stem cells. *Mol. Cell. Neurosci.,* 40**,** 1-13.

Loser, P., Schirm, J., Guhr, A., Wobus, A. M. & Kurtz, A. 2010. Human embryonic stem cell lines and their use in international research. *Stem Cells,* 28**,** 240-6.

Lowry, W. E., Richter, L., Yachechko, R., Pyle, A. D., Tchieu, J., Sridharan, R., Clark, A. T. & Plath, K. 2008. Generation of human induced pluripotent stem cells from dermal fibroblasts. *Proc. Natl. Acad. Sci. U. S. A.,* 105**,** 2883-8.

Lu, B. & Palacino, J. 2013. A novel human embryonic stem cell-derived Huntington's disease neuronal model exhibits mutant huntingtin (mHTT) aggregates and soluble mHTT-dependent neurodegeneration. *FASEB journal : official publication of the Federation of American Societies for Experimental Biology,* 27**,** 1820-9.

Ludwig, T. & J, A. T. 2007. Defined, feeder-independent medium for human embryonic stem cell culture. *Curr. Protoc. Stem Cell Biol.,* Chapter 1**,** Unit 1C 2.

Lunkes, A. & Mandel, J. L. 1998. A cellular model that recapitulates major pathogenic steps of Huntington's disease. *Hum. Mol. Genet.,* 7**,** 1355-61.

Ma, D., Wei, H., Lu, J., Ho, S., Zhang, G., Sun, X., Oh, Y., Tan, S. H., Ng, M. L., Shim, W., Wong, P. & Liew, R. 2012. Generation of patient-specific induced pluripotent stem cell-derived cardiomyocytes as a cellular model of arrhythmogenic right ventricular cardiomyopathy. *Eur. Heart J.*

Maherali, N., Ahfeldt, T., Rigamonti, A., Utikal, J., Cowan, C. & Hochedlinger, K. 2008. A high-efficiency system for the generation and study of human induced pluripotent stem cells. *Cell Stem Cell,* 3**,** 340-5.

Maitra, A., Arking, D. E., Shivapurkar, N., Ikeda, M., Stastny, V., Kassauei, K., Sui, G., Cutler, D. J., Liu, Y., Brimble, S. N., Noaksson, K., Hyllner, J., Schulz, T. C., Zeng, X., Freed, W. J., Crook, J., Abraham, S., Colman, A., Sartipy, P., Matsui, S., Carpenter, M., Gazdar, A. F., Rao, M. & Chakravarti, A. 2005. Genomic alterations in cultured human embryonic stem cells. *Nat. Genet.,* 37**,** 1099-103.

Mandal, P. K. & Rossi, D. J. 2013. Reprogramming human fibroblasts to pluripotency using modified mRNA. *Nat. Protoc.,* 8**,** 568-82.

Mangiarini, L., Sathasivam, K., Seller, M., Cozens, B., Harper, A., Hetherington, C., Lawton, M., Trottier, Y., Lehrach, H., Davies, S. W. & Bates, G. P. 1996. Exon 1 of the HD gene with an expanded CAG repeat is sufficient to cause a progressive neurological phenotype in transgenic mice. *Cell,* 87**,** 493-506.

Margolis, R. L. & Ross, C. A. 2003. Diagnosis of Huntington disease. *Clin. Chem.,* 49**,** 1726-32.

Marion, R. M., Strati, K., Li, H., Murga, M., Blanco, R., Ortega, S., Fernandez-Capetillo, O., Serrano, M. & Blasco, M. A. 2009. A p53-mediated DNA damage response limits reprogramming to ensure iPS cell genomic integrity. *Nature,* 460**,** 1149-53.

Mason, R. P. & Giorgini, F. 2011. Modeling Huntington disease in yeast: perspectives and future directions. *Prion,* 5**,** 269-76.

Mayshar, Y., Ben-David, U., Lavon, N., Biancotti, J. C., Yakir, B., Clark, A. T., Plath, K., Lowry, W. E. & Benvenisty, N. 2010. Identification and classification of chromosomal aberrations in human induced pluripotent stem cells. *Cell Stem Cell,* 7**,** 521-31.

Mcmullan, R., Lax, S., Robertson, V. H., Radford, D. J., Broad, S., Watt, F. M., Rowles, A., Croft, D. R., Olson, M. F. & Hotchin, N. A. 2003. Keratinocyte differentiation is regulated by the Rho and ROCK signaling pathway. *Current biology : CB,* 13**,** 2185-9.

Melkoumian, Z., Weber, J. L., Weber, D. M., Fadeev, A. G., Zhou, Y., Dolley-Sonneville, P., Yang, J., Qiu, L., Priest, C. A., Shogbon, C., Martin, A. W., Nelson, J., West, P., Beltzer, J. P., Pal, S. & Brandenberger, R. 2010. Synthetic peptide-acrylate surfaces for long-term self-renewal and cardiomyocyte differentiation of human embryonic stem cells. *Nat. Biotechnol.,* 28**,** 606-10.

Menalled, L. B., Sison, J. D., Dragatsis, I., Zeitlin, S. & Chesselet, M. F. 2003. Time course of early motor and neuropathological anomalies in a knock-in mouse model of Huntington's disease with 140 CAG repeats. *The Journal of comparative neurology,* 465**,** 11-26.

Mendel, G. 1865. Versuche über Pflanzenhybriden. *Proc. Nat. Hist. Soc. Brunn* 4**,** 3-47.

Mihm, M. J., Amann, D. M., Schanbacher, B. L., Altschuld, R. A., Bauer, J. A. & Hoyt, K. R. 2007. Cardiac dysfunction in the R6/2 mouse model of Huntington's disease. *Neurobiol. Dis.,* 25**,** 297-308.

Miller, J. C., Tan, S., Qiao, G., Barlow, K. A., Wang, J., Xia, D. F., Meng, X., Paschon, D. E., Leung, E., Hinkley, S. J., Dulay, G. P., Hua, K. L., Ankoudinova, I., Cost, G. J., Urnov, F. D., Zhang, H. S., Holmes, M. C., Zhang, L., Gregory, P. D. & Rebar, E. J. 2011. A TALE nuclease architecture for efficient genome editing. *Nat. Biotechnol.,* 29**,** 143-8.

Minami, I., Yamada, K., Otsuji, T. G., Yamamoto, T., Shen, Y., Otsuka, S., Kadota, S., Morone, N., Barve, M., Asai, Y., Tenkova-Heuser, T., Heuser, J. E., Uesugi, M., Aiba, K. & Nakatsuji, N. 2012. A small molecule that promotes cardiac differentiation of human pluripotent stem cells under defined, cytokine- and xeno-free conditions. *Cell reports,* 2**,** 1448-60.

Miyoshi, N., Ishii, H., Nagano, H., Haraguchi, N., Dewi, D. L., Kano, Y., Nishikawa, S., Tanemura, M., Mimori, K., Tanaka, F., Saito, T., Nishimura, J., Takemasa, I., Mizushima, T., Ikeda, M., Yamamoto, H., Sekimoto, M., Doki, Y. & Mori, M. 2011. Reprogramming of mouse and human cells to pluripotency using mature microRNAs. *Cell Stem Cell,* 8**,** 633-8.

Moffitt, H., Mcphail, G. D., Woodman, B., Hobbs, C. & Bates, G. P. 2009. Formation of polyglutamine inclusions in a wide range of non-CNS tissues in the HdhQ150 knock-in mouse model of Huntington's disease. *PLoS One,* 4**,** e8025.

Morton, A. J. & Avanzo, L. 2011. Executive decision-making in the domestic sheep. *PLoS One,* 6**,** e15752.

Mullis, K., Faloona, F., Scharf, S., Saiki, R., Horn, G. & Erlich, H. 1986. Specific enzymatic amplification of DNA in vitro: the polymerase chain reaction. *Cold Spring Harb. Symp. Quant. Biol.,* 51 Pt 1**,** 263-73.

Mummery, C., Ward-Van Oostwaard, D., Doevendans, P., Spijker, R., Van Den Brink, S., Hassink, R., Van Der Heyden, M., Opthof, T., Pera, M., De La Riviere, A. B., Passier, R. & Tertoolen, L. 2003. Differentiation of human embryonic stem cells to cardiomyocytes: role of coculture with visceral endoderm-like cells. *Circulation,* 107**,** 2733-40.

Nagaoka, M., Si-Tayeb, K., Akaike, T. & Duncan, S. A. 2010. Culture of human pluripotent stem cells using completely defined conditions on a recombinant E-cadherin substratum. *BMC Dev. Biol.,* 10**,** 60.

Ng, E. S., Davis, R., Stanley, E. G. & Elefanty, A. G. 2008. A protocol describing the use of a recombinant protein-based, animal product-free medium (APEL) for human embryonic stem cell differentiation as spin embryoid bodies. *Nat. Protoc.,* 3**,** 768-76.

Ng, S. B., Turner, E. H., Robertson, P. D., Flygare, S. D., Bigham, A. W., Lee, C., Shaffer, T., Wong, M., Bhattacharjee, A., Eichler, E. E., Bamshad, M., Nickerson, D. A. & Shendure, J. 2009. Targeted capture and massively parallel sequencing of 12 human exomes. *Nature,* 461**,** 272-6.

Niclis, J. C., Trounson, A. O., Dottori, M., Ellisdon, A. M., Bottomley, S. P., Verlinsky, Y. & Cram, D. S. 2009a. Human embryonic stem cell models of Huntington disease. *Reprod Biomed Online,* 19**,** 106-13.

Niclis, J. C., Trounson, A. O., Dottori, M., Ellisdon, A. M., Bottomley, S. P., Verlinsky, Y. & Cram, D. S. 2009b. Human embryonic stem cell models of Huntington disease. *Reproductive Biomedicine Online,* 19**,** 106-13.

Novak, A., Shtrichman, R., Germanguz, I., Segev, H., Zeevi-Levin, N., Fishman, B., Mandel, Y. E., Barad, L., Domev, H., Kotton, D., Mostoslavsky, G., Binah, O. & Itskovitz-Eldor, J. 2010. Enhanced reprogramming and cardiac differentiation of human keratinocytes derived from plucked hair follicles, using a single excisable lentivirus. *Cellular Reprogramming,* 12**,** 665-78.

Ojala, M., Rajala, K., Pekkanen-Mattila, M., Miettinen, M., Huhtala, H. & Aalto-Setala, K. 2012. Culture conditions affect cardiac differentiation potential of human pluripotent stem cells. *PLoS One,* 7**,** e48659.

Okita, K., Nakagawa, M., Hyenjong, H., Ichisaka, T. & Yamanaka, S. 2008. Generation of mouse induced pluripotent stem cells without viral vectors. *Science,* 322**,** 949-53.

Olmer, R., Haase, A., Merkert, S., Cui, W., Palecek, J., Ran, C., Kirschning, A., Scheper, T., Glage, S., Miller, K., Curnow, E. C., Hayes, E. S. & Martin, U. 2010. Long term expansion of undifferentiated human iPS and ES cells in suspension culture using a defined medium. *Stem cell research,* 5**,** 51-64.

Park, Y., Kim, J. H., Lee, S. J., Choi, I. Y., Park, S. J., Lee, S. R., Sung, H. J., Yoo, Y. D., Geum, D. H., Choi, C. W., Kim, S. H. & Kim, B. S. 2011. Human Feeder Cells Can Support the Undifferentiated Growth of Human and Mouse Embryonic Stem Cells Using Their Own Basic Fibroblast Growth Factors. *Stem Cells Dev*.

Parker, J. A., Connolly, J. B., Wellington, C., Hayden, M., Dausset, J. & Neri, C. 2001. Expanded polyglutamines in Caenorhabditis elegans cause axonal abnormalities and

severe dysfunction of PLM mechanosensory neurons without cell death. *Proc. Natl. Acad. Sci. U. S. A.,* 98**,** 13318-23.

Pasca, S. P., Portmann, T., Voineagu, I., Yazawa, M., Shcheglovitov, A., Pasca, A. M., Cord, B., Palmer, T. D., Chikahisa, S., Nishino, S., Bernstein, J. A., Hallmayer, J., Geschwind, D. H. & Dolmetsch, R. E. 2011. Using iPSC-derived neurons to uncover cellular phenotypes associated with Timothy syndrome. *Nat. Med.,* 17**,** 1657-62.

Pattison, J. S., Sanbe, A., Maloyan, A., Osinska, H., Klevitsky, R. & Robbins, J. 2008. Cardiomyocyte expression of a polyglutamine preamyloid oligomer causes heart failure. *Circulation,* 117**,** 2743-51.

Petit, I., Kesner, N. S., Karry, R., Robicsek, O., Aberdam, E., Muller, F. J., Aberdam, D. & Ben-Shachar, D. 2012. Induced pluripotent stem cells from hair follicles as a cellular model for neurodevelopmental disorders. *Stem Cell Res,* 8**,** 134-40.

Puppala, D., Collis, L. P., Sun, S. Z., Bonato, V., Chen, X., Anson, B., Pletcher, M., Fermini, B. & Engle, S. J. 2013. Comparative gene expression profiling in human-induced pluripotent stem cell--derived cardiocytes and human and cynomolgus heart tissue. *Toxicological sciences : an official journal of the Society of Toxicology,* 131**,** 292-301.

Ramaswamy, S., Mcbride, J. L. & Kordower, J. H. 2007. Animal models of Huntington's disease. *ILAR journal / National Research Council, Institute of Laboratory Animal Resources,* 48**,** 356-73.

Reik, W. 2007. Stability and flexibility of epigenetic gene regulation in mammalian development. *Nature,* 447**,** 425-32.

Rigamonti, D., Bauer, J. H., De-Fraja, C., Conti, L., Sipione, S., Sciorati, C., Clementi, E., Hackam, A., Hayden, M. R., Li, Y., Cooper, J. K., Ross, C. A., Govoni, S., Vincenz, C. & Cattaneo, E. 2000. Wild-type huntingtin protects from apoptosis upstream of caspase-3. *The Journal of neuroscience : the official journal of the Society for Neuroscience,* 20**,** 3705-13.

Ritner, C., Wong, S. S., King, F. W., Mihardja, S. S., Liszewski, W., Erle, D. J., Lee, R. J. & Bernstein, H. S. 2011. An engineered cardiac reporter cell line identifies human embryonic stem cell-derived myocardial precursors. *PLoS One,* 6**,** e16004.

Robinton, D. A. & Daley, G. Q. 2012. The promise of induced pluripotent stem cells in research and therapy. *Nature,* 481**,** 295-305.

Ruiz, S., Diep, D., Gore, A., Panopoulos, A. D., Montserrat, N., Plongthongkum, N., Kumar, S., Fung, H. L., Giorgetti, A., Bilic, J., Batchelder, E. M., Zaehres, H., Kan, N. G., Scholer, H. R., Mercola, M., Zhang, K. & Izpisua Belmonte, J. C. 2012. Identification of a specific reprogramming-associated epigenetic signature in human induced pluripotent stem cells. *Proc. Natl. Acad. Sci. U. S. A.,* 109**,** 16196-201.

Rust, W., Balakrishnan, T. & Zweigerdt, R. 2009. Cardiomyocyte enrichment from human embryonic stem cell cultures by selection of ALCAM surface expression. *Regen. Med.,* 4**,** 225-37.

Rutland, C. S., Polo-Parada, L., Ehler, E., Alibhai, A., Thorpe, A., Suren, S., Emes, R. D., Patel, B. & Loughna, S. 2011. Knockdown of embryonic myosin heavy chain reveals an essential role in the morphology and function of the developing heart. *Development,* 138**,** 3955-66.

Sahl, S. J., Weiss, L. E., Duim, W. C., Frydman, J. & Moerner, W. E. 2012. Cellular inclusion bodies of mutant huntingtin exon 1 obscure small fibrillar aggregate species. *Sci. Rep.,* 2**,** 895.

Sassone, J., Colciago, C., Cislaghi, G., Silani, V. & Ciammola, A. 2009. Huntington's disease: the current state of research with peripheral tissues. *Exp. Neurol.,* 219**,** 385-97.

Sathasivam, K., Hobbs, C., Turmaine, M., Mangiarini, L., Mahal, A., Bertaux, F., Wanker, E. E., Doherty, P., Davies, S. W. & Bates, G. P. 1999. Formation of polyglutamine inclusions in non-CNS tissue. *Hum. Mol. Genet.,* 8**,** 813-22.

Saudou, F., Finkbeiner, S., Devys, D. & Greenberg, M. E. 1998. Huntingtin acts in the nucleus to induce apoptosis but death does not correlate with the formation of intranuclear inclusions. *Cell,* 95**,** 55-66.

Scherzinger, E., Lurz, R., Turmaine, M., Mangiarini, L., Hollenbach, B., Hasenbank, R., Bates, G. P., Davies, S. W., Lehrach, H. & Wanker, E. E. 1997. Huntingtin-encoded polyglutamine expansions form amyloid-like protein aggregates in vitro and in vivo. *Cell,* 90**,** 549-58.

Schulman, J. D., Black, S. H., Handyside, A. & Nance, W. E. 1996. Preimplantation genetic testing for Huntington disease and certain other dominantly inherited disorders. *Clin. Genet.,* 49**,** 57-8.

Segev, H., Kenyagin-Karsenti, D., Fishman, B., Gerecht-Nir, S., Ziskind, A., Amit, M., Coleman, R. & Itskovitz-Eldor, J. 2005. Molecular analysis of cardiomyocytes derived from human embryonic stem cells. *Development, growth & differentiation,* 47**,** 295-306.

Seriola, A., Spits, C., Simard, J. P., Hilven, P., Haentjens, P., Pearson, C. E. & Sermon, K. 2011. Huntington's and myotonic dystrophy hESCs: down-regulated trinucleotide repeat instability and mismatch repair machinery expression upon differentiation. *Hum. Mol. Genet.,* 20**,** 176-85.

Sharp, A. H., Loev, S. J., Schilling, G., Li, S. H., Li, X. J., Bao, J., Wagster, M. V., Kotzuk, J. A., Steiner, J. P., Lo, A. & Et Al. 1995. Widespread expression of Huntington's disease gene (IT15) protein product. *Neuron,* 14**,** 1065-74.

Shelbourne, P. F., Killeen, N., Hevner, R. F., Johnston, H. M., Tecott, L., Lewandoski, M., Ennis, M., Ramirez, L., Li, Z., Iannicola, C., Littman, D. R. & Myers, R. M. 1999. A Huntington's disease CAG expansion at the murine Hdh locus is unstable and associated with behavioural abnormalities in mice. *Hum. Mol. Genet.,* 8**,** 763-74.

Si-Tayeb, K., Noto, F. K., Sepac, A., Sedlic, F., Bosnjak, Z. J., Lough, J. W. & Duncan, S. A. 2010. Generation of human induced pluripotent stem cells by simple transient transfection of plasmid DNA encoding reprogramming factors. *BMC Dev. Biol.,* 10**,** 81.

Siesling, S., Vegter-Van Der Vlis, M. & Roos, R. A. 1997. Juvenile Huntington disease in the Netherlands. *Pediatr. Neurol.,* 17**,** 37-43.

Sipione, S. & Cattaneo, E. 2001. Modeling Huntington's disease in cells, flies, and mice. *Mol. Neurobiol.,* 23**,** 21-51.

Sipione, S., Rigamonti, D., Valenza, M., Zuccato, C., Conti, L., Pritchard, J., Kooperberg, C., Olson, J. M. & Cattaneo, E. 2002. Early transcriptional profiles in huntingtin-inducible striatal cells by microarray analyses. *Hum. Mol. Genet.,* 11**,** 1953-65.

Slow, E. J., Van Raamsdonk, J., Rogers, D., Coleman, S. H., Graham, R. K., Deng, Y., Oh, R., Bissada, N., Hossain, S. M., Yang, Y. Z., Li, X. J., Simpson, E. M., Gutekunst, C. A., Leavitt, B. R. & Hayden, M. R. 2003. Selective striatal neuronal loss in a YAC128 mouse model of Huntington disease. *Hum. Mol. Genet.,* 12**,** 1555-67.

Smith, D. L. & Bates, G. P. 2004. Monitoring aggregate formation in organotypic slice cultures from transgenic mice. *Methods Mol. Biol.,* 277**,** 161-71.

Soldner, F., Laganiere, J., Cheng, A. W., Hockemeyer, D., Gao, Q., Alagappan, R., Khurana, V., Golbe, L. I., Myers, R. H., Lindquist, S., Zhang, L., Guschin, D., Fong, L. K., Vu, B. J., Meng, X., Urnov, F. D., Rebar, E. J., Gregory, P. D., Zhang, H. S. & Jaenisch, R. 2011. Generation of isogenic pluripotent stem cells differing exclusively at two early onset Parkinson point mutations. *Cell,* 146**,** 318-31.

Somers, A., Jean, J. C., Sommer, C. A., Omari, A., Ford, C. C., Mills, J. A., Ying, L., Sommer, A. G., Jean, J. M., Smith, B. W., Lafyatis, R. A., Demierre, M. F., Weiss, D. J., French, D. L., Gadue, P., Murphy, G. J., Mostoslavsky, G. & Kotton, D. N. 2010. Generation of Transgene-Free Lung Disease-Specific Human iPS Cells Using a Single Excisable Lentiviral Stem Cell Cassette. *Stem Cells*.

Sommer, C. A., Stadtfeld, M., Murphy, G. J., Hochedlinger, K., Kotton, D. N. & Mostoslavsky, G. 2009. Induced pluripotent stem cell generation using a single lentiviral stem cell cassette. *Stem Cells,* 27**,** 543-9.

Sontag, E. M., Lotz, G. P., Agrawal, N., Tran, A., Aron, R., Yang, G., Necula, M., Lau, A., Finkbeiner, S., Glabe, C., Marsh, J. L., Muchowski, P. J. & Thompson, L. M. 2012. Methylene blue modulates huntingtin aggregation intermediates and is protective in Huntington's disease models. *The Journal of neuroscience : the official journal of the Society for Neuroscience,* 32**,** 11109-19.

Sorensen, S. A. & Fenger, K. 1992. Causes of death in patients with Huntington's disease and in unaffected first degree relatives. *J. Med. Genet.,* 29**,** 911-4.

Squitieri, F., Cannella, M., Giallonardo, P., Maglione, V., Mariotti, C. & Hayden, M. R. 2001. Onset and pre-onset studies to define the Huntington's disease natural history. *Brain Res. Bull.,* 56**,** 233-8.

Stadtfeld, M., Brennand, K. & Hochedlinger, K. 2008a. Reprogramming of pancreatic beta cells into induced pluripotent stem cells. *Current biology : CB,* 18**,** 890-4.

Stadtfeld, M., Maherali, N., Breault, D. T. & Hochedlinger, K. 2008b. Defining molecular cornerstones during fibroblast to iPS cell reprogramming in mouse. *Cell Stem Cell,* 2**,** 230-40.

Stadtfeld, M., Nagaya, M., Utikal, J., Weir, G. & Hochedlinger, K. 2008c. Induced pluripotent stem cells generated without viral integration. *Science,* 322**,** 945-9.

Stephenson, E., Ilic, D., Jacquet, L., Genbacev, O. & Fisher, S. J. 2014. PGD and Human Embryonic Stem Cell Technology. *In:* T. El-Toukhy (ed.) *Preimplantation Genetic Diagnosis in Clinical Practice.* London: Springer-Verlag London 2014.

Stephenson, E., Jacquet, L., Miere, C., Wood, V., Kadeva, N., Cornwell, G., Codognotto, S., Dajani, Y., Braude, P. & Ilic, D. 2012. Derivation and propagation of human embryonic stem cell lines from frozen embryos in an animal product-free environment. *Nat. Protoc.,* 7**,** 1366-81.

Stojkovic, P., Lako, M., Przyborski, S., Stewart, R., Armstrong, L., Evans, J., Zhang, X. & Stojkovic, M. 2005. Human-serum matrix supports undifferentiated growth of human embryonic stem cells. *Stem Cells,* 23**,** 895-902.

Streckfuss-Bomeke, K., Wolf, F., Azizian, A., Stauske, M., Tiburcy, M., Wagner, S., Hubscher, D., Dressel, R., Chen, S., Jende, J., Wulf, G., Lorenz, V., Schon, M. P., Maier, L. S., Zimmermann, W. H., Hasenfuss, G. & Guan, K. 2012. Comparative study of human-induced pluripotent stem cells derived from bone marrow cells, hair keratinocytes, and skin fibroblasts. *Eur. Heart J.*

Strong, T. V., Tagle, D. A., Valdes, J. M., Elmer, L. W., Boehm, K., Swaroop, M., Kaatz, K. W., Collins, F. S. & Albin, R. L. 1993. Widespread expression of the human and rat Huntington's disease gene in brain and nonneural tissues. *Nat. Genet.,* 5**,** 259-65.

Strulovici, Y., Leopold, P. L., O'connor, T. P., Pergolizzi, R. G. & Crystal, R. G. 2007. Human embryonic stem cells and gene therapy. *Molecular therapy : the journal of the American Society of Gene Therapy,* 15**,** 850-66.

Takahashi, K., Tanabe, K., Ohnuki, M., Narita, M., Ichisaka, T., Tomoda, K. & Yamanaka, S. 2007. Induction of pluripotent stem cells from adult human fibroblasts by defined factors. *Cell,* 131**,** 861-72.

Takahashi, K. & Yamanaka, S. 2006. Induction of pluripotent stem cells from mouse embryonic and adult fibroblast cultures by defined factors. *Cell,* 126**,** 663-76.

Takai, N., Desmond, J. C., Kumagai, T., Gui, D., Said, J. W., Whittaker, S., Miyakawa, I. & Koeffler, H. P. 2004. Histone deacetylase inhibitors have a profound antigrowth activity in endometrial cancer cells. *Clinical cancer research : an official journal of the American Association for Cancer Research,* 10**,** 1141-9.

Telenius, H., Kremer, B., Goldberg, Y. P., Theilmann, J., Andrew, S. E., Zeisler, J., Adam, S., Greenberg, C., Ives, E. J., Clarke, L. A. & Et Al. 1994. Somatic and gonadal mosaicism of the Huntington disease gene CAG repeat in brain and sperm. *Nat. Genet.,* 6**,** 409-14.

Telenius, H., Kremer, H. P., Theilmann, J., Andrew, S. E., Almqvist, E., Anvret, M., Greenberg, C., Greenberg, J., Lucotte, G., Squitieri, F. & Et Al. 1993. Molecular analysis of juvenile Huntington disease: the major influence on (CAG)n repeat length is the sex of the affected parent. *Hum. Mol. Genet.,* 2**,** 1535-40.

The HD iPSC Consortium. 2012. Induced Pluripotent Stem Cells from Patients with Huntington's Disease Show CAG-Repeat Expansion Associated Phenotypes. *Cell Stem Cell,* 11**,** 264-278.

The Huntington Disease Collaborative Research Group 1993. A novel gene containing a trinucleotide repeat that is expanded and unstable on Huntington's disease chromosomes. The Huntington's Disease Collaborative Research Group. *Cell,* 72**,** 971-83.

Thomson, J. A., Itskovitz-Eldor, J., Shapiro, S. S., Waknitz, M. A., Swiergiel, J. J., Marshall, V. S. & Jones, J. M. 1998. Embryonic Stem Cell Lines Derived from Human Blastocysts. *Science,* 282**,** 1145-1147.

Tiscornia, G., Vivas, E. L., Matalonga, L., Berniakovich, I., Barragan Monasterio, M., Eguizabal, C., Gort, L., Gonzalez, F., Ortiz Mellet, C., Garcia Fernandez, J. M., Ribes, A., Veiga, A. & Izpisua Belmonte, J. C. 2013. Neuronopathic Gaucher's disease: induced pluripotent stem cells for disease modelling and testing chaperone activity of small compounds. *Hum. Mol. Genet.,* 22**,** 633-45.

Tong, Y., Ha, T. J., Liu, L., Nishimoto, A., Reiner, A. & Goldowitz, D. 2011. Spatial and temporal requirements for huntingtin (Htt) in neuronal migration and survival during brain development. *The Journal of neuroscience : the official journal of the Society for Neuroscience,* 31**,** 14794-9.

Trettel, F., Rigamonti, D., Hilditch-Maguire, P., Wheeler, V. C., Sharp, A. H., Persichetti, F., Cattaneo, E. & Macdonald, M. E. 2000. Dominant phenotypes produced by the HD mutation in STHdh(Q111) striatal cells. *Hum. Mol. Genet.,* 9**,** 2799-809.

Trottier, Y., Biancalana, V. & Mandel, J. L. 1994. Instability of CAG repeats in Huntington's disease: relation to parental transmission and age of onset. *J. Med. Genet.,* 31**,** 377-82.

Tse, H. F., Ho, J. C., Choi, S. W., Lee, Y. K., Butler, A. W., Ng, K. M., Siu, C. W., Simpson, M. A., Lai, W. H., Chan, Y. C., Au, K. W., Zhang, J., Lay, K. W., Esteban, M. A., Nicholls, J. M., Colman, A. & Sham, P. C. 2013. Patient-specific induced-pluripotent stem cells-derived cardiomyocytes recapitulate the pathogenic phenotypes of dilated

cardiomyopathy due to a novel DES mutation identified by whole exome sequencing. *Hum. Mol. Genet.,* 22**,** 1395-403.

Van Der Burg, J. M., Bjorkqvist, M. & Brundin, P. 2009. Beyond the brain: widespread pathology in Huntington's disease. *Lancet Neurol.,* 8**,** 765-74.

Verlinsky, Y., Strelchenko, N., Kukharenko, V., Rechitsky, S., Verlinsky, O., Galat, V. & Kuliev, A. 2005. Human embryonic stem cell lines with genetic disorders. *Reproductive Biomedicine Online,* 10**,** 105-110.

Vlodavsky, I. 2001. Preparation of extracellular matrices produced by cultured corneal endothelial and PF-HR9 endodermal cells. *Curr. Protoc. Cell Biol.,* Chapter 10**,** Unit 10 4.

Waelter, S., Boeddrich, A., Lurz, R., Scherzinger, E., Lueder, G., Lehrach, H. & Wanker, E. E. 2001. Accumulation of mutant huntingtin fragments in aggresome-like inclusion bodies as a result of insufficient protein degradation. *Mol. Biol. Cell,* 12**,** 1393-407.

Wang, G. H., Mitsui, K., Kotliarova, S., Yamashita, A., Nagao, Y., Tokuhiro, S., Iwatsubo, T., Kanazawa, I. & Nukina, N. 1999. Caspase activation during apoptotic cell death induced by expanded polyglutamine in N2a cells. *Neuroreport,* 10**,** 2435-8.

Wang, Q., Mou, X., Cao, H., Meng, Q., Ma, Y., Han, P., Jiang, J. & Zhang, H. 2012. A novel xeno-free and feeder-cell-free system for human pluripotent stem cell culture. *Protein & cell,* 3**,** 51-9.

Warren, L., Manos, P. D., Ahfeldt, T., Loh, Y. H., Li, H., Lau, F., Ebina, W., Mandal, P. K., Smith, Z. D., Meissner, A., Daley, G. Q., Brack, A. S., Collins, J. J., Cowan, C., Schlaeger, T. M. & Rossi, D. J. 2010. Highly Efficient Reprogramming to Pluripotency and Directed Differentiation of Human Cells with Synthetic Modified mRNA. *Cell Stem Cell*.

Warren, L., Ni, Y., Wang, J. & Guo, X. 2012. Feeder-free derivation of human induced pluripotent stem cells with messenger RNA. *Sci. Rep.,* 2**,** 657.

Watanabe, K., Ueno, M., Kamiya, D., Nishiyama, A., Matsumura, M., Wataya, T., Takahashi, J. B., Nishikawa, S., Muguruma, K. & Sasai, Y. 2007. A ROCK inhibitor permits survival of dissociated human embryonic stem cells. *Nat. Biotechnol.,* 25**,** 681-6.

Weiss, A., Roscic, A. & Paganetti, P. 2009. Inducible mutant huntingtin expression in HN10 cells reproduces Huntington's disease-like neuronal dysfunction. *Mol. Neurodegener.,* 4**,** 11.

Wheeler, V. C., White, J. K., Gutekunst, C. A., Vrbanac, V., Weaver, M., Li, X. J., Li, S. H., Yi, H., Vonsattel, J. P., Gusella, J. F., Hersch, S., Auerbach, W., Joyner, A. L. & Macdonald, M. E. 2000. Long glutamine tracts cause nuclear localization of a novel form of huntingtin in medium spiny striatal neurons in HdhQ92 and HdhQ111 knock-in mice. *Hum. Mol. Genet.,* 9**,** 503-13.

Woltjen, K., Michael, I. P., Mohseni, P., Desai, R., Mileikovsky, M., Hamalainen, R., Cowling, R., Wang, W., Liu, P., Gertsenstein, M., Kaji, K., Sung, H. K. & Nagy, A. 2009. piggyBac transposition reprograms fibroblasts to induced pluripotent stem cells. *Nature,* 458**,** 766-70.

Wood, N. I., Sawiak, S.J., Buonincontri, G., Niu, Y., Kane, A.D., Carpenter, T.A., Giussanic, D.A., & Morton, J.A 2012. Direct Evidence of Progressive Cardiac Dysfunction in a Transgenic Mouse Model of Huntington's Disease. *Journal of Huntington's Disease* 1**,** 57–64.

Wulhfard, S., Baldi, L., Hacker, D. L. & Wurm, F. 2010. Valproic acid enhances recombinant mRNA and protein levels in transiently transfected Chinese hamster ovary cells. *J. Biotechnol.,* 148**,** 128-132.

Xu, C., Inokuma, M. S., Denham, J., Golds, K., Kundu, P., Gold, J. D. & Carpenter, M. K. 2001. Feeder-free growth of undifferentiated human embryonic stem cells. *Nat. Biotechnol.,* 19**,** 971-4.

Xu, C., Police, S., Rao, N. & Carpenter, M. K. 2002. Characterization and enrichment of cardiomyocytes derived from human embryonic stem cells. *Circ. Res.,* 91**,** 501-8.

Yagi, T., Ito, D., Okada, Y., Akamatsu, W., Nihei, Y., Yoshizaki, T., Yamanaka, S., Okano, H. & Suzuki, N. 2011. Modeling familial Alzheimer's disease with induced pluripotent stem cells. *Hum. Mol. Genet.,* 20**,** 4530-9.

Yamamoto, A., Cremona, M. L. & Rothman, J. E. 2006. Autophagy-mediated clearance of huntingtin aggregates triggered by the insulin-signaling pathway. *The Journal of cell biology,* 172**,** 719-31.

Yang, D., Wang, C. E., Zhao, B., Li, W., Ouyang, Z., Liu, Z., Yang, H., Fan, P., O'neill, A., Gu, W., Yi, H., Li, S., Lai, L. & Li, X. J. 2010. Expression of Huntington's disease protein results in apoptotic neurons in the brains of cloned transgenic pigs. *Hum. Mol. Genet.,* 19**,** 3983-94.

Yang, L., Soonpaa, M. H., Adler, E. D., Roepke, T. K., Kattman, S. J., Kennedy, M., Henckaerts, E., Bonham, K., Abbott, G. W., Linden, R. M., Field, L. J. & Keller, G. M. 2008. Human cardiovascular progenitor cells develop from a KDR+ embryonic-stem-cell-derived population. *Nature,* 453**,** 524-8.

Yang, S. H., Cheng, P. H., Banta, H., Piotrowska-Nitsche, K., Yang, J. J., Cheng, E. C., Snyder, B., Larkin, K., Liu, J., Orkin, J., Fang, Z. H., Smith, Y., Bachevalier, J., Zola, S. M., Li, S. H., Li, X. J. & Chan, A. W. 2008. Towards a transgenic model of Huntington's disease in a non-human primate. *Nature,* 453**,** 921-4.

Yazawa, M., Hsueh, B., Jia, X., Pasca, A. M., Bernstein, J. A., Hallmayer, J. & Dolmetsch, R. E. 2011. Using induced pluripotent stem cells to investigate cardiac phenotypes in Timothy syndrome. *Nature,* 471**,** 230-4.

Yoon, T. M., Chang, B., Kim, H. T., Jee, J. H., Kim, D. W. & Hwang, D. Y. 2010. Human embryonic stem cells (hESCs) cultured under distinctive feeder-free culture conditions display global gene expression patterns similar to hESCs from feeder-dependent culture conditions. *Stem cell reviews,* 6**,** 425-37.

Yu, J., Vodyanik, M. A., Smuga-Otto, K., Antosiewicz-Bourget, J., Frane, J. L., Tian, S., Nie, J., Jonsdottir, G. A., Ruotti, V., Stewart, R., Slukvin, Ii & Thomson, J. A. 2007. Induced pluripotent stem cell lines derived from human somatic cells. *Science,* 318**,** 1917-20.

Yu, T., Miyagawa, S., Miki, K., Saito, A., Fukushima, S., Higuchi, T., Kawamura, M., Kawamura, T., Ito, E., Kawaguchi, N., Sawa, Y. & Matsuura, N. 2013. In vivo differentiation of induced pluripotent stem cell-derived cardiomyocytes. *Circulation journal : official journal of the Japanese Circulation Society,* 77**,** 1297-306.

Zeitlin, S., Liu, J. P., Chapman, D. L., Papaioannou, V. E. & Efstratiadis, A. 1995. Increased apoptosis and early embryonic lethality in mice nullizygous for the Huntington's disease gene homologue. *Nat. Genet.,* 11**,** 155-63.

Zhang, J., Klos, M., Wilson, G. F., Herman, A. M., Lian, X., Raval, K. K., Barron, M. R., Hou, L., Soerens, A. G., Yu, J., Palecek, S. P., Lyons, G. E., Thomson, J. A., Herron, T. J., Jalife, J. & Kamp, T. J. 2012. Extracellular matrix promotes highly efficient cardiac differentiation of human pluripotent stem cells: the matrix sandwich method. *Circ. Res.,* 111**,** 1125-36.

Zhang, N., An, M. C., Montoro, D. & Ellerby, L. M. 2010. Characterization of Human Huntington's Disease Cell Model from Induced Pluripotent Stem Cells. *PLoS Curr,* 2**,** RRN1193.

Zhang, Z., Gao, Y., Gordon, A., Wang, Z. Z., Qian, Z. & Wu, W. S. 2011. Efficient generation of fully reprogrammed human iPS cells via polycistronic retroviral vector and a new cocktail of chemical compounds. *PLoS One,* 6**,** e26592.

Zhao, M., Yang, H., Jiang, X., Zhou, W., Zhu, B., Zeng, Y., Yao, K. & Ren, C. 2008. Lipofectamine RNAiMAX: an efficient siRNA transfection reagent in human embryonic stem cells. *Mol. Biotechnol.,* 40**,** 19-26.

Zhao, Y., Yin, X., Qin, H., Zhu, F., Liu, H., Yang, W., Zhang, Q., Xiang, C., Hou, P., Song, Z., Liu, Y., Yong, J., Zhang, P., Cai, J., Liu, M., Li, H., Li, Y., Qu, X., Cui, K., Zhang, W., Xiang, T., Wu, Y., Liu, C., Yu, C., Yuan, K., Lou, J., Ding, M. & Deng, H. 2008. Two supporting factors greatly improve the efficiency of human iPSC generation. *Cell Stem Cell,* 3**,** 475-9.

Zhou, H., Wu, S., Joo, J. Y., Zhu, S., Han, D. W., Lin, T., Trauger, S., Bien, G., Yao, S., Zhu, Y., Siuzdak, G., Scholer, H. R., Duan, L. & Ding, S. 2009. Generation of induced pluripotent stem cells using recombinant proteins. *Cell Stem Cell,* 4**,** 381-4.

Zhou, W. & Freed, C. R. 2009. Adenoviral gene delivery can reprogram human fibroblasts to induced pluripotent stem cells. *Stem Cells,* 27**,** 2667-74.

Zhu, S., Li, W., Zhou, H., Wei, W., Ambasudhan, R., Lin, T., Kim, J., Zhang, K. & Ding, S. 2010. Reprogramming of human primary somatic cells by OCT4 and chemical compounds. *Cell Stem Cell,* 7**,** 651-5.

LIST OF PUBLICATIONS

Stephenson, E., Ilic, D., **Jacquet, L.**, Genbacev, O. & Fisher, S. J. 2014. PGD and Human Embryonic Stem Cell Technology. *In:* T. El-Toukhy (ed.) *Preimplantation Genetic Diagnosis in Clinical Practice.* London: Springer-Verlag London 2014.

Jacquet, L., Stephenson, E., Collins, R., Patel, H., Trussler, J., Al-Bedaery, R., Renwick, P., Ogilvie, C., Vaughan, R. & Ilic, D. 2013. Strategy for the creation of clinical grade hESC line banks that HLA-match a target population. *EMBO Mol. Med.,* 5**,** 10-7.

Stephenson, E., **Jacquet, L.**, Miere, C., Wood, V., Kadeva, N., Cornwell, G., Codognotto, S., Dajani, Y., Braude, P. & Ilic, D. 2012. Derivation and propagation of human embryonic stem cell lines from frozen embryos in an animal product-free environment. *Nat. Protoc.,* 7**,** 1366-81.

Ilic, D., Stephenson, E., Wood, V., **Jacquet, L.**, Stevenson, D., Petrova, A., Kadeva, N., Codognotto, S., Patel, H., Semple, M., Cornwell, G., Ogilvie, C. & Braude, P. 2012. Derivation and feeder-free propagation of human embryonic stem cells under xeno-free conditions. *Cytotherapy,* 14**,** 122-8.

Stephenson, E., Ogilvie, C. M., Patel, H., Cornwell, G., **Jacquet, L.**, Kadeva, N., Braude, P. & Ilic, D. 2010. Safety paradigm: genetic evaluation of therapeutic grade human embryonic stem cells. *Journal of the Royal Society, Interface / the Royal Society,* 7 Suppl 6**,** S677-88.

APPENDIX I hESC Characterisation

KCL013_HD4

a

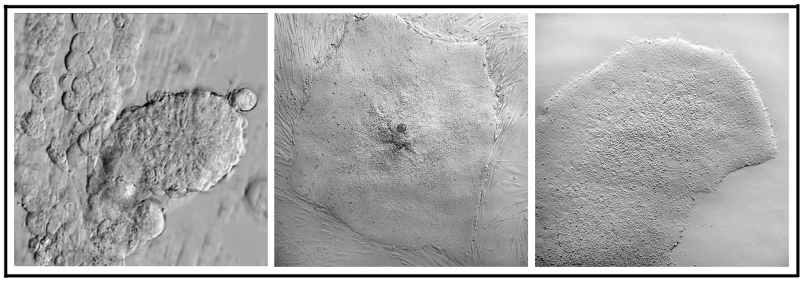

b

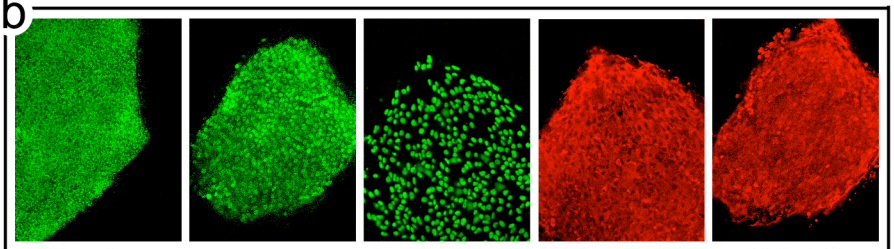

c

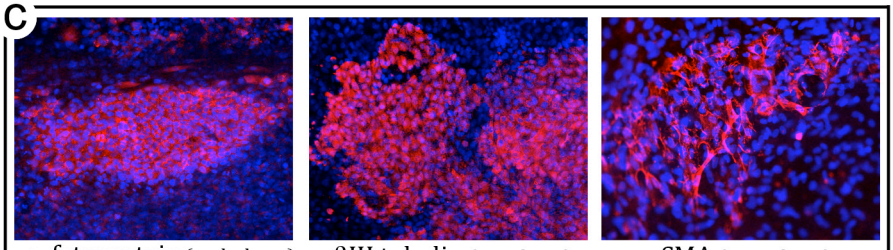

d

Marker	Allele 1	Allele 2
D13S252	278	299
D13S305	451	455
D13S325	297	301
D13S628	446	457
D13S634	397	405
D18S386	356	356
D18S390	364	368
D18S391	217	217
D18S535	478	499
D18S819	412	420
D18S976	480	483
D18S978	211	211
D21S11	241	241
D21S1409	212	220
D21S1411	324	324
D21S1435	184	188
D21S1437	319	339

e

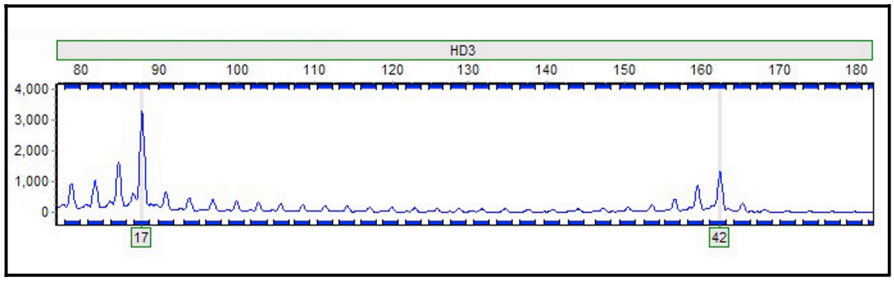

KCL013_HD4 Characterisation. a) Morphological criteria. Initial outgrowth (left), KCL012_HD4 cell colony on HFF (middle) and feeder-free condition (right). **b)** Pluripotency markers: alkaline phosphatase (AP) activity, NANOG, OCT4, TRA-1–60 and TRA-1–81. **c)** *In vitro* differentiation markers for the three germ layers: α-fetoprotein (endoderm), β-III tubulin (ectoderm) and smooth muscle actin (mesoderm). **d)** Genotyping: microsatellite markers specific for chromosomes 13, 18, 21, X and Y were amplified. The allele sizes in base pair for markers on chromosomes 13, 18, and 21 are listed in the table. Array comparative genomic hybridization (CGH) did not detect any copy number changes using Promega female G1521 as a standard. **e)** CAG repeat sizing. Images were taken at 40x magnification.

KCL020

a

Marker	Allele 1	Allele 2
D13S252	299	299
D13S305	443	451
D13S325	285	289
D13S628	453	453
D13S634	405	407
D18S386	352	367
D18S390	372	376
D18S391	217	217
D18S535	482	486
D18S819	408	408
D18S976	477	483
D18S978	207	215
D21S11	249	255
D21S1409	212	228
D21S1411	320	320
D21S1435	185	196
D21S1446	331	331

b

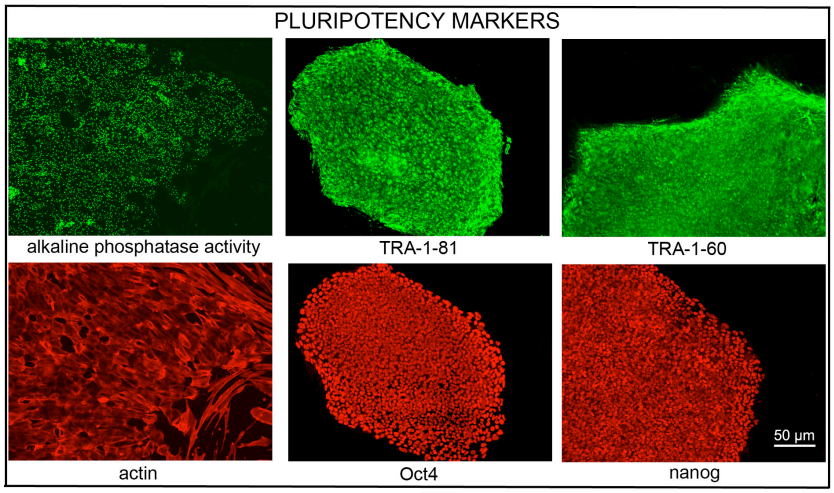

c

HLA		
HLA A	01	
HLA B	08	37
HLA C	07	06
HLA DRB1	03:01/19/22/28/37	15
HLA DRB3/4/5	3*01, 5*01	
HLA DQB1	02:01	06:02/0/11/33

d

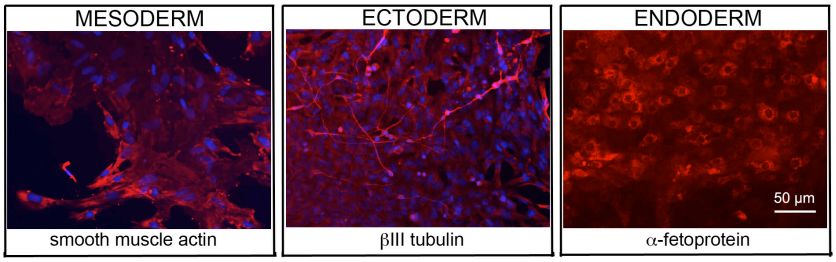

KCL020 Characterisation. a) Genotyping: microsatellite markers specific for chromosomes 13, 18, 21, X and Y were amplified. The allele sizes in base pair for markers on chromosomes 13, 18, and 21 are listed in the table. Array comparative genomic hybridization (CGH) did not detect any copy number changes using Promega female G1521 as a standard. **b)** Pluripotency markers: alkaline phosphatase activity, NANOG, OCT4, TRA-1–60 and TRA-1–81. **c)** HLA typing. **d)** *In vitro* differentiation markers for the three germ layers: smooth muscle actin (mesoderm), β-III tubulin (ectoderm) and α-fetoprotein (endoderm). Images were taken at 40x magnification.

KCL027_HD5

a

Marker	Allele 1	Allele 2
D13S252	299	299
D13S305	443	451
D13S325	285	289
D13S628	453	453
D13S634	405	407
D18S386	352	367
D18S390	372	376
D18S391	217	217
D18S535	482	486
D18S819	408	408
D18S976	477	483
D18S978	207	215
D21S11	249	255
D21S1409	212	228
D21S1411	320	320
D21S1435	185	196
D21S1446	331	331

b

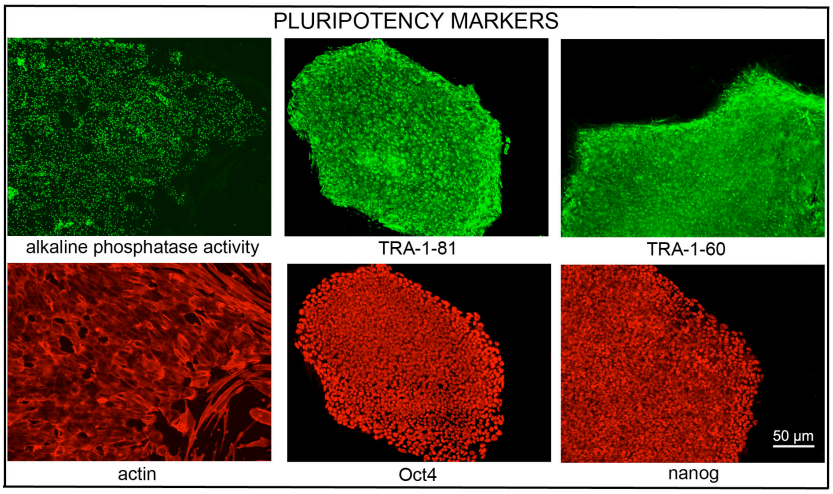

c

HLA	
HLA A	01
HLA B	08 37
HLA C	07 06
HLA DRB1	03:01/19/22/28/37 15
HLA DRB3/4/5	3*01, 5*01
HLA DQB1	02:01 06:02/0/11/33

d

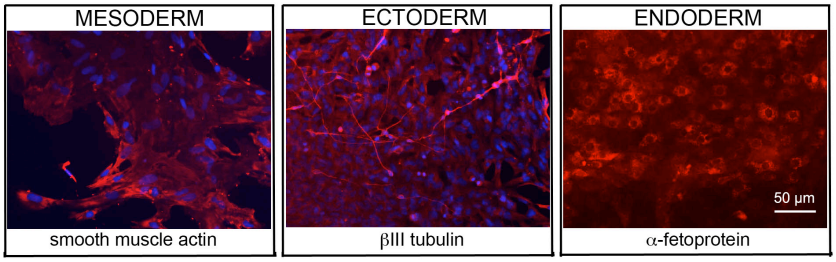

e

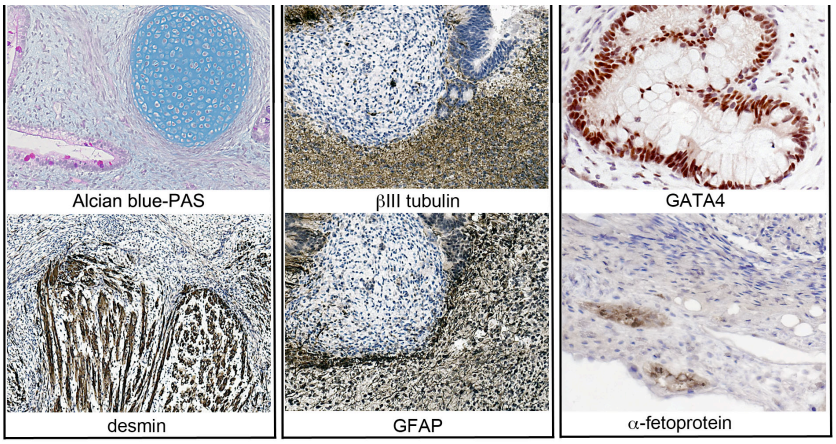

KCL027_HD5 Characterisation. a) Genotyping: microsatellite markers specific for chromosomes 13, 18, 21, X and Y were amplified. The allele sizes in base pair for markers on chromosomes 13, 18, and 21 are listed in the table. Array comparative genomic hybridization (CGH) did not detect any copy number changes using Promega female G1521 as a standard. **b)** Pluripotency markers: alkaline phosphatase activity, NANOG, OCT4, TRA-1–60 and TRA-1–81. **c)** HLA typing. **d)** *In vitro* differentiation markers for the three germ layers: smooth muscle actin (mesoderm), β-III tubulin (ectoderm) and α-fetoprotein (endoderm). **e)** *In vivo* differentiation. Teratoma sections were counterstained with hematoxylin and eosin and specific stains are either light blue (Alcian blue) or brown (all immunohistochemistry). Mesoderm germ layer markers: Alcian blue– and periodic acid–Schiff (PAS)-stained cartilage and desmin. Ectoderm germ layer markers: β-III tubulin and glial fibrillary acidic protein (GFAP). Endoderm germ layer marker: GATA4 and α-fetoprotein. Positive immunostaining for complex IV type II marker confirms the human origin of the tumour (adjacent section of the one stained for desmin). Images were taken at 40x magnification. Images were taken at 40x magnification.

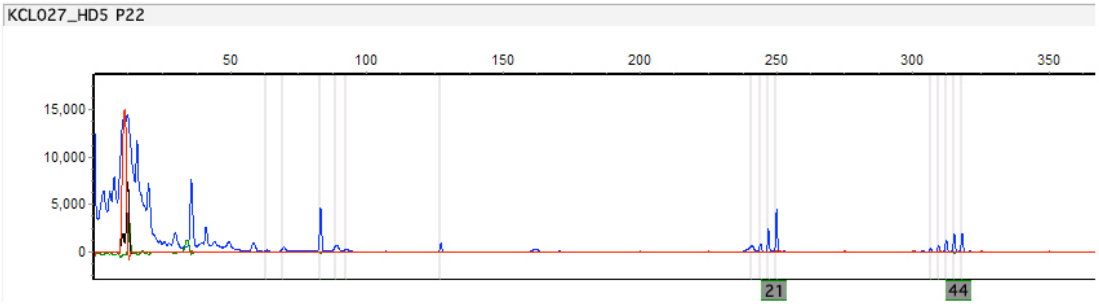

KCL027_HD5 CAG repeat sizing.

KCL028_HD6

a

Marker	Allele 1	Allele 2
D13S252	299	303
D13S305	443	462
D13S325	289	293
D13S628	450	458
D13S634	394	405
D18S386	356	386
D18S390	372	372
D18S391	217	217
D18S535	486	486
D18S819	412	420
D18S976	473	483
D18S978	211	211
D21S11	244	244
D21S1409	212	220
D21S1411	312	324
D21S1435	192	192
D21S1446	311	315

b

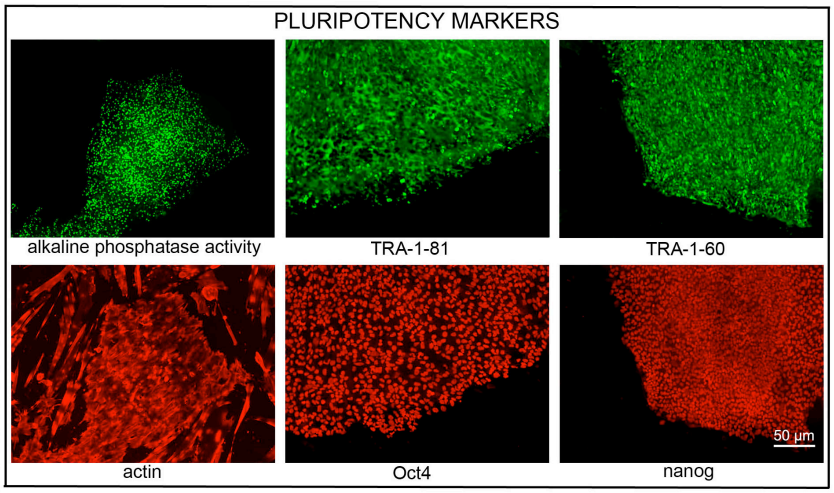

c

	HLA	
HLA A	02	03
HLA B	07	35
HLA C	04	07
HLA DRB1	01	
HLA DRB3/4/5		
HLA DQB1	05	

d

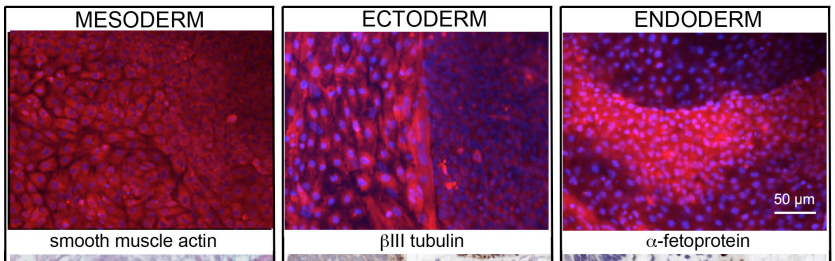

e

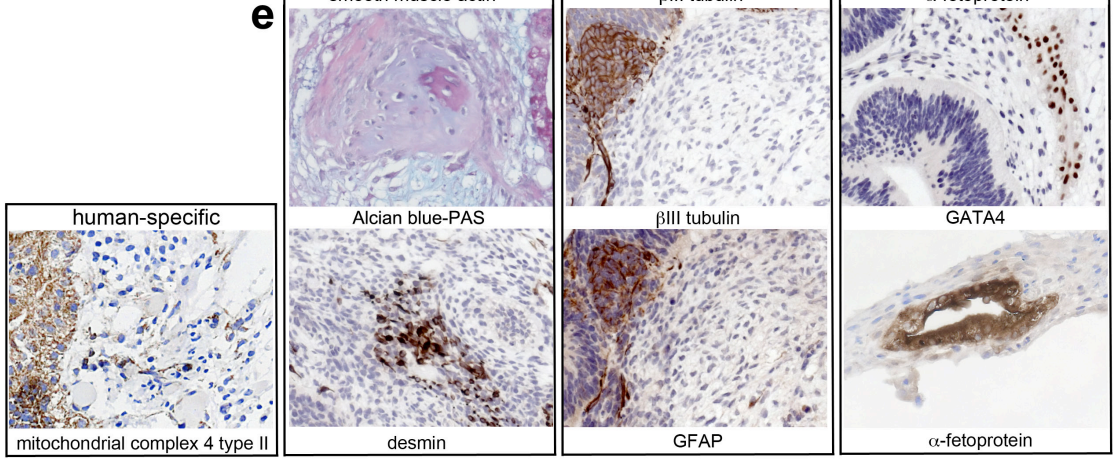

KCL026_HD6 Characterisation. a) Genotyping: microsatellite markers specific for chromosomes 13, 18, 21, X and Y were amplified. The allele sizes in base pair for markers on chromosomes 13, 18, and 21 are listed in the table. Array comparative genomic hybridization (CGH) did not detect any copy number changes using Promega female G1521 as a standard. **b)** Pluripotency markers: alkaline phosphatase activity, NANOG, OCT4, TRA-1–60 and TRA-1–81. **c)** HLA typing. **d)** *In vitro* differentiation markers for the three germ layers: smooth muscle actin (mesoderm), β-III tubulin (ectoderm) and α-fetoprotein (endoderm). **e)** *In vivo* differentiation. Teratoma sections were counterstained with hematoxylin and eosin and specific stains are either light blue (Alcian blue) or brown (all immunohistochemistry). Mesoderm germ layer markers: Alcian blue– and periodic acid–Schiff (PAS)-stained cartilage and desmin. Ectoderm germ layer markers: β-III tubulin and glial fibrillary acidic protein (GFAP). Endoderm germ layer marker: GATA4 and α-fetoprotein. Positive immunostaining for complex IV type II marker confirms the human origin of the tumour (adjacent section of the one stained for desmin). Images were taken at 40x magnification. Images were taken at 40x magnification.

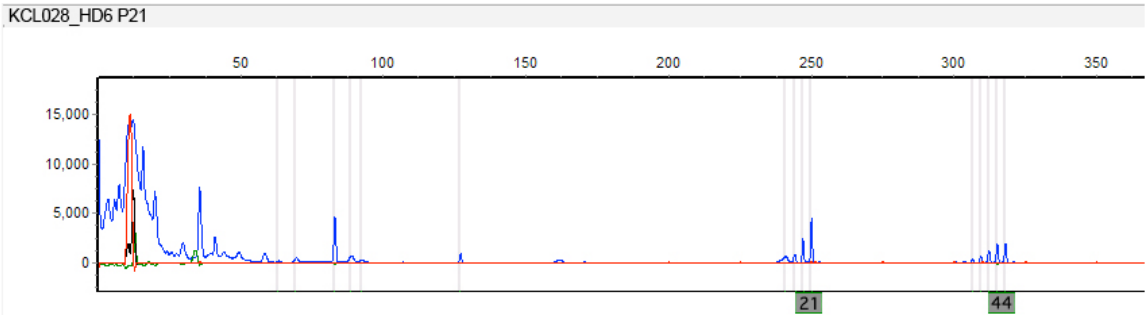

KCL028_HD6 CAG repeat sizing.

KCL031

a

Marker	Allele 1	Allele 2
D13S252	295	299
D13S325	293	293
D13S628	454	457
D13S634	397	401
D18S386	363	382
D18S390	372	372
D18S391	209	221
D18S535	478	486
D18S819	416	416
D18S976	476	481
D18S978	207	211
D21S11	245	255
D21S1409	212	212
D21S1411	304	320
D21S1435	184	188
D21S1446	311	311

b

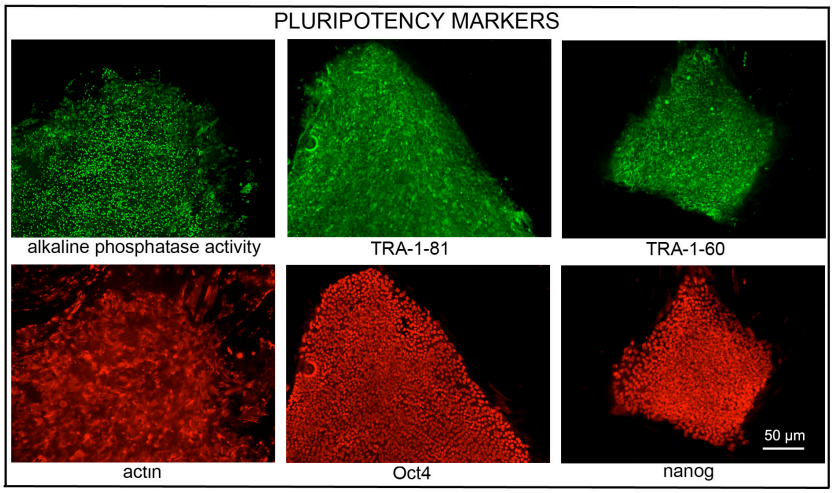

c

HLA		
HLA A	02	24
HLA B	51	52:01/04/07/13
HLA C	14	12
HLA DRB1	11	15
HLA DRB3/4/5	3*02	5*01
HLA DQB1	03	06

d

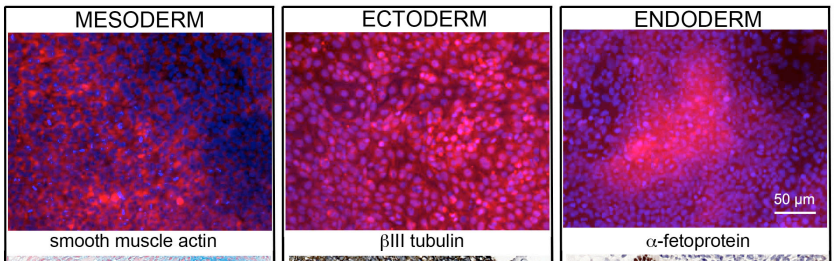

e

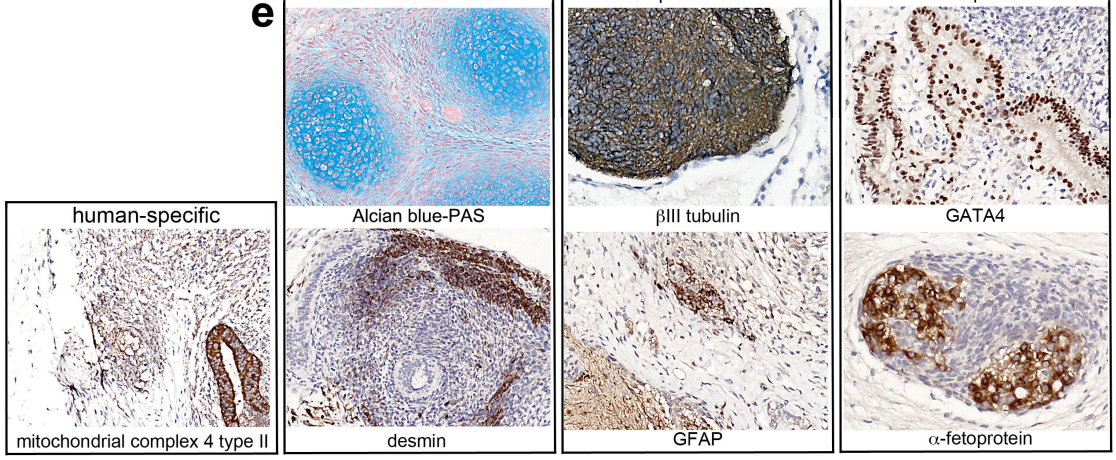

KCL031 Characterisation. a) Genotyping: microsatellite markers specific for chromosomes 13, 18, 21, X and Y were amplified. The allele sizes in base pair for markers on chromosomes 13, 18, and 21 are listed in the table. Array comparative genomic hybridization (CGH) did not detect any copy number changes using Promega female G1521 as a standard. **b)** Pluripotency markers: alkaline phosphatase activity, NANOG, OCT4, TRA-1–60 and TRA-1–81. **c)** HLA typing. **d)** *In vitro* differentiation markers for the three germ layers: smooth muscle actin (mesoderm), β-III tubulin (ectoderm) and α-fetoprotein (endoderm). **e)** *In vivo* differentiation. Teratoma sections were counterstained with hematoxylin and eosin and specific stains are either light blue (Alcian blue) or brown (all immunohistochemistry). Mesoderm germ layer markers: Alcian blue– and periodic acid–Schiff (PAS)-stained cartilage and desmin. Ectoderm germ layer markers: β-III tubulin and glial fibrillary acidic protein (GFAP). Endoderm germ layer marker: GATA4 and α-fetoprotein. Positive immunostaining for complex IV type II marker confirms the human origin of the tumour (adjacent section of the one stained for desmin). Images were taken at 40x magnification.

KCL034

a

Marker	Allele 1	Allele 2
D13S252	283	295
D13S325	285	289
D13S628	450	458
D13S634	405	407
D18S386	356	386
D18S390	364	372
D18S391	217	217
D18S535	479	482
D18S819	408	416
D18S976	473	480
D18S978	211	215
D21S11	241	249
D21S1409	212	212
D21S1411	312	316
D21S1435	184	184
D21S1446	311	325

b

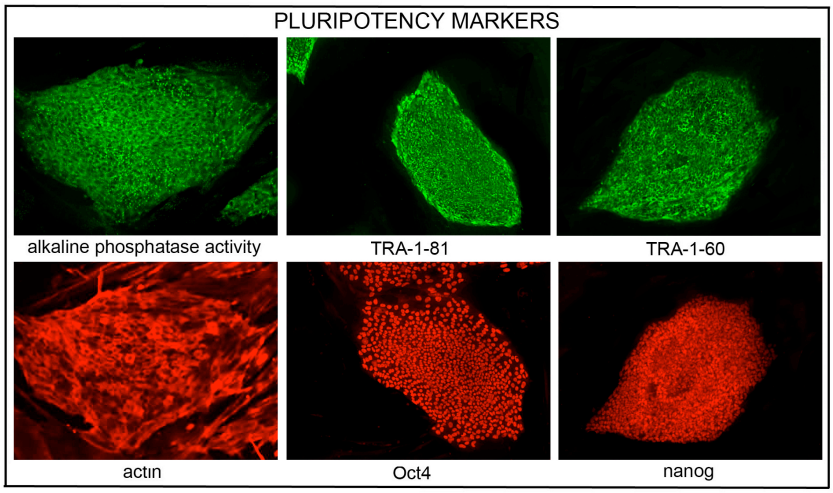

c

HLA		
HLA A	11	29
HLA B	44	51
HLA C	16	04
HLA DRB1	04:07	07
HLA DRB3/4/5	4*01	
HLA DQB1	03	02

d

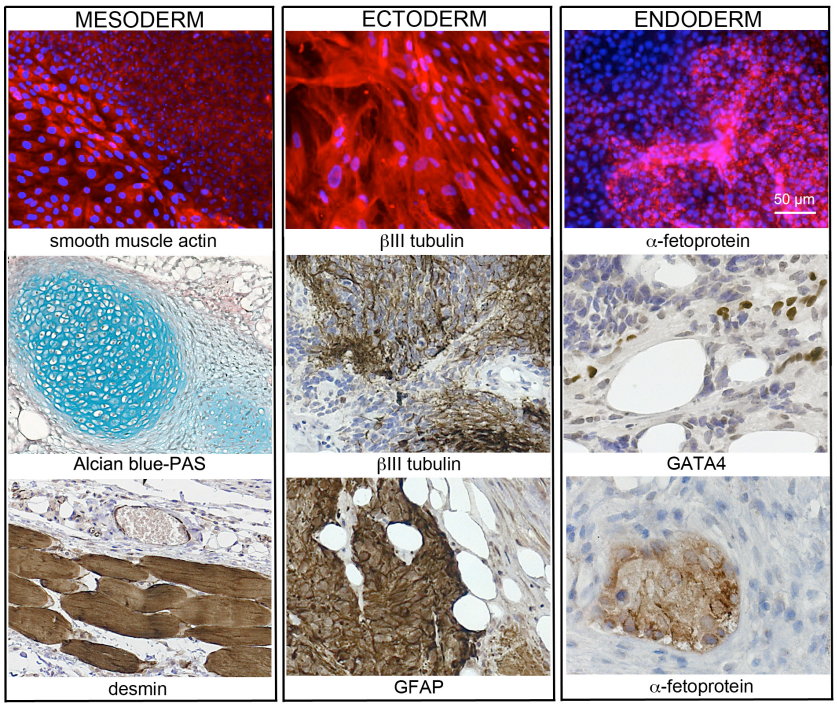

e

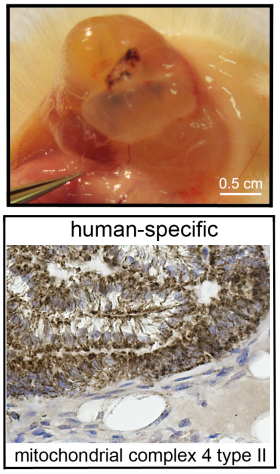

KCL034 Characterisation. a) Genotyping: microsatellite markers specific for chromosomes 13, 18, 21, X and Y were amplified. The allele sizes in base pair for markers on chromosomes 13, 18, and 21 are listed in the table. Array comparative genomic hybridization (CGH) did not detect any copy number changes using Promega female G1521 as a standard. **b)** Pluripotency markers: alkaline phosphatase activity, NANOG, OCT4, TRA-1–60 and TRA-1–81. **c)** HLA typing. **d)** *In vitro* differentiation markers for the three germ layers: smooth muscle actin (mesoderm), β-III tubulin (ectoderm) and α-fetoprotein (endoderm). **e)** *In vivo* differentiation. Teratoma sections were counterstained with hematoxylin and eosin and specific stains are either light blue (Alcian blue) or brown (all immunohistochemistry). Mesoderm germ layer markers: Alcian blue– and periodic acid–Schiff (PAS)-stained cartilage and desmin. Ectoderm germ layer markers: β-III tubulin and glial fibrillary acidic protein (GFAP). Endoderm germ layer marker: GATA4 and α-fetoprotein. Positive immunostaining for complex IV type II marker confirms the human origin of the tumour (adjacent section of the one stained for desmin). Images were taken at 40x magnification. Images were taken at 40x magnification.

KCL036_HD7

a

Marker	Allele 1	Allele 2
D13S252	278	299
D13S325	293	301
D13S628	453	453
D13S634	397	401
D18S386	379	382
D18S390	368	372
D18S391	209	217
D18S535	478	482
D18S819	400	408
D18S976	476	483
D18S978	211	211
D21S11	249	259
D21S1409	216	224
D21S1411	312	316
D21S1435	188	188
D21S1446	311	325

b

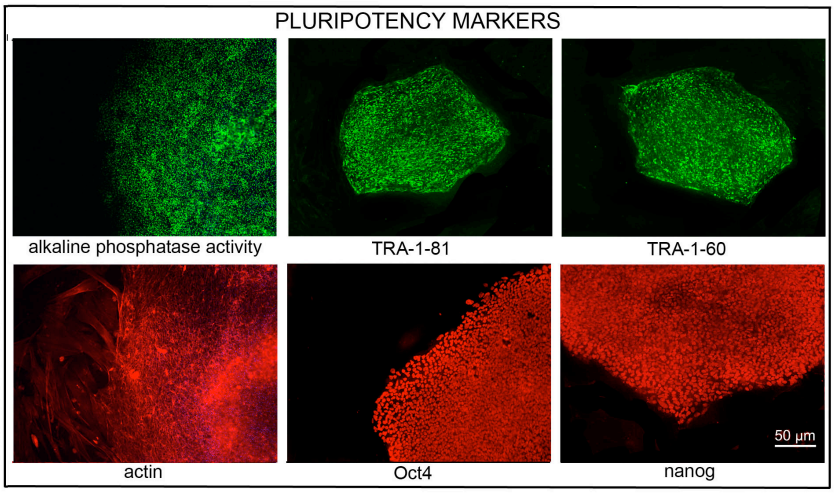

c

HLA		
HLA A	03	24
HLA B	07	44
HLA C	05	07
HLA DRB1	04	
HLA DRB3/4/5	DRB4*01	
HLA DQB1	03	04
Bw	Bw6	Bw4

d

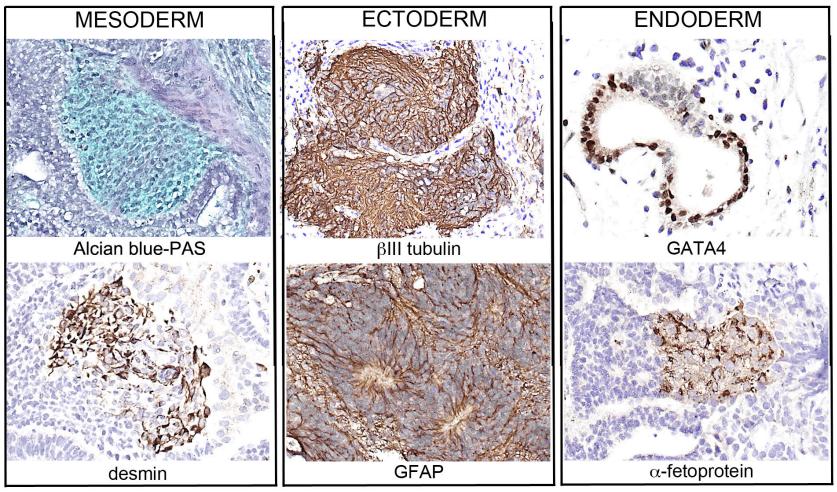

KCL036_HD7 Characterisation. a) Genotyping: microsatellite markers specific for chromosomes 13, 18, 21, X and Y were amplified. The allele sizes in base pair for markers on chromosomes 13, 18, and 21 are listed in the table. Array comparative genomic hybridization (CGH) did not detect any copy number changes using Promega female G1521 as a standard. **b)** Pluripotency markers: alkaline phosphatase activity, NANOG, OCT4, TRA-1–60 and TRA-1–81. **c)** HLA typing. **d)** *In vitro* differentiation markers for the three germ layers: smooth muscle actin (mesoderm), β-III tubulin (ectoderm) and α-fetoprotein (endoderm). **e)** *In vivo* differentiation. Teratoma sections were counterstained with hematoxylin and eosin and specific stains are either light blue (Alcian blue) or brown (all immunohistochemistry). Mesoderm germ layer markers: Alcian blue– and periodic acid–Schiff (PAS)-stained cartilage and desmin. Ectoderm germ layer markers: β-III tubulin and glial fibrillary acidic protein (GFAP). Endoderm germ layer marker: GATA4 and α-fetoprotein. Positive immunostaining for complex IV type II marker confirms the human origin of the tumour (adjacent section of the one stained for desmin). Images were taken at 40x magnification. Images were taken at 40x magnification.

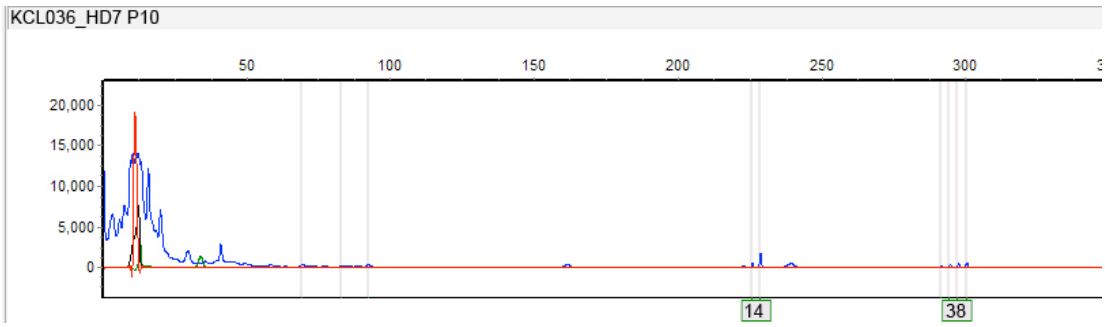

KCL036_HD7 CAG repeat sizing

KCL040

a

Marker	Allele 1	Allele 2
D13S252	295	305
D13S325	285	293
D13S628	453	457
D13S634	401	401
D18S386	360	382
D18S390	372	372
D18S391	217	217
D18S535	478	494
D18S819	412	412
D18S976	476	476
D18S978	215	219
D21S11	249	249
D21S1409	224	228
D21S1411	320	328
D21S1435	189	189
D21S1446	316	324

b

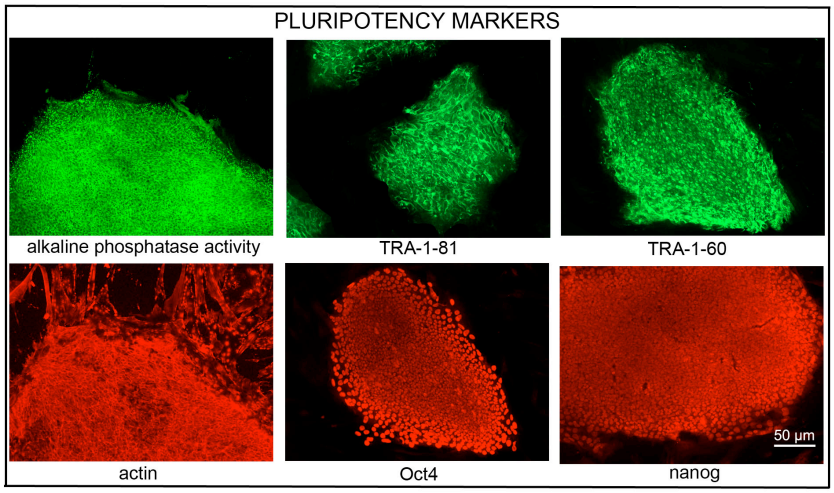

c

HLA		
HLA A	03	24
HLA B	07	15(62)
HLA C	04	15
HLA DRB1	03	24
HLA DRB3/4/5		
HLA DQB1		

d

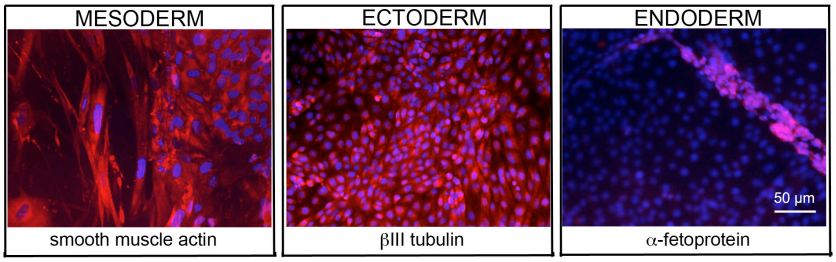

KCL040 Characterisation. a) Genotyping: microsatellite markers specific for chromosomes 13, 18, 21, X and Y were amplified. The allele sizes in base pair for markers on chromosomes 13, 18, and 21 are listed in the table. Array comparative genomic hybridization (CGH) did not detect any copy number changes using Promega female G1521 as a standard. **b)** Pluripotency markers: alkaline phosphatase activity, NANOG, OCT4, TRA-1–60 and TRA-1–81. **c)** HLA typing. **d)** *In vitro* differentiation markers for the three germ layers: smooth muscle actin (mesoderm), β-III tubulin (ectoderm) and α-fetoprotein (endoderm). Images were taken at 40x magnification.

APPENDIX II Modified mRNA synthesis

Coding sequences of the different genes used for the generation of modified synthetic mRNA.

SOX2 954bp NM_003106.2 CDS Gene ID: 6657

ATGTACAACATGATGGAGACGGAGCTGAAGCCGCCGGGCCCGCAGCAAACTTCGGGGGG
CGGCGGCGGCAACTCCACCGCGGCGGCGGCCGGCGGCAACCAGAAAAACAGCCCGGAC
CGCGTCAAGCGGCCCATGAATGCCTTCATGGTGTGGTCCCGCGGGCAGCGGCGCAAGAT
GGCCCAGGAGAACCCCAAGATGCACAACTCGGAGATCAGCAAGCGCCTGGGCGCCGAGT
GGAAACTTTTGTCGGAGACGGAGAAGCGGCCGTTCATCGACGAGGCTAAGCGGCTGCGA
GCGCTGCACATGAAGGAGCACCCGGATTATAAATACCGGCCCCGGCGGAAAACCAAGAC
GCTCATGAAGAAGGATAAGTACACGCTGCCCGGCGGGCTGCTGGCCCCCGGCGGCAATA
GCATGGCGAGCGGGGTCGGGGTGGGCGCCGGCCTGGGCGCGGGCGTGAACCAGCGCA
TGGACAGTTACGCGCACATGAACGGCTGGAGCAACGGCAGCTACAGCATGATGCAGGAC
CAGCTGGGCTACCCGCAGCACCCGGGCCTCAATGCGCACGGCGCAGCGCAGATGCAGCC
CATGCACCGCTACGACGTGAGCGCCCTGCAGTACAACTCCATGACCAGCTCGCAGACCTA
CATGAACGGCTCGCCCACCTACAGCATGTCCTACTCGCAGCAGGGCACCCCTGGCATGGC
TCTTGGCTCCATGGGTTCGGTGGTCAAGTCCGAGGCCAGCTCCAGCCCCCCTGTGGTTAC
CTCTTCCTCCCACTCCAGGGCGCCCTGCCAGGCCGGGGACCTCCGGGACATGATCAGCA
TGTATCTCCCCGGCGCCGAGGTGCCGGAACCCGCCGCCCCCAGCAGACTTCACATGTCC
CAGCACTACCAGAGCGGCCCGGTGCCCGGCACGGCCATTAACGGCACACTGCCCCTCTC
ACACATGTGA

OCT-4 1,083bp NM_002701.4 CDS CDS GENE ID: 5460

ATGGCGGGACACCTGGCTTCGGATTTCGCCTTCTCGCCCCCTCCAGGTGGTGGAGGTGAT
GGGCCAGGGGGGCCGGAGCCGGGCTGGGTTGATCCTCGGACCTGGCTAAGCTTCCAAG
GCCCTCCTGGAGGGCCAGGAATCGGGCCGGGGGTTGGGCCAGGCTCTGAGGTGTGGGG
GATTCCCCCATGCCCCCCGCCGTATGAGTTCTGTGGGGGGATGGCGTACTGTGGGCCCC
AGGTTGGAGTGGGGCTAGTGCCCCAAGGCGGCTTGGAGACCTCTCAGCCTGAGGGCGAA
GCAGGAGTCGGGGTGGAGAGCAACTCCGATGGGGCCTCCCCGGAGCCCTGCACCGTCAC
CCCTGGTGCCGTGAAGCTGGAGAAGGAGAAGCTGGAGCAAAACCCGGAGGAGTCCCAGG
ACATCAAAGCTCTGCAGAAAGAACTCGAGCAATTTGCCAAGCTCCTGAAGCAGAAGAGGAT
CACCCTGGGATATACACAGGCCGATGTGGGGCTCACCCTGGGGGTTCTATTTGGGAAGGT
ATTCAGCCAAACGACCATCTGCCGCTTTGAGGCTCTGCAGCTTAGCTTCAAGAACATGTGT
AAGCTGCGGCCCTTGCTGCAGAAGTGGGTGGAGGAAGCTGACAACAATGAAAATCTTCAG
GAGATATGCAAAGCAGAAACCCTCGTGCAGGCCCGAAAGAGAAAGCGAACCAGTATCGAG
AACCGAGTGAGAGGCAACCTGGAGAATTTGTTCCTGCAGTGCCCGAAACCCACACTGCAG
CAGATCAGCCACATCGCCCAGCAGCTTGGGCTCGAGAAGGATGTGGTCCGAGTGTGGTTC
TGTAACCGGCGCCAGAAGGGCAAGCGATCAAGCAGCGACTATGCACAACGAGAGGATTTT
GAGGCTGCTGGGTCTCCTTTCTCAGGGGGACCAGTGTCCTTTCCTCTGGCCCCAGGGCCC
CATTTTGGTACCCCAGGCTATGGGAGCCCTCACTTCACTGCACTGTACTCCTCGGTCCCTT
TCCCTGAGGGGGAAGCCTTTCCCCCTGTCTCCGTCACCACTCTGGGCTCTCCCATGCATT
CAAACTGA

KLF4 1,440bp NM_004235.4 CDS gene ID: 9314

ATGAGGCAGCCACCTGGCGAGTCTGACATGGCTGTCAGCGACGCGCTGCTCCCATCTTTC
TCCACGTTCGCGTCTGGCCCGGCGGGAAGGGAGAAGACACTGCGTCAAGCAGGTGCCCC
GAATAACCGCTGGCGGGAGGAGCTCTCCCACATGAAGCGACTTCCCCCAGTGCTTCCCGG
CCGCCCCTATGACCTGGCGGCGGCGACCGTGGCCACAGACCTGGAGAGCGGCGGAGCC
GGTGCGGCTTGCGGCGGTAGCAACCTGGCGCCCCTACCTCGGAGAGAGACCGAGGAGTT
CAACGATCTCCTGGACCTGGACTTTATTCTCTCCAATTCGCTGACCCATCCTCCGGAGTCA
GTGGCCGCCACCGTGTCCTCGTCAGCGTCAGCCTCCTCTTCGTCGTCGCCGTCGAGCAG
CGGCCCTGCCAGCGCGCCCTCCACCTGCAGCTTCACCTATCCGATCCGGGCCGGGAACG
ACCCGGGCGTGGCGCCGGGCGGCACGGGCGGAGGCCTCCTCTATGGCAGGGAGTCCGC
TCCCCCTCCGACGGCTCCCTTCAACCTGGCGGACATCAACGACGTGAGCCCCTCGGGCG
GCTTCGTGGCCGAGCTCCTGCGGCCAGAATTGGACCCGGTGTACATTCCGCCGCAGCAG
CCGCAGCCGCCAGGTGGCGGGCTGATGGGCAAGTTCGTGCTGAAGGCGTCGCTGAGCG
CCCCTGGCAGCGAGTACGGCAGCCCGTCGGTCATCAGCGTCAGCAAAGGCAGCCCTGAC
GGCAGCCACCCGGTGGTGGTGGCGCCCTACAACGGCGGGCCGCCGCGCACGTGCCCCA
AGATCAAGCAGGAGGCGGTCTCTTCGTGCACCCACTTGGGCGCTGGACCCCCTCTCAGCA
ATGGCCACCGGCCGGCTGCACACGACTTCCCCCTGGGGCGGCAGCTCCCCAGCAGGACT
ACCCCGACCCTGGGTCTTGAGGAAGTGCTGAGCAGCAGGGACTGTCACCCTGCCCTGCC
GCTTCCTCCCGGCTTCCATCCCCACCCGGGGCCCAATTACCCATCCTTCCTGCCCGATCA
GATGCAGCCGCAAGTCCCGCCGCTCCATTACCAAGAGCTCATGCCACCCGGTTCCTGCAT
GCCAGAGGAGCCCAAGCCAAAGAGGGGAAGACGATCGTGGCCCCGGAAAAGGACCGCCA
CCCACACTTGTGATTACGCGGGCTGCGGCAAAACCTACACAAAGAGTTCCCATCTCAAGG
CACACCTGCGAACCCACACAGGTGAGAAACCTTACCACTGTGACTGGGACGGCTGTGGAT
GGAAATTCGCCCGCTCAGATGAACTGACCAGGCACTACCGTAAACACACGGGGCACCGCC
CGTTCCAGTGCCAAAAATGCGACCGAGCATTTTCCAGGTCGGACCACCTCGCCTTACACAT
GAAGAGGCATTTTTAA

MYC v-myc myelocytomatosis viral oncogene homolog 1,365bp NM_002467.4 Gene ID: 4609

CTGGATTTTTTTCGGGTAGTGGAAAACCAGCAGCCTCCCGCGACGATGCCCCTCAACGTTA
GCTTCACCAACAGGAACTATGACCTCGACTACGACTCGGTGCAGCCGTATTTCTACTGCGA
CGAGGAGGAGAACTTCTACCAGCAGCAGCAGCAGAGCGAGCTGCAGCCCCCGGCGCCCA
GCGAGGATATCTGGAAGAAATTCGAGCTGCTGCCCACCCCGCCCCTGTCCCCTAGCCGCC
GCTCCGGGCTCTGCTCGCCCTCCTACGTTGCGGTCACACCCTTCTCCCTTCGGGGAGACA
ACGACGGCGGTGGCGGGAGCTTCTCCACGGCCGACCAGCTGGAGATGGTGACCGAGCTG
CTGGGAGGAGACATGGTGAACCAGAGTTTCATCTGCGACCCGGACGACGAGACCTTCATC
AAAAACATCATCATCCAGGACTGTATGTGGAGCGGCTTCTCGGCCGCCGCCAAGCTCGTC
TCAGAGAAGCTGGCCTCCTACCAGGCTGCGCGCAAAGACAGCGGCAGCCCGAACCCCGC
CCGCGGCCACAGCGTCTGCTCCACCTCCAGCTTGTACCTGCAGGATCTGAGCGCCGCCG
CCTCAGAGTGCATCGACCCCTCGGTGGTCTTCCCCTACCCTCTCAACGACAGCAGCTCGC
CCAAGTCCTGCGCCTCGCAAGACTCCAGCGCCTTCTCTCCGTCCTCGGATTCTCTGCTCTC
CTCGACGGAGTCCTCCCCGCAGGGCAGCCCCGAGCCCCTGGTGCTCCATGAGGAGACAC

CGCCCACCACCAGCAGCGACTCTGAGGAGGAACAAGAAGATGAGGAAGAAATCGATGTTG
TTTCTGTGGAAAAGAGGCAGGCTCCTGGCAAAAGGTCAGAGTCTGGATCACCTTCTGCTG
GAGGCCACAGCAAACCTCCTCACAGCCCACTGGTCCTCAAGAGGTGCCACGTCTCCACAC
ATCAGCACAACTACGCAGCGCCTCCCTCCACTCGGAAGGACTATCCTGCTGCCAAGAGGG
TCAAGTTGGACAGTGTCAGAGTCCTGAGACAGATCAGCAACAACCGAAAATGCACCAGCC
CCAGGTCCTCGGACACCGAGGAGAATGTCAAGAGGCGAACACACAACGTCTTGGAGCGC
CAGAGGAGGAACGAGCTAAAACGGAGCTTTTTTGCCCTGCGTGACCAGATCCCGGAGTTG
GAAAACAATGAAAAGGCCCCCAAGGTAGTTATCCTTAAAAAAGCCACAGCATACATCCTGT
CCGTCCAAGCAGAGGAGCAAAAGCTCATTTCTGAAGAGGACTTGTTGCGGAAACGACGAG
AACAGTTGAAACACAAACTTGAACAGCTACGGAACTCTTGTGCGTAA

LIN28A lin-28 homolog A (C. elegans) [*Homo sapiens*] NM_024674.4 630bp Gene ID: 79727

ATGGGCTCCGTGTCCAACCAGCAGTTTGCAGGTGGCTGCGCCAAGGCGGCAGAAGAGGC
GCCCGAGGAGGCGCCGGAGGACGCGGCCCGGGCGGCGGACGAGCCTCAGCTGCTGCA
CGGTGCGGGCATCTGTAAGTGGTTCAACGTGCGCATGGGGTTCGGCTTCCTGTCCATGAC
CGCCCGCGCCGGGGTCGCGCTCGACCCCCCAGTGGATGTCTTTGTGCACCAGAGTAAGC
TGCACATGGAAGGGTTCCGGAGCTTGAAGGAGGGTGAGGCAGTGGAGTTCACCTTTAAGA
AGTCAGCCAAGGGTCTGGAATCCATCCGTGTCACCGGACCTGGTGGAGTATTCTGTATTG
GGAGTGAGAGGCGGCCAAAAGGAAAGAGCATGCAGAAGCGCAGATCAAAAGGAGACAGG
TGCTACAACTGTGGAGGTCTAGATCATCATGCCAAGGAATGCAAGCTGCCACCCCAGCCC
AAGAAGTGCCACTTCTGCCAGAGCATCAGCCATATGGTAGCCTCATGTCCGCTGAAGGCC
CAGCAGGGCCCTAGTGCACAGGGAAAGCCAACCTACTTTCGAGAGGAAGAAGAAGAAATC
CACAGCCCTACCCTGCTCCCGGAGGCACAGAATTGA

pTNT vector circular map (Promega).

Promega

4. pTNT™ Vector Multiple Cloning Site and Circle Map (continued)

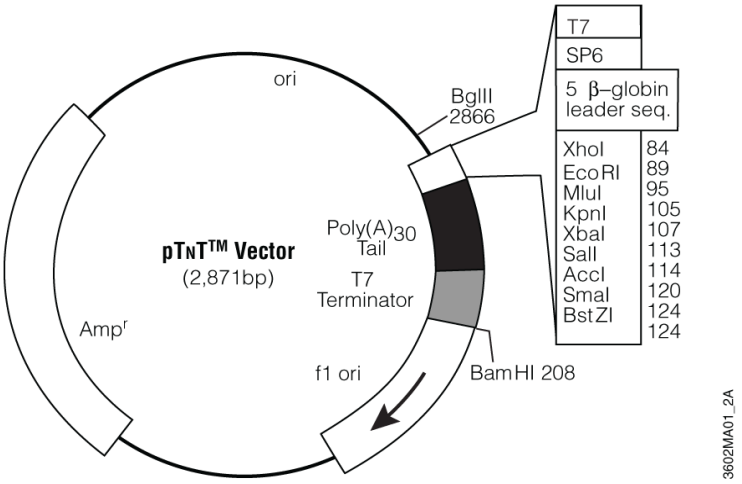

Figure 2. pTNT™ Vector circle map and sequence reference points.

T7 RNA polymerase promoter	16–34
SP6 RNA polymerase promoter	40–56
5´ β-globin leader sequence	57–83
Multiple cloning region	84–130
Synthetic poly(A)$_{30}$ region	131–160
T7 transcription terminator sequence	161–208
Phage f1 region	287–742
β-Lactamase (Amp^r) coding region	1179–2039